UNIVERSIDAD DE OVIEDO

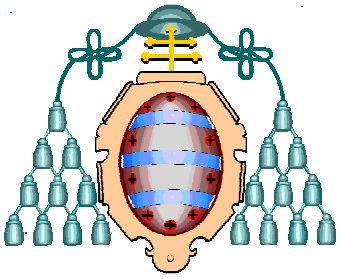

PROGRAMA DE DOCTORADO
DE PSICOLOGÍA

INFLUENCIA DE LA HIPERTENSIÓN PORTAL EN LA CONDUCTA DE LA ORIENTACIÓN ESPACIAL

Natalia Arias del Castillo

Oviedo, 2014

RESUMEN

La encefalopatía hepática (EH) es un síndrome neuropsiquiátrico y neurocognitivo ocasionado por un daño hepático agudo o crónico. En la actualidad se ha visto que la EH tiene carácter multifactorial, interviniendo en su patogénesis tanto la hipertensión portal como el incremento del amonio. Primeramente, nos centramos en analizar la contribución diferencial de estos factores al metabolismo oxidativo de las regiones cerebrales implicadas en los procesos de aprendizaje y memoria. Los resultados nos permiten observar que los animales con hipertensión portal ven reducida su actividad metabólica en la corteza prefrontal, el estriado ventral, los núcleos talámicos y el hipocampo, manifestando una mayor alteración en el modelo de hiperamonemia, donde las demandas energéticas se ven incrementadas por encima de los niveles convencionales en todas las estructuras cerebrales.

Hemos observado que durante el estadio crónico de la EH, reproducido mediante animales hiperamonémicos, estos fueron incapaces de alcanzar el criterio de aprendizaje en las tareas alocéntrica y de guía. A su vez, detectamos diferencias en la actividad metabólica cerebral en las cortezas prefrontal, parietal y temporal, así como en el estriado dorsal, el tálamo, el hipocampo ventral y los núcleos amigdalinos. Contrariamente, el estudio de la EH mínima (EHM) mediante el modelo de hipertensión portal no mostró alteraciones en la memoria de referencia espacial, pero sí una implicación diferencial de áreas cerebrales como el hipocampo y la amígdala. Por otra parte, el análisis conductual mediante la combinación de la estrategia alocéntrica y de guía reveló una falta de flexibilidad por parte de los animales hipertensos. Además, el análisis de las redes cerebrales basado en la actividad metabólica manifestó que estructuras cerebrales como la corteza parietal, el estriado dorsal y el núcleo accumbens eran comunes a los cambios de estrategia estudiados. Sin embargo, en los sujetos que realizaron el cambio desde la estrategia alocéntrica a la de guía, la corteza prefrontal se reveló primordial, no siendo así en los grupos que realizaron el cambio opuesto donde la relevancia mayor recayó sobre el hipocampo y la amígdala.

Por último, diseñamos diferentes tareas conductuales con el fin de detectar las estructuras cerebrales pioneras en la adquisición del déficit temprano de la EHM. La incapacidad de los animales hipertensos para realizar tanto la tarea de reconocimiento objeto-lugar como el aprendizaje de reversión, junto con los resultados obtenidos mediante la inmunocitoquímica de la proteína c-Fos, nos revelaron la existencia de dos circuitos, un "circuito neural corto" donde el grupo hipertenso muestra una elevada inmunoreactividad en CA1, CA3 y la corteza entorrinal, y un "circuito neural largo" caracterizado por una disminución significativa de actividad c-Fos en CA1, CA3, giro dentado y las cortezas prelímbica e infralímbica en el citado grupo hipertenso en frente al grupo pseudo-operado. Igualmente, los animales hipertensos fueron incapaces de alcanzar el criterio de aprendizaje en la tarea de hábitos, lo que iba acompañado de una reducción en la actividad citocromo c-oxidasa en el estriado ventral, hipocampo y los núcleo amigdalinos de los animales con EHM, un incremento del factor necrótico de tumores α en el núcleo estriado, una disminución de células GFAP inmunoreactivas en el estriado dorsal y un incremento en el volumen nuclear neuronal del estriado ventral.

De nuestro trabajo se puede concluir que la existencia de deficiencias en la adquisición de los aprendizajes a corto plazo, correlacionan con los cambios observados en el metabolismo oxidativo cerebral y en la expresión génica de aquellas estructuras cerebrales que se ven primeramente afectadas por la EHM. Asimismo, pudimos relacionar el núcleo estriado con procesos inflamatorios, daños astrocitarios y cambios en el volumen nuclear neuronal, lo que nos permite demostrar la existencia de cambios tempranos antes de que tenga lugar la cronicidad de la EH.

ABSTRACT

Hepatic encephalopathy (HE) is a neuropsychiatric and neurocognitive syndrome caused by acute or chronic liver damage. Recently, it has been shown that the EH is a multifactorial disorder, being involved in its pathogenesis portal hypertension and elevated ammonia levels. We analyzed the differential contribution of these factors to brain oxidative metabolism related to learning and memory processes. The results show that portal hypertension animals present a decrease in their metabolic activity in the prefrontal cortex, the ventral striatum, thalamic nuclei and hippocampus, whereas the severest alteration was found in the model of hyperammonemia, where energy demands are increased above the conventional levels in all brain structures.

We observed that during the chronic stage of HE, reproduced by hyperammonemic animals, they were unable to reach the learning criterion in allocentric and cue-guided tasks. In turn, we detected differences in brain metabolic activity in the prefrontal, parietal and temporal cortices and in the dorsal striatum, thalamus, the ventral hippocampus and amygdala nuclei. Conversely, the minimal HE (MHE) studied in the portal hypertension model showed no abnormalities in spatial reference memory, but a differential involvement of brain areas such as the hippocampus and amygdala. Furthermore, behavioral analysis, combining the allocentric and cue-guided strategies, revealed a lack of flexibility by portal hypertension animals. Furthermore, the analysis of brain networks based on the metabolic activity showed that brain structures such as the parietal cortex, the dorsal striatum and nucleus accumbens were common to both strategy changes studied. However, subjects who performed the change from allocentric strategy to cue-guided revealed changes in prefrontal cortex. This is not the case in the groups that made the opposite change where the most important change was shown in the hippocampus and amygdala.

Finally, we design different behavioral tasks in order to detect the pioneering brain structures involved in the deficits in the early acquisition of MHE. The inability of portal hypertension animals to make both the object-place recognition

task and reversal learning, together with the results obtained by immunocytochemistry of c- Fos protein, revealed the existence of two circuits, a "short neural circuit" where the portal hypertension group showed high immunoreactivity in CA1, CA3 and the entorhinal cortex, and a" long neural circuit" characterized by a significant decrease of c -Fos activity in CA1, CA3, dentate gyrus, infralimbic and prelimbic cortices in portal hypertension group compared to sham group. Similarly, portal hypertension animals were unable to reach the learning criterion in the stimulus-response task, which was accompanied by a reduction in cytochrome c-oxidase activity in the ventral striatum, hippocampus and amygdala nuclei, an increase in tumor necrosis factor α in the striatum, decreased GFAP immunoreactive cells in the dorsal striatum and increased nuclear volume neuron in the ventral striatum.

From our work it can be concluded that the existence of deficits in the acquisition of short term learnings correlated with observed changes in brain oxidative metabolism and gene expression in those brain structures that are primarily affected by MHE. Also, we could relate the striatum with inflammatory processes, astrocytic damage and changes in neuronal nuclear volume, which allows us to demonstrate the existence of early changes that take place before the chronicity of the EH.

1. INTRODUCCIÓN

1.1 La Encefalopatía Hepática

La cirrosis hepática, lejos de ser un daño aislado del hígado, tiene consecuencias bien conocidas sobre el funcionamiento cerebral. Desde la antigua Grecia y los tiempos romanos se conocen alteraciones mentales relacionadas con un mal funcionamiento hepático. Hipócrates reconocía un "delirio sintomático" asociado con una "ictericia y supresión de la evacuación natural" (Moffat, 1788). En 1765, Morgagni describió la presencia de coma en la cirrosis (Morgagni, 1765), la cual fue denominada encefalopatía portal sistémica (Sherlock y cols., 1954), y posteriormente recibiría el nombre de encefalopatía hepática (EH) (Fazekas y cols., 1957).

La EH es un síndrome neuropsiquiátrico y neurocognitivo potencialmente reversible y frecuente en los pacientes cirróticos (Kappus y Bajaj, 2012; Perazzo y cols., 2012), que se manifiesta a través de un amplio espectro de síntomas como son los cambios en la conciencia, la personalidad y anormalidades en el comportamiento donde se incluyen alteraciones en el ciclo del sueño, daños en las funciones cognitivas e intelectuales, así como trastornos en la actividad motora y la coordinación, pudiendo derivar a un coma profundo y la muerte (Felipo, 2013; Perazzo y cols., 2012).

Debido al amplio espectro de síntomas neurológicos, los cuales varían en severidad, la EH ha sido clasificada en base a sus síntomas clínicos (ver la Tabla 1) o su etiología. A nivel clínico, la forma de monitorizar el curso de la EH, así como el efecto de sus tratamientos, consiste en asignar cuatro grados a sus manifestaciones neurológicas, siendo a tal efecto, la escala de West Haven, también denominada puntuación de Conn, la que nos permite llevarlo a cabo mediante la asignación de valores del 0 al 4, donde las altas puntuaciones refieren una alteración severa (Bass y cols., 2010).

Definición Clínica	Definición Investigación	Nivel de Conciencia	Síntomas Neuropsiquiátricos	Síntomas Neurológicos
Encubierta	**Grado 0=EHM**	Normal	Daños sólo apreciables mediante test psicométricos	Ninguno
	Grado 1	Ligera lentitud mental	Eudisforia, irritabilidad y ansiedad, corta amplitud atencional	Deterioro de las habilidades motoras finas (daño en la escritura, temblor de dedos)
Abierta	**Grado 2**	Incremento de la fatiga, apatía o letargia	Desorden ligero de la personalidad, ligera desorientación respecto al tiempo y al espacio	Asterixis (o flapping tremor), ataxia, dificultad para hablar
	Grado 3	Somnolencia	Agresividad marcada desorientación del tiempo y el espacio	Rigidez, asterixis
	Grado 4	Coma	_____	Signos de incremento de la presión intracraneal

- **Tabla 1.** Clasificación semicuantitativa del estado mental en la EH utilizando el criterio de West Haven, modificado de Conn y Bircher (1993). El grado 0 se corresponde con la encefalopatía hepática mínima (EHM).

En referencia a su etiología, la working party de 1998 (Ferenci y cols., 2002; Rivera Ramos y Rodríguez Leal, 2011), así como su posterior reclasificación en 2009 por los miembros de la Sociedad Internacional para la Encefalopatía Hepática y el Metabolismo del Nitrógeno (ISHEN) (Bleibel y Al-Osaimi, 2013; Butterworth y cols., 2009) establecieron tres categorías: la EH **tipo A** típicamente asociada con un daño hepático agudo resultado de una severa inflamación y/o de una enfermedad

necrótica de evolución rápida, la **tipo B** resultado de una derivación portosistémica con ausencia de daño en el parénquima hepático, y la denominada **tipo C** que acompaña a un daño hepático crónico (cirrosis).

Atendiendo a estas clasificaciones es importante resaltar como la encefalopatía hepática mínima (EHM), previamente conocida como encefalopatía hepática subclínica o latente, se encuentra al principio del espectro de evolución de la EH (Zhan y Stremmel, 2012). Por tanto, la EHM se define como una EH carente de síntomas clínicos o neurológicos, pero con déficits en algunas áreas cognitivas que solamente se ponen de manifiesto mediante pruebas neuropsicométricas (Ferenci y cols., 2002). Siendo la atención, la percepción visuoespacial, la velocidad en el procesamiento de la información, especialmente en el área psicomotora, las habilidades motoras finas y la memoria a corto plazo (Weissenborn y cols., 2001) las áreas principalmente dañadas.

El reto que supone para la clínica el diagnóstico de los pacientes con EHM, junto con el interés creciente por el efectivo diagnóstico de la misma debido a su progresión hacia una EH abierta, así como su elevada incidencia, comprendida entre un 33-50% de los pacientes cirróticos (Felipo, 2013), convierten a la EHM en un serio problema sanitario, social y económico.

1.2 Modelos experimentales de la Encefalopatía Hepática

El desarrollo de un modelo de EH que guarde similitudes con los trastornos hepáticos en humanos es difícil de obtener. Esto es debido a que su etiología (alcohólica, vírica, tóxica, autoinmune, isquémica o genética) varía, así como también lo hacen los diferentes grados de derivación sistémica portal, el daño a órganos internos, y el hecho de que, en la mayoría de los casos, esté asociada con factores precipitantes como infecciones, hipoglucemias, uso de sedantes, etc. Por todo ello, no es posible reproducir todos los aspectos de la EH en modelos animales. Basándose en esto, los modelos actuales tratan de reproducir, de manera aislada, los síntomas de los distintos tipos de EH descritos en humanos (Butterworth y cols, 2009) (Ver Figura 1).

Siguiendo la clasificación propuesta por Butterworth y cols. (2009), el modelo animal de EH mejor caracterizado de fallo agudo hepático es el llamado tipo A, este modelo consta de dos variantes, una de ellas se basa en una anhepatectomía que puede llevarse a cabo bien por la devascularización hepática donde se mantiene el hígado pero se reconduce la circulación (anastomosis portocava), se interrumpe (ligación de la arteria hepática), o bien por la hepatectomía total, donde el hígado es extraído. La segunda de las variantes consiste en un modelo de toxicidad hepática para el que se emplean una gran variedad de sustancias hepatotóxicas como son la galactosamina, acetaminofeno, tioacetamida y azoxymetano. También se conocen otras sustancias potenciales como el fósforo, las nitrosaminas y el tetracloruro de carbono pero no están bien caracterizadas. Estas sustancias o son hepatotóxicas de manera directa, como la galactosamina, o se convierten en tales tras metabolizarse en el hígado. La patología causada por dichas sustancias varía, de ahí la heterogeneidad de los modelos potenciales para el estudio de diversos síntomas de la EH tipo A (Butterworth y cols, 2009).

Para el estudio de la EH tipo B, se ha propuesto un modelo basado en una derivación porto-sistémica. Esta anastomosis portocava ha sido empleada en ratas, conejos, perros y cerdos, siendo no sólo fácil de realizar, sino que, además, ha mostrado alteraciones tales como pérdidas de actividad, alteración de los ritmos circadianos, hiperamonemia y un incremento de la proporción amonio/glutamina cerebral (Butterworth y cols., 2009).

Otro de los modelos animales para el desarrollo de EH tipo B es la utilización de la triple ligadura de la vena porta (Aller y cols., 2005). Este modelo supone una modificación de la ligadura parcial de la vena porta, que conllevaba una rápida reversión de los síntomas circulatorios, al evitar la disminución del flujo sanguíneo, con la creación de un bypass. La realización de la triple ligadura aumenta el tramo estenosado de la vena porta con lo que impide la formación del bypass y reproduce los síntomas de la encefalopatía.

Desafortunadamente la EH tipo C carece de un modelo animal satisfactorio que se correlacione con el daño hepático causado por un estadío avanzado de alcoholismo, así como de la EH tipo C causada por una hepatitis vírica, siendo

ambas las etiologías más comunes encontradas en los pacientes que cursan con este síndrome (Butterworth y cols., 2009).

Por último, se han desarrollado modelos para estudiar los efectos del exceso de amonio *per se*, en ausencia de una disfunción hepática, sobre la función cerebral. Estos modelos consisten en alimentar a los animales con dietas ricas en amonio o ureasa (Butterworth y cols., 2009), creándose en dichos animales una hiperamonemia aguda o crónica que nos permite estudiar de manera aislada uno de los principales factores que contribuyen al desarrollo de la EH (Felipo y cols., 2012).

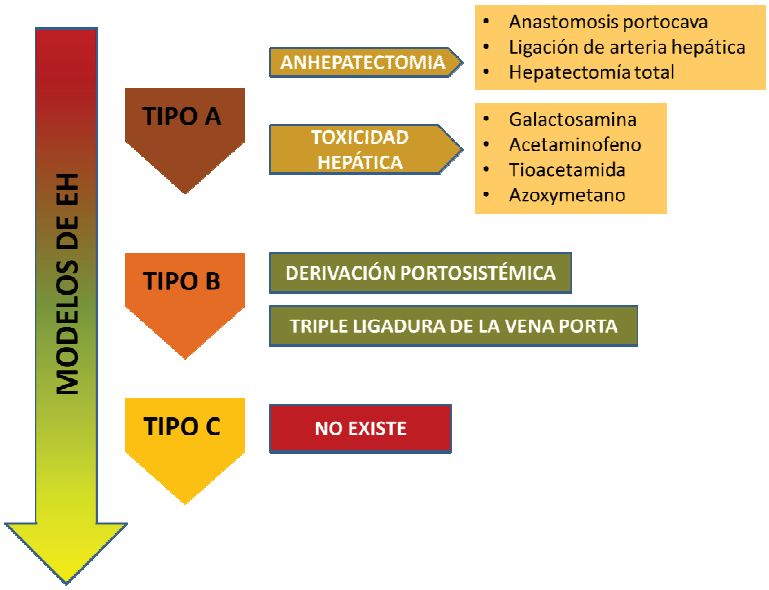

➢ **Figura 1.** Modelos experimentales actuales de la EH siguiendo la clasificación propuesta por Butterworth y cols. (2009).

1.3 Patogénesis de la Encefalopatía Hepática

1.3.1 Relación entre la Encefalopatía Hepática y la Hipertensión Portal

La hipertensión portal es un síndrome clínico común definido por la elevación de la presión venosa por encima de 5 mm Hg. La presión portal es causada por la combinación de dos procesos hemodinámicos simultáneos: el incremento de la resistencia intrahepática al paso del flujo sanguíneo a través del hígado debido a la cirrosis, y el incremento del flujo sanguíneo esplácnico secundario a la vasodilatación dentro del lecho esplácnico vascular (Al-Busafi y cols., 2012). Es

importante destacar la dificultad de su estudio de manera aislada debido a su asociación con mayores o menores grados de daño hepático. Sus signos clínicos más notables son la ascitis, la encefalopatía hepática o portosistémica y las varices esofágicas (Aller y cols., 2007).

El incremento de la presión de la vena porta, conocida como hipertensión portal, está relacionado con una obstrucción del flujo portal. Dependiendo del nivel al que tenga lugar la obstrucción, se clasificará como posthepática, intrahepática o prehepática. La hipertensión portal prehepática en humanos es causada por una obstrucción de la vena portal extra-hepática con la formación de circulación portosistémica y una función hepática normal, asociada a la denominada EH tipo B (Minguez y cols., 2006; Yadav y cols., 2010).

Ese aumento del flujo sanguíneo en el sistema venoso portal es estabilizado a través de una vasodilatación arteriolar esplácnica que produce la denominada "circulación esplácnica hiperdinámica" o "hiperemia esplácnica". Conjuntamente, y fruto de la reducción de la luz de la vena porta, se produce un aumento de la resistencia vascular al flujo sanguíneo que conlleva la creación de una circulación colateral portosistémica a nivel esplenorrenal y paraesofageal, bien por la apertura de vasos preexistentes o por la formación de nuevos vasos. Siendo por tanto la vasodilatación y la respuesta angiogénica los representantes de la **respuesta inflamatoria** que tiene un papel central en la progresión de la disfunción cerebral (Rolando y cols., 2000).

1.3.2 Relación entre la Encefalopatía Hepática y la Inflamación

Se ha visto una creciente evidencia tanto en modelos animales (Tanaka y cols., 2006; Marini y Broussard, 2006; Jover y cols., 2006; Cauli y cols., 2007; Wright y cols., 2007; Aller y cols., 2012), como en pacientes con cirrosis (Shawcross y cols., 2004; Shawcross y cols., 2007; Shawcross y cols., 2011; Montoliu y cols., 2011) sobre el papel de la inflamación en la exacerbación de las manifestaciones de la EH desde una EH mínima (encubierta) hasta abierta (grados 2-4), ya que se ha corroborado que la severidad del daño neurocognitivo correlaciona con marcadores

de inflamación (Tranah y cols., 2013). Dicha inflamación proviene de infecciones, sangrado gastrointestinal, obesidad y alteraciones en la flora intestinal, factores que confluyen en los pacientes con cirrosis.

Asimismo, la presencia de inflamación queda patente ante la respuesta por parte de las células cebadas, estratégicamente localizadas cerca de los vasos sanguíneos (Galli y cols., 2005), frente al estímulo mecánico que inicia la inflamación esplácnica en ratas con hipertensión portal prehepática (Aller y cols., 2007). Estas células tienen la habilidad de sintetizar y liberar mediadores de la respuesta inflamatoria (Galli y cols., 2005; Dawicki y Marshall, 2007) que alcanzan el sistema nervioso central. De hecho, fruto de dicha inflamación, a nivel molecular se describe un fenotipo de "tormenta citoquímica" caracterizado por un marcado incremento sistémico de citoquinas proinflamatorias como son el factor necrótico de tumores α (TNF-α) y las interleuquinas 1β, 6 y 12 (IL-1β, IL-6 e IL-12) (Tranah y cols., 2013). Dicha regulación al alza de factores como el TNF estimula las células gliales cerebrales en su secreción de Il-1 e IL-6 (Silen y cols., 1989). Por último, serán el TNF, la IL-1 y la IL-6 los que producirán un incremento de la permeabilidad de la barrera hematoencefálica (Didier y cols., 2003; de Vries, 1996). Además, el TNF incrementará la difusión del amonio al interior de los astrocitos (Duchini y cols., 1996). La combinación de todos estos eventos contribuirá a la inflamación crónica, así como a la patogénesis de la EHM.

1.3.3 Relación entre la Encefalopatía Hepática y el Amonio

Existe evidencia de la asociación entre el amonio y la EHM (Lockwood y cols., 1991a, 1991b), pero los mecanismos por los cuales el amonio causa la disfunción cerebral no están claros. De manera natural, el amonio circulante deriva del metabolismo de la glutamina en el epitelio intestinal, de la actividad ureasa en la flora intestinal y de la producción renal. Dicho amonio es excretado por los riñones, utilizado para la síntesis de glutamina en los músculos esqueléticos o para la síntesis de urea a nivel hepático, siendo este el más importante.

El ciclo de la urea regula la circulación sistémica del amonio sanguíneo en torno a valores de 50-100 μM. Durante el fallo hepático que acontece a la obstrucción de la circulación portal, se produce una situación de hiperamonemia, acumulándose altos niveles de amonio en el cerebro que alcanzan valores en torno a 1-5 mM.

El ciclo consiste en la captación de la glutamina por el intestino y los riñones donde es metabolizado por la glutaminasa a amonio. El amonio generado en el riñón es excretado en la orina o liberado a la vena renal. Tanto el amonio renal liberado a la circulación como el generado en el intestino es metabolizado en el hígado en los hepatocitos periportales para formar urea que posteriormente será excretada en la orina.

Ante la existencia del fallo hepático, la síntesis de urea se ve disminuida y el amonio procedente del intestino o los riñones se escapa de su transformación periportal a urea. Se sabe que cuando se incrementan las concentraciones de amonio periférico resulta tóxico para el cuerpo y debe ser retirado (Cooper y Plum, 1987; Zieve, 1987). Ese amonio es retirado de la circulación por los hepatocitos perivenosos portadores de la glutamina sintetasa formando glutamina. Esta glutamina es liberada de nuevo a la circulación sistémica con lo que será degradada por la glutaminasa intestinal y renal, convirtiéndose el riñón en el órgano central de la detoxificación del amonio (Olde Damink Steven y cols., 2009).

En pacientes con EHM se encontró un incremento en la expresión del gen que codifica la glutaminasa (Romero-Gómez y cols., 2004). Además, otros estudios mostraron incrementos en la expresión intestinal de glutaminasa en los enterocitos de ratas con derivación portocava (Romero-Gómez y cols., 2006). Ambos resultados ofrecen indicios de una mayor producción de amonio desde la flora intestinal en comparación con la habitual.

Sin embargo, la relevancia del aumento del amonio a nivel sistémico radica en su capacidad para afectar a la función del sistema nervioso central, en concreto a los astrocitos. Los astrocitos son un tipo de célula glial que, contrariamente a las neuronas u otras células gliales, son particularmente sensibles a los efectos del amonio; por ello son portadores de la enzima glutamina sintetasa, la cual puede

eliminar el amonio a través de la amidación del glutamato para formar glutamina. Eso permite al cerebro actuar como una vía alternativa de detoxificación del amonio durante una insuficiencia hepática (Coltart y cols., 2013). A pesar de esto, la acumulación de la glutamina resultante dentro de los astrocitos ejerce un estrés osmótico que conlleva el hinchazón de la célula (Norenberg, 1987) y ocasiona la alteración de la expresión de la proteína glial fibrilar ácida (GFAP) (Méndez y cols., 2008a). Dicho fenómeno del hinchazón astrocitario se ha demostrado tanto en el fallo hepático agudo (Blei y cols., 1994) como en el crónico (Häussinger y cols., 2000), siendo en este estadio cuando se habla de una astrocitosis Alzheimer tipo II debido a las características morfológicas de los astrocitos (Plum y Hindfelt, 1976).

Asimismo, la glutamina no actúa solamente como un osmolito. Gran parte de la glutamina sintetizada en los astrocitos es transportada desde el citoplasma a la mitocondria, donde es metabolizada por la glutaminasa activada por fosfato (PAG) produciendo amonio y glutamato. Esta generación del amonio por la PAG puede alcanzar niveles elevados, los cuales inducen una transición en la permeabilidad mitocondrial (mPT) en respuesta a un incremento en los niveles mitocondriales de Ca^{2+}. Esto conlleva un colapso del potencial de la membrana interna mitocondrial ocasionando el bombeo hacia el exterior de los protones de la cadena de transporte de electrones. La pérdida del potencial de membrana produce un hinchamiento de la matriz mitocondrial, movimiento de metabolitos a través de la membrana interna (por ejemplo, Ca^{2+}, Mg^{2+}, glutatión y NADPH), una fosforilación oxidativa defectuosa, un cese de la síntesis del ATP, así como la generación de especies reactivas de oxígeno (Rama Rao y Norenberg, 2012) que contribuyen a la mPT (Canevari y cols., 2004).

Al mismo tiempo, los astrocitos están implicados en la formación de la barrera hematoencefálica, por lo que una disfunción astrocitaria o la inflamación derivada de una activación astrocitaria, dado que los astrocitos son capaces de secretar citoquinas y factores neurotróficos, puede ocasionar daños en la integridad de dicha barrera (Coltart y cols., 2013). A este respecto, los estudios han demostrado que la barrera hematoencefálica permanece anatómicamente intacta en

la EH (Wright y cols., 2007), sin embargo, la tomografía de emisión de positrones (PET) sugiere un incremento de la permeabilidad de la misma al amonio (Lockwood y cols., 1991b).

Por último, también debemos resaltar el efecto que tiene el incremento del amonio a nivel metabólico. Un efecto tradicionalmente asociado con un metabolismo cerebral de la glucosa disminuido (Hazell y Butterworth, 1999). Sin embargo, estudios recientes han demostrado la falta de correlación entre cambios en el metabolismo de la glucosa y el grado de encefalopatía (Rama Rao y Norenberg, 2012). No obstante, se ha visto el papel del amonio en el incremento no sólo de los niveles de intermediarios glicolíticos, sino también de la actividad de numerosos enzimas glicolíticos (Ratnakumari y Murthy, 1992, 1993), lo cual ocasiona un aumento de la glicolisis que no va acompañada de un incremento del ciclo de los ácidos tricarboxílicos y subsecuentemente de la cadena de transporte de electrones. De hecho en modelos congénitos de ratones spf de hiperamonemia crónica se ha visto una progresiva inhibición de la actividad citocromo c-oxidasa (complejo IV de la cadena de transporte de electrones) (Rao y cols., 1997). Este incremento no tiene lugar debido a que el piruvato generado en la glicolisis se convierte a lactato en vez de continuar su natural paso por dicha cadena electrónica (Rama Rao y Norenberg, 2012). Dicho aumento en los niveles de lactato se ha relacionado con el desarrollo de edema cerebral y el incremento de la presión intracraneal (Toftengi y Larsen, 2004) (Ver Figura 2).

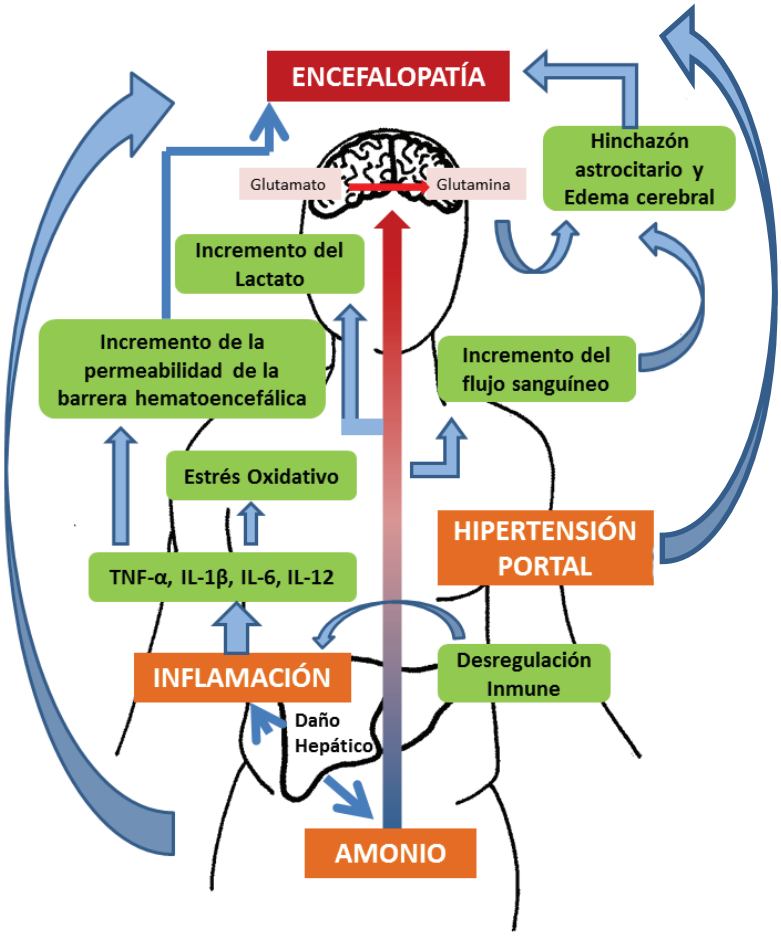

- **Figura 2.** Contribución del amonio y la inflamación en el desarrollo de la encefalopatía hepática, modificado de Coltart y cols. (2013).

1.4 Alteraciones Neurológicas de la Encefalopatía Hepática

Al diagnóstico de EH se llega tras la exclusión de otras disfunciones cerebrales u otras fuentes de encefalopatía. Más complicado resulta la determinación de la EHM dado que son ligeros cambios neurocognitivos en los ámbitos de la cognición y la atención los que se encuentran afectados, viéndose reflejados por déficits en la desinhibición, daños en la memoria de trabajo y en la coordinación visuomotora.

Estas alteraciones en la atención afectan a la habilidad del paciente para orientarse y realizar funciones ejecutivas, así como el aprendizaje y la memoria (Kappus y Bajaj, 2012). Aunque tradicionalmente han sido los tests neuropsicológicos y psicométricos los que nos han ayudado en su diagnóstico, en la

actualidad se han incorporado las pruebas de frecuencia crítica de parpadeo (Kircheis y cols., 2002) y los tiempos de reacción continuos (Lauridsen y cols., 2011) como pruebas diagnósticas.

Es lógico pensar que dichos déficits van acompañados de un gradual deterioro de la función cerebral. Se ha visto que la severidad de la EH se correlaciona con un enlentecimiento global de la actividad oscilatoria cerebral (Butz y cols., 2013). De hecho, los daños cognitivos detectados mediante tests neuropsiquiátricos en pacientes cuyo grado de afección de la EH varía de mínima a abierta, están acompañados de un enlentecimiento de las oscilaciones gamma corticales mientras realizan una tarea de atención bimodal (Kahlbrock y cols., 2012). Las interneuronas GABAérgicas corticales que contienen parvalbumina son las responsables de la generación de estas oscilaciones gamma (Sohal, 2012), por lo que es probable que el daño en la transmisión GABAérgica sea el responsable de estos déficits.

Asimismo, en la EH se produce una disminución en la conciencia que correlaciona con una disminución de la conectividad cortical antero-posterior medida mediante resonancia magnética funcional (Chen y cols., 2012a). Dicha alteración en la conectividad podría ser explicada tanto por una disminución en la transmisión glutamatérgica como por un incremento en el tono GABAérgico (Sergeeva, 2013).

No sólo estos síntomas de neurotransmisión se encuentran alterados en la EH. Debido a las alteraciones en la barrera hematoencefálica, numerosas moléculas son transportadas, entre ellos los aminoácidos de cadena ramificada y los aminoácidos aromáticos (Ciécko-Michalska y cols., 2012). El transporte de estos últimos afecta a la síntesis de catecolaminas (serotonina y dopamina) y produce "falsos neurotransmisores" (octopamina y feniletilamina) ocasionando daños en la neurotransmisión GABAérgica, serotoninérgica y glutamatérgica (Cauli y cols., 2009; Skowrońska y Albrecht, 2012).

No obstante, estas alteraciones en la comunicación neuronal también se han visto favorecidas por la acumulación de otras sustancias. En los pacientes cirróticos aumentan los niveles plasmáticos de manganeso, que en condiciones normales reciben una eliminación hepatobiliar. Debido al fallo hepático, este metal se acumula en el tejido cerebral. Consistentemente con esto, en los pacientes cirróticos

se han encontrado depósitos de manganeso en los ganglios basales (Pomier-Layrargues y cols., 1995; Spahr y cols., 2000) y en el globo pálido (Rivera-Mancía y cols., 2012). La peligrosidad de la acumulación del manganeso está relacionada con el papel que juega en la estimulación de la entrada del amonio en el cerebro, su participación en el sistema de señalización de neuroinflamación y el estrés oxidativo y nitrosativo (Butterworth, 2013), así como la estimulación que ejerce sobre la microglía para la generación de especies reactivas de oxígeno que podrían ser mediadoras en la pérdida de neuronas dopaminérgicas (Zhang y cols., 2010).

Por último, estudios recientes han encontrado acúmulos anormales de hierro en el cerebro de pacientes con EHM, sugiriendo que el metabolismo anormal del hierro puede subyacer a los daños neurocognitivos de los pacientes con EHM. Además, estos depósitos de hierro correlacionan con una disminución de la señal T2 que se observa en la resonancia magnética funcional en el circuito frontal-cortical-ganglios basales de dichos pacientes (Liu y cols., 2013).

Las alteraciones en la señalización de estos circuitos cerebrales, y sus correspondientes sistemas de neurotransmisión pueden explicar las dificultades en el aprendizaje de distintas tareas que muestran los distintos modelos de la EH, tales como el condicionamiento clásico (Aguilar y cols., 2000), la discriminación condicionada (Erceg y cols., 2005; Monfort y cols., 2007), la memoria de referencia (Arias y cols., 2012) y la memoria de trabajo (Méndez y cols., 2009a).

2. OBJETIVOS

La EH es una enfermedad común en los países occidentales (World Health Organization, 2003), a pesar de ello su etiología sigue entendiéndose como el resultado de numerosos procesos patológicos entre los que se encuentran el daño hepático, la inflamación y el amonio (Arias y cols., 2013). En este contexto la EHM se considera la etapa inicial del espectro de desórdenes neurocognitivos asociados con la EH, por tanto, la patogénesis de la EH abierta y la EHM podría ser similar (Kappus y Bajaj, 2012).

Sin embargo, a pesar de su importancia, pocos estudios se han llevado a cabo para evaluar las alteraciones de memoria de los pacientes con cirrosis que desarrollan EH, llegando algunos autores a afirmar que los daños en la memoria no son uno de los síntomas más importantes de la EH (Weissenborn, 2003). Asimismo, el tratamiento de los pacientes con EH no es uniforme y requiere del desarrollo de nuevas herramientas que permitan evaluar el deterioro cognitivo (Córdoba, 2011).

Es por ello que debido al continuo que supone la evolución de la EH, entender la fase incial conocida como EHM se hace necesario desde un punto de vista preventivo. Dentro de este marco conceptual, la presente tesis persiguió los siguientes objetivos:

1. Los principales desencadenantes de la EH son: el daño hepático, la hipertensión portal y la hiperamonemia. Nosotros pretendemos elucidar su contribución diferencial sobre el metabolismo oxidativo neuronal en el sistema límbico (artículo I).

2. Estudiar los déficits conductuales producidos en el estadio crónico de la EH, mediante un modelo de hiperamonemia, asociados con el funcionamiento de las redes cerebrales (artículos II).

3. Detectar si los cambios neurofisiológicos manifestados en el modelo crónico aparecen en su expresión leve en el modelo subclínico de la EH, como es la encefalopatía hepática mínima (artículos III, IV, V y VI).

4. Establecer los parámetros relacionados con la EHM a nivel de presión sanguínea, cambios morfométricos de los órganos, así como verificar la hipotética etiopatogenia inflamatoria de la EHM a través del estudio de algunos mediadores involucrados en la respuesta inflamatoria en las principales áreas cerebrales relacionadas con la memoria (artículo III, IV, V, VI).

5. Evaluar la existencia de déficits psicobiológicos tempranos tanto a nivel de la función cognitiva como de la función motora en el modelo de EHM mediante pruebas conductuales que nos permitan evaluar los cambios subclínicos en la EH (artículos III, IV, V y VI).

6. Destacar las principales estructuras cerebrales que se encuentran relacionadas con los déficits subclínicos y crónicos de la EH tanto a nivel metabólico, como de genes tempranos y morfometría celular (artículos I, II, III, IV, V y VI).

3. MATERIAL Y MÉTODOS

3.1 Animales

Todos los experimentos se han realizado empleando ratas (*Rattus norvegicus*) macho de la cepa Wistar (250-330 g) procedentes del bioterio de la Universidad de Oviedo. Los sujetos se seleccionaron de manera aleatoria de diferentes camadas y fueron alojados en grupos de 4-5 animales por jaula (38×55×20 cm) con acceso libre a comida y bebida. Asimismo, los animales se mantuvieron bajo un ciclo regular de luz/oscuridad de 12 horas (período de luz: 08:00-20:00h), siendo la temperatura ambiental de 23 ± 2ºC y una humedad relativa de 65 ± 5%. El uso y la manipulación de los animales se realizaron en todo momento de acuerdo con las Comunidades Europeas 2010/63/UE y legislados en nuestro país mediante el Real Decreto 53/2013.

Según el requerimiento de los experimentos realizados en cada artículo, los animales fueron divididos en varios grupos tal como se indica en la Tabla 2.

Grupos / Artículos	CO	PS	HP	CHA	HA	TAA
I			12		8	8
II				19	15	
III		12	12			
IV	10	18	16			
V		16	14			
VI		13	13			

- **Tabla 2.** Número de animales empleados. En las filas se representan los artículos y en las columnas se muestran los grupos utilizados. CO: control nado; PS: pseudo-operado; HP: hipertenso portal; CHA: control de hiperamonemia; HA: hiperamonemia; TAA: tioacetamida.

3.2 Producción de los modelos experimentales

Los modelos experimentales utilizados en los experimentos de cada uno de los artículos fueron realizados empleando los procedimientos que se describen brevemente a continuación:

Control nado (IV): Consistió en animales que fueron manipulados y se introdujeron en la piscina el mismo número de veces y días que los animales experimentales que adquirieron el aprendizaje, de forma que el tiempo de nado fuera equivalente. Los intervalos entre los ensayos y entre sesiones fueron los mismos que en el grupo experimental, aunque en este caso no se utilizó plataforma de escape. Este grupo se utilizó con el fin de controlar factores como el estrés, la manipulación o la actividad motora.

Hiperamonemia (I y II): El método utilizado para reproducir la hiperamonemia en nuestros animales fue el mismo realizado por Azorín y cols. (1989). Brevemente, los animales fueron alimentados con una dieta estándar suplementada con acetato de amonio (30 gramos por rata al día) durante un período de 27 días.

Control hiperamonemia (II): Los animales fueron alimentados con la dieta estándar sin suplementar, alojándose en las mismas condiciones que los animales hiperamonémicos y realizando las mismas tareas de aprendizaje.

Tioacetamida (I): El método empleado para la producción de daño hepático consistió en la administración semanal de pequeñas concentraciones de tioacetamida acordes con el peso corporal de los animales (Xiangnong y cols., 2002). Los animales recibieron concentraciones de tioacetamida (Sigma, Germany) diluidas en los biberones de agua durante un período total de 12 semanas. Se partía de una concentración inicial de tioacetamida al 0.03%, la cual se modificaba en base al incremento semanal del peso corporal de los animales. Para controlar el consumo de cada sujeto, los animales se mantuvieron en cajas individuales de Plexiglas transparente, disponiendo cada uno de su propio biberón que contenía 200 ml de dilución por semana. Cada semana se registraba tanto el peso corporal del animal como su consumo de líquido. En función del peso ganado por el animal se

elaboraban las nuevas concentraciones. En cualquier caso, se tenía presente que el peso del animal no debía verse incrementado en más de 20 g durante cada semana, y que el peso total alcanzado al final de esas 12 semanas no podía sobrepasar la ganancia de 60 g. Al finalizar las 12 semanas, los animales se agrupaban (4-5 por caja) con el fin de evitar la influencia causada por el aislamiento en los parámetros evaluados. A partir de ese momento, todos los animales recibieron una concentración estable de tioacetamida al 0.04%.

Modelos con intervención quirúrgica:

Para la obtención de los animales pseudo-operados e hipertensos es necesaria la realización de una intervención quirúrgica, por ello, se procedió a anestesiar a ambos grupos. La anestesia se realizó mediante inyección intraperitoneal donde se combinó ketamina (80mg/kg) y xilacina (12mg/kg). En relación al cuidado postquirúrgico, las ratas se mantuvieron cercanas a una fuente de calor hasta recuperar la conciencia (10-15 min) con el fin de impedir la hipotermia postoperatoria. Después, fueron alojadas en cajas de policarbonato individuales durante 15 días y posteriormente agrupadas en cajas de 6 animales hasta la evaluación del comportamiento. Los procedimientos quirúrgicos y los protocolos utilizados para cada modelo experimental se describen a continuación.

Pseudo-operado (III, IV, V y VI): Se realizó una laparotomía bilateral subcostal prolongada hasta la apófisis xifoidea, seguida de la disecación de la vena porta. El campo de operación fue irrigado con suero salino durante la intervención. Finalmente la laparotomía fue cerrada por una sutura continua en dos planos con seda 2/0. El período postoperatorio comenzó inmediatamente después de la intervención y se prolongó durante 45 días hasta la evaluación del comportamiento.

Hipertensión portal (I, III, IV, V y VI): Se colocó al animal en decúbito supino y se realizó una laparotomía media xifopubiana. El duodeno se movilizó y se extrayeron las asas intestinales, colocándolas hacia la izquierda del animal protegidas por una gasa humedecida en solución salina isotónica. Igualmente se desplazaron cranealmente los lóbulos superiores hepáticos protegiéndolos con algodón húmedo. Todo ello permitió una correcta exposición del hilio hepático.

Posteriormente, se realizó la disección hiliar para individualizar las estructuras vasculares y biliares. Se disecó la vena porta a lo largo de toda su longitud. Las tres ligaduras estenosantes se realizaron a nivel de la porción superior, medial e inferior de la vena porta respectivamente, y su posición se mantuvo por la situación previa de las ligaduras a una guía plástica con muestras equidistantes a 1.5 mm. Las tres ligaduras se anudaron secuencialmente alrededor de la vena porta (seda 4/0) y de una aguja 20 G con un diámetro externo 1.2 mm. Finalizado el anudamiento, se retiró la aguja quedando una estenosis triple de la vena porta de calibre conocido (1.2 mm).

Fue necesario comprobar que la guía se encuentra correctamente colocada no produciendo angulaciones ni rotaciones de la vena porta, así como verificar la inexistencia de congestión mesentérica la cual es indicativa de hipertensión portal y conlleva la muerte del animal en las primeras veinticuatro horas del postoperatorio.

Por último, se reintegraron las asas intestinales a la cavidad abdominal y se procedió a su cierre mediante un plano peritoneo- aponeurático- muscular con seda 2/0 y un plano cutáneo con seda 2/0.

Tanto en los animales pseudo-operados como en los hipertensos portales, el período postoperatorio empezó inmediatamente después de la intervención y acabó antes de la evaluación del comportamiento, habiendo transcurrido un período de 45 días.

3.3 Evaluación de los parámetros fisiológicos e inflamatorios relacionados con la Encefalopatía Hepática Mínima

La determinación de dichos parámetros (artículos III, IV, V y VI) se realizó empleando los métodos que se describen a continuación:

- Método para la medición de la presión portal: La presión portal se midió mediante una técnica indirecta de punción intraesplécnica, en la cual se inserta una aguja de diámetro 20 gauge en el parénquima esplénico, que a su vez está conectado a un registrador de presión (Powerlab 200 ML 201) y a un transductor de presión (Sensonor SN-844), ambos asociados a un programa de ordenador Chart V 4.0 (ADI

Instruments). El sistema de registro es calibrado antes de iniciar una nueva medición.

- Peso de los órganos: Debido a la relación existente entre el cambio en el volumen de los órganos y el desarrollo de la encefalopatía hepática, era necesario obtener el peso relativo del hígado, glándulas adrenales, riñones, bazo y testículos. Para ello, se realizó una extracción cautelosa con el fin de separar los órganos del tejido que los rodeaba, cometiendo de esta manera un error mínimo en la pesada de los mismos. El peso de los órganos se efectuó en una balanza de precisión (Mettler Toledo AB54-S), expresándose el peso de los órganos en relación al peso corporal del animal.

- Procesamiento del bazo para obtener células mononucleares: El bazo fue inmediatamente introducido en RPMI-1640 estéril (Sigma-Aldrich), y posteriormente se pasó a través de una malla de alambre con el fin de obtener suspensiones individuales. Las células resultantes fueron lavadas tres veces en un medio celular estéril y viable, y fueron contadas utilizando la técnica de exclusión del colorante azul de Trypan (0.5%v/v). La viabilidad fue siempre superior al 80%. Las células mononucleares fueron aisladas de la suspensión celular del bazo utilizando el centrifugador (400 g durante 30 min) Ficoll-Plaque ^{TM} PLUS (GE Healthcare Bio Sciences, Uppasala, Swedea) a temperatura ambiente. El gradiente de sedimentación establecido mediante la utilización del Ficoll-Plaque ^{TM} PLUS permite la sedimentación de los eritrocitos, los granulocitos y las células muertas que quedan por debajo, junto con las células mononucleares (linfocitos y monocitos) que se distinguen en la interfase entre el Ficoll-Plaque y el medio RPMI-1640. Las células recogidas en dicha interfase fueron lavadas tres veces, su viabilidad fue determinada de nuevo, y sus concentraciones se ajustaron a 2.5×10^{6} células/ml con RPMI-1640 suplementado con un 10% de suero fetal de ternero (Gibco, Life Technologies, MD, USA), 25 mM de HEPES, 2 mM de L-glutamina, 5×10^{-5} M de 2-mercaptoetanol (Sigma-Aldrich, Madrid, Spain) y 2 g/l de bicarbonato sódico (Sigma-Aldrich, Spain). Una vez que las células mononucleares fueron obtenidas, se prepararon los cultivos celulares para determinar la capacidad proliferativa in vitro de los linfocitos B y T.

- Determinación de la capacidad proliferativa de los linfocitos B y T: Sobre una placa Falcon plana de 96 pocillos (Becton-Dickinson, Meylan, France), 15 pocillos fueron sembrados por sujeto con 100 µl del medio en el cual se suspendieron las células obtenidas en el proceso de extracción. A continuación, 5 de esos pocillos fueron sembrados con 100 µl del medio RPMI-1640 suplementado con un 20% del suero fetal de ternero y 5 µl/ml de Concanavalin-A (Con-A, Sigma-Aldrich, Madrid, Spain), con el fin de estimular la proliferación de los linfocitos T. Finalmente, los otros 5 pocillos fueron sembrados con 100 µl del medio RPMI-1640 suplementado con un 20% del suero fetal de ternero y 1 mg/ml de lipopolisacáridos procedentes de *Salmonella* (LPS, Sigma-Aldrich, Madrid, Spain) con el fin de estimular la proliferación de los linfocitos B. Una vez sembrados, todas estas muestras fueron cultivadas durante 72 horas en un medio con 95% aire/5% CO_2 y una atmósfera humidificada en una incubadora (Jouan, Saint Herblain, Cedex, France) a 37 ºC. La proliferación celular fue determinada mediante el empleo del kit de proliferación colorimétrica celular II (XTT) siguiendo las instrucciones del fabricante (Roche, Mannheim, Germany) y las mediciones se realizaron con un lector de colorimetría Synergy HT (BioTek Instruments, INC, Winoosku, Ve, USA) utilizando un filtro de absorción de 450 nm. Los datos se expresaron como puntuaciones del índice de proliferación, siendo el índice de proliferación de los linfocitos T = densidad óptica (DO) de la media de los pocillos estimulados con ConA dividido entre la DO de la media de los pocillos sin ninguna estimulación mitogénica. Asimismo, el índice de proliferación de los linfocitos B = DO de la media de los pocillos estimulados con LPS fue dividida entre la DO de la media de los pocillos sin ninguna estimulación mitogénica.

- Medición de la expresión del ARNm mediante la PCR de Tiempo Real (RT-PCR): el tejido cerebral fue homogeneizado mediante la utilización de Trizol (Invitrogen, Madrid, Spain) y el ARN total fue aislado utilizando un método estándar de fenol, como es la extracción por cloroformo (Chomczynski y Sacchi, 1987). Se realizó un análisis espectrofotométrico, por luz ultravioleta de 450 nm, de los ácidos nucleicos con el fin de determinar las concentraciones, utilizando un radio de absorbancia de 260:280 para evaluar la pureza de los ácidos nucleicos. Las muestras fueron tratadas

con DNasas (DNase I, Invitrogen, Madrid, Spain) para eliminar la contaminación previa del ADN antes de llevar a cabo la síntesis de la cadena complementaria del ADN (ADNc). La cantidad total de ARN fue retranscrito a la inversa mediante el kit PrimeScript ™ RT (Takara Bio Inc., Madrid, Spain), obteniendo niveles de ADNc los cuales fueron cuantificados mediante la RT-PCR de tiempo real basada en SybrGreen (SYBR® Premix Ex Taq ™, Takara Bio Inc., Madrid, Spain). La formación de los productos de la PCR fueron monitorizados en tiempo real mediante los Applied BioSystems 7500 de la PCR de tiempo real. Las secuencias del ADNc se obtuvieron del GenBank en el Centro Nacional de Información Biotecnológica (NCBI; www.ncbi.nlm.nih.gov). Para conservar los genes se utilizó la gliceraldehido-6-fosfato dehidrogenasa (GAPDH). Las secuencias primarias fueron diseñadas mediante el software Prime Express v3.0 (Applied BioSystems). Los primers fueron obtenidos por Applied BioSystems (Madrid, Spain). La especificidad del primer fue verificada mediante curvas de análisis de derretimiento. La expresión relativa a los genes se determinó mediante el método $2^{-\Delta\Delta t}$ (Livak y Schmittgen, 2001).

Las secuencias utilizadas en la PCR fueron las siguientes (la dirección de la secuencia del primer es 5´….3´):

IL-1β, directo: CAACTGTCCCTGAACTAACTG

inverso: CTCATCTGGACAGCCAAGTC

IL-6, directo: CCACCAGGAACGAAAGTCAAC

inverso: CTTGCGGAGAGAAACTTCATAGC

TNF-α, directo: GCCACCGGCAAGGATTC

inverso: TCGACATTCCGGGATCCA

GAPDH, directo: GCTCTCTGCTCCTCCCTGTTC

inverso: GAGGCTGGCACTGCACAA

3.4 Examen neurológico

Todos los animales fueron manipulados y sometidos a observación neurológica, en el caso de los animales intervenidos quirúrgicamente la observación fue pre y postoperatoria, para descartar aquellos con algún déficit neurológico.

En el examen neurológico se evalúa el tono muscular mediante la abducción de las patas traseras, donde a mayor distancia entre las patas traseras, tras la caída desde una altura de 30 cm, puede indicar alteración; también mediante la capacidad de asimiento a un alambre.

Por otro lado se pone de manifiesto la ausencia de alteraciones en el equilibrio del animal mediante la respuesta geotáctica negativa, prueba en la que se sitúa al animal en posición descendente sobre un plataforma inclinada 30º por la que éste girará 180º para subir por ella, y se complementa con la evaluación de su capacidad para permanecer sobre una barra horizontal sin apoyo externo durante 3 minutos.

También se observan las respuestas sensoriomotoras a través del reflejo de flexión, pellizcando la pata para observar cómo la retira de manera inmediata, o igualmente colocándola en el extremo de una mesa dejando una de sus patas traseras fuera de la superficie, viendo como la retrae apoyándola sobre la mesa. Asimismo, se evalúa el reflejo de extensión de dos formas distintas, bien suspendiendo verticalmente al animal para observar cómo extiende sus patas hacia la superficie cercana para soportar su peso, o acercando la cabeza del animal a dicha superficie viendo la extensión que realiza de sus patas delanteras hacia la mesa.

También se evalúa la respuesta al tacto, donde el animal dirige su cabeza hacia el lugar donde se le aplica el estímulo, y la respuesta vestibular/auditiva donde se suelta al animal boca arriba desde una altura de 30 cm, y éste usará la cola para, durante la bajada, caer sobre sus cuatro patas; en esta prueba también se le somete a un estímulo sonoro fuerte (como un aplauso) reaccionando el animal con una extensión súbita de los miembros posteriores, flexión de los anteriores, arqueamiento del cuerpo, cierre de ojos y un movimiento de orejas hacia abajo.

También se valora la sacudida de la cabeza (head shaking) que consiste en aplicar un soplo de aire cerca de uno de los oídos para ver la respuesta de agitación brusca de la cabeza según el eje antero- posterior de su cuerpo. Por último, se observa el reflejo de enderezamiento donde se coloca a la rata boca arriba en una superficie plana aprisionando su cola y zona ventral para observar su inmediata tendencia a volver a colocarse sobre sus cuatro patas.

3.5 Evaluación de la actividad motora

Para evaluar dicha función se utiliza un aparato conocido como Rotarod (Acceder Rota-Rod, Ugo Basile Model, Jones y Roberts, para ratas 775a 63×50×49cm), mediante la utilización de este aparato podemos determinar la coordinación motora y la resistencia a la fatiga (Jones y Roberts, 1968). El aparato está formado por una barra horizontal a modo de rodillo dividido de manera equidistante por cinco discos opacos que nos permiten aislar entre sí a los cuatro animales que serán evaluados conjuntamente en cada prueba. Cada uno de los cuatro huecos o carriles consta de un contador digital de la ejecución, el cual es detenido al accionar el animal las almohadillas situadas debajo de cada carril.

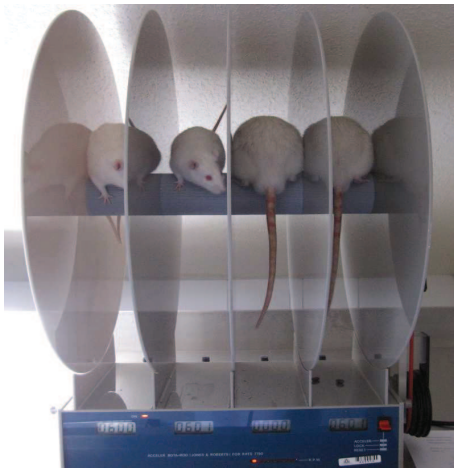

- **Figura 3:** Se ilustra el aparato Rota-Rod mientras un grupo de animales ejecutan la prueba colocados sobre el rodillo.

El procedimiento consta de dos partes, en la primera de ellas los animales se sitúan en el aparato y la velocidad de rotación del rodillo se mantiene constante a 2 rpm durante 60 s; en la segunda parte, la actividad de las ratas se evalúa durante 5

minutos en una sesión de velocidad acelerada donde la rotación se ve incrementada de manera constante hasta alcanzar las 20 rpm. Se registra el número de rpm alcanzadas por el rodillo en el momento de caída del animal, así como los segundos transcurridos.

3.6 Evaluación de la Memoria de Referencia Espacial

La memoria de referencia espacial fue evaluada en la piscina circular diseñada por Morris (Morris, 1984) conocida como el laberinto acuático de Morris (MWM, del inglés: Morris Water Maze). Dicho laberinto es una de las pruebas conductuales más utilizadas en la neurociencia para el estudio de los procesos psicológicos y los mecanismos neurales implicados en el aprendizaje espacial y la memoria. Esta memoria fue evaluada en los artículos I y III.

La piscina funciona como un campo abierto en el que las ratas se entrenan para escapar del agua mediante el nado hasta una plataforma oculta de reducidas dimensiones. El MWM es un tanque fabricado en fibra de vidrio y cuyas dimensiones son 150 cm de diámetro y unas paredes de 40 cm de altura. El nivel del agua alcanza 30 cm y su temperatura se mantiene en torno a 21±2ºC. La plataforma utilizada consiste en un cilindro de 10 cm de diámetro y 28 cm de altura sumergida 2 cm por debajo de la superficie del agua. El MWM se sitúa en el centro de una habitación de 16 m^2 (con dos lámparas halógenas de 4000 lx) rodeada de paneles negros donde se colocaron las pistas visuales. Estas pistas fueron amarillas, verdes y azules. Con el fin de facilitar los procedimientos de entrenamiento y análisis de los resultados se estableció una división imaginaria de la piscina en cuatro cuadrantes iguales (A, B, C, D). Toda la conducta se registró mediante una cámara de vídeo (Sony V88E) conectada a un ordenador con un sistema de análisis de imagen (Ethovision 3.1, Noldus Information Technology, Leesburg, VA).

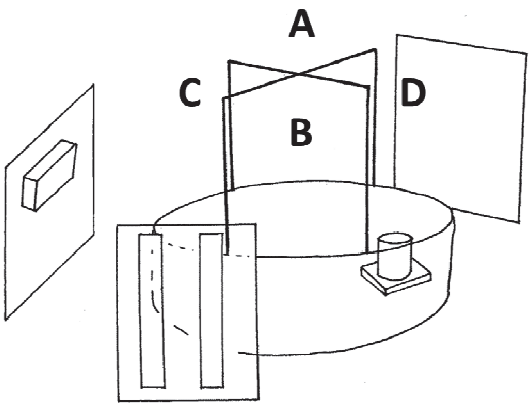

- **Figura 4:** Esquema del laberinto acuático de Morris donde se ilustra la localización de las pistas alocéntricas.

El protocolo de aprendizaje consistió en un primer día destinado a la habituación de los animales a la tarea, en ella los animales nadan durante cuatro ensayos manteniendo la plataforma visible en el centro de la piscina a 4 cm por encima de la superficie del agua. Durante los días siguientes, se realizaron cuatro ensayos cada día en los cuales la plataforma estuvo oculta, 2 cm por debajo del nivel del agua, localizada en el centro del cuadrante D a 30 cm de la pared de la piscina. Cada ensayo consistió en liberar al animal desde la pared de la piscina de cada cuadrante y dejar que nade hasta alcanzar la plataforma o hasta que hayan transcurrido 60 s. Si el animal no alcanzó la plataforma después de este tiempo, se le guio hasta la plataforma dejándole en esta durante 15 s. Durante el intervalo entre ensayos, los animales se alojaron en un recipiente negro opaco por un período de tiempo de 30 s. Tanto el tiempo como la distancia de nado fueron registradas. Diariamente, al final de la sesión, la plataforma fue retirada y la rata se introdujo en la piscina desde el cuadrante opuesto a la localización previa de la plataforma, dejando que el animal nade durante un período de 25 s. Inmediatamente después de esta prueba de recuerdo o transfer la plataforma fue colocada en su posición habitual y los animales fueron entrenados con un nuevo ensayo con el fin de evitar cualquier posible interferencia con la prueba o extinción del aprendizaje. Se registraron tanto las latencias durante la adquisición como el tiempo de permanencia en cada cuadrante en el ensayo de transfer.

3.7 Evaluación del Aprendizaje de Reversión

Dicho aprendizaje va siempre precedido de la evaluación de la memoria de referencia espacial, por tanto, es realizado utilizando el mismo paradigma experimental (laberinto acuático de Morris) y en las mismas condiciones experimentales. Este tipo de aprendizaje fue llevado a cabo en el artículo V.

Para llevarlo a cabo necesitamos que los animales hayan alcanzado el criterio de aprendizaje establecido para la memoria de referencia espacial. Tras esto, los animales fueron sometidos a un día más de aprendizaje en el que se le realizaron cuatro ensayos de adquisición, donde la plataforma fue colocada en el cuadrante opuesto a las localizaciones previas, en el cuadrante C (anteriormente la ubicación de dicha plataforma era el cuadrante D, ver figura 4). Por último, al igual que en la evaluación de la memoria de referencia espacial, los animales realizaron una prueba de recuerdo o transfer al final de la sesión de entrenamiento.

3.8 Evaluación de la Tarea Estímulo-Respuesta o Tarea de Hábitos

Esta tarea se realizó bajo las mismas condiciones ambientales y experimentales de luz, temperatura y registro del comportamiento que la evaluación de la memoria de referencia y el aprendizaje de reversión. Este aprendizaje está reflejado en el artículo VI.

En este aprendizaje las ratas fueron entrenadas durante una única sesión, de unos 10 minutos de duración de media. El criterio de aprendizaje fue establecido gracias a la ejecución previa de dicha tarea por los animales pseudo-operados, consistiendo dicho criterio en alcanzar una latencia de retención inferior a 8 segundos en los dos últimos ensayos; sabiendo que para alcanzar este criterio los animales no podrían destinar más de 10 ensayos.

En cada ensayo, se liberó al animal desde la pared de la piscina de cada cuadrante y se le permitió escapar a la plataforma visible con pistas. La plataforma visible de escape fue localizada en un cuadrante diferente en cada ensayo. Asimismo, un punto diferente de salida fue empleado en cada ensayo. Cada ensayo finalizó una vez que el animal encontró la plataforma o cuando transcurrieron 60 s

sin que el animal fuera capaz de alcanzar dicha plataforma. Si el animal no ha alcanzó la plataforma después de este tiempo, se le guio hasta la plataforma dejándole en esta durante 15 s. Durante el intervalo entre ensayos, los animales se alojaron en un recipiente negro opaco por un período de tiempo de 30 s. La latencia empleada en alcanzar la plataforma de escape fue registrada y utilizada como una medida de evaluación de la adquisición de la tarea.

3.9 Evaluación del Cambio de Estrategia

El propósito de dicho estudio fue evaluar las redes cerebrales que se encuentran implicadas en la codificación y el recuerdo de la información espacial requerida para efectuar cambios en la utilización de la estrategia de aprendizaje y, específicamente, determinar cómo difieren en su activación las distintas regiones cerebrales de la rata cuando el orden de administración de la tarea alocéntrica o de guía es cambiado. Durante la tarea alocéntrica, las ratas tuvieron que adquirir memorias a largo plazo acerca de la localización de la plataforma sumergida basándose en su orientación en relación con las posiciones de los estímulos distales colocados en la habitación experimental. En la tarea de guía, las ratas fueron entrenadas para localizar la plataforma basándose únicamente en un globo amarillo que fue situado 20 cm por encima de la plataforma. Esta versión de la tarea requiere de la ejecución de la misma respuesta (ir hacia la guía), en vez de nadar hacia el mismo lugar. El cambio de estrategia fue estudiado en los artículos II y IV.

Los animales fueron entrenados en un laberinto radial de agua (RAWM, del inglés: radial arm water maze) de fibra de vidrio negra (80 cm×12 cm), el cual fue situado 50 cm por encima del nivel del suelo. El laberinto tenía 4 brazos en forma de cruz disponibles para la entrada del animal. El nivel del agua alcanzó 30 cm y su temperatura se mantuvo en torno a 21±2ºC. La plataforma utilizada consistió en un cuadrado de 10 cm de diámetro y 24 cm de altura sumergido 2 cm por debajo de la superficie del agua. El RAWM se situó en el centro de una habitación de 16 m^2 (con dos lámparas halógenas de 4000 lx) rodeada de paneles negros donde se colocaron las pistas visuales. El comportamiento de los animales se registró mediante una cámara de vídeo (Sony V88E) conectada a un ordenador con un

sistema de análisis de imagen (Ethovision 3.1, Noldus Information Technology, Leesburg, VA).

El protocolo de aprendizaje consistió en 10 ensayos diarios durante 6 días, de los cuales los 3 primeros días fueron designados para la adquisición de una de las tareas y los 3 últimos para la adquisición de la otra tarea (por ejemplo, 3 días destinados para el aprendizaje alocéntrico, y los 3 siguientes se emplearon para el aprendizaje de la tarea de guía; otros animales realizaron el cambio de aprendizaje inverso comenzando por la tarea de guía). En cada ensayo, los animales fueron colocados en el centro de la piscina mirando hacia un brazo diferente cada vez, y se les permitió nadar hacia la plataforma de escape. Si el animal no ha alcanzó la plataforma después de este tiempo, se le guio hasta la plataforma dejándoles en esta durante 15 s. Durante el intervalo entre ensayos, los animales se alojaron en un recipiente negro opaco por un período de tiempo de 30 s. La plataforma permaneció en el mismo brazo a lo largo de los 10 ensayos diarios, pero su localización varió en cada día de entrenamiento.

Cada día al finalizar la sesión de 10 ensayos, se realizó una prueba de recuerdo o transfer donde la plataforma fue retirada y la rata se introdujo en la piscina durante un período de 25 s. Inmediatamente después de esta prueba la plataforma fue colocada en su posición habitual y los animales fueron entrenados con un nuevo ensayo con el fin de evitar cualquier posible interferencia con la prueba o extinción del aprendizaje.

Se estableció que un animal adquiría el criterio de aprendizaje cuando elegía el brazo correcto, donde se localizaba la plataforma de escape, en un 70% de los ensayos diarios.

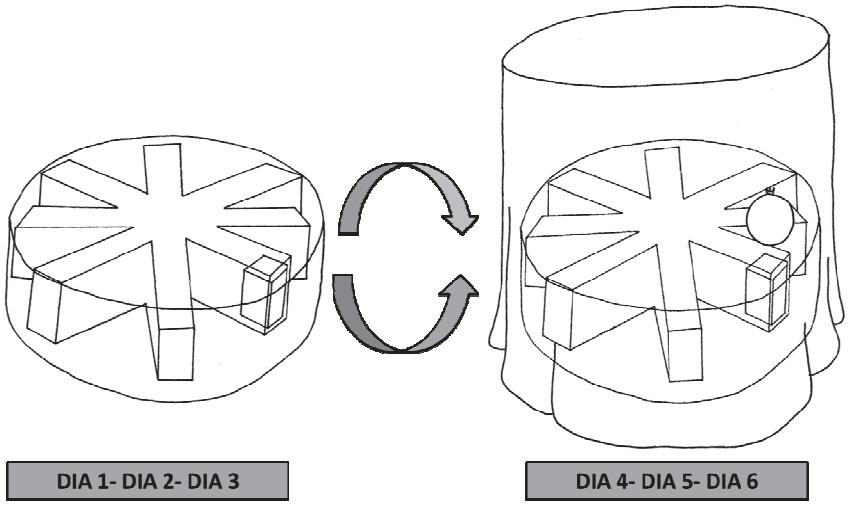

- **Figura 5.** Representación del protocolo de aprendizaje utilizado en la evaluación del cambio de estrategia en el que se indican las diferencias en la localización de los estímulos guía entre ambas estrategias de aprendizaje, alocéntrica y de guía.

3.10 Evaluación de la Tarea de Reconocimiento de Objeto-Lugar

La exploración de los objetos se evaluó en un campo abierto cuadrado (100×100×40 (altura) cm) de fibra de vidrio gris, situado en una habitación rectangular con numerosas pistas distales y una pista proximal, una pequeña etiqueta engomada localizada en la pared este del campo abierto. Dos luces blancas difusas, localizadas en lados opuestos de la habitación, proporcionaron una densidad de iluminación de 50 lux en el centro del campo abierto. Dos ventiladores produjeron un ruido de fondo en los lados este y oeste de la habitación. Una cámara de vídeo conectada a un ordenador con un sistema de análisis de imagen fue colocada encima del campo abierto para grabar tanto los ensayos de habituación, como la prueba. Después de cada ensayo, el campo abierto fue cuidadosamente limpiado con una solución de etanol al 75%. Cuatro objetos diferentes fueron construidos a partir de diferentes combinaciones de piezas de plástico, variando tanto el color como el tamaño desde 13×13×16 cm a 16×16×19 cm. Todos los objetos tuvieron suficiente peso para asegurar que las ratas no podían desplazarlos, asimismo, los objetos se contrabalancearon dentro de cada grupo experimental para evitar posibles efectos de preferencia. Igualmente, después de cada ensayo, los

objetos fueron cuidadosamente limpiados con una solución de etanol al 75% para eliminar pistas olfativas. Esta tarea fue la estudiada en el artículo V.

3.10.1 Habituación

Previamente a la fase de prueba, todos los animales fueron manipulados durante cuatro días consecutivos 10 minutos diarios, así como habituados al campo abierto vacío durante tres días consecutivos. En el primer día de habituación, grupos de tres a cinco ratas fueron colocados juntos en el campo abierto, permitiéndoles explorarlo durante 6 minutos en ausencia de objetos. Al día siguiente, las ratas exploraron durante 6 minutos el campo abierto pero de manera individual. En el tercer y último día de la habituación, las ratas recibieron 3 sesiones diarias de 6 minutos de duración, con 20 minutos de intervalo entre ensayo, con la presencia de dos objetos destinados únicamente para la habituación. Los objetos fueron colocados en paredes opuestas del campo abierto a una distancia de 10 cm de la pared. Durante estas sesiones, los animales fueron llevados individualmente a la habitación de la prueba y fueron colocados en el campo abierto mirando hacia una de las paredes donde no se encontraba ningún objeto.

3.10.2 Fase de prueba

En ella tiene lugar la evaluación del reconocimiento del objeto-lugar y consiste en 2 ensayos: un ensayo de muestra y un ensayo de prueba, ambos de 4 minutos de duración con un intervalo entre ensayos de 50 minutos. En el ensayo de muestra, se presentaron dos copias del mismo objeto. Sin embargo, en el ensayo de prueba, una de las dos copias fue localizada en la esquina opuesta del campo abierto. Esta tarea se utiliza para determinar si las ratas pueden detectar un desajuste entre la localización pasada y presente de un objeto familiar.

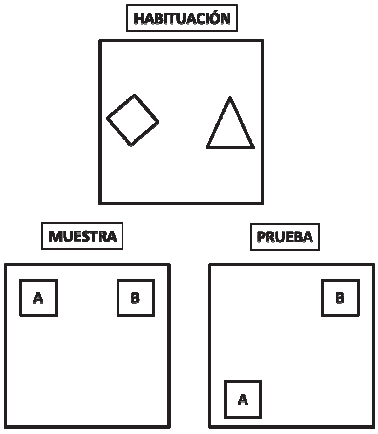

- **Figura 6.** Esquema de las tres fases de evaluación en la tarea de reconocimiento de objeto-lugar en la cual se aprecian las diferencias entre los objetos utilizados en la prueba de habituación respecto a las otras pruebas, así como la diferente ubicación de los objetos entre el ensayo de muestra y de prueba.

3.11 Procesamiento del tejido cerebral para citocromo c-oxidasa y c-Fos

Una vez finalizado el último día de aprendizaje, tal como se muestra en los artículos I, II, III, IV, V y VI, los animales fueron decapitados a los 90 minutos, siendo sus cerebros rápidamente extraídos y los encéfalos congelados por inmersión en isopentano a - 70º C, durante dos minutos, conservándoslos en un congelador a - 40º C para prevenir el deterioro del tejido con la consiguiente pérdida de actividad enzimática.

Posteriormente, los encéfalos fueron seccionados coronalmente mediante un microtomo criostático (Leica CM 1900, Alemania) en cortes de 30 µm de grosor que se colocaron en portaobjetos que previamente habían sido limpiados con alcohol de 100º. Para realizar un muestreo completo y sistemático de las distintas áreas cerebrales a estudiar, se seleccionaron las estructuras a analizar utilizando el atlas de Paxinos y Watson (1997). Las secciones se colocaron sobre un portaobjetos y se almacenaron a -40ºC. Posteriormente, se aplicaron las técnicas de tinción histoquímicas e inmunocitoquímicas que se detallan a continuación.

3.11.1 Histoquímica de la citocromo c-oxidasa

Esta técnica histoquímica consiste en el marcaje de la citocromo c-oxidasa, enzima presente en la membrana interna mitocondrial, que pertenece a la clase óxido-reductasa. Esta enzima cataliza el último paso en la cadena de transporte electrónico, en el proceso de fosforilación oxidativa, permitiendo la producción de

energía en forma de ATP. Esta tinción fue aplicada en los siguientes artículos: I, II, III, IV, VI.

El procedimiento seguido fue el descrito por Wong-Riley (1979) basándonos en ciertas modificaciones propuestas por González-Lima y Cada (1994). Con el fin de corregir las posibles variaciones de la tinción citocromo c-oxidasa en los distintos baños de incubación, se utilizaron una serie de secciones de diferentes grosores (10, 30, 40 y 60 μm) como estándares, obtenidas de homogeneizados cerebrales de rata. Este tejido homogeneizado se obtuvo de la decapitación y extracción de los cerebros de 12 ratas macho adultas Wistar, los cuales se sumergieron en tampón fosfato de pH 7,6 a 4ºC. Posteriormente, se realizó la homogeneización a 4º C y mediante espectrofotometría se determinó la actividad de la citocromo c-oxidasa (COx) del homogeneizado obtenido. Estos valores de actividad permiten realizar una curva de regresión lineal para convertir los valores de medida de densidad óptica de las estructuras seleccionadas en valores de actividad citocromo oxidasa. El homogeneizado cerebral, al igual que las secciones de cerebro de rata seleccionado, se congelaron con isopentano y se almacenaron a -40 ºC.

Para realizar la tinción se emplearon cubetas de 800 ml, en las que se introdujeron gradillas con una capacidad para 60 portaobjetos en las que se incluye el portaobjeto donde se colocaron las secciones del homogeneizado. Las secciones congeladas se introdujeron en una solución de tampón fosfato con sacarosa (pH 7.6; 0.1 M, 100g de sacarosa por litro de tampón) con glutaraldehido al 0.5% durante 5 min para favorecer la adhesión del tejido al portaobjetos. A continuación las secciones se lavaron en tres cambios de tampón fosfato con sacarosa durante 5 min antes de introducirlas 4 min en la solución TRIS, cuya composición para un litro es: 363 ml de agua bidestilada, 387 ml de ácido clorhídrico 0.1 N, 5 ml de dimetilsulfóxido (DMSO), 250 ml de trizma base, 100 g de sacarosa y 0.275 g de cloruro de cobalto. Se realiza un lavado en tampón fosfato (pH 7.6; 0.1 M) para posteriormente incubarlas en oscuridad durante una hora en la solución de tinción, en agitación lenta y a 37ºC. La composición de dicha solución es la siguiente: 800 ml de tampón fosfato 0.1 M, 0.06 g de citocromo c, 0.016 g de catalasa, 40 g de sacarosa, 2 ml de DMSO y 0.4 g de diaminobencidina (DAB). La DAB actúa como

un cromógeno, tras haber sido oxidada por la COx (endógena y exógena), se fija a la membrana mitocondrial. Esta solución de tinción se prepara en oscuridad ya que la presencia de luz podría dar lugar a una tinción inespecífica como consecuencia de la oxidación espontánea de la DAB.

Posteriormente, y a temperatura ambiente, se bloqueó la reacción con un baño de formol (Prolabo, España) tamponado al 10%, durante 30 min. Finalmente, el tejido se deshidrató mediante baños de cinco minutos en una cadena de alcoholes de concentración creciente (30%, 50%, 70%, 95%, 95%, 100%, 100%). Una vez deshidratado el tejido, las secciones se aclararon en un baño de xileno (Prolabo, Barcelona, España) durante 10 minutos, y posteriormente se realizó el montaje con Entellán (Merck, Darmstadt, Alemania), para la correcta conservación del tejido.

Análisis de imagen y transformación de la actividad enzimática

Mediante la utilización de un sistema de análisis de imágenes informatizado (MCID Elite Interfocus Linton, Inglaterra), se analizó y cuantificó la intensidad de la tinción COx mediante densitometría óptica.

Inicialmente, se realizaron las medidas densitométricas de los estándares que acompañan a cada baño de tinción para confeccionar la curva de regresión que va a permitir comparar las distintas series/ baños de tinción. A continuación, se seleccionaron las estructuras de interés con la ayuda del atlas de Paxinos y Watson (1997), para posteriormente iniciar la medición. Con el fin de evitar errores al delimitar la estructura, se tomaron pequeñas medidas dibujando con el ratón del ordenador cuadrados distribuidos de forma aleatoria dentro de la estructura. De cada estructura se realizan cuatro medidas en 3 secciones consecutivas.

3.11.2 Inmunocitoquímica de la c-Fos

Esta técnica de marcaje de la proteína c-Fos fue utilizada en el artículo V. Para llevarla a cabo, las secciones que estaban montadas en portaobjetos gelatinizados, recibieron una postfijación en paraformaldehido al 4% (0.1 M, pH 7.4) durante 30 min y fueron lavadas en tampón fosfato salino (0.01 M, pH 7.4). A continuación, fueron incubadas en peróxido de hidrógeno al 3% en tampón fosfato salino con el

fin de eliminar la actividad peroxidasa endógena. Tras ser lavadas en tampón fosfato salino, se introdujeron en una solución de tampón fosfato salino (solución de incubación) que contenía Tritón X-100 al 10% (Sigma, USA) y suero de albúmina bovino al 3% durante 30 minutos. Inmediatamente después, las secciones se incubaron en una cámara húmeda durante toda la noche a una temperatura de 4ºC con el anticuerpo primario policlonal de conejo anti-c-Fos (1:10.000) (Santa Cruz Biotech, sc-52, USA) diluido en tampón fosfato salino con Triton X-100 al 10%. Seguidamente, las secciones se lavaron en tampón fosfato salino y se incubaron con el anticuerpo secundario de cabra anti-conejo biotinilado IgG (1:200) (Pierce, USA) diluido en tampón fosfato salino con Triton X-100 durante 2 horas. Tras ser lavadas con tampón fosfato salino, las secciones fueron incubadas con el complejo avidina-biotina peroxidasa (Vectastain ABC Ultrasensitive Elite Kit, Pierce) durante 1 hora. Tras lavar las secciones en tampón fosfato salino, la reacción fue visualizada con una solución de diaminobencidina intensificada con níquel/cobalto (Pierce) durante 3 minutos. Tras visualizar la reacción, las secciones se lavaron en tampón fosfato salino y se procedió a la deshidratación, así como al posterior montaje para su visualización a microscopía óptica.

Estimación numérica de las neuronas inmunoreactivas a la c-Fos

Brevemente, la cuantificación se realizó por muestreo de dos secciones por animal separadas una distancia de 30 μm, habiendo sido el área de interés previamente delimitada. Sobre las secciones se superpusieron disectores de conteo con un área conocida y diseñados específicamente para cada núcleo. En base a estos disectores se realizó el conteo utilizando un microscopio (Olympus BH-2, Japón) acoplado a una cámara (Sony XC-77, Japón) y a una pantalla de televisión (300x aumentos totales). El criterio para discriminar las neuronas inmunoreactivas a la c-Fos fue la existencia de puntos de color gris-negro homogéneo con unos bordes bien delimitados. Finalmente, para cada sujeto y región, se calculó la media del conteo realizado sobre las dos secciones.

3.12 Procesamiento del tejido cerebral para GFAP-IR y volumen nuclear

Tal como se detalla en el artículo VI, los animales fueron anestesiados con pentobarbital sódico (100mg/Kg) (Sigma, USA). A continuación, se les perfundió intracardiacamente con un tampón fosfato salino al 0.9% (0.1 M, pH 7.4), seguido de paraformaldehído al 4% en tampón fosfato (0.1 M, pH 7.4). Los cerebros fueron extraídos e introducidos en parafina. Posteriormente, se realizaron cortes sistemáticos con la ayuda de un micrótomo (Leica, Germany) de 30 μm de grosor a intervalos conocidos desde el principio hasta el final del cerebro.

3.12.1 Inmunohistoquímica de la proteína glial fibrilar ácida (GFAP)

Brevemente, la técnica consiste en un lavado previo de las secciones para llevar a cabo el desparafinado en tampón salino Tris con Triton X-100 al 0.1%, bloqueándolos posteriormente con suero humano. Después, las secciones fueron incubadas durante un día con anticuerpo primario policlonal de conejo anti-GFAP (1:800) diluido en albúmina bovina. Al dia siguiente, después de lavarlas las secciones en tampón fosfato salino con Triton X-100, se incubaron en anticuerpo secundario de cabra anti-conejo biotinilado IgG (1:30) (Pierce, USA) diluido en albúmina bovina. El tratamiento posterior es el mismo seguido para la inmunocitoquímica de la c-Fos, siendo las secciones incubadas con el complejo avidina-biotina peroxidasa (Vectastain ABC Ultrasensitive Elite Kit, Pierce) y visualizándose la reacción con una solución de diaminobencidina intensificada con níquel/cobalto (Pierce).

Cuantificación de la GFAP

El proceso completo de la cuantificación del número de proteína glial fibrilar ácida de los astrocitos inmunoreactivos (GFAP-IR) fue llevado a cabo mediante un microscopio óptico acoplado a Leica LAS Live Image Builder (Leica, Microsystems). Para estimar la densidad de GFAP-IR se utilizaron tres secciones equidistantes en las estructuras seleccionadas para cada animal. La cuantificación fue realizada situando 4 regiones de conteo equidistantes en la imagen de la pantalla (tamaño del marco 0.150 mm×0.150 mm). Solamente fueron cuantificados

los cuerpos celulares dentro de cada cuadrante o disector centrado en la sección de interés. El grosor total medido en cada sección fue de 30 µm, descontando 5 µm de grosor por encima y por debajo del eje Z para evitar posibles sobreestimaciones.

3.12.2 Cálculo del volumen nuclear neuronal mediante cuantificación en violeta de cresilo

La tinción en violeta de cresilo conlleva un desparafinado del tejido y posterior hidratación de las secciones en violeta de cresilo al 0.5% en H_2O (Sigma, USA) durante 3 minutos. A continuación, las secciones son lavadas con H_2O, deshidratadas y montadas en portaobjetos para su posterior visualización.

Cuantificación del volumen nuclear neuronal

El volumen nuclear neuronal fue cuantificado con el sistema CAST2 (Olympus, Denmark) en un microscopio Olympus-BX61. En nuestro estudio sólo fue cuantificado el lado derecho de cada estructura cerebral. Las imágenes de las células sobre las que se realizó la cuantificación fueron tomadas por un objetivo ×100. El criterio utilizado para identificar las neuronas y las células de glía fue morfológico. Las neuronas muestran un nucleolo claramente definido, la presencia de eucromatina en el núcleo y un citoplasma visible rodeando dicho núcleo, mientras que las células de glía muestran heterocromatina en el núcleo, ausencia de nucleolo y de citoplasma.

El método elegido para comparar el volumen nuclear neuronal en las diferentes estructuras cerebrales entre animales pseudo-operados e hipertensos fue el Nucleador (Méndez y cols., 2008a). La prueba del Nucleador se lleva a cabo marcando un único punto dentro del núcleo neuronal, el nucléolo. El sistema, sucesivamente crea 6 líneas de intersección con el punto marcado por nosotros. A continuación, nosotros marcamos la intersección de cada una de esas 6 líneas con la membrana nuclear de nuestra neurona objeto de estudio. Sólo se cuantificaron los núcleos celulares definidos dentro de la zona del disector (1141 μm^2). Se muestrearon cuatro secciones por cada animal y los núcleos fueron muestreados a

una distancia constante y conocida entre ellos de 30 µm. En cada sección se realizaron 25 medidas celulares, obteniendo un total de 100 neuronas muestreadas.

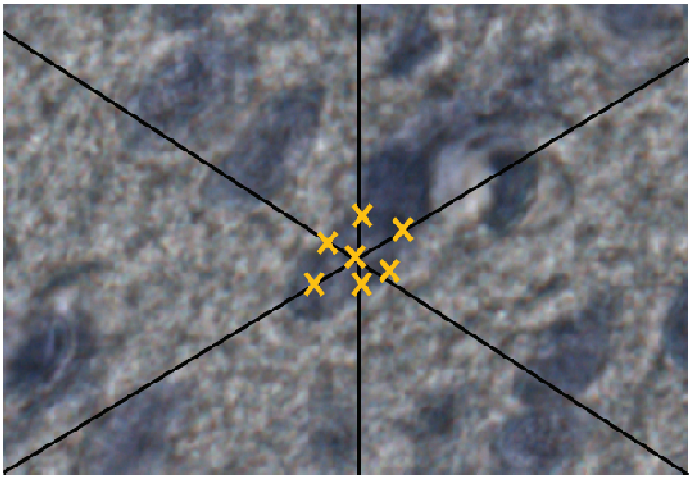

- **Figura 7.** Muestra las intersecciones de las seis líneas generadas por el Nucleador con la membrana nuclear neuronal objeto de estudio.

3.13 Análisis estadísticos

Todos los datos obtenidos se analizaron estadísticamente utilizando el programa SigmaStat 3.2 (Systat, Richmond, EEUU) y el SAS 9.3 (SAS Institute, 2011), representándose gráficamente por medio del programa SigmaPlot 8.0 (Systat, Richmond, EEUU), empleando la media y el error estándar de la media para dichos cálculos. Los resultados se consideraron estadísticamente significativos cuando $p \leq 0.05$. A continuación, se describen brevemente los análisis realizados con los diferentes datos obtenidos.

3.13.1 Evaluación de los parámetros fisiológicos e inflamatorios

Los datos cuantitativos referentes a la presión portal (artículos III, IV, V y VI), el peso de los órganos y las determinaciones fisiológicas como son el factor necrótico de tumores α, las interleuquinas 1β, 6 y la proliferación de células T y B (artículo VI), fueron comparados entre los dos grupos empleados mediante la prueba *t* de Student para muestras independientes.

3.13.2 Análisis de los procedimientos conductuales

Los datos obtenidos en la evaluación de la función motora en el Rota Rod, como son el tiempo sobre el rodillo y la velocidad de rotación en la que se produjo la caída (artículos II y III) fueron analizados mediante una prueba de *t* de Student para muestras independientes.

Los datos obtenidos en la prueba de memoria de referencia espacial y el aprendizaje de reversión (artículos III y V) fueron analizados como se describe a continuación. La velocidad de nado y la distancia recorrida se compararon entre los grupos experimentales como medida directa de la ejecución motora mediante un ANOVA de dos factores de medidas repetidas con los días como factor de medidas repetidas y el grupo como factor entre sujetos. Las variables dependientes registradas fueron las latencias de escape, cuya media fue calculada individualmente para cada uno de los días de registro, así como el tiempo de permanencia en cada uno de los cuatro cuadrantes durante la prueba de recuerdo o transfer. Las latencias de escape fueron comparadas mediante un ANOVA de dos factores de medidas repetidas, en donde el factor de medidas repetidas fue las distintas sesiones, y el factor entre sujetos fue la variable grupo. Cuando el factor sesión resultó significativo, se realizó un ANOVA de medidas repetidas para comparar las sesiones de cada grupo de forma independiente. El tiempo de permanencia en cada cuadrante durante la prueba de recuerdo o transfer fue analizado separadamente para cada grupo y día mediante un ANOVA unifactorial, siendo el factor cuadrante la variable independiente. Las comparaciones a posteriori realizadas en cada caso fueron la prueba de Tukey para pares de medias (artículo V) y el método Holm-Sidak (artículo III). Además, en el caso de que la normalidad o la igualdad de varianzas no se cumplieran, se llevó a cabo un test no paramétrico como es la *U* de Mann-Whitney para muestras independientes (artículo III y V).

Los datos registrados en la prueba de estímulo-respuesta o tarea de hábitos (artículo VI) fueron las latencias de escape. Se calculó la media para los ensayos realizados en el día de prueba que fueron comparados mediante un ANOVA unifactorial, donde el factor latencia fue la variable independiente. Cuando se

encontró un efecto significativo de la variable, se realizaron comparaciones a posteriori mediante la prueba Tukey para pares de medias. Asimismo, se compararon la velocidad de nado y la distancia recorrida entre los grupos experimentales mediante un ANOVA unifactorial.

Los análisis realizados para la comprensión de la tarea de cambio de estrategia discernieron en función del grado de patología a analizar, hiperamonemia o hipertensión portal, dado que en función de su afectación se requirieron análisis más o menos sensibles.

Cuando se analizó el cambio de estrategia en los animales hiperamonémicos (artículo II), se registró como medida de análisis el número de veces que escogían el brazo correcto, y se analizó mediante un ANOVA de dos factores de medidas repetidas, en donde el factor de medidas repetidas fue las distintas sesiones, y el factor entre sujetos fue la variable grupo. El análisis a posteriori realizado fue la prueba Tukey para pares de medias.

Para el análisis del cambio de estrategia en los animales hipertensos (artículo VI) se utilizó un diseño de ensayo controlado aleatorio longitudinal. El uso de este tipo de análisis se debe a que en estudios previos (Vallejo y cols., 2011) se ha mostrado como los modelos de efectos mixtos basados en la probabilidad suponen marcos analíticos generales apropiados para determinar si hay perfiles de respuesta diferentes a lo largo del tiempo entre grupos de animales distintos. Además, se llevó a cabo un análisis del modelo de efectos mixtos de medidas repetidas (MMRM), el cual incluye un modelado estructurado del tiempo y una estructura de correlación de errores entre sujetos. En la versión del MMRM que llevamos a cabo, el tiempo fue considerado como una clasificación en vez de una variable continua. Tras el rechazo de la hipótesis general, determinamos los contrastes entre las poblaciones en las cuales las medias no eran iguales a cero. Para controlar la tasa de error familiar (FWE) para todas las posibles comparaciones por pares, se utilizó un Hochberg (1988) que pasó la desigualdad de Bonferroni y fue realizado mediante la declaración ESTIMATE en el SAS PROC MIXED y la opción HOC en el SAS

PROC MULTTEST. El conjunto de datos fue analizado utilizando MMRM con la estimación REML.

El análisis de los datos obtenidos en la tarea de reconocimiento Objeto-Lugar (artículo V) se realizó tal como se describe a continuación. La exploración de un objeto fue definida como: dirigir la nariz hacia el objeto a una distancia menor de 2 cm, así como una exploración activa del mismo. Sentarse o dar la vuelta alrededor del objeto no fueron considerados comportamientos exploratorios. Para cada rata, el tiempo destinado en la exploración de los objetos en ambas sesiones de exploración, así como en la sesión de prueba, fueron cuantificados mediante cronómetros. Estas medidas fueron recogidas para examinar tanto la exploración como la discriminación. La proporción de exploración en las fases de muestra y de prueba fue considerada como e1 y e2 respectivamente, y fueron calculadas dividiendo la exploración de todos los objetos en cada fase entre el tiempo total disponible para la exploración. Para el cálculo de la discriminación se tomaron dos medidas: el índice de discriminación (d1) y el radio de discriminación (d2) (Ennaceur y Delacour, 1988). El índice de discriminación, d1, se basa en la diferencia en el tiempo empleado en explorar los dos objetos en la fase de prueba, el objeto que ha cambiado de posición menos el objeto que permanece en la misma posición. El radio de discriminación, d2, también se calculó en la fase de prueba. En este caso, consiste en la diferencia del tiempo de exploración en los dos objetos dividido por el tiempo total de exploración de los objetos, esto es, d1/tiempo empleado en explorar ambos objetos. La exploración en la fase de muestra y la de prueba (e1 y e2) fueron comparadas con una *t* de Student para muestras relacionadas. Además, también se utilizó la *t* de Student para comparar d1 y d2, con el fin de determinar si sus medias diferían del cero, puntuación que indica la igualdad de exploración de los dos objetos, indicando que las ratas han discriminado satisfactoriamente entre los dos objetos.

3.13.3 Análisis de la actividad citocromo c-oxidasa

Para comparar los valores de actividad citocromo c-oxidasa se utilizaron la prueba *t* de Student para muestras independientes (artículos II, III y VI) y el

ANOVA unifactorial (artículo I), dependiendo la elección de la prueba del número de grupos estudiados en cada caso.

En cuanto al artículo III, resultaba especialmente interesante el análisis de la conectividad funcional de las distintas estructuras cerebrales implicadas en dicho aprendizaje. Por ello, se utilizó la correlación de Pearson entre las regiones de cada grupo experimental. Previamente los valores de la actividad CO se normalizaron dividiendo la actividad obtenida en cada región cerebral entre la media de la actividad CO de todas las regiones en cada animal, de esta manera se reducen las variaciones en la actividad CO que no fueron consecuencia del aprendizaje. A continuación, para evitar errores debidos a tamaños de muestra muy pequeños, se empleó el método "Jackknife" (Shao y Tu, 1995). Este procedimiento consiste en calcular todas las posibles correlaciones que resultan de eliminar un sujeto cada vez teniendo en consideración únicamente las correlaciones que sean significativas a lo largo de todas las combinaciones.

Sin embargo, y a pesar de la validez de los datos obtenidos con las correlaciones de Pearson, quisimos afinar aún más en el análisis de las redes neuronales. Es por ello, que en el artículo IV llevamos a cabo un análisis de los componentes principales (PCA). En primer lugar se realiza el test de esfericidad de Barlett para confirmar la existencia de relaciones entre las variables, así como también se lleva a cabo el test Kaiser-Meyer-Olkin (KMO) para evaluar la medida en que las puntuaciones de la variable podrían predecirse a partir de las puntuaciones de las demás (Ferrando y Anguiano-Carrasco, 2010). El segundo paso fue determinar el número de componentes (redes). Por último, se realizó una rotación oblimin no ortogonal, siendo las puntuaciones para cada uno de los componentes analizadas por separado mediante ANOVAs con componentes entre sujetos (tres niveles).

3.13.4 Inmunoreactividad c-Fos, GFAP y análisis del volumen nuclear

Los datos obtenidos mediante la cuantificación del número de neuronas inmunoreactivas c-Fos (artículo V), la cuantificación del número de astrocitos inmunoreactivos GFAP y el volumen de los núcleos neuronales (artículo VI), fueron comparados mediante una prueba *t* de Student para muestras independientes.

Las comparaciones a posteriori se realizaron empleando una prueba de Tukey. Por último, en el caso de que la normalidad o la igualdad de varianzas no se cumplieran, se llevó a cabo un test no paramétrico como es la *U* de Mann-Whitney para muestras independientes.

4. RESULTADOS

Los principales resultados obtenidos en los diferentes experimentos realizados se describen brevemente en este apartado.

4.1 Evaluación de los parámetros fisiológicos e inflamatorios

En primer lugar, los resultados indican que los animales que han sido sometidos a la cirugía de la triple ligadura estenosante de la vena porta muestran un incremento en los valores de presión portal en comparación con los animales que han sido pseudo-operados (artículos III, IV, V y VI).

En cuanto al peso corporal, no se han encontrado diferencias significativas entre los animales hipertensos y pseudo-operados. Sin embargo, el peso relativo de sus órganos indica un aumento en las glándulas adrenales en el grupo hipertenso en relación al pseudo-operado ($p=0.006$). Asimismo, se observó esplenomegalia causada por la hipertensión portal ($p=0.038$) (artículo VI).

Por último, las determinaciones fisiológicas en tejido cerebral mostraron un incremento en la presencia de TNF-α ($p=0.024$) en el estriado de los animales hipertensos en relación con los pseudo-operados. No se encontraron diferencias significativas entre los grupos en regiones cerebrales como la corteza prefrontal, el hipocampo y la amígdala para el TNF-α, las interleuquinas 1β y 6, así como diferencias en la proliferación de células T y B medidas a una longitud de onda de 450 nm (artículo VI).

4.2 Tareas conductuales

4.2.1 Función Motora

Los resultados de la evaluación de la función motora en el Rota Rod (artículo II y III) indican que tanto la hiperamonemia como la hipertensión portal no afectan a la función motora. Los animales hiperamonémicos y los hipertensos no se diferencian de sus controles en el tiempo de permanencia sobre el rodillo a velocidad acelerada. Asimismo, tampoco existen diferencias en las revoluciones por minuto alcanzadas. Consecuentemente, los diferentes grupos experimentales muestran una coordinación motora similar a la de sus controles.

4.2.2 Memoria de Referencia Espacial

Los resultados obtenidos en la prueba de memoria de referencia espacial (artículo III) muestran ausencia de diferencias entre los grupos hipertenso y pseudo-operado tanto en la velocidad como en la distancia recorrida durante el proceso de aprendizaje a lo largo de los días. Igualmente, no se encontraron diferencias en las latencias de escape hacia la plataforma sumergida. Ambos grupos muestran una disminución de las latencias de escape con el entrenamiento espacial ($p<0.05$). Sin embargo, aunque la memoria de referencia no esté dañada en los hipertensos, este grupo muestra un retraso de un día en la adquisición de la tarea ($p=0.007$).

4.2.3 Aprendizaje de Reversión

Los resultados obtenidos en la prueba de reversión (artículo V) indican que no hay diferencias entre los grupos, hipertenso y pseudo-operado en las latencias de escape para alcanzar la plataforma sumergida durante los ensayos de adquisición en la prueba de reversión ($p=0.837$). Sin embargo, los grupos difieren en el tiempo de permanencia en los cuadrantes durante la prueba de recuerdo o transfer. El grupo pseudo-operado prefiere la nueva localización de la plataforma (cuadrante C) frente a los demás cuadrantes ($p<0.001$). Por el contrario, el grupo hipertenso prefiere el cuadrante D, es decir que son incapaces de recordar el lugar en el que se encontraba la plataforma de escape, ya que no cumplen el criterio de aprendizaje, permanencia

de un tiempo significativamente mayor en el cuadrante reforzado con respecto al resto de cuadrantes de la piscina, en ninguno de los días de entrenamiento.

4.2.4 Estímulo-Respuesta o Tarea de Hábitos

Los resultados obtenidos en la prueba estímulo-respuesta o tarea de hábitos (artículo VI) reflejan que el modelo animal de encefalopatía hepática mínima presenta un deterioro en la capacidad para localizar eficazmente una plataforma de escape visible a lo largo de un entrenamiento masivo de 10 ensayos en un día, como reflejan las diferencias en la ejecución con respecto a sus animales controles, pseudo-operados, los cuales son capaces de dirigirse hacia la plataforma que cambia de lugar en cada uno de los ensayos. Por tanto, se encuentran diferencias en las latencias de escape entre los grupos hipertenso y peudo-operado ($p=0.016$), donde el grupo hipertenso no muestra una disminución en las latencias de escape durante los ensayos ($p=0.313$) en comparación con la reducción presentada por el grupo pseudo-operado a partir del segundo ensayo ($p=0.034$). Finalmente, no existieron diferencias en cuanto a la velocidad y la distancia recorrida entre los grupos experimentales.

4.2.5 Cambio de Estrategia

Hiperamonemia

Los resultados obtenidos en la prueba de cambio de estrategia (artículo II) mostraron que los animales hiperamonémicos no alcanzaron el criterio de aprendizaje, donde los animales debían de escoger el brazo correcto en 7 de los 12 ensayos presentados. Consecuentemente, se encontraron diferencias significativas entre los grupos (control e hiperamonemia) que realizaron la tarea de guía a lo largo de los días de aprendizaje ($p<0.001$). Además, se observaron incrementos significativos en las latencias de escape entre los días 1 y 3 en el grupo control que realizó el aprendizaje guía ($p=0.024$). En los demás grupos experimentales no se encontraron diferencias a lo largo de los días de entrenamiento.

Hipertensión Portal

El análisis MMRM (artículo IV) reveló diferencias estadísticamente significativas entre los grupos hipertenso y pseudo-operado ($p=0.029$) durante la realización de la tarea a lo largo de los días de aprendizaje. Interesantemente, no se encontraron diferencias significativas entre los grupos a comparar a lo largo del tiempo, esto es debido a que a pesar de que la realización de la tarea cambió a lo largo del tiempo, este cambio se produjo de manera similar en todos los grupos de aprendizaje.

Cuando se procedió a contrastar los grupos experimentales entre sí, se encontraron diferencias significativas entre el grupo pseudo-operado A-C (cambio de estrategia en la dirección de tarea alocéntrica a tarea de guía) y el grupo hipertenso C-A (cambio de estrategia en la dirección de tarea de guía a tarea alocéntrica) ($p=0.015$).

Por último, los análisis intragrupo que se llevaron a cabo, seguidos de las comparaciones post hoc por pares de Hochberg, mostraron un incremento significativo de las latencias en el grupo HP A-C entre el dia 1 y todos los demás días de aprendizaje, así como entre el día 2 y el día 6, diferencias en el grupo PS A-C entre el dia 6 y los días 1 y 2, diferencias estadísticamente significativas en el grupo HP C-A entre los días 5 y 6 respecto de los días 1 y 2, y finalmente, también se hallaron diferencias en el grupo PS C-A entre todos los días de aprendizaje frente a los días 1 y 2.

4.2.6 Reconocimiento de Objeto-Lugar

Los resultados obtenidos en la prueba de reconocimiento de Objeto-Lugar indican la presencia de una alteración en la tarea por parte de los animales hipertensos, mostrando la incapacidad de dichos animales para realizar juicios acerca de si el estímulo se ha encontrado anteriormente en la misma localización. Los animales pseudo-operados son capaces de discriminar entre el objeto que ha permanecido en la posición constante, y aquel que se ha movido de lugar. Sin embargo, los animales hipertensos son incapaces de realizar dicha distinción. Este

comportamiento se ve reflejado en las diferencias significativas encontradas entre los grupos hipertenso y pseudo-operado en los índices d1 ($p=0.004$) y d2 ($p=0.005$), es importante destacar que dichas diferencias no vienen provocadas por una ausencia en la exploración por parte de los animales hipertensos, ya que los índices de exploración e1 ($p=0.569$) y e2 ($p=0.298$) no mostraron diferencias estadísticamente significativas.

4.3 Actividad Metabólica

4.3.1 Comparación de los tres modelos de Encefalopatía Hepática (artículo I)

El análisis de la cuantificación densitométrica de la actividad citocromo c-oxidasa cerebral (COx) reveló diferencias significativas entre los tres grupos experimentales, siendo mayor la actividad metabólica entre el grupo hiperamonemia seguido del grupo hipertensión portal y tioacetamida en la corteza prelímbica ($p<0.001$), la corteza infralímbica ($p<0.001$) y la subregión CA3 del hipocampo dorsal ($p<0.001$). Además, se encontró una mayor actividad COx en el grupo HA, seguido del grupo TAA y del grupo HP en el estriado ventral ($p<0.01$), tanto en la corteza del accumbens como en el núcleo, el tálamo anterodorsal ($p<0.001$) y el giro dentado ($p<0.01$). Asimismo, sólo se encontraron diferencias entre el grupo HA y el resto de los grupos experimentales en el tálamo anteroventral ($p<0.05$), el tálamo mediodorsal ($p<0.001$) y la subregión CA1 del hipocampo dorsal ($p<0.001$), siendo en todos los casos el grupo HA el que mostró una actividad metabólica significativamente elevada con respecto a los grupos HP y TAA. Finalmente, no se encontraron diferencias entre los grupos experimentales en ninguno de los núcleos mamilares estudiados, como son el mamilar medial medial, el mamilar medial lateral y el mamilar lateral.

4.3.2 Memoria de Referencia Espacial (artículo III)

El estudio de la actividad citocromo c-oxidasa mostró una menor actividad COx en el grupo HP en comparación con el grupo PS en las subregiones del hipocampo dorsal CA3 ($p=0.039$) y giro dentado ($p=0.018$), en los núcleos amigdalinos, entre los que se encuentran, el núcleo basolateral ($p=0.045$), el núcleo lateral ($p=0.045$),

el núcleo central (p=0.029) y el núcleo medial (p=0.013). No encontrándose diferencias entre los grupos en la corteza prefrontal, la cual incluye la corteza prelímbica, infralímbica y la corteza cingulada.

A continuación, estudiamos las correlaciones interregionales entre los grupos experimentales en base a su actividad COx. Se encontraron correlaciones interregionales significativas en ambos grupos. En el caso del grupo PS, se halló una alta correlación entre la amígdala medial y la subregión CA3 del hipocampo dorsal, así como entre las subregiones CA3 y CA1, y la subregión CA1 y la amígdala central (p<0.005). En referencia al grupo HP, se establecieron dos circuitos independientes; el primero de ellos comprende la corteza cingulada que correlaciona con la amígdala central, la cual se relaciona con la corteza infralímbica, y ésta a su vez con la corteza prelímbica, el segundo circuito muestra una alta correlación entre las subregiones del hipocampo dorsal CA3 y CA1, la cual correlaciona con la amígdala lateral, que a su vez se relaciona con la amígdala medial (p<0.015).

4.3.3 Estímulo-Respuesta o Tarea de Hábitos (artículo VI)

La medida de la actividad metabólica cerebral se mostró significativamente reducida en los animales HP en comparación con los animales PS en el núcleo del accumbens (p=0.024), el giro dentado dorsal (p=0.046) y en núcleos amigdalinos como el basolateral (p=0.017), lateral (p=0.014) y el central (p=0.007). No se encontraron diferencias entre los grupos en la corteza prefrontal, el tálamo, el estriado dorsal, la corteza del núcleo accumbens, la corteza parietal, las subregiones del hipocampo dorsal CA1 y CA3, la amígdala medial, el hipocampo ventral, las cortezas perirrinal y entorrinal, así como en los núcleos de los cuerpos mamilares.

4.3.4 Cambio de Estrategia en el modelo de Hipertensión Portal (artículo IV)

Los cambios obtenidos en los valores COx inducidos por el aprendizaje de ambas tareas (alocéntrica y de guía) se estudiaron mediante el análisis de los componentes principales, el cual nos permite establecer posibles grupos funcionales entre las regiones cerebrales analizadas.

En referencia a la tarea de guía (se corresponde con los grupo que efectuaron el cambio A-C), el componente 1, el cual juega un papel principal en el aprendizaje de la tarea, incluye a la corteza prefrontal, la corteza parietal, el estriado dorsal y ventral, encontrándose únicamente diferencias para las puntuaciones de este componente entre el control puro respecto de los grupos HP y PS ($p<0.001$).

Los componentes principales 2, 3 y 4 incluyen un número más limitado de regiones cerebrales. El componente 2 solamente incluye los cuerpos mamilares y la amígdala basolateral. El componente 3, incluye los núcleos amigdalinos basolateral y central, y el componente 4 incluye el hipocampo. No se encontraron diferencias entre los grupos en ninguno de estos componentes.

En referencia a la tarea alocéntrica (grupos que efectuaron el cambio de estrategia C-A), el componente principal 1 incluyó 7 regiones cerebrales con una alta carga de componente (>0.7). La carga del componente indica hasta qué punto cada estructura se encuentra relacionada con cada componente. De esta manera, una mayor carga de componente indica mayor importancia de la estructura asociada y, por tanto, menor error de influencia. La carga en el componente 1 es alta para la corteza parietal, el estriado dorsal y ventral, el giro dentado y la amígdala basolateral y central, encontrándose diferencias entre el control puro y el grupo PS ($p<0.05$). En el componente 2 sólo el mamilar medial mostró una carga positiva fuerte sin encontrarse diferencias entre los grupos. Por último, el componente 3 incluyó la corteza prefrontal, el estriado dorsal y ventral y el giro dentado, hallándose diferencias entre el grupo control y los demás grupos experimentales ($p<0.05$). Estos resultados mostraron que algunas áreas como el estriado dorsal, ventral y el giro dentado, pueden presentarse tanto en el componente 1 como en el 3, sugiriendo que estas regiones podrían ser parte de ambos circuitos y, probablemente podrían dichos circuitos interaccionar durante el proceso de aprendizaje.

4.3.5 Cambio de Estrategia en el modelo de Hiperamonemia (artículo II)

Los resultados de la cuantificación histoquímica de la COx revelaron que los animales HA entrenados en la tarea alocéntrica, mostraban mayor actividad COx en

el tálamo anterodorsal (p=0.01) que sus controles en dicha tarea. Igualmente, se encontró una mayor actividad metabólica en los animales HA que realizaron la tarea de guía en las cortezas prelímbica (p=0.048), infralímbica (p=0.044), parietal (p=0.001), entorrinal (p=0.002) y perirrinal (p=0.002) en comparación con el grupo CO. Además, este mismo patrón de actividad se encontró entre los grupos en el estriado dorsal lateral (p=0.038), el estriado dorsal medial (p=0.05), la subregión del hipocampo ventral CA1 (p=0.01), y los núcleos amigdalinos basolateral (p=0.005) y central (p=0.005). Finalmente, no se encontraron diferencias significativas en la parte dorsal del estriado dorsal, en el estriado ventral, el tálamo, el hipocampo dorsal, la amígdala lateral y medial, así como la subregión del hipocampo ventral CA3 y el giro dentado.

4.4 Inmunoreactividad c-Fos en el Aprendizaje de Reversión y el Reconocimiento de Objetos-Lugar (artículo V)

Los resultados hallados en el análisis de la cuantificación del número de neuronas con marcaje c-Fos en la tarea de reversión revelan que los animales con hipertensión presentan menor número de células con marcaje c-Fos que el grupo pseudo-operado en las regiones de la corteza cingulada (p=0.026), prelímbica (p=0.015), infralímbica (p=0.008), CA1 septal (p=0.004), CA3 septal (p<0.001) y giro dentado septal (p<0.001).

El patrón opuesto de células con marcaje c-Fos, siendo mayor el marcaje en los hipertensos, se encuentra entre los grupos experimentales entrenados en el reconocimiento de Objetos-Lugar, concretamente en las regiones CA1 dorsal (p=0.045), CA3 dorsal (p=0.035) y la corteza entorrinal (p=0.012). No se encontraron diferencias entre los grupos hipertenso y pseudo-operado en la corteza prefrontal (prelímbica, infralímbica y cingulada), el giro dentado dorsal y la corteza perirrinal.

4.5 Inmunoreactividad GFAP (artículo VI)

Se encontraron diferencias en el número de los astrocitos GFAP inmunoreactivos entre los grupos HP y PS en el estriado dorsal, tanto en la zona

dorsal (p=0.002) como en la zona medial (p=0.002), siendo el número de astrocitos inmunoreactivos mayor en el grupo PS que en el grupo HP.

4.6 Volumen Neuronal Nuclear (artículo VI)

Se hallaron diferencias estadísticamente significativas entre los grupos HP y PS en cuanto al volumen neuronal nuclear, siendo mayor dicho volumen en los animales PS en comparación con los HP en el estriado dorsal, el cual se subdivide en la zona dorsal (p=0.027), la zona medial (p=0.012) y la zona lateral (p=0.019). El patrón opuesto se observa en el estriado ventral, donde el mayor volumen núclear lo presentan los animales HP en comparación con los PS en el núcleo (p=0.015) y la corteza (p=0.004) del accumbens.

5. DISCUSIÓN

Encefalopatía hepática (EH) es el término utilizado para describir una seria complicación neuropsiquiátrica y neurocognitiva ocasionada por un daño hepático agudo o crónico (Kappus y Bajaj, 2012). Sin embargo, en la actualidad se ha visto que la EH no es un síndrome único (Felipo, 2013), interviniendo en su patogénesis tanto la hipertensión portal como el incremento del amonio sistémico y cerebral.

Numerosos son los estudios que revelan una disminución de la tasa metabólica cerebral de la glucosa en los pacientes con EH, sugiriendo que el hipometabolismo contribuye a los síntomas neuropsiquiátricos que se observan comúnmente en la EH. Asimismo, se encontraron disminuciones en el metabolismo cerebral del oxígeno y en el flujo sanguíneo (Dam y cols., 2013) de dichos pacientes, revelando la resonancia magnética funcional una relación entre los déficits cognitivos y una aberrante actividad cerebral basal (Chen y cols., 2012b). Sin embargo, la existencia de una contribución diferencial de estos factores, hipertensión portal, hiperamonemia y daño hepático no había sido explorada. Por tanto, nuestro primer objetivo consistió en estudiar cómo dichos factores afectaban al metabolismo oxidativo de las regiones cerebrales implicadas en los procesos de aprendizaje y memoria.

Los animales con hipertensión portal vieron reducida su actividad metabólica en la corteza prefrontal, el estriado ventral, los núcleos talámicos y el hipocampo, siendo comparable dicho patrón al de sujetos con ausencia de patología. Esta similitud puede explicarse por el desarrollo de colaterales portosistémicas, consecuencia del incremento de presión que tiene lugar en la vena porta, las cuales aminoran el incremento de la resistencia (Miñano y Garcia-Tsao, 2010; Méndez-López y cols., 2007).

La situación opuesta es la observada en los animales hiperamonémicos, donde las demandas energéticas se ven incrementadas por encima de los niveles convencionales en todas las estructuras cerebrales. Este incremento en la utilización de oxígeno podría ser debido a un proceso inflamatorio en dichas áreas cerebrales (Arias y cols., 2006) dado que la inflamación incrementaría el uso del oxígeno produciendo un exceso de especies reactivas de oxígeno y nitrógeno, las cuales causarían el estrés oxidativo y nitrosativo (Norenberg, 2003; Nathan, 2003).

Asimismo, el amonio, una vez atravesada la barrera hematoencefálica, podría disminuir el metabolismo oxidativo debido a la inhibición de enzimas tales como la piruvato deshidrogenesa y el α-cetoglutarato (Bjerring y cols., 2009). Además, numerosos neurotransmisores como el GABA, dopamina, serotonina y glutamato pueden verse alterados por un exceso de amonio. En concreto, la neurotransmisión glutamatérgica se ve comprometida por el daño que ocasiona el amonio en la inducción de los receptores NMDA, los cuales alteran la vía glutamato-óxido nítrico-GMP, que está involucrada en el aprendizaje y la memoria (Aguilar y cols., 2000; Erceg y cols., 2005).

Por otra parte, durante el fallo hepático, modelo de tioacetamida, también se produce un incremento de los niveles de amonio en el cerebro (Keiding y cols., 2006), los cuales pueden provocar un alteración en la utilización de la glucosa similar a la encontrada en los modelos de hiperamonemia (Rama Rao y Norenberg, 2012). Pero, mientras que los pacientes con cirrosis hepática tienen mecanismos compensatorios que previenen de la ocurrencia del edema cerebral y de la hipertensión intracraneal (Jover y cols., 2005), fruto del carácter osmolítico de la

glutamina derivada del amonio, el cerebro hiperamonémico es incapaz de establecer estos mecanismos.

Estos resultados muestran que las alteraciones en la actividad metabólica cerebral no se desarrollan por igual en los tres modelos experimentales, daño hepático, hiperamonemia e hipertensión portal. La mayor alteración se encuentra en el modelo que simula la intoxicación por amonio, en el cual las estructuras cerebrales deben realizar un gran esfuerzo metabólico en comparación con los otros dos modelos experimentales.

A la luz de los resultados obtenidos, y debido al continuo que representa la progresión de la EH, nos pareció interesante abordar el estudio tanto del estadio crónico de la enfermedad como del estadio temprano utilizando como modelos experimentales aquellos que se identifican con los principales factores que contribuyen a la EH, como son la hiperamonemia y la hipertensión portal. Esto no sólo arrojará luz sobre los déficits tempranos que se encuentran en la EH, con su potencial carácter preventivo, sino que nos permitirá establecer la progresión desde los estadios tempranos a crónicos de este síndrome.

El amonio es uno de los factores etiológicos de la EH, así como de otras condiciones hiperamonémicas como errores innatos en el ciclo de la urea, el síndrome de Reye, la toxicidad por valproato (Rao y Norenberg, 2001) y la hiperamonemia idiopática (Butterworth, 1991). Así pues, la hiperamonemia se considera uno de los factores más importantes en las alteraciones neurológicas encontradas en el daño hepático agudo y crónico (Wang y Saab, 2003).

Para discernir la contribución del exceso de amonio en las alteraciones neurológicas de la EH, desarrollamos un modelo de hiperamonemia crónica con ausencia de daño hepático. Asimismo, nos propusimos estudiar hasta qué punto el amonio cerebral afectaba al aprendizaje mediante el desarrollo de dos protocolos que pusieran de manifiesto el empleo de dos estrategias de aprendizaje diferentes, la alocéntrica y la de guía. El primer protocolo define la relación entre la meta y otra localización, siendo la meta independiente del sujeto (estrategia alocéntrica). El

segundo protocolo define la relación entre la meta y la aproximación a ésta a través de una pista distintiva (estrategia de guía) (de Bruin y cols., 2001).

Los resultados conductuales mostraron la incapacidad de los animales hiperamonémicos de alcanzar el criterio de aprendizaje en ambas tareas. A su vez, esto fue reflejado por las diferencias en la actividad metabólica cerebral encontradas en las estructuras límbicas implicadas en estos procesos de aprendizaje.

Como era de esperar, en base a los resultados obtenidos previamente (Arias y cols., 2013), las estructuras cerebrales estudiadas en los animales hiperamonémicos incrementaron sus demandas energéticas en un intento por alcanzar dicho criterio. Además, el nivel de dificultad de ambas tareas era diferente, tal como reveló la ejecución de dichas tareas por parte de los controles. Mientras que durante la realización de la tarea de guía se vio una mejora a lo largo de los días, en la tarea alocéntrica no se observó este patrón, dado que la tarea fue realizada sin dificultad desde el primer día del aprendizaje. Esta dificultad diferencial podría explicar el incremento de la actividad metabólica del tálamo, estructura requerida al inicio de la adquisición de una tarea de aprendizaje espacial (Conejo y cols., 2010), en los animales hiperamonémicos que realizan la tarea alocéntrica. Mientras que en los animales hiperamonémicos que realizan la tarea de guía se ve aumentada la actividad metabólica en aquellas regiones cerebrales que se requieren en diferentes momentos del proceso de aprendizaje.

El estudio de la EHM se llevó a cabo mediante un modelo de triple ligadura estenosante de la vena porta en un estadio de evolución temprana de cuarenta y cinco días en cuyo transcurso se desarrolla la hipertensión portal. La hipertensión portal es una complicación común de la cirrosis, la cual se asocia con diferentes riesgos entre los que se incluyen, sangrado intestinal, ascitis y EH (Carey, 2011).

En primer lugar, evaluamos el modelo de EHM mediante la medida de la hipertensión portal, el peso de los órganos así como su actividad motora. Se encontraron diferencias en la presión portal entre los grupos hipertenso y pseudo-operado. Además, la presión portal fue confirmada por la presencia de esplenomegalia (Aller y cols., 2005b), así como por la insuficiencia adrenal, la cual

es común en paciente con cirrosis y sepsis severa. Sin embargo, nosotros encontramos esta deficiencia en estadios tempranos de la EH, lo cual podría ayudar a reformular una definición fisiopatológica de la EHM.

La evaluación de la actividad motora se llevó a cabo mediante el Rota Rod y no reveló alteraciones en los animales hipertensos. Nuestro grupo experimental mostró una coordinación motora balanceada y un desplazamiento similar en velocidad y distancia en comparación con los animales pseudo-operados, lo cual está en concordancia con lo obtenido por otros autores (Méndez y cols., 2008b). Por tanto, los déficits motores no podrán explicar las diferencias halladas en la realización de los distintos aprendizajes por parte de los animales con EHM.

Comenzamos evaluando la memoria de referencia espacial en los animales con EHM. Aunque ambos grupos experimentales, hipertensos y pseudo-operados, alcanzaron el criterio de aprendizaje, el grupo hipertenso tiende a realizar peor la tarea en comparación con el grupo pseudo-operado. De hecho, se encontró un retraso de un día en la reducción de las latencias de escape hacia la plataforma escondida durante el proceso de aprendizaje. Este dato podría indicar una deficiencia de los animales hipertensos en la memoria a corto plazo en relación con la memoria a largo plazo espacial. Numerosos estudios con diferentes modelos experimentales de EH confirmaron que la memoria de trabajo espacial está dañada en animales cirróticos por administración de tioacetamida (Méndez y cols., 2009a). Además, estudios que evaluaron la respuesta de evitación revelaron que tanto los animales con tioacetamida, como con shunt portocava tuvieron déficits en su adquisición (Méndez y cols., 2009b). Todos estos datos nos permitieron establecer la hipótesis de que una exposición masiva a la adquisición de una tarea, como es el caso de los cinco días de duración de la memoria de referencia, es probablemente la causa de la ausencia de diferencias entre los grupos.

El patrón de actividad metabólica que subyace a la memoria de referencia espacial nos reveló una implicación de áreas cerebrales como el hipocampo y la amígdala. El hipocampo ha sido tradicionalmente relacionado no sólo en la representación del entorno, sino también en la codificación de la meta y el recuerdo

en asociación con la memoria espacial (Dupret y cols., 2010). Además, estos autores mostraron cómo la reactivación de las representaciones de la meta es dependiente de los receptores NMDA presentes en el hipocampo. Estos receptores también se han hallado en el complejo basolateral y el núcleo central de la amígdala (Llansola y cols., 2007). Por lo que alteraciones tempranas en la transmisión glutamatérgica, las cuales ya se han datado en estadios crónicos de la EH (Montoliu y cols., 2010), podrían explicar la escasa activación metabólica encontrada en los animales hipertensos.

Por último, el estudio de las correlaciones nos permitió identificar distintos patrones de interacción entre las redes cerebrales en los distintos grupos. El grupo pseudo-operado, el cual muestra mayor actividad metabólica que el grupo hipertenso, mostró un único circuito en el que se integran las distintas estructuras cerebrales; mientras que el grupo hipertenso mostró dos redes cerebrales complejas. Este incremento en el número de redes cerebrales y estructuras podría indicar los esfuerzos metabólicos cerebrales del grupo hipertenso, los cuales son necesarios para adquirir la memoria de referencia espacial en el mismo tiempo que el grupo pseudo-operado.

A la vista de los resultados obtenidos en el análisis de la memoria de referencia espacial por los animales con EHM, nuestro siguiente objetivo consistió en examinar si también podrían ocurrir alteraciones en la flexibilidad conductual.

La flexibilidad conductual se refiere a la habilidad para aprender una nueva estrategia al mismo tiempo que se inhibe la ejecución de una estrategia previa bajo unas condiciones ambientales cambiantes (Ragozzino y cols., 1999). La flexibilidad conductual es el concepto general que subyace a los cambios en las tareas los cuales requieren modificar tanto la dimensión del estímulo relevante (por ejemplo, cambiar del aprendizaje alocéntrico al aprendizaje de guía y viceversa) como el sistema de memoria implicado (White y McDonald, 2002). A lo largo de los años, son muchos los estudios que demuestran cómo las diferentes estrategias de aprendizaje requieren de diferentes redes neurales, las cuales podrían superponerse parcialmente (Rubio y cols., 2012).

Para acceder al estudio tanto de la flexibilidad conductual como de las redes implicadas en el modelo de EHM, combinamos la estrategia alocéntrica y la guía. Asimismo, variando el orden de adquisición de cada una de las estrategias pudimos observar el efecto de la facilitación.

Estudios previos realizados por de Bruin y cols. (2001) mostraron que al comienzo del entrenamiento las ratas intentan localizar la plataforma en la piscina utilizando una estrategia que implica el procesamiento de la información referente a la localización espacial. Cuando las ratas fallan, cambian su estrategia y aprenden la ruta hacia la plataforma basándose en una estrategia táxica, por ejemplo una estrategia de guía. Estos hallazgos son similares a nuestros resultados.

Comparando los grupos experimentales que realizan el cambio alocéntrico-guía (A-C), el grupo pseudo-operado exhibió un aumento en el número de elecciones correctas en lo que respecta a la adquisición de la tarea alocéntrica (desde el día 1 al 3). Sin embargo, cuando se realizó el cambio para favorecer la tarea de guía, se observó una disminución en el número de elecciones correctas, a pesar de que los animales alcanzaron el criterio al final del entrenamiento.

Cuando nos centramos en el cambio de la tarea de guía a la alocéntrica (C-A), el bajo número de elecciones correctas por parte de los animales pseudo-operados nos refleja la preferencia de los animales por una utilización de la información espacial. De hecho, cuando se inicia la tarea alocéntrica no se observan disminuciones en el número de respuestas correctas, lo cual no sólo apoya las investigaciones previas, sino que muestra cómo el comienzo con una tarea favorecida podría facilitar la adquisición de una tarea de mayor dificultad.

Sin embargo, en el caso del grupo hipertenso, la identidad de la primera tarea presentada no fue importante dado que el número de elecciones correctas fue siempre bajo. Esta falta de flexibilidad había sido observada en estudios previos (de Bruin y cols., 1994) asociada a lesiones en el prefrontal medial con cambios de estrategias, desde alocéntrica a pista visual. Por tanto, el siguiente paso consistió en estudiar la actividad citocromo c-oxidasa, que se encontraba disminuida en el grupo hipertenso en relación al grupo pseudo-operado, para formar redes basadas en la

actividad metabólica cerebral que puedan explicar las diferencias cerebrales entre las distintas estrategias.

El análisis reveló un complejo de estructuras comunes a ambos cambios de estrategia, tales como la corteza parietal, el estriado dorsal y el accumbens. La evidencia experimental apoya estos resultados sugiriendo que sistemas de memoria diferentes podrían interactuar bajo algunas condiciones (Byrne y cols., 2007; Fidalgo y cols., 2012). La existencia de un conjunto común de estructuras involucradas en ambas estrategias sugiere un sistema central que facilita alternancias entre los requerimientos de las dos estrategias diferentes.

A parte de las estructuras comunes, la corteza prefrontal en los grupos A-C se reveló primordial, mientras que la ausencia del hipocampo o la amígdala podrían entenderse como parte de la inhibición que el prefrontal ejerce sobre ambas estructuras (Quirk y cols., 2003; Rich y Shapiro, 2007). En contraposición se encuentran los resultados observados en los grupos C-A, donde la relevancia mayor recae sobre el hipocampo y la amígdala. Por tanto, no resulta difícil entender que cualquier daño en una de esas estructuras que conforman las redes podría causar alteraciones en la flexibilidad cognitiva de manera similar a la encontrada en enfermedades como el Huntington, el Alzheimer (Menzie y cols., 2012) y la EH (Amodio y cols., 2005). Este estudio nos permitió proponer la corteza prefrontal, el estriado, el hipocampo y los núcleos amigdalinos como las estructuras cerebrales concretas que podrían encontrarse afectadas en los estadios tempranos de la EH. A continuación, diseñamos diferentes tareas conductuales con el fin de detectar la existencia de un déficit temprano en ellas consecuencia de la EHM.

Así pues, en primer lugar, nos preguntamos cómo el hipocampo de un animal con EHM sería capaz de tratar con distintos niveles de dificultad en tareas hipocampo-dependientes. Para ello llevamos a cabo dos tareas, una tarea de reconocimiento objeto-lugar que sólo implica juzgar si un objeto ha sido encontrado previamente, mientras que la segunda tarea fue un aprendizaje de reversión, el cual implica el manejo de información contextual, un comportamiento

extendido en el tiempo, así como la integración de la ruta con la recompensa produciendo la selección adecuada de la ruta (Young y Shapiro, 2011).

El primer experimento nos reveló la incapacidad de los animales hipertensos para recordar el cambio de posición que tuvo lugar en el objeto desplazado. Además, esta disminución en su capacidad de discriminación no fue consecuencia de una disminución en la exploración, ya que el grupo hipertenso no mostró diferencias en los tiempos totales de exploración en comparación con los animales pseudo-operados.

El segundo experimento mostró la incapacidad del grupo hipertenso para recordar la nueva localización de la plataforma durante la prueba test de la tarea de reversión en comparación con los animales pseudo-operados. En este experimento las demandas para resolver la tarea son mayores que en el primer experimento. Consecuentemente, como la complejidad de la tarea se incrementa, el número de regiones cerebrales involucradas será mayor.

Esto viene avalado por el estudio de la expresión de la proteína c-Fos, resultado de la activación del protooncogen c-fos, cuya expresión es indicativa de la actividad neuronal que se produce en diferentes tipos de aprendizajes (Kaczmarek, 1993; Santín y cols., 2003; Radulovic y cols., 1998). Nuestros resultados muestran elevada inmunoreactividad c-Fos en CA1, CA3 y la corteza entorrinal del grupo hipertenso en comparación con el grupo pseudo-operado en la tarea de reconocimiento objeto-lugar. Sin embargo, el patrón opuesto se encontró en la tarea de reversión, donde una disminución de las neuronas con marcaje c-Fos apareció en CA1, CA3, giro dentado, y las cortezas prelímbica e infralímbica en el grupo hipertenso en comparación con el grupo pseudo-operado.

A la luz de estos resultados, comprobamos la contribución diferencial del hipocampo y su dependencia según el requerimiento de la tarea, así como los déficits que presentan los animales con EHM en la realización de ambas tareas. Cuando el requerimiento de la tarea es bajo, tal como la tarea de reconocimiento objeto-lugar, se ve implicado un "circuito neural corto" donde los animales hipertensos muestran incrementos en la inmunoreactividad c-Fos en comparación

con los animales pseudo-operados. Esto puede deberse a los esfuerzos realizados por los animales afectados por EHM en realizar la tarea satisfactoriamente.

Consecuentemente, un incremento en la dificultad de la tarea espacial reflejada por el aprendizaje de reversión, conlleva un reclutamiento de estructuras adicionales formando un "circuito neural largo" que implica no sólo el hipocampo sino también la corteza prefrontal. Ambas estructuras se encuentran conectadas, ya que CA1 es el mayor eferente de la corteza prelímbica (Jay y cols., 1992; Gigg y cols., 1994). Asimismo, la vía trisináptica entre las diferentes subregiones hipocampales, la corteza entorrinal y el subículo es dependiente de glutamato (Amaral y Witter, 1989; O´Reilly y McClelland, 1994; McClelland y cols., 1995; Eichenbaum, 2000; Witter y cols., 2000). Además, Seamans y cols. (1998) han sugerido un papel modulador de la dopamina en el flujo de información entre el hipocampo y la corteza prefrontal. Todas ellas, son vías de neurotransmisión que se han visto alteradas en estadios agudos y crónicos de la EH, pero basándonos en los resultados obtenidos podrían sugerir una alteración desde estadios tempranos de la enfermedad.

Igualmente, desarrollamos una herramienta simple de evaluación de las alteraciones en el aprendizaje en los animales con EHM. Con este propósito, llevamos a cabo una tarea de hábitos o estímulo-respuesta, la cual es estriado-dependiente (Packard y McGaugh, 1992; McDonald y White, 1994). Para ello, evaluamos la realización de los animales con EHM en una tarea estímulo-respuesta en la cual la plataforma visible fue reposicionada pseudo-aleatoriamente a lo largo de los días para variar su relación con las pistas distales triviales del entorno (Morris, 1981).

Los resultados conductuales mostraron la incapacidad de los animales hipertensos para alcanzar el criterio de aprendizaje establecido por los animales pseudo-operados. A este respecto, son numerosos los estudios que han señalado cómo las lesiones en el caudado-putamen pueden dañar la adquisición de dicha tarea (Block y cols., 1993; Dunbar y cols., 1993) siendo dichas alteraciones independientes de déficits motores (Furtado y Mazurek, 1996; Arias y cols., 2012).

Estos resultados podrían sugerir el daño estriatal como primario en el desarrollo de la EHM. Asimismo, las disminuciones en la actividad citocromo c-oxidasa encontradas en el grupo hipertenso en el estriado ventral, el hipocampo y los núcleos amigdalinos podrían subrayar dicha hipótesis.

En último lugar, quisimos relacionar dichos déficits en el aprendizaje y la actividad metabólica con el estudio de los posibles procesos inflamatorios cerebrales que subyacen a la EH, así como explorar los cambios morfológicos gliales y neuronales que pueden acaecer en la EHM.

Hay una evidencia creciente que apoya el papel de la inflamación en la exacerbación de las manifestaciones neurológicas de la EH. La inflamación en el contexto de la EH puede producirse directamente dentro del cerebro ocasionando una disfunción astrocítica, microglial y neuronal, contribuyendo al daño cerebral (Tranah y cols., 2013). Por otra parte, la inflamación también puede desarrollarse a nivel sistémico (Aller y cols., 2012) e influenciar la función cerebral de manera indirecta (Aller y cols., 2005a,b). Es por ello que nosotros consideramos interesante determinar la presencia de algunos mediadores involucrados en la respuesta inflamatoria, entre ellos incluimos el TNF-α, la IL-1β y la IL-6 con el fin de verificar la hipotética etiopatogenia inflamatoria de la EHM.

Nuestros resultados no mostraron diferencias en la IL-1β y la IL-6 entre los grupos hipertenso y pseudo-operado en las principales estructuras cerebrales del sistema límbico que se encuentran relacionadas con el aprendizaje estriado-dependiente. Tampoco hallamos diferencias en la proliferación de células T y B. Sin embargo, encontramos un incremento del TNF-α en el estriado del grupo hipertenso. La producción del TNF-α, a menudo, tiene acciones sobre procesos inflamatorios, amplificando dichas respuestas mediante la inducción de mediadores secundarios (Moore y cols., 2001).

Asimismo, el incremento del TNF-α en los animales con EHM podría estar relacionado con la disminución de la actividad metabólica encontrada. De hecho, el TNF-α podría disminuir la actividad citocromo c-oxidasa a través de dos vías: directamente, inhibiendo la fosforilación oxidativa mitocondrial donde la citocromo

c-oxidasa, como enzima mitocondrial, está involucrada en los procesos de fosforilación que generan ATP; e indirectamente, porque el TNF-α podría incrementar la síntesis del óxido nítrico a través de la regulación a la alza de la óxido nítrico sintasa inducible (Aller y cols., 2005a). Por tanto, el estrés oxidativo y nitrosativo podrían causar el daño mitocondrial neuronal y una fosforilación oxidativa defectiva la cual se reflejaría en una actividad citocromo c-oxidasa alterada (Arias y cols., 2012).

Quisimos estudiar también los posibles daños neuronales y gliales en la EHM que podrían subyacer a los déficits conductales. Para ello, exploramos los cambios en el volumen nuclear neuronal y la proteína citoesquelética glial fibrilar ácida (GFAP). Encontramos disminución de células GFAP inmunoreactivas en el estriado dorsal del grupo hipertenso en comparación con el pseudo-operado. Cambios en la GFAP astrocitaria habían sido reportados en la corteza cerebral de ratas con daño hepático crónico (Norenberg, 1977), así como en los ganglios basales, la corteza cerebral y las estructuras talámicas de humanos en estadios crónicos de la EH (Sobel y cols., 1981). Además, mediadores inflamatorios como el TNF-α pueden disminuir la expresión de GFAP (Chastre y cols., 2010). Nuestros resultados son pioneros en señalar cambios en la GFAP estriatal y su relación con los déficits encontrados en el aprendizaje en la EHM.

Por último, encontramos un incremento en el volumen nuclear neuronal del estriado ventral, estructura sobre la que descansa la correcta realización de la tarea estriatal (artículo VI). Existe evidencia de la actuación sinérgica de las citoquinas proinflamatorias y el amonio cerebral, en el daño hepático agudo, para causar edema cerebral (Chastre y cols., 2010). Asimismo, también se han encontrado incrementos en el volumen nuclear neuronal en los cuerpos mamilares y el hipocampo en modelos crónicos de la EH (Méndez y cols., 2008a). Sin embargo, estos resultados apoyan la existencia de una hipertrofia nuclear neuronal temprana en la evolución de la EH.

Así pues, en la presente tesis intentamos correlacionar deficiencias en numerosos aprendizajes que nos permitieran poner de manifiesto las alteraciones en el

metabolismo oxidativo cerebral, así como en la expresión génica de aquellas estructuras cerebrales que son las primeras en ser afectadas por la EHM. Asimismo, intentamos establecer la relación entre dichas alteraciones y los procesos inflamatorios, los daños astrocitarios y los cambios neuronales que subyacen a los mismos, entendiéndolos como parte de un continuo en el desarrollo de la cronicidad de la EH. Estos hallazgos dejan una puerta abierta para los futuros tratamientos sobre dianas tempranas ya presentes en los pacientes con EHM.

6. CONCLUSIONES

1. El estudio de la actividad metabólica cerebral de los modelos experimentales de daño hepático, hipertensión portal e hiperamonemia ha revelado una alteración diferencial en las estructuras del sistema límbico. La mayor alteración fue hallada en el modelo hiperamonémico, seguido del modelo tratado con tioacetamida y el modelo de hipertensión portal en las regiones prefrontales, los núcleos talámicos, el estriado y el hipocampo dorsal.

2. El estudio del modelo crónico de hiperamonemia durante la ejecución de las tareas alocéntrica y de guía ha manifestado un deficiente aprendizaje en ambas tareas.

3. El aprendizaje espacial incrementa la actividad metabólica de una manera significativa en las regiones cerebrales implicadas en el modelo de hiperamonemia. Asimismo, encontramos una mayor implicación de estructuras límbicas en la tarea de guía (cortezas prelímbica, infralímbica, parietal, entorrinal y perirrinal, el estriado dorsal y los núcleos amigdalinos) en comparación con la alocéntrica (tálamo anterodorsal) en dicho modelo de EH crónica.

4. La presión portal sanguínea medida en el grupo con EHM fue significativamente superior a la encontrada en el grupo pseudo-operado.

5. Se observa esplenomegalia e insuficiencia adrenal en el modelo de EHM en comparación con el grupo pseudo-operado.

6. Se demuestra, por primera vez en la literatura, que el desarrollo de la inflamación en la EHM se inicia en el núcleo estriado a través de un incremento del TNF-α, proponiendo dicha estructura cerebral como centinela inicial del desarrollo de la EH.

7. Los sujetos con EHM no manifiestan déficit en la memoria espacial tras un aprendizaje que requiere la repetición a lo largo de los días.

8. Los sujetos con EHM siempre presentaron deficiencias en la ejecución de tareas que requerían un aprendizaje no extendido en el tiempo.

9. Se han observado variaciones significativas en la expresión cerebral de los genes tempranos en los animales con EHM cuando se incrementa el nivel de dificultad presentado en las tareas espaciales.

10. La morfología celular ha revelado una reducción en el volumen nuclear neuronal y en la expresión de la proteína glial fibrilar ácida en el núcleo estriatal de los animales con EHM, lo que recalca la importancia de dicha estructura como potencial diana terapéutica.

11. El análisis de la actividad metabólica mediante la técnica citocromo c-oxidasa ha permitido delimitar el circuito cerebral, constituido por la corteza prefrontal, el estriado, el hipocampo y los núcleos amigdalinos, causante de los déficits cognitivos encontrados en la EHM.

CONCLUSIONS

1. The brain metabolic activity of the experimental models of liver injury, hyperammonemia and portal hypertension revealed a differential alteration in the structures of the limbic system. The greater alteration was found in the hyperammonemic model, followed by thioacetamide -treated and portal hypertension in the prefrontal cortex, the thalamic nuclei, striatum and dorsal hippocampus.

2. The chronic hyperammonemia model was unable to acquire both the allocentric and the cue-guided tasks.

3. The spatial learning increases the metabolic activity in the brain regions involved in the chronic hyperammonemia model. At the same time, we found more limbic structures involved in the cue-guided task (prelimbic, infralimbic, parietal, entorrhinal and perirhinal cortices, the dorsal striatum and amygdala nuclei) compared to the allocentric one (anterodorsal thalamus).

4. The portal blood pressure measured in the minimal hepatic encephalopathy (MHE) model was significantly higher than that found in sham group.

5. In contrast to the sham group, the model of MHE shows splenomegaly and adrenal insufficiency.

6. It is shown, for the first time in the literature, that the development of the inflammation in MHE it is started in the striatum through an increase in TNF-α, proposing this brain structure as precocious in the development of HE.

7. The MHE subjects did not show spatial memory impairment in a learning task which requires repetition over days.

8. The MHE subjects always showed deficiencies in the execution of tasks requiring no extended in time learning.

9. Significant differences in the brain early gene expression in the MHE animals have been shown when the difficulty of the task was increased.

10. The cellular morphology has revealed a reduction in the neuronal nuclear volume and the glial fibrillar acid protein in the striatal nuclei of the MHE animals, as a consequence it is highlighted the potential of this brain structure as a therapeutic target.

11. The analysis of the brain metabolic activity using the histochemical technique of the cytochrome c-oxidase allows us to define the brain circuitry, composed by the prefrontal cortex, striatum, hippocampus and amygdala nuclei, which causes the cognitive deficits found in MHE.

7. REFERENCIAS

Aguilar, M.A., Miñarro, J., Felipo, V. (2000). Chronic moderate hyperammonemia impairs active and passive avoidance behavior and conditional discrimination learning in rats. *Exp Neurol*, 161, 704-713.

Al-Busafi, S.A., McNabb-Baltar, J., Farag, A., Hilzenrat, N. (2012). Clinical manifestations of portal hypertension. *Int J Hepatol*, 2012, 203794.

Aller, M.A., Nava, M.P., López, L., Méndez, M., Méndez, M., Arias, J.L., Arias, J. (2005a). *Hipertensión portal clínica y experimental*. Madrid: Ed. Complutense.

Aller, M.A., Vara, E., Garcia, C., Palma, M.D., Arias, J.L., Nava, M.P., Arias, J. (2005b). Proinflammatory liver and antiinflammatory intestinal mediators involved in portal hypertensive rats. *Mediators Inflamm*, 2, 101-111.

Aller, M.A., Arias, J.L., Arias, J. (2007). The mast cells integrates the splanchnic and systemic inflammatory response in portal hypertension. *J Transl Med*, 5, 44.

Aller, M.A., Arias, N., Fuentes-Julian, S., Blazquez-Martinez, A., Argudo, S., Miguel, M.P., Arias, J.L., Arias, J. (2012). Coupling inflammation with evo-devo. *Med Hypotheses*, 78, 721-731.

Amaral, D.G., Witter, M.P. (1989). The three-dimensional organization of the hippocampal formation: a review of anatomical data. *Neuroscience*, 31, 571-591.

Amodio, P., Schiff, S., Del Piccolo, F., Mapelli, D., Gatta, A., Umiltà, C. (2005). Attention dysfunction in cirrhotic patients: An inquiry on the role of executive control, attention orienting and focusing. *Metab Brain Dis*, 20, 115-127.

Arias, J.L., Aller, M.A., Sánchez-Patan, F., Arias, J. (2006). The inflammatory bases of hepatic encephalopathy. *Eur J Gastroenterol Hepatol*, 18, 1297-310.

Arias, N., Méndez, M., Arias, J., Arias, J.L. (2012). Brain metabolism and spatial memory are affected by portal hypertension. *Metab Brain Dis*, 27, 183-191.

Arias, N., Méndez, M., Fidalgo, C., Aller, M.A., Arias, J., Arias, J.L. (2013). Mapping metabolic brain activity in three models of hepatic encephalopathy. *Int J Hypertens*, 2013, 390872.

Azorín, I., Miñana, M.D., Felipo, V., Grisolía, S. (1989). A simple animal model of hyperammonemia. *Hepatology*, 10, 311-314.

Bass, N.M., Mullen, K.D., Sanyal, A., Poordad, F., Neff, G., Leevy, C.B., Sigal, S., Sheikh, M.Y., Beavers, K., Frederick, T., Teperman, L., Hillebrand, D., Huang, S., Merchant, K., Shaw, A., Bortey, E., Forbes, W.P. (2010). Rifaximin treatment in hepatic encephalopathy. *N Engl J Med*, 362, 1071-1081.

Bjerring, P.N., Eefsen, M., Hansen, B.A., Larsen, F.S. (2009). The brain in acute liver failure. A tortuous path from hyperammonemia to cerebral edema. *Metab Brain Dis*, 24, 5-14.

Blei, A.T., Olafsson, S., Therrien, G., Butterworth, R.F. (1994), Ammonia-induced brain edema and intracranial hypertension in rats after portacaval anastomosis. *Hepatology*, 19, 1437-1444.

Bleibel, W., Al-Osaimi, A.M.S. (2013). Hepatic encephalopathy. *SJG*, 18, 301-309.

Block, F., Kunkel, M., Schwarz, M. (1993). Quinolinic acid lesion of the striatum induces impairment in spatial learning and motor performance in rats. *Neurosci Lett*, 149, 126-128.

Butterworth, R.F. (1991). Pathophysiology of hepatic encephalopathy: The ammonia hypothesis revisited. In: F. Bengtsson, B. Jeppsson, T. Aamdal, H. Vistrup (Eds.), *Progress in hepatic encephalopathy and metabolic nitrogen exchange* (pp. 9-24). Florida: CRC Press, Boca Raton.

Butterworth, R.F., Norenberg, M.D., Felipo, V., Ferenci, P., Albrecht, J., Blei, A.T. (2009). Members of the ISHEN Commission on Experimental Models of HE. Experimental models of hepatic encephalopathy: ISHEN guidelines. *Liver Int*, 29, 783-788.

Butterworth, R.F. (2013). The liver-brain axis in liver failure: neuroinflammation and encephalopathy. *Nat Rev Gastroenterol Hepatol*, 10, 522-528.

Butz, M., May, E.S., Häussinger, D., Schnitzler, A. (2013). The slowed brain: cortical oscillatory activity in hepatic encephalopathy. *Arch Biochem Biophys*, 536, 197-203.

Byrne, P., Becker, S., Burgess, N. (2007). Remembering the past and imagining the future: A neural model of spatial memory and imagery. *Psychol Rev*, 114, 340-375.

Canevari, L., Abramov, A.Y., Duchen, M.R. (2004). Toxicity of amyloid beta peptide: tales of calcium, mitochondria, and oxidative stress. *Neurochem Res*, 29, 637-650.

Carey, W. (2011). Portal hypertension: diagnosis and management with particular reference to variceal hemorrhage. *J Dig Dis*, 12, 25-32.

Cauli, O., Rodrigo, R., Piedrafita, B., Boix, J., Felipo, V. (2007). Inflammation and hepatic encephalopathy: ibuprofen restores learning ability in rats with portacaval shunts. *Hepatology*, 46, 514-519.

Cauli, O., Rodrigo, R., Llansola, M., Montoliu, C., Monfort, P., Piedrafita, B., El Mlili, N., Boix, J., Agustí, A., Felipo, V. (2009). Glutamatergic and gabaergic neurotransmission and neuronal circuits in hepatic encephalopathy. *Metab Brain Dis*, 24, 69-80.

Chastre, A., Jiang, W., Desjardins, P., Butterworth, R.F. (2010). Ammonia and proinflammatory cytokines modify expression of genes coding for astrocytic proteins implicated in brain edema in acute liver failure. *Metab Brain Dis*, 25, 17-21.

Chen, H.J., Zhu, X.Q., Jiao, Y., Li, P.C., Wang, Y., Teng, G.J. (2012a). Abnormal baseline brain activity in low-grade hepatic encephalopathy: a resting-state fMRI study. *J Neurol Sci*, 318, 140-145.

Chen, B.R., Cheng, H.H., Lin, W.C., Wang, K.H., Liou, J.Y., Chen, P.F., Wu, K.K. (2012b). Quiescent fibroblasts are more active in mounting robust inflammatory responses than proliferative fibroblasts. *PLoS One*, 7, e49232.

Chomczynski, P., Sacchi, N. (1987). Single-step method of RNA isolation by acid guanidinium thiocyanate-phenol-chloroform extraction. *Anal Biochem*, 162, 156-159.

Ciećko-Michalska, I., Szczepanek, M., Słowik, A., Mach, T. (2012). Pathogenesis of hepatic encephalopathy. *Gastroenterol Res Pract*, 2012, 642108.

Coltart, I., Tranah, T.H., Shawcross, D.L. (2013). Inflammation and hepatic encephalopathy. *Arch Biochem Biophys*, 536, 189-196.

Conejo, N.M., González-Pardo, H., González-Lima, F., Arias, J.L. (2010), Spatial learning of the water maze: Progression of brain circuits mapped with cytochrome oxidase histochemistry. *Neurobiol Learn Mem*, 93, 362-371.

Conn, H.O., Bircher, J. (1993). Quantifying the severity of hepatic encephalopathy: syndromes and therapies. In H.O. Conn, J. Bricher (Eds.) *Hepatic encephalopathy: syndromes and therapies* (pp. 13-26). East Lansing MI: Medi Ed Press.

Cooper, A.J., Plum, F. (1987). Biochemistry and physiology of brain ammonia. *Physiol Rev*, 67, 440-519.

Córdoba, J. (2011). New assessment of hepatic encephalopathy. *J Hepatol*, 54, 1030-1040.

Dam, G., Keiding, S., Munk, O.L., Ott, P., Vilstrup, H., Bak, L.K., Waagepetersen, H.S., Schousboe, A., Sørensen, M. (2013). Hepatic encephalopathy is associated with decreased cerebral oxygen metabolism and blood flow, not increased ammonia uptake. *Hepatology*, 57, 258-265.

Dawicki, W., Marshall, J.S. (2007). New and emerging roles for mast cells in host defense. *Curret Opin. Immunol*, 19, 31-38.

de Bruin, J.P., Sànchez-Santed, F., Heinsbroek, R.P., Donker, A., Postmes, P. (1994). A behavioural analysis of rats with damage to the medial prefrontal cortex using the Morris water maze: Evidence for behavioural flexibility, but not for impaired spatial navigation. *Brain Res*, 652, 323-333.

de Bruin, J.P., Moita, M.P., de Brabander, H.M., Joosten, R.N. (2001). Place and response learning of rats in a Morris water maze: Differential effects of fimbria fornix and medial prefrontal cortex lesions. *Neurobiol Learn Mem*, 75, 164-178.

de Vries, H.E., Blom-Roosemalen, M.C., van Oosten, M., de Boer, A.G., van Berkel, T.J., Breimer, D.D., Kuiper, J. (1996). The influence of cytokines on the integrity of the blood-brain barrier in vitro. *J Neuroimmunol*, 64, 37-43.

Didier, N., Romero, I.A., Créminon, C., Wijkhuisen, A., Grassi, J., Mabondzo, A. (2003), Secretion of interleukin-1beta by astrocytes mediates endothelin-1 and tumour necrosis factor-alpha effects on human brain microvascular endothelial cell permeability. *J Neurochem*, 86, 246-254.

Duchini, A., Govindarajan, S., Santucci, M., Zampi, G., Hofman, F.M. (1996). Effects of tumor necrosis factor-alpha and interleukin-6 on fluid-phase permeability and ammonia diffusion in CNS-derived endothelial cells. *J Investig Med*, 44, 474-482.

Dunbar, G.L., Lescaudron, L.L., Stein, D.G. (1993). Comparison of GM1 ganglioside, AGF2, and D-amphetamine as treatments for spatial reversal and place learning deficits following lesions of the neostriatum. *Behav Brain Res*, 54, 67-79.

Dupret, D., O'Neill, J., Pleydell-Bouverie, B., Csicsvari, J. (2010), The reorganization and reactivation of hippocampal maps predict spatial memory performance. *Nat Neurosci*, 13, 995-1002.

Eichenbaum, H. (2000). A cortical-hippocampal system for declarative memory. *Nat Rev Neurosci*, 1, 41-50.

Ennaceur, A., Delacour, J. (1988), A new one-trial test for neurobiological studies of memory in rats. 1: Behavioral data. *Behav Brain Res*, 31, 47-59.

Erceg, S., Monfort, P., Hernández-Viadel, M., Rodrigo, R., Montoliu, C., Felipo, V. (2005). Oral administration of sildenafil restores learning ability in rats with hyperammonemia and with portacaval shunts. *Hepatology*, 41, 299-306.

Fazekas, J.E., Ticktin, H.E., Shea, J.G. (1957). Effects of L-arginine on hepatic encephalopathy. *Am Med Sci*, 234, 462-467.

Felipo, V., Urios, A., Montesinos, E., Molina, I., Garcia-Torres, M.L., Civera, M., Olmo, J.A., Ortega, J., Martinez-Valls, J., Serra, M.A., Cassinello, N., Wassel, A., Jordá, E., Montoliu, C. (2012). Contribution of hyperammonemia and inflammatory factors to cognitive impairment in minimal hepatic encephalopathy. *Metab Brain Dis*, 27, 51-58.

Felipo, V. (2013). Hepatic encephalopathy: effects of liver failure on brain function. *Nat Rev Neurosci*, 14, 851-858.

Ferenci, P., Lockwood, A., Mullen, K., Tarter, R., Weissenborn, K., Blei, A.T. (2002), Hepatic encephalopathy--definition, nomenclature, diagnosis, and quantification: final report of the working party at the 11th World Congresses of Gastroenterology, Vienna, 1998. *Hepatology*, 35, 716-721.

Ferrando, P.J., Anguiano-Carrasco, C. (2010). El análisis factorial como técnica de investigación en psicología. *Papeles del Psicólogo*, 31, 18-33.

Fidalgo, C., Conejo, N.M., González-Pardo, H., Arias, J.L. (2012). Functional interaction between the dorsal hippocampus and the striatum in visual discrimination learning. *J Neurosci Res*, 90, 715-720.

Furtado, J.C., Mazurek, M.F. (1996). Behavioral characterization of quinolinate-induced lesions of the medial striatum: relevance for Huntington's disease. *Exp Neurol*, 138, 158-168.

Galli, S.J., Kalesnikoff, J., Grimbakleston, M.A., Piliponsky, A.M., Williams, C.M.M., Tsai, M. (2005), Mast cells as "cunable" effector and immunoregulatory cells: Recent advances. *Ann Rev Immunol*, 23, 749-786.

Gigg, J., Tan, A.M., Finch, D.M. (1994). Glutamatergic hippocampal formation projections to prefrontal cortex in the rat are regulated by GABAergic inhibition and show convergence with glutamatergic projections from the limbic thalamus. *Hippocampus*, 4, 189-198.

González-Lima, F., Cada, A. (1994). Cytochrome oxidase activity in the auditory system of the mouse: A qualitative and quantitative histochemical study. *Neuroscience*, 63, 559-578.

González-Lima, F., Valla, J., Matos-Collazo, S. (1997). Quantitative cytochemistry of cytochrome oxidase and cellular morphometry of the human inferior colliculus in control and Alzheimer´s patients. *Brain Res*, 752, 117-126.

Häussinger, D., Kircheis, G., Fischer, R., Schliess, F., vom Dahl, S. (2000). Hepatic encephalopathy in chronic liver disease: a clinical manifestation of astrocyte swelling and low-grade cerebral edema? *J Hepatol*, 32, 1035-1038.

Hazell, A.S., Butterworth, R.F. (1999). Hepatic encephalopathy: An update of pathophysiologic mechanisms. *Proc Soc Exp Biol Med*, 222, 99-112.

Hochberg, Y. (1988). A sharper Bonferroni procedure for multiple tests of significance. *Biometrika*, 75, 800-802.

Jay, T.M., Thierry, A.M., Wiklund, L., Glowinski, J. (1992), Excitatory Amino Acid Pathway from the Hippocampus to the Prefrontal Cortex. Contribution of AMPA Receptors in Hippocampo-prefrontal Cortex Transmission. *Eur J Neurosci*, 4, 1285-1295.

Jones, B.J., Roberts, D.J. (1968). The quantitative measurement of motor incoordination in naïve mice using an accelerating rotarod. *J Pharm Pharmacol*, 20, 302-304.

Jover, R., Madaria, E., Felipo, V., Rodrigo, R., Candela, A., Compañ, A. (2005), Animal models in the study of episodic hepatic encephalopathy in cirrhosis. *Metab Brain Dis*, 20, 399-408.

Jover, R., Rodrigo, R., Felipo, V., Insausti, R., Sáez-Valero, J., García-Ayllón, M.S., Suárez, I., Candela, A., Compañ, A., Esteban, A., Cauli, O., Ausó, E., Rodríguez, E., Gutiérrez, A., Girona, E., Erceg, S., Berbel, P., Pérez-Mateo, M. (2006). Brain edema and inflammatory activation in bile duct ligated rats with diet-induced hyperammonemia: A model of hepatic encephalopathy in cirrhosis. *Hepatology*, 43, 1257-1266.

Kaczmarek, L. (1993). Molecular biology of vertebrate learning: is c-fos a new beginning? *J Neurosci Res*, 34, 377-381.

Kahlbrock, N., Butz, M., May, E.S., Brenner, M., Kircheis, G., Häussinger, D., Schnitzler, A. (2012). Lowered frequency and impaired modulation of gamma band oscillations in a bimodal attention task are associated with reduced critical flicker frequency. *Neuroimage*, 61, 216-227.

Kappus, M.R., Bajaj, J.S. (2012). Covert hepatic encephalopathy: not as minimal as you might think. *Clin Gastroenterol Hepatol*, 10, 1208-1219.

Keiding S, Sørensen M, Bender D, Munk OL, Ott P, Vilstrup H. (2006) Brain metabolism of 13N-ammonia during acute hepatic encephalopathy in cirrhosis measured by positron emission tomography. *Hepatology*. 43:42-50.

Kircheis, G., Wettstein, M., Timmermann, L., Schnitzler, A., Häussinger, D. (2002). Critical flicker frequency for quantification of low-grade hepatic encephalopathy. *Hepatology*, 35, 357-366.

Lauridsen, M.M., Jepsen, P., Vilstrup, H. (2011). Critical flicker frequency and continuous reaction times for the diagnosis of minimal hepatic encephalopathy: a comparative study of 154 patients with liver disease. *Metab Brain Dis*, 26, 135-139.

Liu, J.Y., Ding, J., Lin, D., He, Y.F., Dai, Z., Chen, C.Z., Cheng, W.Z., Wang, H., Zhou, J., Wang, X. (2013). T2* MRI of minimal hepatic encephalopathy and cognitive correlates in vivo. *J Magn Reson Imaging*, 37, 179-186.

Livak, K.J., Schmittgen, T.D. (2001). Analysis of relative gene expression data using real-time quantitative PCR and the 2(-Delta Delta C(T)). *Method Methods*, 25, 402-408.

Llansola, M., Rodrigo, R., Monfort, P., Montoliu, C., Kosenko, E., Cauli, O., Piedrafita, B., El Mlili, N., Felipo, V. (2007). NMDA receptors in hyperammonemia and hepatic encephalopathy. *Metab Brain Dis*, 22, 321-335.

Lockwood, A.H., Yap, E.W., Rhoades, H.M., Wong, W.H. (1991a). Altered cerebral blood flow and glucose metabolism in patients with liver disease and minimal encephalopathy. *J Cereb Blood Flow Metab*, 11, 331-336.

Lockwood, A.H., Yap, E.W., Wong, W.H. (1991b). Cerebral ammonia metabolism in patients with severe liver disease and minimal hepatic encephalopathy. J Cereb Blood Flow Metab, 11, 337-341.

Marini, J.C., Broussard, S.R. (2006). Hyperammonemia increases sensitivity to LPS. *Mol Genet Metab*, 88, 131-137.

McClelland, J.L., McNaughton, B.L., O'Reilly, R.C. (1995). Why there are complementary learning systems in the hippocampus and neocortex: insights from the successes and failures of connectionist models of learning and memory. *Psychol Rev*, 102, 419-457.

McDonald, R.J., White, N.M. (1994). Parallel information processing in the water maze: evidence for independent memory systems involving dorsal striatum and hippocampus. *Behav Neural Biol*, 61, 260-270.

Méndez-López, M., Méndez, M., Sánchez-Patán, F., Casado, I., Aller, M.A., López, L., Corcuera, M.T., Alonso, M.J., Nava, M.P., Arias, J., Arias, J.L. (2007). Partial portal vein ligation plus thioacetamide: a method to obtain a new model of cirrhosis and chronic portal hypertension in the rat. *J Gastrointest Surg*, 11, 187-194.

Méndez, M., Méndez-López, M., López, L., Aller, M.A., Arias, J., Arias, J.L. (2008a). Mammillary body alterations and spatial memory impairment in Wistar rats with thioacetamide-induced cirrhosis. *Brain Res*, 1233, 185-195.

Méndez, M., Méndez-López, M., López, L., Aller, M.A., Arias, J., Cimadevilla, J.M., Arias, J.L. (2008b). Spatial memory alterations in three models of hepatic encephalopathy. *Behav Brain Res*, 188, 32-40.

Méndez, M., Méndez-López, M., López, L., Aller, M.A., Arias, J., Arias, J.L. (2009a). Basal and learning task-related brain oxidative metabolism in cirrhotic rats. *Brain Res Bull*, 78, 195-201.

Méndez, M., Méndez-López, M., López, L., Aller, M.A., Arias, J., Arias, J.L. (2009b). Associative learning deficit in two experimental models of hepatic encephalopathy. *Behav Brain Res*, 198, 346-351.

Menzie, J., Pan, C., Prentice, H., Wu, J.Y. (2012). Taurine and central nervous system disorders. *Amino Acids*, 46, 31-46.

Miñano, C., Garcia-Tsao, G. (2010), Clinical pharmacology of portal hypertension. *Gastroenterol Clin North Am*, 39, 681-695.

Minguez, B., Garcia-Pagan, J.C., Bosch, J., Turnes, J., Alonso, J., Rovira, A., Cordoba, J. (2006) Noncirrhotic portal vein trombosis exhibits neuropsychological and MR changes consistent with minimal hepatic encephalopathy. *Hepatology*, 46, 707-714.

Moffat, J. (1788). *Prognostics and Prorrhetics of Hipocrates Translated From the Original Greek*. London, UK: Bensle.

Monfort, P., Erceg, S., Piedrafita, B., Llansola, M., Felipo, V. (2007). Chronic liver failure in rats impairs glutamatergic synaptic transmission and long-term potentiation in hippocampus and learning ability. *Eur J Neurosci*, 25, 2103-2111.

Montoliu, C., Rodrigo, R., Monfort, P., Llansola, M., Cauli, O., Boix, J., El Mlili, N., Agusti, A., Felipo, V. (2010). Cyclic GMP pathways in hepatic encephalopathy. Neurological and therapeutic implications. *Metab Brain Dis*, 25, 39-48.

Montoliu, C., Cauli, O., Urios, A., ElMlili, N., Serra, M.A., Giner-Duran, R., González-Lopez, O., Del Olmo, J.A., Wassel, A., Rodrigo, J.M., Felipo, V. (2011). 3-nitro-tyrosine as a peripheral biomarker of minimal hepatic encephalopathy in patients with liver cirrhosis. *Am J Gastroenterol*, 106, 1629-1637.

Moore, K.W., de Waal Malefyt, R., Coffman, R.L., O'Garra, A. (2001). Interleukin-10 and the interleukin-10 receptor. *Annu Rev Immunol*, 19, 683-765.

Morgagni, G.B. (1765). *De sedibus er causis morborum per anatomen indagatis: libri quinque*. Padova, Italy: Remondinus.

Morris, R.G.M. (1981). Spatial localization does not require the presence of local cues. *Learn Motiv*., 12, 239-260.

Morris, R.G.M. (1984). Developments of a water-maze procedure for studying spatial learning in the rat. *J Neurosci Meth*, 11, 47-60.

Nathan, C. (2003). Specificity of a third kind: reactive oxygen and nitrogen intermediates in cell signaling. *J Clin Invest*, 111, 769-778.

Norenberg, M.D. (1977). A light and electron microscopic study of experimental portal-systemic (ammonia) encephalopathy. *Lab Investigat*, 36, 618-627.

Norenberg, M.D. (1987). The role of astrocytes in hepatic encephalopathy. *Neurochem Pathol*, 6:, 13-33.

Norenberg, M.D. (2003). Oxidative and nitrosative stress in ammonia neurotoxicity. *Hepatology*, 37, 245-248.

Olde Damink Steven, W.M., Jalan, R., Dejong Cornelius, H.C. (2009). Interorgan ammonia trafficking in liver disease. *Metab. Brain Dis*, 24, 169-181.

O'Reilly, R.C., McClelland, J.L. (1994). Hippocampal conjunctive encoding, storage, and recall: avoiding a trade-off. *Hippocampus*, 4, 661-682.

Packard, M.G., McGaugh, J.L. (1992). Double dissociation of fornix and caudate nucleus lesions on acquisition of two water maze tasks: further evidence for multiple memory systems. *Behav Neurosci*., 106, 439-446.

Paxinos, G., Watson, G. (1997). *The Rat Brain in Stereotaxic Coordinates* (Compact Third Edition). New York: Academic Press.

Perazzo, J.C., Tallis, S., Delfante, A., Souto, P.A., Lemberg, A., Eizayaga, F.X., Romay, S. (2012). Hepatic encephalopathy: An approach to its multiple pathophysiological features. *World J Hepatol*, 4, 50-65.

Plum, F., Hindfelt, B. (1976). The neurological complications of liver disease. In: O. Vinken, G. Bruyn (Eds.), *Handbook of Clinical Neurology* (pp. 349-377). New York: American Elsevier.

Pomier-Layrargues, G., Spahr, L., Butterworth, R.F. (1995). Increased manganese concentrations in pallidum of cirrhotic patients. *Lancet*, 345, 735.

Quirk, G.J., Likhtik, E., Pelletier, J.G., Paré, D. (2003), Stimulation of medial prefrontal cortex decreases the responsiveness of central amygdala output neurons. *J Neurosci*, 23, 8800-8807.

Radulovic, J., Kammermeier, J., Spiess, J. (1998). Relationship between fos production and classical fear conditioning: effects of novelty, latent inhibition, and unconditioned stimulus preexposure. *J Neurosci*, 18, 7452-7461.

Ragozzino, M.E., Detrick, S., Kesner, R.P. (1999). Involvement of the prelimbic-infralimbic areas of the rodent prefrontal cortex in behavioral flexibility for place and response learning. *J Neurosci*, 19, 4585-4594.

Rama Rao, K.V., Norenberg, M.D. (2012). Brain energy metabolism and mitochondrial dysfunction in acute and chronic hepatic encephalopathy. *Neurochem Int*, 60, 697-706.

Rao, K.V., Mawal, Y.R., Qureshi, I.A. (1997). Progressive decrease of cerebral cytochrome C oxidase activity in sparse-fur mice: role of acetyl-L-carnitine in restoring the ammonia-induced cerebral energy depletion. *Neurosci Lett*, 224, 83-86.

Rao, K.V., Norenberg, M.D. (2001). Cerebral energy metabolism in hepatic encephalopathy and hyperammonemia. *Metab Brain Dis*, 16, 67-78.

Ratnakumari, L., Murthy, C.R. (1992). In vitro and in vivo effects of ammonia on glucose metabolism in the astrocytes of rat cerebral cortex. *Neurosci Lett*, 148, 85-88.

Ratnakumari, L., Murthy, C.R. (1993). Response of rat cerebral glycolytic enzymes to hyperammonemic states. *Neurosci Lett*, 161, 37-40.

Rich, E.L., Shapiro, M.L. (2007). Prelimbic/infralimbic inactivation impairs memory for multiple task switches, but not flexible selection of familiar tasks. *J Neurosci*, 27, 4747-4755.

Rivera Ramos, J.F., Rodríguez Leal, C. (2011). Review of the final report of the 1998 Working Party on definition, nomenclature and diagnosis of hepatic encephalopathy. *Ann Hepatol*, 10, S36-39.

Rivera-Mancía, S., Ríos, C., Montes, S. (2012). Manganese and ammonia interactions in the brain of cirrhotic rats: effects on brain ammonia metabolism. *Neurochem Res*, 37, 1074-1084.

Rolando, N., Wade, J., Davalos, M., Wendon, J., Philpott-Howard, J., Williams, R. (2000). The systemic inflammatory response syndrome in acute liver failure. *Hepatology*, 32, 734-739.

Romero-Gómez, M., Ramos-Guerrero, R., Grande, L., de Terán, L.C., Corpas, R., Camacho, I., Bautista, J.D. (2004). Intestinal glutaminase activity is increased in liver cirrhosis and correlates with minimal hepatic encephalopathy. *J Hepatol*, 41, 49-54.

Romero-Gómez, M., Jover, M., Diaz-Gomez, D., de Teran, L.C., Rodrigo, R., Camacho, I., Echevarria, M., Felipo, V., Bautista, J.D. (2006). Phosphate-activated glutaminase activity is enhanced in brain, intestine and kidneys of rats following portacaval anastomosis. *World J Gastroenterol*, 12, 2406-2411.

Rubio, S., Begega, A., Méndez, M., Méndez-López, M., Arias, J.L. (2012). Similarities and differences between the brain networks underlying allocentric and egocentric spatial learning in rat revealed by cytochrome oxidase histochemistry. *Neuroscience*, 223, 174-182.

Santín, L.J., Aguirre, J.A., Rubio, S., Begega, A., Miranda, R., Arias, J.L. (2003). c-Fos expression in supramammillary and medial mammillary nuclei following spatial reference and working memory tasks. *Physiol Behav*, 78, 733-739.

SAS Institute Inc (2011) SAS PROC MIXED (Software). Cary, NC: SAS Institute.

Seamans, J.K., Floresco, S.B., Phillips, A.G. (1998). D1 receptor modulation of hippocampal-prefrontal cortical circuits integrating spatial memory with executive functions in the rat. *J Neurosci*, 18, 1613-1621.

Sergeeva, O.A. (2013). GABAergic transmission in hepatic encephalopathy. *Arch Biochem Biophys*, 536, 122-130.

Shao, J., Tu, D. (1995). *The Jacknife and Bootstrap*. New York: Springer Series in Stadistics,

Shawcross, D.L., Davies, N.A., Williams, R., Jalan, R. (2004). Systemic inflammatory response exacerbates the neuropsychological effects of induced hyperammonemia in cirrhosis. *J Hepatol*, 40, 247-254.

Shawcross, D.L., Wright, G., Olde Damink, S.W., Jalan, R. (2007). Role of ammonia and inflammation in minimal hepatic encephalopathy. *Metab Brain Dis*, 22, 125-138.

Shawcross, D.L., Sharifi, Y., Canavan, J.B., Yeoman, A.D., Abeles, R.D., Taylor, N.J., Auzinger, G., Bernal, W., Wendon, J.A. (2011). Infection and systemic inflammation, not ammonia, are associated with Grade 3/4 hepatic encephalopathy, but not mortality in cirrhosis. *J Hepatol*, 54, 640-649.

Sherlock, S., Summerskill, W.H.J., White, L.P., Phear, E.A. (1954). Portal-systemic encephalopathy. Neurological complicarions of liver disease. *Lancet*, 267, 453-457.

Silen, M.L., Hesse, D.G., Felsen, D., Moldawer, L.L., Calvano, S.E., Seniuk, S., Cerami, A., Lowry, S.F. (1989), Cachectin/tumor necrosis factor production by fetal and newborn rat hepatic macrophages. *J Pediatr Surg*, 24, 34-38.

Skowrońska, M., Albrecht, J. (2012). Alterations of blood brain barrier function in hyperammonemia: an overview. *Neurotox Res*, 21, 236-244.

Sobel, R.A., DeArmond, S.J., Forno, L.S., Eng, L.F. (1981). Glial fibrillary acid protein in hepatic encephalopathy. An immunohistochemical study. *J Neuropathol Exp Neurol*, 40, 625-632.

Sohal, V.S. (2012). Insights into cortical oscillations arising from optogenetic studies. *Biol Psychiatry*, 71, 1039-1045.

Spahr, L., Vingerhoets, F., Lazeyras, F., Delavelle, J., DuPasquier, R., Giostra, E., Mentha, G., Terrier, F., Hadengue, A. (2000). Magnetic resonance imaging and proton spectroscopic alterations correlate with parkinsonian signs in patients with cirrhosis. *Gastroenterology*, 119, 774-781.

Tanaka, S., Ide, M., Shibutani, T., Ohtaki, H., Numazawa, S., Shioda, S., Yoshida, T. (2006). Lipopolysaccharide-induced microglial activation induces learning and memory deficits without neuronal cell death in rats. *J Neurosci Res*. 83, 557-566.

Toftengi, F., Larsen, F.S. (2004). Management of patients with fulminant hepatic failure and brain edema. *Metab Brain Dis*, 19, 207-214.

Tranah, T.H., Vijay, G.K., Ryan, J.M., Shawcross, D.L. (2013). Systemic inflammation and ammonia in hepatic encephalopathy. *Metab Brain Dis*, 28, 1-5.

Vallejo, G., Fernández, M.P., Livacic-Rojas, P.E., Tuero-Herrero, E. (2011). Comparison of modern methods for analyzing unbalanced repeated measures data with missing values. *Multivariate Behavioral Research*, 46, 900-937.

Wang, V., Saab, S. (2003). Ammonia levels and the severity of hepatic encephalopathy. *Am J Med*, 114, 237-238.

Weissenborn, K., Ennen, J.C., Schomerus, H., Rückert, N., Hecker, H. (2001). Neuropsychological characterization of hepatic encephalopathy. *J Hepatol*, 34, 768-773.

Weissenborn, K., Heidenreich, S., Giewekemeyer, K., Rückert, N., Hecker, H. (2003). Memory function in early hepatic encephalopathy. *J Hepatology*, 39, 320-325.

White, N.M., McDonald, R.J. (2002). Multiple parallel memory systems in the brain of the rat. *Neurobiol Learn Mem*, 77, 125-184.

Witter, M.P., Wouterlood, F.G., Naber, P.A., Van Haeften, T. (2000). Anatomical organization of the parahippocampal-hippocampal network. *Ann N Y Acad Sci*, 911, 1-24.

Wong-Riley, M. (1979). Changes in the visual system of monocularly sutured or enucleated cats demonstrable with cytochrome oxidase histochemistry. *Brain Res*, 171, 11-28.

World Health Organization. (2003). *WHO Global Burden of Disease: 2002 Global Summary*. Geneva, Switzerland: World Health Organization.

Wright, G., Davies, N.A., Shawcross, D.L., Hodges, S.J., Zwingmann, C., Brooks, H.F., Mani, A.R., Harry, D., Stadlbauer, V., Zou, Z., Williams, R., Davies, C., Moore, K.P., Jalan, R. (2007). Endotoxemia produces coma and brain swelling in bile duct ligated rats. *Hepatology*, 45, 1517-1526.

Xianong, L., Irving, S.B., Barry, A. (2002). Reproducible production of thioacetamide-induced macronodular cirrhosis in the rat with no mortality. *J Hepatol*, 36, 488-493.

Yadav, S.K., Srivastaba, A., Thomas, M.A., Agarwal, J., Pandey, C.M., Lal, R., Dacha, S.K., Saraswat, V.A., Gupta, R.K. (2010). Encephalopathy assessment in children with

extra-hepatic portal vein obstruction with MR, psycometry and critical flicker frequency. *J Hepatology*, 52, 348-354.

Young, J.J., Shapiro, M.L. (2011). Dynamic coding of goal-directed paths by orbital prefrontal cortex. *J Neurosci*, 31, 5989-6000.

Zhan, T., Stremmel, W. (2012). The diagnosis and treatment of minimal hepatic encephalopathy. *Dtsch Arztebl Int*, 109, 180-187.

Zhang, P., Lokuta, K.M., Turner, D.E., Liu, B. (2010). Synergistic dopaminergic neurotoxicity of manganese and lipopolysaccharide: differential involvement of microglia and astroglia. *J Neurochem*., 112, 434-443.

Zieve, L. (1987). Pathogenesis of hepatic encephalopathy. *Metab Brain Dis*, 2, 147-165.

Hindawi Publishing Corporation
International Journal of Hypertension
Volume 2013, Article ID 390872, 7 pages
http://dx.doi.org/10.1155/2013/390872

Research Article

Mapping Metabolic Brain Activity in Three Models of Hepatic Encephalopathy

Natalia Arias,[1] Marta Méndez,[1] Camino Fidalgo,[1] María Ángeles Aller,[2] Jaime Arias,[2] and Jorge L. Arias[1]

[1] *Laboratorio de Neurociencias, Departamento de Psicología, Universidad de Oviedo, Plaza Feijoo s/n., 33003 Oviedo, Spain*
[2] *Departamento de Cirugía I, Facultad de Medicina, Universidad Complutense de Madrid, Ciudad Universitaria s/n., 28040 Madrid, Spain*

Correspondence should be addressed to Jorge L. Arias; jarias@uniovi.es

Received 28 November 2012; Accepted 19 February 2013

Academic Editor: Natalia de las Heras

Cirrhosis is a common disease in Western countries. Liver failure, hyperammonemia, and portal hypertension are the main factors that contribute to human cirrhosis that frequently leads to a neuropsychiatric disorder known as hepatic encephalopathy (HE). In this study, we examined the differential contribution of these leading factors to the oxidative metabolism of diverse brain limbic system regions frequently involved in memory process by histochemical labelling of cytochrome oxidase (COx). We have analyzed cortical structures such as the infralimbic and prelimbic cotices, subcortical structures such as hippocampus and ventral striatum, at thalamic level like the anterodorsal, anteroventral, and mediodorsal thalamus, and, finally, the hypothalamus, where the mammillary nuclei (medial and lateral) were measured. The severest alteration is found in the model that mimics intoxication by ammonia, followed by the thioacetamide-treated group and the portal hypertension group. No changes were found at the mammillary bodies for any of the experimental groups.

1. Introduction

Portal hypertension is one of the main complications of human cirrhosis that frequently leads to a neuropsychiatric disorder known as hepatic encephalopathy (HE). The genesis of portal hypertension implies an increase in vascular resistance that can occur at any level within the portal venous system [1]. Elevated blood flow and brain ammonia levels have been strongly implicated in the pathogenesis of HE [2]. Ammonia is a common etiological factor in HE as well as in various hyperammonemic conditions, including inborn errors of the urea cycle, Reye's syndrome, valproate toxicity, idiopathic hyperammonemia, and other conditions [3–6]. Elevated ammonia and its chief metabolite, glutamine, are believed to be important factors responsible for altered cerebral functions, including multiple neurotransmitter system failures, altered bioenergetics, and oxidative stress [7].

Likewise, patients with liver disease have HE, which incorporates a spectrum of manifestations including psychomotor dysfunction, increased reaction time, sensory abnormalities, and poor concentration [8]. Depending on the definition used, HE prevalence varies between 30–84% in patients with cirrhosis [9], a common disease in Western countries [10]. In humans, few studies have been carried out on memory alterations in patients with cirrhosis who develop HE, and, although some authors argue that memory disturbances are not a major symptom of HE [11], others state that patients with HE present clear mnesic alterations. Hence, Bahceci et al. [12] found a poorer performance in several memory tests in patients with cirrhosis, whereas Ortiz et al. [13] showed a learning deficit and impairment in long-term memory.

Taken together, liver disease, portal hypertension, and hyperammonemia appear to be the main contributing factors that lead to the occurrence of HE.

According to the proposal of Butterworth et al. [14], HE is reclassified into different types, depending on its origin or cause. Type B concerns HE related to portosystemic shunt,

which does not necessarily involve any hepatocytic alteration and includes portocaval shunt, partial ligature of the portal vein, and triple portal vein ligation [15]. Type C is associated with chronic liver failure (cirrhosis). As HE can be derived from different causes, diverse experimental models have been developed to reproduce the characteristics of HE as closely as possible and to study brain dysfunction in this syndrome [14]. In this study, we try to isolate the main factors leading to HE through the use of three experimental models: portal hypertension, hyperammonemia, and thioacetamide. Portal hypertension by triple portal vein ligation [16] involves collateral circulation but with a discrete hepatocellular insufficiency. The model of hyperammonemia [17] allowed us to study the effect of ammonia as a toxic brain substance but it lacks also liver failure [18]. Therefore, to explore cirrhosis, a model of chronic thioacetamide administration was used [19].

Difficulties learning diverse types of tasks have been shown in these experimental models, such as classical conditioning [20], conditional discrimination [21, 22], reference [23], and working memory [24]. However, less is known about the specific role of liver failure, portal hypertension, and hyperammonemia in the development of bioenergetic brain disturbances.

The aim of this study is to elucidate the differential contribution of these leading factors to the oxidative metabolism of diverse brain limbic system regions frequently involved in memory process by histochemical labelling of cytochrome oxidase (COx). COx is a mitochondrial enzyme involved in the phosphorylation process that generates ATP. This energy is used to maintain the resting membrane potential and the synthesis of molecules and neurotransmitters, among other functions [25]. Because metabolic activity is tightly coupled with neuronal activity, this technique can be used as an index of regional functional activity in the brain, reflecting changes in tissue metabolic capacity induced by sustained energy requirements of the nervous system associated with learning [23, 26].

2. Material and Methods

2.1. Subject. A total of 28 male adult Wistar rats were used (230–260 g at the start of the experiments) from the animalarium of Oviedo University. All the animals had ad libitum access to food and tap water and were maintained under standard laboratory conditions (20–22°C, 65–70% relative humidity, and a 12 h light/dark cycle). The procedures and manipulation of the animals used in this study were carried out according to the European Parliament and the Council of the European Union 2010/63/UE and were approved by the Oviedo University committee for animal studies.

2.2. Procurement of Experimental Models. The animals were randomly distributed into 3 groups: portal hypertension (PH group, $n = 12$), hyperammonemia (HA group, $n = 8$), and animals with cirrhosis by administration of thioacetamide (TAA group, $n = 8$). The surgical procedures and protocols used for the different experimental models are described below.

2.2.1. Portal Hypertension. The portal hypertension model was carried out under induction of anaesthesia by i.m. injection of ketamine (100 mg/kg) and xylacine (12 mg/kg). A midline abdominal incision was performed and a part of the intestinal loops was gently shifted to the left and covered with saline-moistened gauze. The portal vein was isolated along its length. Portal hypertension was produced by triple partial ligation [16]. Three stenosing ligatures were performed in the superior, medial, and inferior portions of the portal vein, respectively, and maintained in position by the previous fixation of the ligatures to a sylastic guide. The stenoses were also calibrated by a simultaneous ligature (3–0 silk) around the portal vein and a 20 G needle. The abdominal incision was closed in two layers with an absorbable suture (polyglycolic acid) and 3–0 silk. With respect to postsurgical care, the rats were maintained close to a source of heat until they recovered consciousness (10–15 min) to avoid postoperative hypothermia. Brains were assessed 45 days later.

2.2.2. Thioacetamide. The method used to produce cirrhosis was weekly administration of thioacetamide (Sigma, Germany) in drinking water as described by Li et al. [19]. The thioacetamide (TAA) was administered for 12 weeks and its concentration was modified weekly depending on the animals' weight gain or weight loss. The initial concentration of TAA was 0.03%. After twelve weeks of treatment, they were placed in groups of 5 rats per cage and they were assessed after two weeks. During this period, the animals received TAA at 0.04%.

2.2.3. Hyperammonemia. The method used to produce hyperammonemia was performed according to Azorín et al. [17]. Briefly, the animals were fed with a standard diet supplemented with ammonium acetate ad libitum for up to 27 days.

2.3. Cytochrome Oxidase Histochemistry. 90 minutes after the performance of a spatial reference memory task, animals were decapitated, and the brains were removed intact, frozen rapidly in isopentane (Sigma-Aldrich), and stored at −40°C. Coronal sections (30 μm) of the brain were cut at −20°C in a cryostat (Leica CM1900, Germany) and were mounted on slides.

We used a quantitative COx histochemistry described by Gonzalez-Lima and Cada [25]. To quantify enzymatic activity and to control staining variability across different baths of staining, sets of tissue homogenate standards obtained from Wistar rat brains were included with each bath of slides. These standards were cut at different thicknesses (10, 30, 40, and 60 μm).

Sections and standards were incubated for 5 min in 0.1 M phosphate buffer with 10% w/v sucrose and 0.5% v/v glutaraldehyde, pH 7.6. After this, four baths of 0.1 M phosphate buffer with 10% w/v sucrose were given for 5 min each. Then 0.05 M Tris buffer, pH 7.6, with 275 mg/L cobalt

chloride, 10% w/v sucrose, and 0.5% v/v dimethylsulfoxide were applied for 10 min, to enhance staining contrast. Subsequently, sections and standards were incubated in a solution of 0.06 g cytochrome c (Sigma, St. Louis, MO, USA), 0.016 g catalase, 40 g sucrose, 2 mL dimethylsulfoxide, and 0.4 g diaminobenzidine tetrahydrochloride in 800 mL of 0.1 M phosphate buffer, at 37°C for 1 h. The reaction was stopped by fixing the tissue in buffered formalin for 30 min at room temperature with 10% w/v sucrose and 4% v/v formalin. Finally, the slides were dehydrated in series of ethanol baths (from 30% to 100% v/v ethanol), cleared with xylene, and coverslipped with Entellan (Merck, Germany).

2.3.1. Quantification. Quantification of COx histochemical staining intensity was done by densitometric analysis using a computer-controlled image analysis workstation (MCID, InterFocus Imaging Ltd., Linton, England) made up of a high-precision illuminator, a digital camera, and a computer with specific software for image analysis. The mean optical density (OD) of each structure was measured on the right side of the bilateral structures using three consecutive sections of each animal. In each section, four nonoverlapping readings were taken using a square-shaped sampling window that was adjusted for each region size. A total of twelve measurements were taken per region. These twelve measurements were averaged to obtain one mean per region for each subject. OD values were then converted to COx activity units, determined by the enzymatic activity of the standards which were measured spectrophotometrically [25]. Measurements were performed by an investigator blind to the groups.

The regions of interest were anatomically defined according to Paxinos and Watson (2005) [27]. The regions of interest and the distance in mm of the regions counted from bregma were: +3.20 mm for prefrontal cortex (the infralimbic cortex and prelimbic cortex (IL and PL, resp.), +2.28 mm for ventral striatum (accumbens core and shell, AcC and AcS), −1.40 for the anterodorsal thalamus (ADT), the anteroventral thalamus (AVT), and the mediodorsal (MDT), −1.20 mm for the CA1, CA3, and the dentate gyrus (DG) subfields of the dorsal hippocampus, and +4.52 mm for the medial part of the medial mammillary nucleus (mMM), the lateral part of the medial mammillary nucleus (lMM), and the lateral mammillary nucleus (LM). See Figure 1.

2.4. Data Analysis. All data were analyzed in the Sigma-Stat 3.2 program (Systat, Richmond, USA) and were expressed as mean ± SEM. A one-way analysis of variance was performed (factor: group). When a significant effect was found post hoc paired Tukey's test was carried out. The results were considered as statistically significant if $P < 0.05$.

3. Results

The post hoc paired Tukey's tests showed differences between groups in their prefrontal cortex COx activity. The HA group showed higher activity than the PH and TAA groups in the PL ($F2, 24 = 47.674$) ($P < 0.001$), and the TAA group also showed higher activity than the PH group ($P < 0.001$). In the IL, the same difference between the HA group and the other groups was found ($F2, 24 = 53.649$, $P < 0.001$). In the ventral striatum, the same pattern of metabolic activity was found in the AcC and AcS, with the HA group showing higher activity, followed by the TAA group, which differed from the PH group ($F2, 25 = 69.662$, $P < 0.001$; $F2, 25 = 76.819$, $P < 0.01$, resp.). These differences were also found in the ADT ($F2, 25 = 63.441$, $P < 0.001$). However, in the AVT ($F2, 25 = 13.610$, $P < 0.05$) and MDT ($F2, 25 = 27.970$, $P < 0.001$), differences were only found when comparing the HA group with the other experimental groups, with the former group being the most highly activated. Examining the dorsal hippocampus, in the DG, the HA group showed higher activity than the PH and TAA groups ($F2, 25 = 47.402$, $P < 0.01$), and the TAA group showed greater activity than the PH group ($P < 0.001$). Similarly, in CA3, the HA group was the most highly activated in relation to the other two groups ($F2, 25 = 63.059$, $P < 0.001$), and the TAA group showed lower activity than the PH group ($P < 0.001$). In CA1, the highest metabolic activity was found in the HA group, which presented differences with the PH and the TAA groups ($F2, 25 = 16.954$, $P < 0.001$). Finally, no differences were found in any of the mammillary nuclei explored: mMM ($F2, 24 = 0.109$, $P = 0.898$), lMM ($F2, 24 = 1.368$, $P = 0.274$), and LM ($F2, 23 = 0.178$, $P = 0.838$). See Table 1.

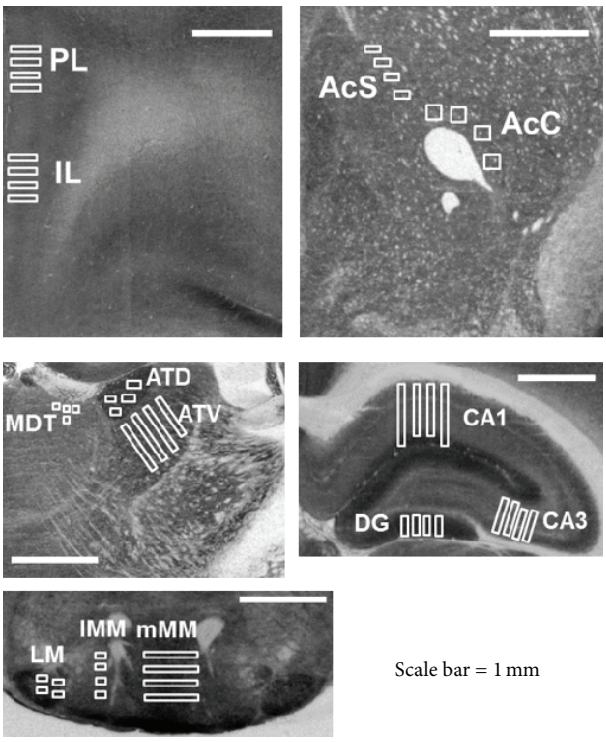

Figure 1: Cytochrome oxidase (COx) histochemistry in the sampled regions in which the squares used to take the measures were presented. Prelimbic (PL) and infralimbic (IL) cortex, accumbens core and shell (AcC and AcS), thalamic nuclei (ADT, AVT, and MDT), dorsal hippocampus (CA1, CA3, and DG) and Mammillary nuclei (mMM, lMM, and LM). Scale bar: 1 mm.

Table 1: Metabolic activity of the selected brain regions in the studied groups.

	PH	HA	TAA
Prefrontal cortex			
PL	18.364 ± 0.460[a,b]	26.781 ± 1.032	22.591 ± 0.379[a]
IL	18.470 ± 0.504[a]	26.988 ± 0.916	19.432 ± 0.401[a]
Ventral Striatum			
AcC	21.362 ± 0.395[a,b]	31.812 ± 1.032	25.552 ± 0.498[a]
AcS	22.210 ± 0.748[a,b]	36.940 ± 1.227	32.409 ± 0.715[a]
Thalamic nuclei			
ADT	30.525 ± 0.736[a,b]	50.930 ± 2.024	40.025 ± 1.302[a]
AVT	24.717 ± 0.525[a]	31.753 ± 1.412	27.631 ± 1.120[a]
MDT	19.307 ± 0.879[a]	27.361 ± 0.809	18.242 ± 0.921[a]
Hippocampus			
DG	23.413 ± 0.500[a,b]	39.550 ± 1.75	32.663 ± 1.739[a]
CA3	16.318 ± 0.488[a,b]	22.633 ± 0.763	12.592 ± 0.568[a]
CA1	18.128 ± 0.707[a]	24.820 ± 0.915	18.250 ± 0.915[a]
Mammillary nuclei			
mMM	22.949 ± 1.151	23.490 ± 1.336	23.769 ± 1.479
lMM	17.643 ± 0.950	16.792 ± 0.633	15.777 ± 0.597
LM	25.923 ± 1.113	26.624 ± 1.246	26.665 ± 0.489

Values are mean ± SEM.
PH: portal hypertension, HA: hyperammonemia, TAA: thioacetamide.
[a] $P < 0.05$ statistically significant value in relation to HA.
[b] $P < 0.05$ statistically significant value in relation to TAA.

4. Discussion

The rationale for the present study arose from evidence that cerebral metabolic rate for glucose has consistently been reported to be decreased in patients with chronic HE, suggesting that hypometabolism contributes to the neuropsychiatric symptoms commonly observed in HE. In fact, it has been shown that cerebral oxygen metabolism and blood flow were decreased in cirrhotic patients with HE [28], and cognitive deficits are closely related to aberrant baseline brain activity measured by fMRI in these patients [29]. However, the existence of a differential contribution of factors, such as portal hypertension, hyperammonemia, and liver disease, to brain metabolic activity has not yet been explored. In this study, we demonstrated that each of these factors affects brain energy requirements to a different extent.

Several studies have assessed these experimental models in a spatial reference memory task. Whereas the portal hypertension model showed only mild impairment in this learning process [23], hyperammonemia and liver failure models were severely affected (Arias et al., unpublished results [30]).

Traditionally, the hippocampus has been widely shown to be involved in reference memory [31]. Specifically, it is important in establishing allocentric relations [32] and also seems to be responsible for correct goal recognition [33]. Together with this brain structure, prefrontal cortex, ventral striatum, anterior thalamus, and mammillary bodies cooperate in diverse memory processes and learning tasks [34, 35]. The role of the prefrontal cortex in the organization of spatially directed behaviours has been shown both in primates and humans. In rats, the main evidence comes from lesion studies in performance of various spatial tasks such as spatial alternation, spatial reversal, elimination in the radial maze, and navigation in the Morris water maze [36]. The connections between this prefrontal cortex and ventral striatum play a role in the transformation of route planning into motor response in memory tasks [37]. Likewise, the prefrontal cortex receives projections from the anterior thalamic nucleus [38], damage to which impairs allocentric memory tasks that are also disrupted by hippocampal dysfunctions [39]. The mammillary nuclei, which can be subdivided into the medial and lateral parts, are connected with the hippocampus and send projections to the anterior thalamus [40] and are involved in spatial memory processes [41, 42].

When we wondered about the possible time-dependent involvement of these structures in the spatial reference memory, we found that most of them were differentially implicated at the beginning and the conclusion of the task in nonpathological conditions [43]. That is, some structures, such as the anterior thalamic nuclei and the mammillary bodies, seem to be more involved in early task acquisition, but it is necessary for these structures to reduce their energy requirements in order to successfully complete the task. But other structures, such as DG, CA3, and the prefrontal cortex, showed an opposite pattern [43].

In view of this tendency, we were willing to explore the metabolic activity of the main contributing factors of HE. Accordingly to our expectations, the portal hypertension group reduced its metabolic activity in almost all studied

regions compared to the other groups. A possible explanation for this behaviour, so similar to that of nonpathological subjects, is that, in the PH model, portosystemic collaterals develop as a consequence of high pressure in the portal vein and ameliorate the increased resistance [1, 44]. However, a different situation takes place in the HA group, in which the energetic demands increase above conventional levels. This increase in oxygen utilization could be due to an inflammation in these areas of the central nervous system [45]. Inflammation will increase the use of oxygen, represented by excess production of reactive oxygen and nitrogen species, which cause oxidative and nitrosative stress [46–48].

Several studies have shown that once ammonia crosses the blood brain barrier, it is immediately used to amidate glutamate to glutamine in the astrocytes in order to prevent its toxicity from damaging the neurons. But this depletion of the substrate of the tricarboxylic acid cycle together with the inhibition by the ammonia to rate limit enzymes such as pyruvate dehydrogenase and α-ketoglutarate will slow down overall oxidative metabolism, leading to depletion of energy-rich phosphate compounds [49]. Moreover, glutamatergic neurotransmission suffers disturbances owing to the fact that ammonia impairs the induction of NMDA receptors, which alters the neural glutamate-nitric oxide cyclic GMP pathway, in turn, involved in learning and memory [20, 21].

At the same time, glutamine, which is an osmotically powerful substance, increases due to ammonia in the brain and can provoke a rapid brain edema, triggering intracranial hypertension. During liver failure, high arterial ammonia levels lead to accumulation in the brain [50] and exert numerous deleterious effects, contributing to the clinical presentation of HE. Subsequent studies carried out in various animal models of acute and chronic HE, such as our TAA model, have reported altered glucose utilization similar to the HA models [51]. But, whereas patients with liver cirrhosis have a compensatory mechanism that prevents the occurrence of brain edema and intracranial hypertension [18], the hyperammonemic brain cannot establish these mechanisms.

Another possible mechanism for impaired energy metabolism in HA is the mitochondrial permeability transition of the inner membrane, which has a critical linkage with disturbed cerebral energy metabolism and oxidative/nitrosative stress [51]. Similar to free radicals, nitric oxide increases in the brain of the TAA-administration rat model [52]. A possible explanation for the alteration of COx activity would be the increased level of oxidative stress [45]. Liver disease is associated with the production of free radicals that override the balance between oxidative stress and antioxidative mechanisms, leading to oxidative stress. Oxidative stress could play a role in the pathogenesis of HE, due to the fact that the brain of patients with HE is particularly susceptible to oxidative damage [47]. Peroxidase damage and increased oxidative stress have been reported in neural membranes of rats with thioacetamide-induced HE [53] and in diverse central nervous system regions of the same animal model [54]. Brain oxidative and nitrosative (superoxide anion with nitric oxide produces peroxynitrite) stress in cirrhotic rats could cause neural mitochondrial damage and defective oxidative phosphorylation, which is reflected in impaired COx activity. Therefore, oxidative and nitrosative stress caused activation of the nuclear factor KB, which is the major inducer of proinflammatory cytokines and chemokines.

The differences found in bioenergetic requirements could indicate a differential affectation of the neural networks underlying different behaviours, so a broad field of future research opens up.

In conclusion, the results obtained show that there is a differential contribution of portal hypertension, hyperammonemia, and liver disease to the brain metabolic dysfunction associated with HE. The most interesting finding is that the alterations in metabolic brain activity do not develop equally in the three models. The severest alteration is found in the model that mimics intoxication by ammonia, where the main cerebral structures have to make a big effort in comparison with the other two experimental models.

Acknowledgments

The authors would like to thank Dr. Vicente Felipo for his helpful assistance during the hyperammonemia model development. This research was supported by Grants MICINN PSI2010-19348, FMMA AP/6977-2009, and MEC AP2009-1714 to N. Arias.

References

[1] C. Miñano and G. Garcia-Tsao, "Clinical pharmacology of portal hypertension," *Gastroenterology Clinics of North America*, vol. 39, no. 3, pp. 681–695, 2010.

[2] R. F. Butterworth, "Pathophysiology of hepatic encephalopathy: a new look at ammonia," *Metabolic Brain Disease*, vol. 17, no. 4, pp. 221–227, 2002.

[3] S. W. Brusilow, "Hyperammonemic encephalopathy," *Medicine*, vol. 81, no. 3, pp. 240–249, 2002.

[4] R. F. Butterworth, "Pathophysiology of hepatic encephalopathy: the ammonia hypotheses revisited," in *Progress in Hepatic Encephalopathy and Metabolic Nitrogen Exchange*, F. Bengtsson, B. Jeppsson, T. Aamdal, and H. Vistrup, Eds., pp. 9–24, CRC Press, Boca Raton, Fla, USA, 2001.

[5] A. J. L. Cooper and F. Plum, "Biochemistry and physiology of brain ammonia," *Physiological Reviews*, vol. 67, no. 2, pp. 440–519, 1987.

[6] C. O. Record, "Neurochemistry of hepatic encephalopathy," *Gut*, vol. 32, no. 11, pp. 1261–1263, 1991.

[7] K. V. R. Rao and M. D. Norenberg, "Cerebral energy metabolism in Hepatic encephalopathy and hyperammonemia," *Metabolic Brain Disease*, vol. 16, no. 1-2, pp. 67–78, 2001.

[8] D. L. Shawcross, G. Wright, S. W. M. Olde Damink, and R. Jalan, "Role of ammonia and inflammation in minimal hepatic encephalopathy," *Metabolic Brain Disease*, vol. 22, no. 1, pp. 125–138, 2007.

[9] M. Groeneweg, J. C. Quero, I. De Bruijn et al., "Subclinical hepatic encephalopathy impairs daily functioning," *Hepatology*, vol. 28, no. 1, pp. 45–49, 1998.

[10] World Health Organization, *WHO Global Burden of Disease: 2002 Global Summary*, World Health Organization, Geneva, Switzerland, 2003.

[11] K. Weissenborn, S. Heidenreich, K. Giewekemeyer, N. Rückert, and H. Hecker, "Memory function in early hepatic encephalopathy," *Journal of Hepatology*, vol. 39, no. 3, pp. 320–325, 2003.

[12] F. Bahceci, B. Yildirim, M. Karincaoglu, I. Dogan, and B. Sipahi, "Memory impairment in patients with cirrhosis," *Journal of the National Medical Association*, vol. 97, no. 2, pp. 213–216, 2005.

[13] M. Ortiz, J. Córdoba, C. Jacas, M. Flavià, R. Esteban, and J. Guardia, "Neuropsychological abnormalities in cirrhosis include learning impairment," *Journal of Hepatology*, vol. 44, no. 1, pp. 104–110, 2006.

[14] R. F. Butterworth, M. D. Norenberg, V. Felipo, P. Ferenci, J. Albrecht, and A. T. Blei, "Experimental models of hepatic encephalopathy: ISHEN guidelines," *Liver International*, vol. 29, no. 6, pp. 783–788, 2009.

[15] M. J. Orloff, "Portal hypertension and portocaval shunt," in *Surgical Research*, W. W. Souba and D. W. Wilmore, Eds., vol. 49, pp. 637–701, Academic Press, London, UK, 2001.

[16] B. Diéguez, M. A. Aller, M. P. Nava et al., "Chronic portal hypertension in the rat by triple-portal stenosing ligation," *Journal of Investigative Surgery*, vol. 15, no. 6, pp. 329–336, 2002.

[17] I. Azorín, M. D. Miñana, V. Felipo, and S. Grisolía, "A simple animal model of hyperammonemia," *Hepatology*, vol. 10, no. 3, pp. 311–314, 1989.

[18] R. Jover, E. de Madaria, V. Felipo, R. Rodrigo, A. Candela, and A. Compañ, "Animal models in the study of episodic hepatic encephalopathy in cirrhosis," *Metabolic Brain Disease*, vol. 20, no. 4, pp. 399–408, 2005.

[19] X. Li, I. S. Benjamin, and B. Alexander, "Reproducible production of thioacetamide-induced macronodular cirrhosis in the rat with no mortality," *Journal of Hepatology*, vol. 36, no. 4, pp. 488–493, 2002.

[20] M. A. Aguilar, J. Miñarro, and V. Felipo, "Chronic moderate hyperammonemia impairs active and passive avoidance behavior and conditional discrimination learning in rats," *Experimental Neurology*, vol. 161, no. 2, pp. 704–713, 2000.

[21] S. Erceg, P. Monfort, M. Hernández-Viadel, R. Rodrigo, C. Montoliu, and V. Felipo, "Oral administration of sildenafil restores learning ability in rats with hyperammonemia and with portacaval shunts," *Hepatology*, vol. 41, no. 2, pp. 299–306, 2005.

[22] P. Monfort, S. Erceg, B. Piedrafita, M. Llansola, and V. Felipo, "Chronic liver failure in rats impairs glutamatergic synaptic transmission and long-term potentiation in hippocampus and learning ability," *European The Journal of Neuroscience*, vol. 25, no. 7, pp. 2103–2111, 2007.

[23] N. Arias, M. Méndez, J. Arias, and J. L. Arias, "Brain metabolism and spatial memory are affected by portal hypertension," *Metabolic Brain Disease*, vol. 27, no. 2, pp. 183–191, 2012.

[24] M. Méndez, M. Méndez-López, L. López, M. A. Aller, J. Arias, and J. L. Arias, "Associative learning deficit in two experimental models of hepatic encephalopathy," *Behavioural Brain Research*, vol. 198, no. 2, pp. 346–351, 2009.

[25] F. Gonzalez-Lima and A. Cada, "Cytochrome oxidase activity in the auditory system of the mouse: a qualitative and quantitative histochemical study," *Neuroscience*, vol. 63, no. 2, pp. 559–578, 1994.

[26] M. Méndez, M. Méndez-López, L. López, M. A. Aller, J. Arias, and J. L. Arias, "Portosystemic hepatic encephalopathy model shows reversal learning impairment and dysfunction of neural activity in the prefrontal cortex and regions involved in motivated behavior," *Journal of Clinical Neuroscience*, vol. 18, no. 5, pp. 690–694, 2011.

[27] G. Paxinos and Ch. Watson, *The Rat Brain in Stereotaxic Coordinates—The New Coronal Set*, Elsevier Academic Press, London, UK, 5th edition, 2005.

[28] G. Dam, S. Keiding, O. L. Munk et al., "Hepatic encephalopathy is associated with decreased ammonia uptake," *Hepatology*, vol. 57, no. 1, pp. 258–265, 2012.

[29] H. J. Chen, X. Q. Zhu, Y. Jiao, P. C. Li, Y. Wang, and G. J. Teng, "Abnormal baseline brain activity in low-grade hepatic encephalopathy: a resting-state fMRI study," *Journal of Neurological Sciences*, vol. 318, no. 1-2, pp. 140–145, 2012.

[30] M. Mendez, M. Mendez- Lopez, L. Lopez et al., "Spatial memory alterations in three models of hepatic encephalopathy," *Behavioural Brain Research*, vol. 188, pp. 32–40, 2008.

[31] R. D'Hooge and P. P. de Deyn, "Applications of the Morris water maze in the study of learning and memory," *Brain Research Reviews*, vol. 36, no. 1, pp. 60–90, 2001.

[32] R. G. M. Morris, P. Garrud, J. N. P. Rawlins, and J. O'Keefe, "Place navigation impaired in rats with hippocampal lesions," *Nature*, vol. 297, no. 5868, pp. 681–683, 1982.

[33] S. A. Hollup, K. G. Kjelstrup, J. Hoff, M. B. Moser, and E. I. Moser, "Impaired recognition of the goal location during spatial navigation in rats with hippocampal lesions," *The Journal of Neuroscience*, vol. 21, no. 12, pp. 4505–4513, 2001.

[34] E. Irle and H. J. Markowitsch, "Connections of the hippocampal formation, mamillary bodies, anterior thalamus and cingulate cortex. A retrograde study using horseradish peroxidase in the cat," *Experimental Brain Research*, vol. 47, no. 1, pp. 79–94, 1982.

[35] A. E. Kelley, V. B. Domesick, and W. J. H. Nauta, "The amygdalostriatal projection in the rat. An anatomical study by anterograde and retrograde tracing methods," *Neuroscience*, vol. 7, no. 3, pp. 615–630, 1982.

[36] B. Delatour and P. Gisquet-Verrier, "Functional role of rat prelimbic-infralimbic cortices in spatial memory: evidence for their involvement in attention and behavioural flexibility," *Behavioural Brain Research*, vol. 109, no. 1, pp. 113–128, 2000.

[37] S. B. Floresco, J. K. Seamans, and A. G. Phillips, "Selective roles for hippocampal, prefrontal cortical, and ventral striatal circuits in radial-arm maze tasks with or without a delay," *The Journal of Neuroscience*, vol. 17, no. 5, pp. 1880–1890, 1997.

[38] V. Ghiglieri, C. Sgobio, C. Costa, B. Picconi, and P. Calabresi, "Striatum-hippocampus balance: from physiological behavior to interneuronal pathology," *Progress in Neurobiology*, vol. 94, no. 2, pp. 102–114, 2011.

[39] M. Wolff, S. J. Gibb, J. C. Cassel, and J. C. Dalrymple-Alford, "Anterior but not intralaminar thalamic nuclei support allocentric spatial memory," *Neurobiology of Learning and Memory*, vol. 90, no. 1, pp. 71–80, 2008.

[40] S. D. Vann and J. P. Aggleton, "The mammillary bodies: two memory systems in one?" *Nature Reviews Neuroscience*, vol. 5, no. 1, pp. 35–44, 2004.

[41] L. J. Santín, J. A. Aguirre, S. Rubio, A. Begega, R. Miranda, and J. L. Arias, "c-fos expression in supramammillary and medial mammillary nuclei following spatial reference and working memory tasks," *Physiology and Behavior*, vol. 78, no. 4-5, pp. 733–739, 2003.

[42] V. Sziklas and M. Petrides, "Selectivity of the spatial learning deficit after lesions of the mammillary region in rats," *Hippocampus*, vol. 10, no. 3, pp. 325–328, 2000.

[43] N. M. Conejo, H. González-Pardo, F. Gonzalez-Lima, and J. L. Arias, "Spatial learning of the water maze: progression of brain circuits mapped with cytochrome oxidase histochemistry,"

Neurobiology of Learning and Memory, vol. 93, no. 3, pp. 362–371, 2010.

[44] M. Méndez-López, M. Méndez, F. Sánchez-Patán et al., "Partial portal vein ligation plus thioacetamide: a method to obtain a new model of cirrhosis and chronic portal hypertension in the rat," *Journal of Gastrointestinal Surgery*, vol. 11, no. 2, pp. 187–194, 2007.

[45] J. L. Arias, M. A. Aller, F. Sánchez-Patan, and J. Arias, "The inflammatory bases of hepatic encephalopathy," *European Journal of Gastroenterology and Hepatology*, vol. 18, no. 12, pp. 1297–1310, 2006.

[46] M. D. Norenberg, "Oxidative and nitrosative stress in ammonia neurotoxicity," *Hepatology*, vol. 37, no. 2, pp. 245–248, 2003.

[47] M. D. Norenberg, A. R. Jayakumar, and K. V. R. Rao, "Oxidative stress in the pathogenesis of hepatic encephalopathy," *Metabolic Brain Disease*, vol. 19, no. 3-4, pp. 313–329, 2004.

[48] C. Nathan, "Specificity of a third kind: reactive oxygen and nitrogen intermediates in cell signaling," *Journal of Clinical Investigation*, vol. 111, no. 6, pp. 769–778, 2003.

[49] P. N. Bjerring, M. Eefsen, B. A. Hansen, and F. S. Larsen, "The brain in acute liver failure. A tortuous path from hyperammonemia to cerebral edema," *Metabolic Brain Disease*, vol. 24, no. 1, pp. 5–14, 2009.

[50] S. Keiding, M. Sørensen, D. Bender, O. L. Munk, P. Ott, and H. Vilstrup, "Brain metabolism of ^{13}N-ammonia during acute hepatic encephalopathy in cirrhosis measured by positron emission tomography," *Hepatology*, vol. 43, no. 1, pp. 42–50, 2006.

[51] K. V. R. Rao and M. D. Norenberg, "Brain energy metabolism and mitochondrial dysfunction in acute and chronic hepatic encephalopathy," *Neurochemistry International*, vol. 60, no. 7, pp. 697–706, 2012.

[52] R. Hernández, E. Martínez-Lara, M. L. Del Moral et al., "Upregulation of endothelial nitric oxide synthase maintains nitric oxide production in the cerebellum of thioacetamide cirrhotic rats," *Neuroscience*, vol. 126, no. 4, pp. 879–887, 2004.

[53] I. Swapna, K. V. SathyaSaikumar, C. R. K. Murthy, A. Dutta-Gupta, and B. Senthilkumaran, "Changes in cerebral membrane lipid composition and fluidity during thioacetamide-induced hepatic encephalopathy," *Journal of Neurochemistry*, vol. 98, no. 6, pp. 1899–1907, 2006.

[54] K. V. SathyaSaikumar, I. Swapna, P. V. B. Reddy et al., "Fulminant hepatic failure in rats induces oxidative stress differentially in cerebral cortex, cerebellum and pons medulla," *Neurochemical Research*, vol. 32, no. 3, pp. 517–524, 2007.

II

Metab Brain Dis (2014) 29:113–120
DOI 10.1007/s11011-013-9477-0

ORIGINAL PAPER

The effects of hyperammonemia in learning and brain metabolic activity

Natalia Arias · Camino Fidalgo · Vicente Felipo · Jorge L. Arias

Received: 10 October 2013 / Accepted: 23 December 2013 / Published online: 12 January 2014

Abstract Ammonia is thought to be central in the development of hepatic encephalopathy. However, the specific relation of ammonia with brain energy depletions and learning has not been studied. Our work attempts to reproduce an increase in rat cerebral ammonia level, study the hyperamonemic animals' performance of two learning tasks, an allocentric (ALLO) and a cue guided (CG) task, and elucidate the contribution of hyperammonemia to the differential energy requirements of the brain limbic system regions involved in these tasks. To assess these goals, four groups of animals were used: a control (CHA) CG group (n=10), a CHA ALLO group (n=9), a hyperammonemia (HA) CG group (n=7), and HA ALLO group (n=8). Oxidative metabolism of the target brain regions were assessed by histochemical labelling of cytochrome oxidase (C.O.). The behavioural results revealed that the hyperammonemic rats were not able to reach the behavioural criterion in either of the two tasks, in contrast to the CHA groups. The metabolic brain consumption revealed increased C.O. activity in the anterodorsal thalamus when comparing the HA ALLO group with the CHA ALLO group. Significant differences between animals trained in the CG task were observed in the prelimbic, infralimbic, parietal, entorhinal and perirhinal cortices, the anterolateral and anteromedial striatum, and the basolateral and central amygdala. Our findings may provide fresh insights to reveal how the differential damage to the brain limbic structures involved in these tasks differs according to the degree of task difficulty.

Keywords Hepatic encephalopathy · Hyperammonemia · Rat · Cytochrome c oxidase · Allocentric task · Cue guided task

N. Arias (✉) · C. Fidalgo · J. L. Arias
Laboratory of Neuroscience, Departamento de Psicología, Universidad de Oviedo, Plaza Feijoo s/n 33003, Oviedo, Spain
e-mail: ariasnatalia@uniovi.es

N. Arias · J. L. Arias
INEUROPA, Instituto de Neurociencias del Principado de Asturias, Oviedo, Spain

V. Felipo
Laboratory of Neurobiology, Centro Investigación Príncipe Felipe, Valencia, Spain

Introduction

Hyperammonemia is considered the most important factor of the neurological alterations found in acute and chronic liver disease (Wang and Saab 2003), although there are other factors, such as inflammation (Aller et al. 2007; Arias et al. 2006 and Shawcross et al. 2007), liver disease (Méndez et al. 2011) and portal hypertension (Arias et al. 2012) that contribute to the neurological alterations found in acute and chronic liver disease (Wang and Saab 2003). Ammonia is a common etiological factor in hepatic encephalopathy (HE) as well as in various hyperammonemic conditions, including inborn errors of the urea cycle, Reye's syndrome, valproate toxicity (Rao and Norenberg 2001) and idiopathic hyperammonemia (Butterworth 1991).

Patients with minimal HE exhibit a decreased ability to perform memory tasks, which appears to be mainly due to deficits in attention and visual perception (Weissenborn et al. 2003). Formerly, several animal models of HE that reproduce some of the neurological alterations found in patients with this disorder displayed impaired conditional discrimination learning in a Y maze and delays in the acquisition of a reference memory task (Aguilar et al. 2000; Erceg et al. 2005 and Azorín et al. 1989).

To discern the contribution of hyperammonemia to the neurological alterations in HE, we developed an animal model of chronic hyperammonemia without liver failure: rats fed an ammonium-containing diet (Azorín et al. 1989). These rats present a level of hyperammonemia similar to that of patients

with liver cirrhosis or of rats with portocaval anastomosis, but they do not present other alterations associated with liver failure and may therefore be considered to be a model of "pure" hyperammonemia (Rodrigo and Felipo 2006).

Multiple navigational strategies in orientation and retention of spatial information have been illustrated both in animals and in humans (Aggleton et al. 2000). But spatial learning and memory are ultimately dependent on searching strategies that can be applied in a spatial orientation task. Thus, rats can use allocentric (place and cue learning) and egocentric strategies to reach a goal (Kolb and Whishaw 2003). We therefore used two testing protocols that may favour an optimal orientation strategy: the first protocol defines the relationship between a goal and another location, where the goal is independent of the subject (allocentric strategy); the second protocol defines the relationship between a goal and the direct approach towards a distinct cue in the environment (cue-guided strategy) (de Bruin et al. 2001). Because these two different learning strategies have been evaluated in our work, the main structures related to these tasks have been taken into account. The hippocampus (Kesner 1990), as well as cortical regions including the frontal, cingulate and parietal areas (Galani et al. 2002), have conventionally been considered to be linked to spatial learning. In fact, the hippocampus and the prefrontal cortex are necessary to encode and store spatial information (Rogers and Kesner 2006). Thus, structures that are connected to these regions, such as the perirhinal and entorhinal cortices, which are part of the main sources of afferent projections to the prelimbic and infralimbic cortices, and the gangliothalamocortical circuits, which exist in analogy with primates (Groenewegen et al. 1990), are involved in these processes. Therefore, the limbic afferents from the prelimbic cortex, the hippocampal formation and the amygdala determine the functioning of the ventral striatum, including the nucleus accumbens (Burns et al. 1996). Finally, it has been shown that lesions in the dorsal and ventral areas of the hippocampal formation impair the working memory for allocentric distance information (Long and Kesner 1996).

The aims of this work were: (i) Identify the crucial limbic brain regions that are affected by this increase in the cerebral ammonia level. (ii) Study to which extent cerebral ammonia level affects learning, accordingly two different strategy tasks, allocentric and cue guided were performed. (iii) Clarify the contribution of hyperammonemia to the differential energy requirements that are necessary to achieve each learning process. To accomplish this goal, oxidative metabolism of diverse brain limbic system regions frequently involved in memory process has been studied by histochemical labelling of cytochrome oxidase (C.O.). C.O. is a mitochondrial enzyme involved in the phosphorylation process that generates ATP. This energy is used to maintain the resting membrane potential and the synthesis of molecules and neurotransmitters, among other functions (González-Lima and Cada 1994). Because metabolic activity is tightly coupled with neuronal activity, C.O. labelling can be used as an index of regional functional activity in the brain, reflecting changes in the tissue metabolic capacity that are induced by the sustained energy requirements of the nervous system associated with learning (Méndez et al. 2011 and Arias et al. 2012).

Materials and methods

Subjects

A total of 34 male Wistar rats weighing between 250 and 300 g were used in this experiment. The animals were obtained from the animalarium of the University of Oviedo and were randomly housed five per cage in a temperature-and humidity-controlled vivarium under a 12-h light/dark cycle (lights on 8.00 A.M.) Experimental procedures were performed in accordance with the Directive of the European Commission (2010/63/EU) and Spanish legislation (R.D. 1201/2005) and approved by the local committee for animal studies.

Procedure of experimental models

The animals were randomly distributed into the following four groups: control cue guided group (CHA CG group, n=10), control allocentric group (CHA ALLO group, n=9), hyperammonemia cue guided group (HA CG group, n=7), and hyperammonemia allocentric group (HA ALLO group, n=8),. Hyperammonemia was induced by feeding a standard diet supplemented with ammonium (30 g per rat and day during 27 days until sacrifice) (Azorín et al. 1989) while control groups were fed the normal diet.

Determination of neurological alterations and motor functions

Neurological test

All animals were handled and evaluated by neurological tests such as flexion reflex, startle reactions, head shacking, righting and equilibrium reflex, placing reactions, grasping and some equilibrium tests. No alteration was displayed by any animal.

Rotarod-accelerod test

This motor performance test consists of a motor-driven rotating rod that enables researchers to assess motor coordination and resistance to fatigue (Jones and Roberts 1968). The accelerating rotarod 7750 of Ugo Basile (Ugo Basile Biological Research Apparatus, Italy) was used for the rats. The procedure consists of two parts. In the first part, the animals were placed on the apparatus and the speed was maintained

constant at 2 rpm for 60s. In the second part, the rats were evaluated for 5 min in the accelerod test session, in which the rotation rate constantly increased until it reached 20 rpm. Latency to fall off the rod and the actual rotation speed were recorded.

Behavioural procedures

The rats were trained in a black fibreglass radial arm water maze (RAWM, each arm measured 80 cm×12 cm) that was placed 50 cm above floor level. The maze had four arms in the shape of a cross. The water depth was 30 cm, and the temperature was 22±2 °C. The RAWM was in the centre of a 16 m^2 lit room (two halogen lamps of 4,000 lx). The behaviour of the rat in the RAWM was recorded with a video camera (Sony V88E) connected to a computer equipped with an EthoVision Pro program (EthoVision 3.1; Noldus Information Technology, Leesburg, VA).

The learning protocol consisted of single 10 trial-sessions each day over 3 days for each task. In each trial, the rats were placed in the centre of the pool facing a different arm and allowed to swim to the platform. If the animal failed to find the platform, it was guided to the platform. Once the rat reached the platform, it remained there for 15 s. Between trials, the rat was placed in a small square box for 30s. The platform was in the same arm throughout the entire 10 trial-sessions each day, but the location of the platform changed each training day.

Every day at the end of each 10 trial-sessions, a probe test was applied in which the pool platform was removed, and the rat was introduced into the pool for 25 s. Immediately after the probe test, the rats were subjected to an additional trial in which the hidden platform was replaced to avoid any possible interference from the probe test.

All subjects in the experimental group reached the learning criterion of choosing the correct arm in 70 % of trials.

During the *allocentric task*, the rats had to acquire long-term memories of the location of the submerged platform, based on orientation relative to the positions of distal stimuli in the experimental room. In the *cue guided task*, the rats were trained to locate the platform based on a yellow globe that was situated 20 cm above the platform. This version requires the execution of the same response (cue guided), rather than navigation to the same place.

Cytochrome oxidase histochemistry

The protocol used was the same as that described by Arias et al. (2010). Ninety minutes after the last training day, the animals were decapitated; brains were removed, frozen rapidly in N-methylbutane (Sigma-Aldrich, Madrid, Spain) and stored at −40ºC until processing with quantitative C.O. histochemistry. To quantify enzymatic activity and to control staining variability across different baths, sets of tissue homogenate standards from Wistar rat brain were cut at different thicknesses (10, 30, 40 and 60 μm) and included with each bath of slides. Quantification of C.O. histochemical staining intensity was performed with densitometric analysis using a computer-assisted image analysis workstation (MCID, Interfocus Imaging Ltd., Linton, England) composed of a high precision illuminator, a digital camera, and a computer with specific image analysis software (Leica Q-Win, Germany). A total of 12 measurements were taken per brain region. These measurements were averaged to obtain one mean value per region for each animal and were expressed as arbitrary units of optical density (OD) in the prefrontal cortex (infralimbic and prelimbic cortex), the striatum (anteromedial, anterolateral and anterodorsal), the accumbens core and shell, the parietal cortex, the thalamus (anterodorsal, anteroventral and mediodorsal), the dorsal and ventral hippocampus (dentate gyrus, CA1 and CA3 areas), the amygdala nuclei (basolateral, medial, lateral and central) and the perirhinal and enthorhinal cortex. The anatomically selected brain regions were defined according to Paxinos and Watson's (2005) atlas. Regression curves between section thickness and known C.O. activity measured in each set of standards were calculated for each incubation bath. Finally, average OD measured in each brain region was converted into C.O. activity units (μmol of cytochrome c oxidized/min/g tissue wet weight), using the calculated regression curve in each homogenate standard.

Statistical analysis

The numbers of correct arm choices measured daily in the trained group were analyzed using two-way repeated measures ANOVA, and when appropriate, Tukey post-hoc tests to evaluate differences between experimental groups and training days. Strategy group differences in C.O. activity of each brain region and the rotarod-accelerod test were assessed by student's *t*-test for independent samples. Moreover, a non-parametric Mann–Whitney *U* test (U) for independent samples was carried out when normality or equal group variances failed.

Data were analyzed with Sigma Stat 3.2 (Systat, Chicago, IL) software and were expressed as mean±SEM. The results were considered statistically significant at $p<0.05$.

Results

Rotarod-accelerod test

A *t*-test for independent samples revealed no significant differences between groups in the rotarod-accelerod. The HA CG group did not differ from the CHA CG group in rpm reached by the rotarod ($U=74.000$, $n_1=7$, $n_2=10$, $p=0.278$) or in the time in seconds that the animals managed to withstand

at fast speed (U=74.500, n_1=7, n_2=10, p=0.257). Similar results were obtained between the HA ALLO and the CHA ALLO groups, where no differences were found in rpm (U =76.000, n_1=8, n_2=9, p=0.726) or in the time in seconds (U=74.000, n_1= 8, n_2=9, p=0.884).

Behavioural results

Concerning the number of correct choices made in the training phase, the hyperammonemic rats could not achieve the criterion of 7 out of 12 correct choices in any of the tasks. In contrast, the animals fed the control diet acquired the established criterion in both tasks. In fact, significant differences were found between the CG groups (F(1,45)=74.074, p<0.001) on all the training days (p<0.001). Significant differences were also found between the ALLO groups (F(1,48)=31.523, p<0.001) across training days (p=0.009 for Day 1, p=0.022 for Day 2 and p<0.001 for Day 3). In addition, significant increases were observed across training days in the control cue guided group (CHA CG) between Day 1 and Day 3 (p=0.024). No significant differences were found across training days in the other groups. See Fig. 1.

C.O. Activity

The results of C.O. histochemistry quantification revealed that the hyperammonemic animals trained in the ALLO task displayed increased C.O. activity in the anterodorsal thalamus when compared to the CHA ALLO group (t_{13}=-3.0, p=0.01), whereas no differences were found in the rest of the studied structures. In contrast, significant differences in several brain regions were observed between animals trained in the cue guided task. In this regard, increased C.O. activity was found in the HA CG group when compared with the CHA CG group in the prelimbic (t_{15}=-2.16, p=0.048), infralimbic (t_{15}=-2.19, p=0.044), parietal (t_{15}=-4.02, p=0.001), enthorhinal (U= 95.000, n_1=7, n_2=10, p=0.002) and perirhinal cortices (U= 95.000, n_1=7, n_2=10, p=0.002). In addition, the same pattern of metabolic activity was found in the anterolateral striatum (t_{13}=-2.31, p=0.038), the anteromedial striatum (t_{15}=-2.14, p=0.05), the ventral CA1 (t_{15}=-2.93, p=0.01), the basolateral amygdala (U=92.000, n_1=7, n_2=10, p=0.005) and the central amygdala (t_{15}=-3.33, p=0.005) in the HA CG group compared with the CHA CG group. See Table 1.

Discussion

Studies in patients with liver disease and hyperammonemia (Hawkins and Mans 1989) or hyperammonemia in the absence of liver disease (Jessy et al. 1990) have shown depression in cerebral metabolic rates of glucose and oxygen. Another important aspect is the impairment in several learning tasks showed by rats exposed to ammonia (Aguilar et al. 2000 and Jover et al. 2005). It has been suspected that ammonia is responsible for this cerebral dysfunction. Therefore, the aim of this study is to assess the functional consequences of hyperammonemia and its contribution to the neurological alterations in HE, specifically in learning processes that involve the limbic system.

Behavioural results have shown that hyperammonemic rats cannot achieve the behavioural criterion in either of the two tasks, the allocentric and the cue guided tasks. This is reflected in the metabolic brain activity differences found in the limbic structures involved in these learning processes.

It is important to highlight the existence of a time-dependent involvement of the limbic brain structures implicated in the learning processes (Conejo et al. 2010). This means that, at the beginning of the task, some structures are more necessary than others, which are needed at the end. In fact, it has been stated that the hippocampal and prefrontal cortex operate in parallel during the acquisition of spatial information. However, during retention, there could be interactions with the prefrontal cortex that are important for binding spatial information, and the hippocampus is necessary for the initial access to spatial information (Rogers and Kesner 2006). Taking into account the studies

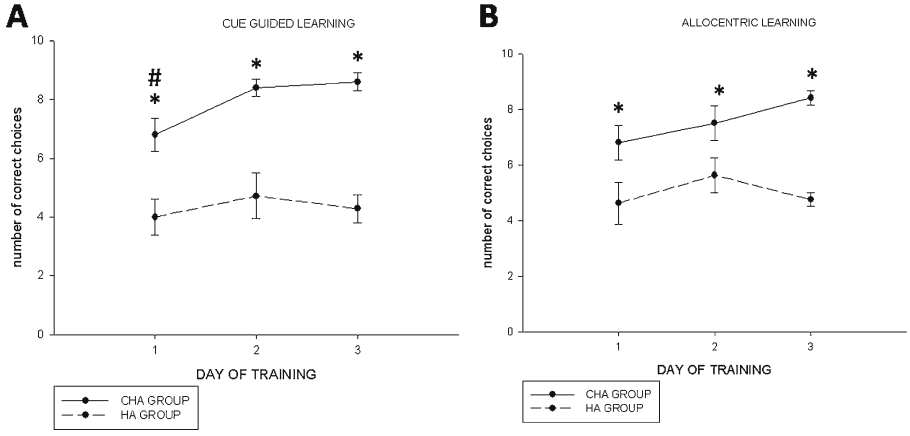

Fig. 1 Number of correct choices across training days in the CG groups (**a**) and the ALLO groups (**b**). Solid and dotted lines represent control hyperammonemia and hyperammonemia groups, respectively. * p<0.05 when comparing the groups' performances, and # p<0.05 when comparing the number of correct choices across training days

Table 1 Cytochrome oxidase activity units (mean±S.E.M.; μmol cytochrome c oxidized/min/g tissue) measured in the selected brain regions

Brain structures	CHA ALLO	HA ALLO	CHA CG	HA CG
Prelimbic cortex	27.3±0.7	26.8±1.0	14.0±0.6	16.1±0,7*
Infralimbic cortex	27,7±0.7	27.0±0.9	13.9±0.5	15.7±0.7*
Parietal cortex	26.8±0.6	26.1±0.1	16.0±0.7	22.3±1.6*
Perirhinal cortex	19.4±0.9	17.4±0.7	14.0±0.4	19.4±1.1*
Enthorhinal cortex	20.1±0.7	19.1±0.6	14.8±0.4	20.5±1.0*
Anterodorsal striatum	29.4±0.7	27.4±0.8	18.4±1.1	20.9±1.1
Anteromedial striatum	29.4±0.8	29.8±0.6	18.6±1.0	22.0±1.2*
Anterolateral striatum	30.6±1.0	28.7±0.9	19.7±2.5	23.0±3.1*
N. accumbens core	32.2±1.0	31.8±1.0	21.3±0.9	23.1±1.5
N. accumbens shell	37.2±1.0	36.9±1.2	25.0±0.7	26.2±1.5
Dorsal CA1 area	24.9±1.1	24.9±1.1	15.8±1.6	17.2±3.5
Dorsal CA3 area	23.7±1.6	22.6±0.8	14.6±0.8	16.1±0.7
Dorsal dentate gyrus	39.3±1.0	39.5±1.6	23.3±0.5	23.4±0.5
Ventral CA1 area	26.6±1.0	24.1±1.2	16.2±0.5	22.2±1.0*
Ventral CA3 area	27.7±1.1	25.2±1.5	20.3±0.4	21.3±0.4
Ventral dentate gyrus	27.0±2.2	26.0±1.2	18.2±0.9	19.5±0.6
Anterodorsal thalamus	42.9±1.7	50.9±2.0*	28.2±0.7	26.7±0.4
Anteroventral thalamus	31.3±1.2	31.7±1.4	19.9±1.0	20.7±0.5
Anteromedial thalamus	26.5±1.1	27.4±0.8	16.9±0.8	18.7±0.6
Basolateral amygdala n.	27.4±0.7	28.1±0.9	19.5±0.6	23.1±1.0*
Lateral amygdala n.	22.9±0.6	23.5±0.7	16.5±0.5	17.4±0.8
Central amygdala n.	20.0±0.7	20.9±0.6	13.9±0.3	17.0±1.0*
Medial amygdala n.	21.7±0.9	22.2±0.4	15.0±0.3	15.2±0.4

* represents significant differences ($p<0.05$) when compared to the control group

of energy depletion in ammonia (Arias et al. 2013 and Stewart et al. 2000) and the differential involvement of structures during a behavioural task, the increase of brain metabolic activity obtained in our HA groups was expected. All the structures studied in the hyperammonemic animals increased their energy requirements in the attempt to reach the learning criterion. However, task difficulty level, as revealed by the performance of the control groups, is different in both tasks: whereas in the cue guided task, an improvement over the days was displayed, in the allocentric task, this pattern did not exist because the task was carried out without any difficulty from the first day. That is probably why the activity of the structures involved at the beginning of the task, such as the anterior thalamic nuclei, was enhanced in the HA ALLO group. Studies of lesions in this structure exhibit clear deficits in the initial acquisition of an allocentric task in the MWM (Wolff et al. 2008 and Sutherland and Hoesing 1993).

In contrast, in the HA CG group, the structures that present enhanced metabolic requirements are necessary at different moments of the learning process; for example, the involvement of the prefrontal cortex in the organization of spatially directed behaviour has been shown both in primates and humans (Delatour and Gisquet-Verrier 2000). The main sources of afferent projections to the prelimbic/infralimbic cortices are the mediodorsal nucleus of thalamus (Moghaddam and Homayoun 2008), the perirhinal and entorhinal cortices, the hippocampus and the basal nuclei of the amygdala, among others (Hoover and Vertes 2007), and this pattern of connections is consistent with a key role at the top of the executive hierarchy and as the ultimate regulator of goal-directed behaviour (Fuster 2001).

Perirhinal and entorhinal cortices showed an increase in C.O. activity in the HA CG group. Regarding the perirhinal cortex, it has been implicated in solving tasks that require spatial awareness, specifically in spatial memory tests. It has been implicated in the spatial reference memory (Wiig and Bilkey 1994 and Abe et al. 2009) and the long-term spatial memory (Glenn et al. 2003), playing a specific role in cue or context recognition (Kealy and Commins 2011). The entorhinal cortex is the primary cortical input region of the hippocampal complex (Calton et al. 2008). The ventral hippocampus is associated with non-spatial functions (Dougherty et al. 2012). In fact, its contribution to temporal ordering processes has been revealed (Hunsaker et al. 2008) and is supported by its projections to the prefrontal cortex and basolateral amygdala (Ishikawa and Nakamura 2006), which is in line with our findings where these structures showed enhanced metabolic requirements. Therefore, the hippocampus and the amygdala, probably in conjunction, clearly play an important role in late memory processes (Burns et al. 1996).

Also, the HA CG group revealed higher C.O. activity in the parietal cortex. This activity could be related to the major role of this structure in the use of landmarks and self-movement cues to update the head direction cell signal, or its generation (Calton et al. 2008). Studies of lesions have shown a more affected performance in tasks that require the processing of proximal landmarks (Save and Poucet 2000). In addition, the same pattern of metabolic activity was found in the striatum of the HA animals which performed the cue guided task. This could support the role of the striatum to assist the navigational system by helping to define future actions (Mizumori et al. 2009), is appropriate for the current context. It has been reported that the dorsal striatum is selectively involved in response or cue learning (McDonald and White 1994). This pattern could also reflect the energy requirement efforts of the brain to perform a task that is facilitated in non-intoxicated rats (Arias et al., unpublished results). But how does ammonia cause these deficits?

Cooper and Lai (1987) have shown that the rate of turnover of glutamine synthetase in acute or chronic hyperammonemia rats is slowed down in comparison to normal rat brains. Therefore, neurons are defenceless against increased ammonia

concentrations due to the absence of this enzyme and are more likely to exhibit impaired function (Butterworth 2003).

Once inside the brain, the consequences of the increase of ammonia range from altered bioenergetics (Hawkins and Mans 1989) to electrophysiological effects (Raabe 1989), disturbances in the neurotransmitter function (Norenberg et al. 1997), altered activity of energy-metabolizing enzymes (Cooper and Plum 1987) and oxidative stress (Murthy et al. 2001).

Alteration of cerebral energy metabolism is a well-documented problem. One of the possible explanations is a disturbance in the glutamate-NO-cGMP pathway. Activation of this pathway, associated to activation of NMDA receptors, increases the production of nitric oxide (NO), resulting in an increased formation of cyclic guanosine monophosphate (cGMP). This pathway modulates important cerebral processes such as long-term potentiation (Boulton et al. 1995 and Hawkins 1996) and other forms of learning and memory (Jover et al. 2005). In fact, cGMP is important in inhibitory avoidance learning (Bernabeu et al. 1996 and Bernabeu et al. 1997), spatial learning in the MWM (Smith et al. 2000), object recognition (Rutten et al. 2005) and conditional discrimination in a Y-maze test (Llansola et al. 2009). It has been recently reported that excess production of NO could cause reversible and irreversible damage to mitochondrial respiration chain enzymes, particularly, to C.O. (Stewart et al. 2000). So, it appears interesting try to analyze the unique effect of ammonia in these structures in order to elucidate the extent to which energy requirements are affected. Acute hyperammonemia or liver failure leads to excessive activation of the glutamate-NO-cGMP pathway and enhanced production of NO which may affect C.O. activity. However, in chronic hyperammonemia or hepatic encephalopathy, there is an adaptive response, leading to reduced function of the glutamate-NO-cGMP pathway (Felipo 2013). The adaptive mechanisms are different in different brain areas. For example activation of soluble guanylate cyclase by NO is educed in cerebellum but enhanced in cortex of rats with chronic hyperammonemia and in cirrhotic patients died in hepatic encephalopathy (Corbalán et al. 2002). However, activation of nitric oxide synthase in response to activation of NMDA receptors is reduced both in cerebellum and cortex in chronic hyperammonemia, resulting in reduced formation of NO and cGMP (Hermenegildo et al. 1998 and Rodrigo et al. 2007). The possible contribution of these changes to altered C.O. activity in different areas remains to be unveiled.

To conclude, the present study revealed impairment in the acquisition of two broadly studied tasks – the allocentric and cued learning tasks – in the animals fed with ammonia. Differences in the metabolic brain consumption were found in cortical regions, striatum and amygdala nuclei between animals trained in the cue guided task. However, only increased C.O. activity in the anterodorsal thalamus was revealed when comparing allocentric groups. The most interesting finding is that the differential brain metabolic activity in the brain limbic structures involved in these tasks differs according to the degree of task difficulty. These findings may be useful in furthering our understanding of a specific contribution of ammonia to different behavioural tasks and its differential relationship with the brain limbic system regions involved.

Acknowledgments This research was supported by Grants MICINN PSI2010-19348 and MEC AP2009-1714 to NA.

References

Abe H, Ishida Y, Nonaka H, Iwasaki T (2009) Functional difference between rat perirhinal cortex and hippocampus in object and place discrimination tasks. Behav Brain Res 197:388–397

Aggleton JP, Vann SD, Oswald CJ, Good M (2000) Identifying cortical inputs to the rat hippocampus that subserve allocentric spatial processes: A simple problem with a complex answer. Hippocampus 10: 466–474

Aguilar MA, Miñarro J, Felipo V (2000) Chronic moderate hyperammonemia impairs active and passive avoidance behavior and conditional discrimination learning in rats. Exp Neurol 161: 704–713

Aller MA, Arias JL, Cruz A, Arias J (2007) Inflammation: A way to understanding the evolution of portal hypertension. Theor Biol Med Model 4:44

Arias JL, Aller MA, Sánchez-Patan F, Arias J (2006) The inflammatory bases of hepatic encephalopathy. Eur J Gastroenterol Hepatol 18: 1297–1310

Arias N, Álvarez C, Conejo N, González-Pardo H, Arias JL (2010) Estrous cycle and sex as regulating factors of baseline brain oxidative metabolism and behavior. Revista Iberoamericana de Psicología y Salud 1:3–16

Arias N, Méndez M, Arias J, Arias JL (2012) Brain metabolism and spatial memory are affected by portal hypertension. Metab Brain Dis 27:183–191

Arias N, Méndez M, Fidalgo C, Aller MA, Arias J, Arias JL (2013) Mapping metabolic brain activity in three models of hepatic encephalopathy. Int J Hypertens 390872

Azorín I, Miñana MD, Felipo V, Grisolía S (1989) A simple animal model of hyperammonemia. Hepatology 10:311–314

Bernabeu R, Schmitz P, Faillace MP, Izquierdo I, Medina JH (1996) Hippocampal cGMP and cAMP are differentially involved in memory processing of inhibitory avoidance learning. Neuroreport 7:585–588

Bernabeu R, Schroder N, Quevedo J, Cammarota M, Izquierdo I, Medina JH (1997) Further evidence for the involvement of a Hippocampal cGMP/cGMP-dependent protein kinase cascade in memory consolidation. Neuroreport 8:2221–2224

Boulton CL, Southam E, Garthwaite J (1995) Nitric oxide-dependent long-term Potentiation is blocked by a specific inhibitor of soluble guanylyl cyclase. Neuroscience 69:699–703

Burns LH, Annett L, Kelley AE, Everitt BJ, Robbins TW (1996) Effects of lesions to amygdala, ventral subiculum, medial prefrontal cortex, and nucleus accumbens on the reaction to novelty: Implication for limbic-striatal interactions. Behav Neurosci 110:60–73

Butterworth RF (1991) Pathophysiology of hepatic encephalopathy: The ammonia hypothesis revisited. In: Bengtsson F, Jeppsson B, Aamdal

T, Vistrup H (eds) Progress in hepatic encephalopathy and metabolic nitrogen exchange. CRC Press, Boca Raton, pp 9–24
Butterworth RF (2003) Hepatic encephalopathy. Alcohol Res Health 27: 240–246
Calton JL, Turner CS, Cyrenne DL, Lee BR, Taube JS (2008) Landmark control and updating of self-movement cues are largely maintained in head direction cells after lesions of the posterior parietal cortex. Behav Neurosci 122:827–840
Conejo NM, González-Pardo H, González-Lima F, Arias JL (2010) Spatial learning of the water maze: Progression of brain circuits mapped with cytochrome oxidase histochemistry. Neurobiol Learn and Mem 93:362–371
Cooper AJ, Lai JC (1987) Cerebral ammonia metabolism in normal and hyperammonemic rats. Neurochem Pathol 6:67–95
Cooper AJ, Plum F (1987) Biochemistry and physiology of brain ammonia. Physiol Rev 67:440–519
Corbalán R, Chatauret N, Behrends S, Butterworth RF, Felipo V (2002) Region selective alterations of soluble guanylate cyclase content and modulation in brain of cirrhotic patients. Hepatology 36:1155–1162
de Bruin JP, Moita MP, de Brabander HM, Joosten RN (2001) Place and response learning of rats in a Morris water maze: Differential effects of fimbria fornix and medial prefrontal cortex lesions. Neurobiol Learn Mem 75:164–178
Delatour B, Gisquet-Verrier P (2000) Functional role of rat prelimbic-infralimbic cortices in spatial memory: Evidence for their involvement in attention and behavioural flexibility. Behav Brain Res 109: 113–128
Dougherty KA, Islam T, Johnston D (2012) Intrinsic excitability of CA1 pyramidal neurones from the rat dorsal and ventral hippocampus. J Physiol 590:5707–5722
Erceg S, Monfort P, Hernández-Viadel M, Rodrigo R, Montoliu C, Felipo V (2005) Oral administration of sildenafil restores learning ability in rats with hyperammonemia and with portacaval shunts. Hepatology 41:299–306
Felipo V (2013) Hepatic encephalopathy: Effects of liver failure on brain function. Nat Rev Neurosci 14:851–858
Fuster JM (2001) The prefrontal cortex–an update: Time is of the essence. Neuron 30:319–333
Galani R, Obis S, Coutureau E, Jarrard L, Cassel JC (2002) A comparison of the effects of fimbria-fornix, Hippocampal, or entorhinal cortex lesions on spatial reference and working memory in rats: Short versus long postsurgical recovery period. Neurobiol Learn Mem 77:1–16
Glenn MJ, Nesbitt C, Mumby DG (2003) Perirhinal cortex lesions produce variable patterns of retrograde amnesia in rats. Behav Brain Res 141:183–193
González-Lima F, Cada A (1994) Cytochrome oxidase activity in the auditory system of the mouse: A qualitative and quantitative histochemical study. Neuroscience 63:559–578
Groenewegen HJ, Berendse HW, Wolters JG, Lohman AH (1990) The anatomical relationship of the prefrontal cortex with the striatopallidal system, the thalamus and the amygdala: Evidence for a parallel organization. Prog Brain Res 85:95–116
Hawkins RA, Mans AM (1989) Brain energy metabolism in hepatic encephalopathy. In: Boulton AA, Baker GB, Butterworth RF (eds) Hepatic encephalopathy. Pathophysiology and treatment. Humana Press, Clifton, pp 159–176
Hawkins RD (1996) NO honey, I don't remember. Neuron 16:465–467
Hermenegildo C, Montoliu C, Llansola M, Muñoz MD, Gaztelu JM, Miñana MD, Felipo V (1998) Chronic hyperammonemia impairs glutamate-nitric oxide-cyclic GMP pathway in cerebellar neurons in culture and in the rat in vivo. Eur J Neurosci 10:3201–3209
Hoover WB, Vertes RP (2007) Anatomical analysis of afferent projections to the medial prefrontal cortex in the rat. Brain Struct Funct 212:149–179
Hunsaker MR, Fieldste PM, Rosenberg JS, Kesner RP (2008) Dissociating the roles of dorsal and ventral CA1 for the temporal processing of spatial locations, visual objects, and odors. Behav Neurosci 122:643–650
Ishikawa A, Nakamura S (2006) Ventral Hippocampal neurons project axons simultaneously to the medial prefrontal cortex and amygdala in the rat. J Neurophysiol 96:2134–2138
Jessy J, Mans AM, DeJoseph MR, Hawkins RA (1990) Hyperammonaemia causes many of the changes found after portacaval shunting. Biochem J 272:311–317
Jones BJ, Roberts DJ (1968) The quantitative measurement of motor incoordination in naïve mice using an accelerating rotarod. J Pharm Pharmacol 20:302–304
Jover R, Madaria E, Felipo V, Rodrigo R, Candela A, Compañ A (2005) Animal models in the study of episodic hepatic encephalopathy in cirrhosis. Metab Brain Dis 20:399–408
Kealy J, Commins S (2011) The rat perirhinal cortex: A review of anatomy, physiology, plasticity, and function. Prog Neurobiol 93: 522–548
Kesner RP (1990) Memory for frequency in rats: Role of the hippocampus and medial prefrontal cortex. Behav Neural Biol 53:402–410
Kolb B, Whishaw IQ (2003) Fundamentals of human neuropsychology. Worth Publishers, New York
Llansola M, Hernandez-Viadel M, Erceg S, Montoliu C, Felipo V (2009) Increasing the function of the glutamate-nitric oxide-cyclic guanosine monophosphate pathway increases the ability to learn a Y-maze task. J Neurosci Res 87:2351–2355
Long JM, Kesner RP (1996) The effects of dorsal versus ventral Hippocampal, total Hippocampal, and parietal cortex lesions on memory for allocentric distance in rats. Behav Neurosci 110:922–932
McDonald RJ, White NM (1994) Parallel information processing in the water maze: Evidence for independent memory systems involving dorsal striatum and hippocampus. Behav Neural Biol 61:260–270
Méndez M, Méndez-López M, López L, Aller MA, Arias J, Arias JL (2011) Portosystemic hepatic encephalopathy model shows reversal learning impairment and dysfunction of neural activity in the prefrontal cortex and regions involved in motivated behavior. J Clin Neurosci 18:690–694
Mizumori SJ, Puryear CB, Martig AK (2009) Basal ganglia contributions to adaptive navigation. Behav Brain Res 199:32–42
Moghaddam B, Homayoun H (2008) Divergent plasticity of prefrontal cortex networks. Neuropsychopharmacology 33:42–55
Murthy CR, Rama Rao KV, Bai G, Norenberg MD (2001) Ammonia-induced production of free radicals in primary cultures of rat astrocytes. J Neurosci Res 66:282–288
Norenberg MD, Huo Z, Neary JT, Roig-Cantesano A (1997) The glial glutamate transporter in hyperammonemia and hepatic encephalopathy: Relation to energy metabolism and glutamatergic neurotransmission. Glia 21:124–133
Paxinos G, Watson CH (2005) The rat brain in Stereotaxic Coordinates—the new coronal set 5th ed. Elsevier Academic Press.
Raabe WA (1989) Neuropathology of ammonia intoxication. In (RF Butterworth and G Pomier Layrargues, eds.) Hepatic encephalopathy: Pathophysiology and Treatment, Humana Press, Clifton, NJ.
Rao KV, Norenberg MD (2001) Cerebral energy metabolism in hepatic encephalopathy and hyperammonemia. Metab Brain Dis 16:67–78
Rodrigo R, Erceg S, Rodriguez-Diaz J, Saez-Valero J, Piedrafita B, Suarez I, Felipo V (2007) Glutamate-induced activation of nitric oxide synthase is impaired in cerebral cortex in vivo in rats with chronic liver failure. J Neurochem 102:51–64
Rodrigo R, Felipo V (2006) Brain regional alterations in the modulation of the glutamate-nitric oxide-cGMP pathway in liver cirrhosis. Role of hyperammonemia and cell types involved. Neurochem Int 48: 472–477

Rogers JL, Kesner RP (2006) Lesions of the dorsal hippocampus or parietal cortex differentially affect spatial information processing. Behav Neurosci 120:852–860

Rutten K, Vente JD, Sik A, Ittersum MM, Prickaerts J, Blokland A (2005) The selective PDE5 inhibitor, sildenafil, improves object memory in Swiss mice and increases cGMP levels in Hippocampal slices. Behav Brain Res 164:11–16

Save E, Poucet B (2000) Involvement of the hippocampus and associative parietal cortex in the use of proximal and distal landmarks for navigation. Behav Brain Res 109:195–206

Shawcross DL, Wright G, Olde Damink SW, Jalan R (2007) Role of ammonia and inflammation in minimal hepatic encephalopathy. Metab Brain Dis 22:125–138

Smith S, Dringenberg HC, Bennett BM, Thatcher GR, Reynolds JN (2000) A novel nitrate ester reverses the cognitive impairment caused by scopolamine in the Morris water maze. Neuroreport 11: 3883–3886

Stewart VC, Sharpe MA, Clark JB, Heales SJ (2000) Astrocyte-derived nitric oxide causes both reversible and irreversible damage to the neuronal mitochondrial respiratory chain. J Neurochem 75:694–700

Sutherland RJ, Hoesing JM (1993) Posterior cingulate cortex and spatial memory: A microlimnology analysis. In: Vogt BA, Gabriel M (eds) Neurobiology of cingulate cortex and limbic thalamus. Birkhauser, Boston

Wang V, Saab S (2003) Ammonia levels and the severity of hepatic encephalopathy. Am J Med 114:237–238

Weissenborn K, Heidenreich S, Giewekemeyer K, Rückert N, Hecker H (2003) Memory function in early hepatic encephalopathy. J Hepatol 39:320–325

Wiig KA, Bilkey DK (1994) The effects of perirhinal cortical lesions on spatial reference memory in the rat. Behav Brain Res 63:101–109

Wolff M, Gibb SJ, Cassel JC, Dalrymple-Alford JC (2008) Anterior but not intralaminar thalamic nuclei support allocentric spatial memory. Neurobiol Learn Mem 90:71–80

III

Metab Brain Dis (2012) 27:183–191
DOI 10.1007/s11011-012-9276-z

ORIGINAL PAPER

Brain metabolism and spatial memory are affected by portal hypertension

Natalia Arias · Marta Méndez · Jaime Arias · Jorge L. Arias

Received: 18 October 2011 / Accepted: 19 January 2012 / Published online: 8 February 2012

Abstract Portal hypertension is a major complication of cirrhosis that frequently leads to a neuropsychiatric disorder that affects cognition. The present study was undertaken in order to compare the performance of sham-operated rats (SHAM) and portal hypertension rats (PH) in reference memory tasks in the Morris water maze (MWM). Two groups of animals were used: SHAM group (n=12) was used as a control group and PH group (n=12) by the triple portal vein ligation method was used as an animal model of early evolutive phase of PH. The portal pressure was measured in the splenic parenchyma. Our work shows that spatial learning in the MWM is not impaired in PH group although this group showed a one-day delay in the task acquisition compared to the SHAM group. We assessed the brain metabolic activity of the animals by means of cytochrome c-oxidase (COx) histochemistry. Significant changes were found in the CA3, dentate gyrus, basolateral, medial, lateral and central amygdala, showing lower COx activity in the PH group as compared to the SHAM group in all cases. We found no changes in metabolic activity in prefrontal cortex and CA1 area between groups. In fact, different neural networks were shown according to the execution level of the subjects. The early PH evolution induced changes in brain metabolic activity without biggest alterations in spatial memory.

Keywords Acute portal hypertension · Memory networks · Cytochrome c-oxidase · Limbic system · Rat

N. Arias · M. Méndez · J. L. Arias (✉)
Laboratorio de Neurociencias, Departamento de Psicología,
Universidad de Oviedo,
Plaza Feijoo s/n,
CP: 33003 Oviedo, Asturias, Spain
e-mail: jarias@uniovi.es

J. Arias
Departamento de Cirugía I, Facultad de Medicina,
Universidad Complutense de Madrid,
Ciudad Universitaria s/n,
28040 Madrid, Spain

Introduction

Hypertension is the single most important risk factor for cardiovascular disease and, thus, remains a global public health challenge (Zubcevic et al. 2011). It has been extremely difficult to manage hypertension in≈40% of hypertensive patients (Primatesta et al. 2001). Studies showed that systemic oxidative stress, inflammation and priming of peripheral polymorphonuclear leukocytes antecede the development of hypertension in experimental model of hypertension in the Sabra rat (Sela et al. 2004).

In humans portal hypertension is characterized by prolonged elevation of portal venous pressure greater than 10 mmHg (Al-Ghamdi 2011). It is estimated that for every 1 mmHg increase in hepatic venous pressure gradient above a threshold level of 10 mmHg, an 11% rise in the risk of clinical decompensation could be expected (Al-Ghamdi 2011). This growth in portal pressure results from both an increase in resistance to portal flow and an increment in portal blood flow (Carey 2011). Portal hypertension (PH) is a common complication of cirrhosis which is in association with distinctive risks, including luminal gut bleeding, ascites and hepatic encephalopathy (HE) (Carey 2011).

There are diverse experimental models that have been developed to study the pathogenic mechanism that may be responsible for HE symptoms (Butterworth et al. 2009). Type B, which concerns HE related to portosystemic shunt and does not require any hepatocytic alteration, includes

portocaval shunt, partial ligature of the portal vein and triple portal vein ligation (Orloff 2001).

Alterations in learning and memory capacity related to spatial memory and object recognition in rats with PH have been previously described in adult animals and in 18-month-old rats (Méndez et al. 2009a; Begega et al. 2010). The brain structures related to this kind of memory are the prefrontal cortex (Ragozzino et al. 1999) and the hippocampus, mainly the rostral part, which is involved in the memory for spatial information (Moser et al. 1995).

The objective of this work was to evaluate motor changes and to assess learning impairment at early evolutive phases of PH. For this purpose, we assessed the impact of PH by triple portal vein ligation on spatial reference memory and we studied oxidative metabolism of different brain limbic system regions involved in memory process by histochemical labelling of cytochrome oxidase (COx). COx is a mitochondrial enzyme involved in the phosphorylation process that generates ATP. This energy is used to maintain the resting membrane potential and the synthesis of molecules and neurotransmitters, among other functions (González-Lima and Cada 1994). Because metabolic activity is tightly coupled with neuronal activity, this technique can be used as an index of regional functional activity in the brain, reflecting changes in tissue metabolic capacity induced by sustained energy requirements of the nervous system associated with learning (Poremba et al. 1998) and spatial memory in the Morris Water Maze (MWM) (Conejo et al. 2007; de la Torre et al. 1997).

Material and Methods

Subject

A total of 24 male Wistar rats were used (3 months at the start of the experiment) from the animalarium of Oviedo University. All the animals had *ad libitum* food and tap water and were maintained at constant room temperature (22±2°C), with a relative humidity of 65±5°C and artificial light–dark cycle of 12 h (08:00–20:00/20:00–08:00). The procedures and manipulation of the animals used in this study were carried out according to the Directive (2010/63/EU) and Royal Decree 1201/2005 of the Ministry of Presidency relating to the protection of the animals used for experimentation and other scientific purposes, and the study was approved by the local committee for animal studies (Oviedo University).

Procurement of experimental models

The animals were randomly distributed into two groups: portal hypertension (PH group, $n=12$) and sham-operated (SHAM group, $n=12$). The experimental models that require surgery were anesthetized by i.m. injection of ketamine (100 mg/kg) and xylacine (12 mg/kg). With regard to postsurgical care, rats were kept near a heat source (10–15 min) until they regained consciousness to prevent postoperative hypothermia. They were then introduced into individual polycarbonate cages for 15 days and subsequently grouped into cages of four animals until their behavioral evaluation.

Portal hypertension

A midline abdominal incision was performed and a section of the intestinal loops was gently shifted to the left and covered with saline-moistened gauze. The portal vein was isolated and three ligatures, fixed on a sylactic guide, were performed in its superior, middle and inferior portions. The stenoses were calibrated by simultaneous ligation (4–0 silk) around the portal vein and a 20-gauge blunt-tipped needle. The abdominal incision was closed in two layers with catgut and 2–0 silk. The postoperative period started immediately after the intervention and lasted until the behavioral evaluation 45 days later.

Sham-operated

A bilateral subcostal laparotomy with prolongation to the xyphoid apophysis, followed by isolation of the portal vein, was performed. The operative field was irrigated with saline solution during the intervention as the portal hypertension ones. Finally, the laparotomics were closed by continuous suture on the two layers with catgut and 2–0 silk. The postoperative period started immediately after the intervention and lasted until the behavioral evaluation 45 days later.

Portal vein pressure measurement

Splenic pulp pressure, an indirect measurement of portal pressure (PP), was measured by the method described by Aller et al. (2006).

Determination of neurological alterations and motor functions

Neurological test

Before intervention and after the postoperative period, all the animals were handled during 10 min and evaluated by neurological tests such as flexion reflex, startle reactions, head shacking, righting and equilibrium reflex, placing reactions, grasping and some equilibrium tests. No alteration was displayed by any animal.

Rotarod-accelerod test

This test of motor performance consists of a motor-driven rotating rod that enables us to assess motor coordination and resistance to fatigue (Jones and Roberts 1968). The accelerating rotarod 7750 of Ugo Basile (Ugo Basile Biological Research Apparatus, Italy) was used for the rats. The procedure followed has two parts. In the first one, the animals were placed in the apparatus and the speed was maintained constant at 2 rpm for 60s. In the second part, the rats were evaluated for 5 min in the accelerod test session, in which the rotation rate constantly increased until it reached 20 rpm. Latency to fall off the rod and the actual rotation speed were recorded.

Evaluation of spatial reference memory

Spatial reference memory was evaluated in the circular pool designed by Morris (Morris 1984) also called the Morris water maze (MWM), one of the experimental paradigms most widely used to evaluate spatial memory. The MWM was made of fibreglass and measured 150 cm in diameter with a wall 40 cm high. The water level was 30 cm and its temperature 22±2°C. The platform used corresponded to a cylinder 10 cm in diameter and 28 cm high, of which 2 cm was below the surface of the water. The MWM was in the centre of a 16 m^2 lit room (two halogen lamps of 4000 lx) and was surrounded by panels on which the spatial clues were placed. The pool was divided into four imaginary quadrants (quadrant A, B, C and D, or right, left, across and correct, respectively). The behaviour of the animal in the MWM was recorded by a video camera (Sony V88E) connected to a computer equipped with an EthoVision Pro programme.

The learning protocol consisted of the first day being destined for habituation of animals to the task, in which the animals carried out four trials with a visible platform that jutted out 4 cm from the water and was located in the centre of the pool. During the following 5 days, the animals were required to locate a hidden platform that remained in the centre of quadrant D in relation to the external visual cues on training days. Training was performed in blocks of six trials per day. To begin each trial, the rats were placed in the water, facing the maze wall, at one of four quadrants, and the daily order of entry into these quadrants was randomized. Each trial ended once the animal had found the hidden platform or when 60 s had elapsed. If the animal had not reached the hidden platform after this time, it was placed on the platform for 15 s. During the inter-trial interval, the animals were placed in a black bucket for 30 s. The time and distance swum in each trial were recorded. At the end of the session, a probe test was applied in which the pool platform was removed and the rat was introduced into the pool in the quadrant opposite to where the platform had been located in previous trials for 25 s in order to check whether the animal remembers the position of the platform (Méndez et al. 2010). Immediately after the probe test, the animals were subjected to an additional trial with the hidden platform placed in its usual position to avoid any possible interference with the probe test. Latencies were recorded during the acquisition and also the time of permanence in each quadrant during the probe test.

Cytochrome oxidase histochemistry

Ninety min after the last training day animals were decapitated. Brains were removed, frozen rapidly in N-methylbutane (Sigma-Aldrich, Madrid, Spain) and stored at −40°C until processing with quantitative COx histochemistry, described by González-Lima and Cada (1994). To quantify enzymatic activity and to control staining variability across different baths, sets of tissue homogenate standards from Wistar rat brain were cut at different thicknesses (10, 30, 40 and 60 μm) and included with each bath of slides. The sections and standards were incubated for 5 min in 0.1 phosphate buffer with 10% (w/v) sucrose and 0.5 (v/v) glutaraldehyde, pH 7.6. After this, baths of 0.1 M phosphate buffer with sucrose were given for 5 min each. Subsequently, 0.05 M Tris buffer, pH 7.6, with 275 mg/l cobalt chloride, sucrose, and 0.5 (v/v) dimethylsulfoxide was applied for 10 min. Then, sections and standards were incubated in a solution of 0.06 g cytochrome c, 0.016 g catalase, 40 g sucrose, 2 ml dimethylsulfoxide and 0.4 g diaminobenzidine tetrahydrochloride (Sigma-Aldrich, Madrid, Spain), in 800 ml of 0.1 M phosphate buffer, at 37°C for 1 h. The reaction was stopped by fixing the tissue in buffered 4% (v/v) formalin for 30 min at room temperature. Finally the slides were dehydrated, cleared with xylene and coverslipped with Entellan (Merck, Germany).

Quantification of COx histochemical staining intensity was done by densitometric analysis, using a computer-assisted image analysis workstation (MCID, Interfocus Imaging Ltd., Linton, England) made up of a high precision illuminator, a digital camera and a computer with specific image analysis software. The mean optical density (OD) of each region was measured on bilateral structures, using three consecutive sections in each subject. In each section, four non-overlapping readings were taken, using a square-shaped sampling window that was adjusted for each region size. A total of twelve measurements were taken per region by an investigator blind to the groups. These measurements were averaged to obtain one mean per region for each animal. OD values were then converted to COx activity units, determined by the enzymatic activity of the standards measured spectrophotometrically (González-Lima and Cada 1994).

The regions of interest were anatomically defined according to Paxinos and Watson´s atlas (2005) (Paxinos and Watson 2005). The regions of interest and the distance in mm of the regions counted from bregma was: +3.20 mm for the infralimbic cortex (IL), prelimbic cortex (PL), the cingulate cortex (CG); -1.20 mm for the CA1, CA3 and the dentate gyrus (DG) subfields of the dorsal hippocampus; -3.12 mm for the basolateral (Bas), medial (MeA), lateral (Lat) and central (Cen) amygdala.

Statistical analysis

Behavioral data

Motor data were analyzed by t-test for independent samples. For the velocity and distance covered, we used a two way repeated measures ANOVA (between factor: group; within factor: day, five levels) as well as to analyse the latencies to reach the hidden platform for each day (average of four trials) during the training phase of the reference memory task. The time spent in each of the four quadrants during the probe test was analysed separately for each group and day, using a one way ANOVA design (factor: quadrants, four levels). Post hoc multiple comparisons analysis was carried out, when allowed, using the Holm-Sidak method. Moreover, a non-parametric Mann–Whitney *U* test (H) for independent samples was carried out when normality or equal group variances failed.

COx activity

Group differences in COx activity measured in each brain region were evaluated by Student's t-test for independent samples. Because training experience in spatial learning might manifest as neural changes in functional connectivity, the possible functional relationships among the regional brain activity data were analysed in terms of pairwise correlations within each experimental group. For the interregional correlation analysis, Pearson´s product–moment correlations between pairs of brain regions in each experimental group were computed. COx activity values were normalized by dividing the measured activity of each brain region by the average COx activity value for all regions measured in each animal. This was done to reduce variation in the intensity of the COx staining not resulting from the experimental manipulation. In addition, in order to avoid errors due to an excessive number of significant correlations using small sample sizes, a "jackknife" procedure was used (Shao and Dongsheng 1995). This procedure is based on the calculation of all possible pairwise correlations resulting from removing one subject each time, and taking into consideration only those correlations that remain significant ($p<0,05$) across all possible combinations.

Results

Portal vein pressure measurement

Portal pressure increases in rats with PH which showed mean values of 14.844±2.08 respect to the SHAM group where portal pressure values were 5.903±0.43.

Rotarod-accelered test

A t-test for independent samples revealed no significant differences between groups in the rotarod/accelerod. The PH group did not differ from the SHAM group in the rpm reached by the rotarod ($t(22)=1.243$, $p=0.227$) or in time in seconds the animals managed to withstand at fast speed ($t(22)=1.294$, $p=0.209$) (Fig. 1).

Reference memory

The two-way repeated measures ANOVA revealed no differences in distance covered ($F(1,88)=2.490$, $p=0.129$) and

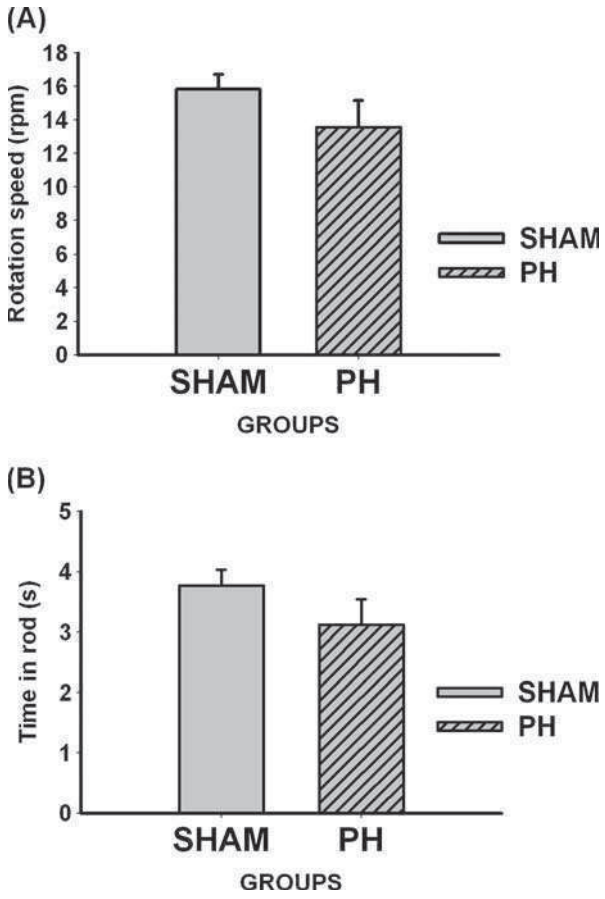

Fig. 1 Rotarod test. Bars charts represent rotation speed **a** and time spent on the rod **b** in the rotarod/accelerod test. There were no statistically significant differences between the groups (mean±SEM)

velocity (F(1,88)=1.321, p=0.263) between PH and SHAM. The variable day, however, did have a significant effect (F(4,88)=26.460, p<0.001) and (F(4,88)=4.040, p=0.005), respectively (Fig. 2).

The two-way repeated measures ANOVA showed no differences in escape latencies between the PH and SHAM groups (F(1,88)=0.462, p=0.504). However, significant differences until day three (p=0.006) in the escape latencies to reach the hidden platform were found in SHAM group respect to the PH group which showed a one-day delay in the task acquisition (p=0.007) (Fig. 3).

Analysis of the time spent in the target quadrant during the probe tests showed an improvement in learning over the 5 days of training for all groups. But, whereas the SHAM group acquired the task in only a few trials, only from Day 3 did permanence in the reinforced quadrant prevail (Day 1: F (3,44)=4.323, p=0.009; Day 2: H(3)=10.122, p=0.018; Day 3: F(3,44)=23.764, p<0.001; Day 4: H(3)=26.423, p<0.001; Day 5: H(3)=26.716, p<0.001). Post hoc tests revealed significant differences between Quadrant D and the rest of quadrants (p≤0.005) on these days. However, the PH group showed a predominant permanence in Quadrant D on

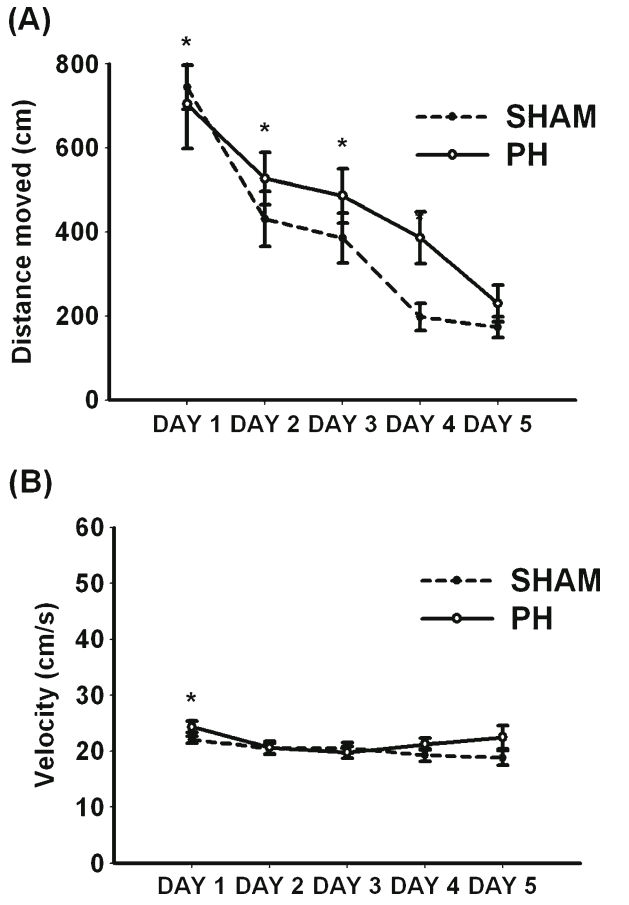

Fig. 2 Distance moved and Velocity. Bars charts (mean±SEM) represent distance moved **a** and velocity **b**. There was a significant effect of the variable day (*p≤0.05)

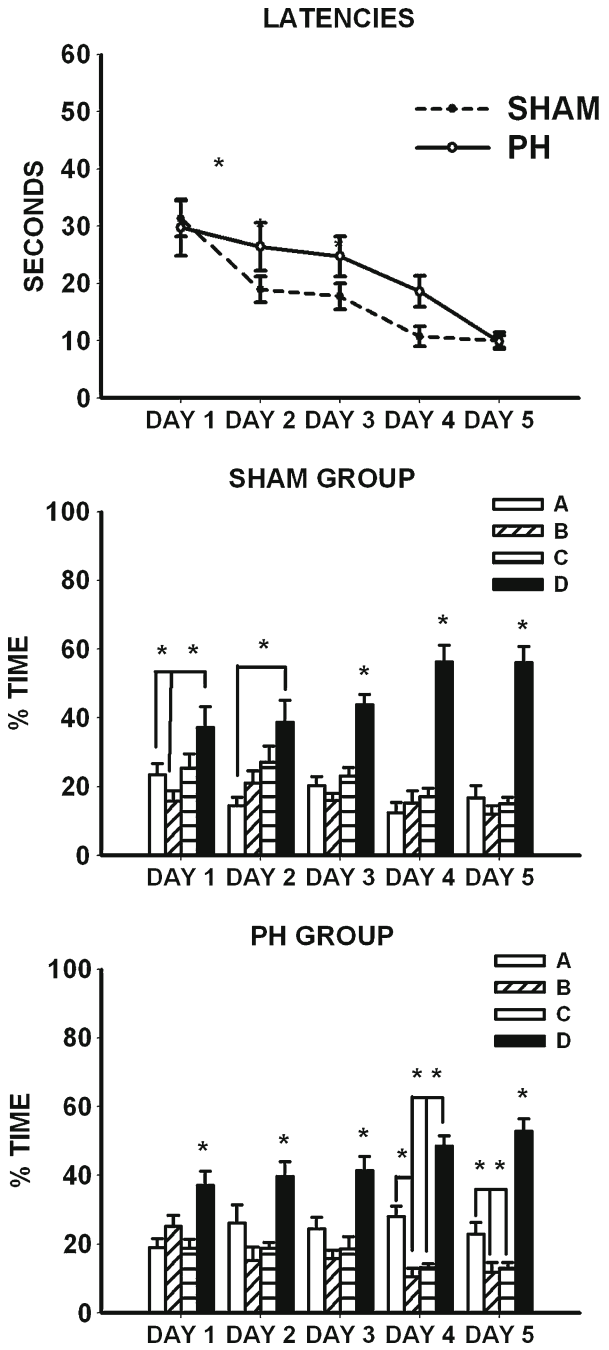

Fig. 3 Escape latencies and probe tests in the spatial reference-memory test during 5 days learning (mean±SEM). The escape platform was located in quadrant D. There was an improvement over days for all groups in escape latencies (*p≤0.05). PH group showed one-day delay in the correct execution of the transfer test respect to the SHAM group

the three first days (Day 1: F(3,44)=7.231, p<0.001; Day 2 : F (3,44)=7.024, p<0.001; Day 3: F(3,44)=11.368, p<0.001) and significant differences between the other quadrants were found on Days 4 and 5 (Day 4: H(3)=33.565, p<0.001; Day 5: F(3,44)=41.253, p<0.001). Post hoc tests for Day 4 revealed significant differences (p≤0.005) between Quadrants D-B, D-C and A-B. But Day 5 showed differences

between Quadrant D and the rest of quadrants ($p<0.001$) and between Quadrants A-B ($p=0.010$) and Quadrant A compared to Quadrant C ($p=0.022$) (Fig. 3).

COx activity

The group comparison of COx activity revealed lower COx activity in the PH group than in the SHAM group in the CA3 ($U=166.000$, n1=11, n2=12; $p=0.039$) and DG ($U=171.000$, n1=11, n2=12; $p=0.018$), Bas ($U=165.000$, n1=11, n2=12; $p=0.045$), Lat ($U=165.000$, n1=11, n2=12; $p=0.045$), Cen ($U=168.000$, n1=11, n2=12; $p=0.029$), and MeA ($U=173.000$, n1=11, n2=12; $p=0.013$). The groups did not differ in their COx activity in the PL ($U=148.000$, n1=11, n2=12; $p=0.340$), IL ($U=156.000$, n1=11, n2=12; $p=0,148$), and CG ($U=153.000$, n1=11, n2=12; $p=0.207$) (Table 1).

Interregional within-group correlations of COx activity

Significant interregional correlations of COx activity were found both in the SHAM and the PH groups. A high cross-correlation between medial amygdala and CA1 subfield ($r=-0.853$, $p<0.001$), between CA1 subfield and CA3 subfield ($r=0.903$, $p<0.001$) as well as between CA3 subfield and central amygdala ($r=-0.794$, $p=0.004$) were found in the SHAM group. In contrast, interregional correlations in the PH group were found between the medial and lateral amygdala ($r=0.766$, $p=0.004$), the lateral amygdala and CA1 subfield ($r=-0.685$, $p=0.014$), the CA1 subfield and CA3 subfield ($r=0.720$, $p=0.008$), as well as between the prelimbic cortex and infralimbic cortex ($r=0.735$, $p=0.006$), the infralimbic cortex and central amygdala ($r=-0.693$, $p=0.012$), the central and cingulate cortex ($r=-0.817$, $p=0.001$) (Fig. 4).

Table 1 Shows the COx values (mean ± SEM) in SHAM and PH groups for all structures studied

Structures	SHAM group	PH group
Cornu ammonis 3	21,74±1,88	16,32±0,49
Dentate gyrus	33,45±3,11	23,41±0,50
Basolateral amygdala	29,68±2,79	20,82±0,38
Lateral amygdala	22,25±1,90	15,64±0,39
Central amygdala	24,19±1,92	17,58±0,53
Medial amygdala	22,31±1,57	16,62±0,37
Prelimbic cortex	22,49±1,75	18,36±0,46
Infralimbic cortex	23,11±1,73	18,47±0,50
Cingulate cortex	22,99±1,83	18,20±0,49

Discussion

Our work shows that spatial learning in the MWM is delayed in rats with acute prehepatic PH, also significant changes could be observed in the COx activity between groups. These differences cannot be justified by motor problems, as indicated in the tests carried out specifically for this purpose.

Patients with cirrhosis show a neuropsychiatric disorder called minimal hepatic encephalopathy (MHE) which, while clinically (neurologically) free of symptoms, manifest abnormalities in central nervous system function where assesed using psychometric tests or electrophysiological techniques. Significant impairment of selective attention and executive function has been reported in MHE, together with abnormalities in prolongation of cognitive evoked potentials, visuomotor activity, response inhibition, slowing of the electroencephalogram and psychomotor speed (Amodio et al. 2004). These deficits have been associated with alterations in the functional connections within the basal ganglia-thalamo-cortical loop (Timmermann et al. 2002; Timmermann et al. 2003). In contrast, in the experimental model of PH employed our results from the rotarod-accelerod test revealed that these alterations were not reflected. Our groups presented a balanced motor coordination and similar displacement speed and distance, in agreement with others authors (Méndez et al. 2008). Indeed, it can be explained by the different neuronal circuits which are activated in normal rats and in rats with HE to modulate motor activity (Cauli et al. 2009). This modulation is due to the sequential alterations in glutamatergic (Canales et al. 2003) and GABAergic neurotransmission in different brain areas involved in these circuits.

Although SHAM and PH groups reached the behavioral criterion, the PH group tended to perform worse than the SHAM group in the reference memory task. In fact, there was a one-day delay in the reduction in the escape latencies to a hidden platform during the learning process for the PH group. Analysis of the probe tests, in which the platform was removed from the pool, revealed that, although there were no group differences in the time of permanence in the target quadrant, the SHAM group increased the time of permanence in the reinforced quadrant during the last 3 days of the acquisition tasks, whereas the PH group showed significant differences between the other quadrants on the last 2 days evaluated. These results are in agreement with those obtained by Méndez and cols (2008) in the study of the working memory. Working memory is a representation of an object, stimulus or spatial location that is typically used within a testing session (Dudchenko 2004), which requires a degree of cognitive flexibility and short-term storage. The data of this study could indicate that the PH group presented more deficits in short-term memory than in long-term spatial memory. In fact, several studies with

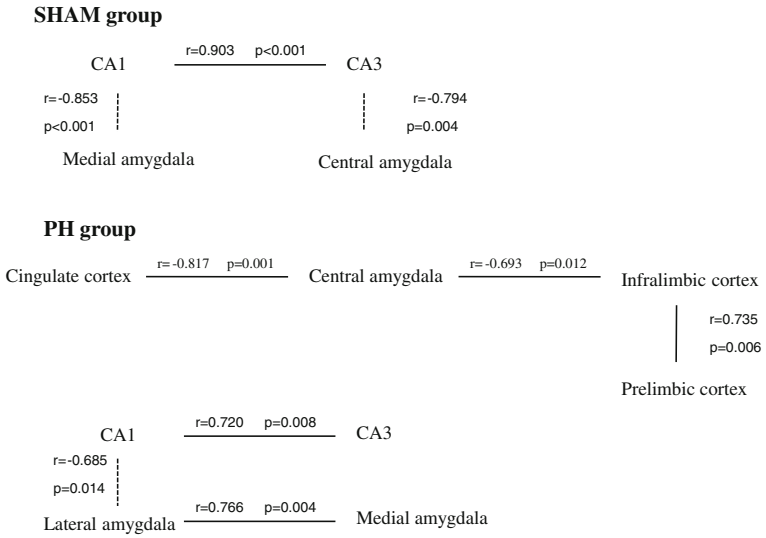

Fig. 4 Schematic diagram showing the significant interregional correlations of COx activity calculated in the studies groups (SHAM and PH). Solid and dotted lines represent respectively highly positive and negative pair-wise Pearson's correlations ($r>0.8$, $P<0.02$)

different experimental models of HE confirms that spatial working memory is damaged in cirrhotic rats due to the weekly administration of thioacetamide. This experimental group was unable to remember the location of platform in the retention trial, displaying difficulties in recalling new spatial information for a short period of time (Méndez et al. 2009a). Moreover, studies that enable us to evaluate the typical avoidance response, where an increase in the number of avoidances on the different acquisition days can be attributed to processes of consolidation and recall, showed that the portacaval shunt group and thioacetamide group had a clear deficit compared to control groups (Méndez et al. 2009b). All these data led to the hypothesis that massive exposition to the acquisition task during the 5 days on which the reference memory is carried out is probably the cause of the absence of differences between groups.

Histochemical labelling of COx revealed an absence of changes between groups in the mPFC area (PL, IL and CG) which is in agreement with the lack of motor dysfunctions, planning (prospective coding) and decision making (Kesner and Churchwell 2011). Dorsal regions of mPFC such as CG have been implicated in various motor behaviours, while ventral regions of mPFC (PL and IL) have been associated with diverse emotional, cognitive and mnemonic processes (Heidbreder and Groenewegen 2003).

The same pattern of activity could be observed in the CA1 subfield of the hippocampus. Previous studies have revealed projections from the hippocampus (CA1/subiculum) to the ventral mPFC (IL/PL) (Carr and Sesack 1996; Jay and Witter 1991), stronger to IL than to PL and to the dorsal mPFC (Hoover and Vertes 2007). It is known that hippocampal neurons encode newly-learnt goal locations through the reorganization of assembly firing patterns in the CA1 region but not in CA3. This suggests specialization within the hippocampus in order to solve spatial problems: whereas CA1 place representations are flexible because it encodes goal locations and the successful retrieval of goal-associated spatial memories, CA3 are stable, providing invariant representations of the whole environment independently of task demand (Dupret et al. 2010). In addition, Dupret and cols. (2011) have shown that enhanced reactivation of newly-established goal representations is NMDA receptor-dependent. These findings highlight the important role of NMDA receptor-dependent hippocampal plasticity during learning and are consistent with other behavioral studies showing that formation of spatial memories involves NMDA receptor (Nakazawa et al. 2004; McDonald et al. 2005).

Regarding the hippocampus, we observed that the dentate gyrus (DG) and CA3 subfield of the hippocampus were under-activated in the PH group. This could be related to the moderate spatial deficit showed in the task. Indeed, in experimental models where the advanced stages of the HE were studied, it has been found that an increase of the ammonia levels impairs induction of NMDA receptor-dependent long-term potentiation in the hippocampus (Méndez et al. 2010) and also alters the function of the glutamate-NO-cGMP pathway, resulting in reduced formation of cGMP (Montoliu et al. 2010). The changes in extracellular cGMP are parallel to changes in learning ability, supporting a role for cGMP levels in learning ability (Llansola et al. 2007). Moreover, behavioral studies suggest that spatial learning both of entire environments and discrete places involves NMDA receptor-dependent plasticity to update the hippocampal representation of space according to task demands and/or environmental changes. But these NMDA receptors are not only located in the hippocampus. Recent research has shown the importance of glutamate receptors in the basolateral complex of the amygdala (Bas) and in the central nucleus of the amygdala (Cen) (Llansola et al. 2007).

Furthermore, significant reciprocal inhibitory connections have been described between the ventral prefrontal cortex and amygdala (Womer et al. 2009).

The neurobehavioral correlations identified different patterns of interactivity in networks of brain regions between groups. In the SHAM group, which showed more metabolic activity than the PH group, we could observe a simple circuit that involves limbic regions associated with the hippocampal formation (CA1 and CA3) and included in Papez´ s circuit, such as the amygdala (Cen and MeA). Others studies revealed CA3-CA1 uncoupling in 5-day trained animals, and these regions correlated with behavioural learning scores in 3-day trained animals (Conejo et al. 2010). It is known that the learning process is reached near Day 3, so we hypothesized that this CA3-CA1 coupling indicates a delay in the brain activity in both groups, which is not reflected in the behavioural learning. In fact, other authors have highlighted that the performance of a laparotomy may cause some alterations that are still uncertain (López et al. 1997).

The PH group showed two more complex networks. The first one included relationships between CA1 and CA3 subfields of the hippocampus with other nuclei of amygdala such as MeA and Lat. The second network involved regions of the mPFC (CG, PL and IL) and Cen nuclei of the amygdala. This amount of structures could indicate metabolic brain efforts in the PH group, which are necessary to acquire the spatial reference memory in the same time as the SHAM group.

The PH rats showed no spatial learning impairment but there were differences in brain metabolic activity. This study is important because it revealed a metabolic deficit associated with some learning impairment at early phases of PH. These results support the complicated diagnosis related to the MHE which are unavailable to most clinicians. In fact, MHE patients have increased risk of developing and a lower survival rate (Romero-Gómez et al. 2007). Thus, others studies could be aimed at early detection of these symptoms in humans in order to prevent the chronic stages of the illness.

Acknowledgements We would like to thank Piedad Burgos, Begoña Valdés for their technical assistance, Lucía Ibañez for her surgical contributions. This research was supported by grant from the Spanish Ministry of Science and Innovation (PSI2010-19348), FMMA (AP/6977-2009) and MEC AP2009-1714 to N. Arias.

References

Al-Ghamdi H (2011) Carvedilol in the treatment of portal hypertension. Saudi J Gastroenterol 17:155–158. doi:10.4103/1319-3767.77251

Aller MA, Vara E, García C, Nava MP, Angulo A, Sánchez-Patán F, Calderón A, Vergara P, Arias J (2006) Hepatic lipid metabolism changes in short- and long-term prehepatic portal hypertensive rats. World J Gastroenterol 12:6828–6834

Amodio P, Montagnese S, Gatta A, Morgan MY (2004) Characteristics of minimal hepatic encephalopathy. Metab Brain Dis 19:253–267. doi:10.1023/B:MEBR.0000043975.01841.de

Begega A, Méndez M, Rubio S, Santín LJ, Aller MA, Arias J, Arias JL (2010) (2010) Portal hypertension in 18-month-old rats: memory deficits and brain metabolic activity. Physiol Behav 100:135–142. doi:10.1016/j.physbeh.2010.02.014

Butterworth RF, Norenberg MD, Felipo V, Ferenci P, Albrecht J, Blei AT, Members of the ISHEN Commission on Experimental Models of HE (2009) Experimental models of hepatic encephalopathy: ISHEN guidelines. Liver Int 29:783–788. doi:10.1111/j.1478-3231.2009.02034.x

Canales JJ, Elayadi A, Errami M, Llansola M, Cauli O, Felipo V (2003) Chronic hyperammonemia alters motor and neurochemical responses to activation of group I metabotropic glutamate receptors in the nucleus accumbens in rats in vivo. Neurobiol Dis 14:380–90. doi:10.1016/j.nbd.2003.08.023

Carey W (2011) Portal hypertension: diagnosis and management with particular reference to variceal hemorrhage. J Dig Dis 12:25–32. doi:10.1111/j.1751-2980.2010.00473.x

Carr DB, Sesack SR (1996) Hippocampal afferents to the rat prefrontal cortex: synaptic targets and relation to dopamine terminals. J Comp Neurol 369:1–15

Cauli O, Rodrigo R, Llansola M, Montoliu C, Monfort P, Piedrafita B, El Mlili N, Boix J, Agustí A, Felipo V (2009) Glutamatergic and gabaergic neurotransmission and neuronal circuits in hepatic encephalopathy. Metab Brain Dis 24:69–80. doi:10.1007/s11011-008-9115-4

Conejo NM, González-Pardo H, González-Lima F, Arias JL (2010) Spatial learning of the water maze: progression of brain circuits mapped with cytochrome oxidase histochemistry. Neurobiol Learn Mem 93:362–371. doi:10.1016/j.nlm.2009.12.002

Conejo NM, González-Pardo H, Vallejo G, Arias JL (2007) Changes in brain oxidative metabolism induced by water maze training. Neuroscience 145:403–412. doi:10.1016/j.neuroscience.2006.11.057

de la Torre JC, Cada A, Nelson N, Davis G, Sutherland RJ, Gonzalez-Lima F (1997) Reduced cytochrome oxidase and memory dysfunction after chronic brain ischemia in aged rats. Neurosci Lett 223:165–168. doi:10.1016/S0304-3940(97)13421-8

Dudchenko PA (2004) An overview of the tasks used to test working memory in rodents. Neurosci Biobehav Rev 28:699–709. doi:10.1016/j.neubiorev.2004.09.002

Dupret D, O'Neill J, Pleydell-Bouverie B, Csicsvari J (2010) The reorganization and reactivation of hippocampal maps predict spatial memory performance. Nat Neurosci 13:995–1002. doi:10.1038/nn.2599

González-Lima F, Cada A (1994) Cytochrome oxidase activity in the auditory system of the mouse: a qualitative and quantitative histochemical study. Neuroscience 63:559–578. doi:10.1016/0306-4522(94)90550-9

Heidbreder CA, Groenewegen HJ (2003) The medial prefrontal cortex in the rat: evidence for a dorso-ventral distinction based upon functional and anatomical characteristics. Neurosci Biobehav Rev 27:555–579. doi:10.1016/j.neubiorev.2003.09.003

Hoover WB, Vertes RP (2007) Anatomical analysis of afferent projections to the medial prefrontal cortex in the rat. Brain Struct Funct 212:149–179. doi:10.1007/s00429-007-0150-4

Jay TM, Witter MP (1991) Distribution of hippocampal CA1 and subicular efferents in the prefrontal cortex of the rat studied by means of anterograde transport of Phaseolus vulgaris-leucoagglutinin. J Comp Neurol 313:574–586

Jones BJ, Roberts DJ (1968) The quantitative measurement of motor incoordination in naïve mice using an accelerating rotarod. J Pharm Pharmacol 20:302–304

Kesner RP, Churchwell JC (2011) An analysis of rat prefrontal cortex in mediating executive function. Neurobiol Learn Mem 96:417–431. doi:10.1016/j.nlm.2011.07.002

Llansola M, Rodrigo R, Monfort P, Montoliu C, Kosenko E, Cauli O, Piedrafita B, El Mlili N, Felipo V (2007) NMDA receptors in hyperammonemia and hepatic encephalopathy. Metab Brain Dis 22:321–335. doi:10.1007/s11011-007-9067-0

López L, Burgos P, Santín LJ, Begega A, Arias J, Lorente L, Arias JL (1997) Portacaval shunt control animals: physiological consequences derived from the sham operation. Lab Anim 31:225–230. doi:10.1258/002367797780596239

McDonald RJ, Hong NS, Craig LA, Holahan MR, Louis M, Muller RU (2005) NMDA-receptor blockade by CPP impairs post-training consolidation of a rapidly acquired spatial representation in rat hippocampus. Eur J Neurosci 22:1201–1213. doi:10.1111/j.1460-9568.2005.04272.x

Méndez M, Méndez-López M, López L, Aller MA, Arias J, Arias JL (2009a) Basal and learning task-related brain oxidative metabolism in cirrhotic rats. Brain Res Bull 78:195–201. doi:10.1016/j.brainresbull.2008.10.008

Méndez M, Méndez-López M, López L, Aller MA, Arias J, Arias JL (2009b) Associative learning deficit in two experimental models of hepatic encephalopathy. Behav Brain Res 198:346–351. doi:10.1016/j.bbr.2008.11.015

Méndez M, Méndez-López M, López L, Aller MA, Arias J, Cimadevilla JM, Arias JL (2008) Spatial memory alterations in three models of hepatic encephalopathy. Behav Brain Res 188:32–40. doi:10.1016/j.bbr.2007.10.019

Méndez M, Méndez-López M, López L, Begega A, Aller MA, Arias J, Arias JL (2010) Reversal learning impairment and alterations in the prefrontal cortex and the hippocampus in a model of portosystemic hepatic encephalopathy. Acta Neurol Belg 110:246–254

Montoliu C, Rodrigo R, Monfort P, Llansola M, Cauli O, Boix J, El Mlili N, Agusti A, Felipo V (2010) Cyclic GMP pathways in hepatic encephalopathy. Neurological and therapeutic implications. Metab Brain Dis 25:39–48. doi:10.1007/s11011-010-9184-z

Morris RGM (1984) Developments of a water-maze procedure for studying spatial learning in the rat. J Neurosci Meth 11:47–60. doi:10.1016/0165-0270(84)90007-4

Moser MB, Moser EI, Forrest E, Andersen P, Morris RG (1995) Spatial learning with a minislab in the dorsal hippocampus. Proc Natl Acad Sci U S A 92:9697–96701

Nakazawa K, McHugh TJ, Wilson MA, Tonegawa S (2004) NMDA receptors, place cells and hippocampal spatial memory. Nat Rev Neurosci 5:361–372. doi:10.1038/nrn1385

Orloff MJ. (2001) Portal hypertension and Portocaval Shunt, Academic Press p. 637–701.

Paxinos G, Watson CH. (2005) The rat brain in stereotaxic coordinates-the new coronal set. 5th ed. Elsevier Academic Press

Poremba A, Jones D, González-Lima F (1998) Classical conditioning modifies cytochrome oxidase activity in the auditory system. Eur J Neurosci 10:3035–3043. doi:10.1046/j.1460-9568.1998.00304.x

Primatesta P, Brookes M, Poulter NR (2001) Improved hypertension management and control: results from the health survey for England 1998. Hypertension 38:827–832

Ragozzino ME, Detrick S, Kesner RP (1999) Involvement of the prelimbic-infralimbic areas of the rodent prefrontal cortex in behavioral flexibility for place and response learning. J Neurosci 19:4585–4594

Romero-Gómez M, Córdoba J, Jover R, del Olmo JA, Ramírez M, Rey R, de Madaria E, Montoliu C, Nuñez D, Flavia M, Compañy L, Rodrigo JM, Felipo V (2007) Value of the critical flicker frequency in patients with minimal hepatic encephalopathy. Hepatology 45:879–885. doi:10.1002/hep.21586

Sela S, Mazor R, Amsalam M, Yagil C, Yagil Y, Kristal B (2004) Primed polymorphonuclear leukocytes, oxidative stress, and inflammation antecede hypertension in the Sabra rat. Hypertension 44:764–769. doi:10.1161/01.HYP.0000144480.10207.34

Shao J, Dongsheng T (1995) The jackknife and bootstrap. Springer, New York

Timmermann L, Gross J, Butz M, Kircheis G, Häussinger D, Schnitzler A (2003) Mini-asterixis in hepatic encephalopathy induced by pathologic thalamo-motor-cortical coupling. Neurology 61:689–692

Timmermann L, Gross J, Kircheis G, Häussinger D, Schnitzler A (2002) Cortical origin of mini-asterixis in hepatic encephalopathy. Neurology 58:295–298

Womer FY, Kalmar JH, Wang F, Blumberg HP (2009) A ventral prefrontal-amygdala neural system in bipolar disorder: A view from neuroimaging research. Acta Neuropsychiatr 21:228–238

Zubcevic J, Waki H, Raizada MK, Paton JF (2011) Autonomic-immune-vascular interaction: an emerging concept for neurogenic hypertension. Hypertension 57:1026–1033. doi:10.1161/HYPERTENSIONAHA.111.169748

IV

Different brain network function during shifts in learning strategies in portal hypertension animals

Natalia Arias[1*], Camino Fidalgo[1], Guillermo Vallejo[2], Jorge L. Arias[1]

[1] *Laboratory of Neuroscience, Department of Psychology, University of Oviedo, Spain*
[2] *Laboratory of Methodology, Department of Psychology, University of Oviedo, Spain*

Corresponding author:

Natalia Arias

University of Oviedo

Department of Psychology

Laboratory of Neuroscience

Plaza Feijoo s/n, 33003

Oviedo, Asturias, Spain

e-mail:ariasnatalia@uniovi.es

Abstract

Patients with minimal hepatic encephalopathy exhibit early impairments in their ability to shift attentional set. We employed a task-switching protocol to evaluate brain network changes. Strategy switching requires the modification of both the relevant stimulus dimension and the required memory system. Rats were trained in an allocentric (A) and a cue-guided (C) task using a four-arm maze. To examine priming, we changed the order in which the tasks were presented. Five groups of animals were used: a SHAM (sham-operated) A-C group (n=10), a SHAM C-A group (n=8), a PH (portal hypertension) A-C group (n=8), PH C-A group (n=8), and a naïve group (n=10). The triple portal vein ligation method was used to create an animal model of the early evolutive phase of PH. The animals were tested in the four-arm radial water maze (RAWM) in a single 10-trial session each day for six days (three days for the allocentric task and three days for the cue-guided task). The metabolic activities of the brains were studied with cytochrome oxidase histochemistry, and brain network changes were assessed with principal component analysis (PCA). The behavioural results revealed significant increases in the numbers of correct choices across training days in all groups studied, and facilitation of the acquisition of the second task was present in the C-A groups. Moreover, different brain network activities were found; in the experimental groups, the performance of A-C switch involved the prefrontal cortex, and the key structures involved in the C-A switch in the other groups were the dentate gyrus of the dorsal hippocampus and the basolateral and central amygdala. These networks have a common nucleus of structures (i.e., the parietal cortex and the dorsal and ventral striatum), whereas other structures were specifically involved in each type of strategy, suggesting that these regions are part of both circuits and may interact with one another during learning.

Keywords

cue-guided task, allocentric task, rat, cytochrome c-oxidase, brain networks, portal hypertension, behavioural flexibility.

1. Introduction

Behavioural flexibility refers to the ability to learn a new strategy while inhibiting the execution of a previous strategy under changing environmental contingencies (Ragozzino et al., 1999). Behavioural flexibility is the general concept behind switching tasks that require modifying both the relevant stimulus dimension (e.g., from allocentric to cued-learning and vice versa) and the required memory system (White and McDonald, 2002). In this regard, different brain regions have traditionally been considered to mediate allocentric- and cued-learning. The hippocampus and the striatum (STR) have conventionally been considered to be key brain regions that are associated with independent memory systems. The hippocampus has been linked to spatial strategies (Bartsch et al., 2010) that require the development of a spatial cognitive map from an internal representation of the relationships between distal landmarks (de Bruin et al., 2001). In contrast, the striatum is involved in the acquisition of stimulus-response (S-R) memories (Fidalgo et al., 2011). More specifically, the striatum appears to be necessary for the formation of associations between cues and rewarded responses (cued-learning) (Miyoshi et al., 2012). This type of flexibility requires the reassignment of brain systems to perform the task correctly and is mediated by the prefrontal cortex in humans and non-human primates (Owen et al., 1990; Dias et al., 1997).

Over the years, studies have shown that different learning strategies require different neural networks that may could partially overlap (Rubio et al., 2012). Indeed, it is well known that the prelimbic area is involved in strategy shifting and that the infralimbic region is involved in the formation of new choice patterns. Furthermore, the interaction between these structures and the striatum during the execution of dynamic behaviour has been shown (Ragozzino, 2007). Indeed, dorsomedial striatal inactivation impairs shifts between visual cues and an egocentric response strategies (Ragozzino et al., 2002) that are revealed when the prelimbic area is inhibited. Furthermore, has been reported that the hippocampus and prefrontal cortex operate in parallel during the acquisition of spatial information (Rogers and Kesner, 2006), which highlights the existence of interactions between learning and memory structures.

Therefore, it is not difficult to understand that damage to one of these structures could cause impairments of cognitive flexibility similar to those that are present in numerous human conditions, including Huntington´s disease, Alzheimer´s disease (Menzie et al., 2012), and hepatic encephalopathy (HE) (Amodio et al., 2005).

The treatment of HE patients is not uniform and requires precise development of several new tools that enable the assessment of cognitive performance (Córdoba, 2011). Because HE is a continuum, understanding the early stages, known as minimal HE (mHE), is necessary from a preventive point of view. Several studies of animal models of mHE have shown delays in the acquisition of reference memory (Arias et al., 2012) and deficits in spatial working memory (Méndez et al, 2008). Thus, we used a model of

triple stenosing ligation of the portal vein (Aller et al., 2005) to create a set of neuropsychological methods that can provide a more objective assessment and be useful in researching the effect of new treatments.

To accomplish this goal, histochemical labelling of cytochrome c-oxidase (COx) was performed. COx is a mitochondrial enzyme that reflects changes in tissue metabolic capacity that are induced by the sustained energy requirements of the nervous system associated with learning (Poremba et al., 1998) and spatial memory in the Morris water maze (MWM) (Conejo et al., 2007). The aim of this study was to examine the brain networks that are involved in the encoding and retrieval of spatial information required for these switching strategies and, specifically, to determine how the selected rat brain regions differed in their activation when the allocentric- and cued-task order was changed. During the *allocentric task*, the rats had to acquire long-term memories of the location of the submerged platform based on their orientation relative to the positions of distal stimuli in the experimental room. In the *cue-guided task,* the rats were trained to locate the platform based on a yellow globe that was situated 20 cm above the platform. This version of the task requires the execution of the same response (cue-guided), rather than navigation to the same place.

2. Material and Methods

2.1. Subjects

Forty-four adult male Wistar rats (250-300 g.) from the animalarium of the University of Oviedo were housed four per cage in a temperature- and humidity-controlled vivarium under a 12-h light/dark cycle (lights on 8.00 A.M.). Experimental procedures were performed in accordance with the Directive of the European Commision (20120/63/EU) and Spanish legislation (R.D. 1201/2005) and approved by the local committee for animal studies.

The rats were randomly distributed into the following five groups: portal hypertension allocentric-cue guided (PH A-C group, n = 8), portal hypertension cue guided-allocentric (PH C-A group, n = 8), sham-operated allocentric-cue guided (SHAM A-C group, n = 10), sham-operated cue guided-allocentric (SHAM C-A group, n = 8), and a group of rats that received only gentle handling (naïve group, n = 10). The microsurgical procedures were carried out as described in Arias et al. (2012).

2.2. Behavioural procedures

The rats were trained in a black fiberglass radial arm water maze (RAWM, each arm was 80 cm×12 cm) that was placed 50 cm above floor level. The maze had four arms in the shape of a cross. The water depth was 30 cm, and the temperature was 22±2°C. The RAWM was in the centre of a 16 m^2 lit room (two halogen lamps of 4000 lx) and was surrounded by panels on which the spatial clues were placed. The behaviour of the rat in the RAWM was recorded by a video camera (Sony V88E)

connected to a computer equipped with the EthoVision Pro program (EthoVision 3.1; Noldus Information Technology, Leesburg, VA).

The learning protocol consisted of single 10 trial-sessions each day over 6 days in which the first 3 days were designated for the acquisition of one task, and the last 3 days were used for the acquisition of the other task (e.g., 3 days were allotted for the allocentric task, and the next 3 days were allotted for the cue-guided task). In each trial, the rats were placed in the centre of the pool facing a different arm and allowed to swim to the platform. If the animal failed to find the platform, it was guided to the platform. Once the rat reached the platform, it remained there for 15 s. Between trials, the rat was placed in a small square box for 30 s. The platform was in the same arm throughout the entire 10 trial-session each day, but the location of the platform each training day.

Every day at the end of each 10 trial-session, a probe test was applied in which the pool platform was removed, and the rat was introduced into the pool for 25 s. Immediately after the probe test, the rats were subjected to an additional trial in which the hidden platform was replaced to avoid any possible interference from the probe test.

All subjects in the experimental groups reached the learning criterion of choosing the correct arm in 70% of trials.

2.3. Cytochrome oxidase histochemistry

The protocol used was the same as that described by Arias et al. (2010). Ninety minutes after the last training day, brains were removed, frozen rapidly in N-methylbutane (Sigma-Aldrich, Madrid, Spain) and stored at -40ºC until processing for quantitative COx histochemistry. To quantify enzymatic activity and to control for staining variability across different baths, sets of tissue homogenate standards from Wistar rat brains were cut at different thicknesses (10, 30, 40 and 60 μm) and included with each bath of slides. Quantification of COx histochemical staining intensity was performed with densitometric analysis using a computer-assisted image analysis workstation (MCID, Interfocus Imaging Ltd., Linton, England) composed of a high-precision illuminator, a digital camera, and a computer with specific image analysis software (Leica Q-Win, Germany). The mean optical density (OD) of each region was measured in the bilateral structures using three consecutive sections in each subject. In each section, four non-overlapping readings were taken using a square-shaped sampling window that was adjusted for the size of each brain region. A total of twelve measurements were taken per region by an investigator who was blind to group membership. These measurements were averaged to obtain one mean value per region for each rat. OD values were then converted to COx activity units that were determined by the spectrophotometrically measured enzymatic activities of the standards (González-Lima and Cada, 1994). The different limbic brain regions studied, which are included in the Papez circuit, have frequently been implicated in memory processes. These regions of interest were anatomically defined according to Paxinos and Watson´s atlas (2005). The regions of interest and their distances (in mm) from bregma were as

follows: +3.20 mm for the infralimbic cortex (IL), prelimbic cortex (PL), and cingulate cortex (CG); +1.20 mm for the dorsal striatum, accumbens core, accumbens shell and parietal cortex; -1.20 mm for CA1, CA3 and the dentate gyrus (DG) subfields of the dorsal hippocampus; -3.12 mm for central and basolateral amygdala; and +4.52 mm for the supramammillary nucleus (SuM) and the medial mammillary bodies.

2.4. Statistical analysis

Portal pressure data were evaluated with student's t-tests for independent samples and are expressed as the mean ± the SEM.

To analyse the behavioural results, a longitudinal randomised controlled trial design was applied. Likelihood-based mixed-effects models provide appropriate general analytic frameworks to determine whether changes in response profiles over time differ between groups of animals (Vallejo et al., 2011). The mixed-effects model repeated measures (MMRM) analysis implemented herein included an unstructured (UN) modelling of time and a within-subject error correlation structure. In the version of MMRM used herein, time is considered as a classification rather than a continuous variable. Following rejection of an omnibus hypothesis, we next determined the contrasts between the populations in which the means were not equal to zero. To control the family-wise error (FWE) rate for all possible pairwise comparisons, the Hochberg (1988) step-up Bonferroni inequality was applied using the ESTIMATE statement in SAS PROC MIXED and the HOC option in SAS PROC MULTTEST. The dataset was analysed using MRM with REML estimation as implemented in SAS Version 9.3 (SAS Institute, 2011) PROC MIXED.

A principal components analysis (PCA) was applied to identify networks of correlated COx values. First, we performed Bartlett's sphericity test to confirm a the relationship between variables and the Kaiser-Meyer-Olkin (KMO) test to evaluate the extent to which the variable scores could be predicted from the other scores (Ferrando and Anguiano-Carrasco, 2010). The second step was to determine the number of components (networks) to be obtained. Lastly, a non-orthogonal oblimin rotation was performed, and the scores of each of the components were analysed by separate ANOVAs with between-subject components (three levels). Statistical analyses were performed with SAS Version 9.3 (SAS Institute, 2011) PROC MIXED.

3. Results

3.1. Portal pressure values

Portal pressure increased in animals with PH; the mean value of the PH animals was 13.9 ± 0.8, and that SHAM group was 5 ± 0.4. Significant differences were found between the groups ($t(18)=-8.258$, $p<0.001$).

3.2. Behavioural results

MMRM analysis revealed statistically significant differences [$F(3,30) = 3.45$, $p = 0.029$] between the comparison groups in their task performances averaged across training days. Additionally, there was a significant increase [$F(5,30) = 26.29$, $p <$

0.0001] in the mean response over time after averaging across the treatment groups. Interestingly, there were no significant differences [$F(15,30) = 1.82$, $p = 0.078$] between the comparison groups over time. Therefore, rat performance changed over time; however, the PH A-C, PH C-A, SHAM A-C, and SHAM C-A groups showed similar patterns of change.

After the overall null hypotheses regarding the groups and trials were rejected, we next determined the contrasts among the population for which the means was not equal to zero. For the group factor, post hoc analysis showed significant differences ($t30 = 3.30$, $p = 0.015$) between the SHAM A-C and the PH C-A groups. No differences were found in the five remaining pairwise comparisons (Fig. 2). For the training-days factor, all possible pairwise comparisons were statistically significant at the 5% family-wise significance level, with the exception of the comparison of day 3 to day 4.

In contrast, the results of the repeated measures ANOVAs for each group (i.e., PH A-C, PH C-A, SHAM A-C, and SHAM C-A) with Hochberg post-hoc pairwise comparisons were as follows: PH A-C [$F(5,35) = 10.35$, $p < 0.0001$] with significant differences between day 1 and the other days ($p<0.01$) and between day 2 compared to day 6 ($p = 0.047$); SHAM A-C [$F(5,45) = 5.35$, $p = 0.0006$] with differences between day 1 and day 6 ($p = 0.012$), and day 2 and day 6 ($p = 0.0012$); PH C-A [$F(5,35) = 8.95$, $p < 0.0001$] with differences between day 1 and days 5 ($p = 0.0002$) and 6 ($p=0.00006$), and between day 2 and days 5 ($p = 0.007$) and 6 ($p = 0.0022$); and SHAM C-A [$F(5,35) = 14.32$, $p < 0.0001$] with significant differences were between day 1 compared to the other days ($p \leq 0.00006$) and between day 2 compared to the other days ($p \leq 0.01$).

3.3. PCA of COx

The changes in COx values induced by both learning tasks were studied using PCA. Thus, we established possible functional groups among the brain regions examined in this study. The final structure obtained is represented in Table 1.

In the cue-guided task (A-C groups), component 1 plays a principal role in the learning task and involves most of the brain regions in each of the three experimental groups. These regions are the prefrontal and parietal cortex and striatum and accumbens. The average component scores for this component differed between groups [$F(2,48)=21.811$, $p<0.001$], and post hoc analysis revealed significant differences between the naïve group and the PH A-C ($p<0.001$) and SHAM A-C ($p<0.001$) groups.

Principal components 2, 3 and 4 seemed to include a more limited number of brain areas. Component 2 only included the mammillary bodies and the basolateral amygdala; component 3 involved the amygdala (basolateral and central), and component 4 is involved the hippocampus. No significant group differences were found in any of these components.

In contrast, three components were required to explain the allocentric task (C-A group). Principal component 1 involved 7 brain areas with high component loadings (>0.7). Component loading indicates the extent to which each structure is related to each component. A higher component loading indicates greater importance of the associated structure and, thus, the lower error influence. Component 1 loaded highest on the parietal cortex, striatum, accumbens, dentate gyrus of the hippocampus, and amygdala. Significant group differences [$F(2,42)=3.797$, $p<0.05$] were found, and post hoc analyses revealed significant differences between the naïve group and the SHAM C-A group ($p<0.05$). No differences were found in the second network in which only the medial mammillary nucleus showed a strong positive loading. However, for component 3, significant group differences [$F(2,42)=3.812$, $p<0.05$] were found, and post hoc analyses revealed significant differences between the naïve and SHAM C-A groups ($p<0.05$) and between the naïve and PH C-A groups ($p<0.05$). The prefrontal cortex, striatum, accumbens and dentate gyrus of the hippocampus showed high loadings on component 3. Additionally, some of these areas (i.e., the striatum, accumbens and dentate gyrus) loaded strongly on components 1 and 3, suggesting that these regions were part of both circuits and may have interacted with each other during the learning process.

4. Discussion

Strategy switching requires animals to distinguish different relationships between the same stimuli and responses to perform well (Rich and Shapiro, 2009), and strategy switching was required in the alternation between cued and allocentric learning. In this study, we combined both strategies while varying the order of acquisition to determine whether one strategy could facilitate the other. To achieve this aim, we used tasks that required the same effort and were matched for the numbers of trials. The RAWM was used as a dual-solution task in which rats can be forced to use one type of learning strategy by pairing the location of the platform with a single cue that guides the rat or with several distal visual cues that allow the rat to locate the target in the spatial environment; the latter solution is associated with increased memory load across trials (Camp et al., 2012). This is an effective procedure for studying behavioural flexibility that can differentiate acquisition strategies.

A previous studies by de Bruin et al. (2001) showed that, at the beginning of training, rats attempt to locate the platform in the pool using a strategy that implies the processing of spatial location information. When the rats fail to succeed, they change their strategy and eventually learn the route to the platform using a taxon strategy (i.e., cue-guided learning). These findings are similar to our results. Compared to the A-C groups (Figure 1), the SHAM group's performances on days 1 to 3 (in the allocentric task) exhibited a high number of correct choices from the beginning of task acquisition. However, when the change to the cue-guided task was made, the new learning process and the new strategy was revealed by the decreases in the numbers of correct choices shown on day 5; although rats eventually reach the criterion by the end of training.

Conversely, in the C-A groups, the low numbers of correct choices of the SHAM group in the cue-guided task reflected the rats' preferences for using spatial information first. Indeed, when the allocentric task was initiated, no decreases in the numbers of correct choices were observed, which supports previous research and shows that beginning with a favoured strategy may facilitate the acquisition of more difficult tasks.

However, the identity of the first task presented to the PH groups was not important because the number of correct choices made was always low. This lack of flexibility has been shown in previous studies (de Bruin et al., 1994) in which rats with medial prefrontal lesions were observed to be less flexible than control animals and required more time to adapt their strategy as reflected by transient impairments that occurred upon strategy changes (from allocentric to visually cued). Indeed, lower metabolic activities in the prefrontal cortices of PH groups compared to SHAM groups and the recruitment of increased numbers of brain regions that reflect the metabolic requirements of the brains of PH groups during the performance of spatial reference tasks have been reported previously (Arias et al., 2012).

The absence of changes in both experimental groups during acquisition allowed us to compare the groups in terms of metabolic brain activity. This comparison is important because, in hepatic encephalopathy and other metabolic encephalopathies, decreases in neuronal function decrease energy requirements (García-Martinez and Córdoba, 2011). We assessed brain metabolism using COx as a reliable index of neuronal oxidative metabolism (Fidalgo et al., 2011). Our data revealed a decrease in COx activity in the PH group compared to the SHAM group. Although this decreased was small and non-significant, the lack of group difference could be due to the metabolic efforts of portal hypertension brains during the early stages of hepatic encephalopathy. Thus, other brain structures might be used to achieve the goals of learning tasks.

Next, we used the COx values to form networks to explain the brain differences between the strategies. There were common structures in both principal networks (both first components in the A-C groups and C-A groups), such as the parietal cortex, dorsal striatum and accumbens. Traditionally, the striatum (STR) has been divided into dorsal and ventral subdivisions. The ventral subdivision contains the nucleus accumbens (ACC), which consists of core and shell sub-regions (Zahm, 2000). The STR is known to assist the navigational system by helping to define future actions that are appropriate for the current context (Mizumori et al., 2009). This role of the STR is reflected in the features that STR head direction cells share with place cells; i.e., preferred orientations shift by an amount that corresponds to shifts in the visual environment, and preferences can shift randomly if the visual cues are altered sufficiently (Mizumori et al., 2000). Thus, STR neuron types exhibit partial reorganisation after changes in allocentric context, and these findings are consistent with the fact that the STR evaluates the consequences of behaviours in a context-dependent manner (Mizumori et al., 2009). In the rodent, the lateral part of the dorsal striatum receives input from frontal and parietal cortices (Wise and Jones, 1977), which are involved in preparing the animal to execute appropriate behavioural responses (Mizumori et al., 2009). Thus, although the learning strategies we examined should have developed in different networks, they shared a

common foundation. Taken together, these data support the idea that, rather than operating as completely segregated neural networks that process and store different types of information as proposed by the multiple memory systems theory, these circuits partially overlap and share at least some structures (Rubio et al., 2012). Accordingly, accumulating recent experimental evidence suggests that the different memory systems may interact under some conditions (Byrne et al., 2007; Fidalgo et al., 2012). The existence of a common set of structures involved in both strategies suggests a central system that facilitates alternations between the requirements of the two different strategies.

In the A-C group, component 1 showed the involvement of the prefrontal cortex (prelimbic, infralimbic and cingulate cortices), which may be critical for the generation of a new strategy (Ragozzino, 2007). Connections between different prefrontal cortical areas and the striatum have been documented (Rich and Shapiro, 2007), and these connections may facilitate the execution of a response pattern that is appropriate for a particular newly generated strategy. According to this supposition, the switch from allocentric to cued-learning should reduce the relative influence of hippocampal processing on on-going behaviour. and increase that of dorsal striatal processing.

Corbit and Balleine (2003) suggested that prelimbic neurons may facilitate switching by integrating multiple task contingencies during goal-directed learning. Furthermore, studies using dopamine receptor blockade or NMDA receptor blockade in this region shown impairments in shifts between egocentric response and visual cue strategies (Floresco et al., 2006; Ragozzino, 2002; Stefani et al., 2003). Together, these findings indicate that the prelimbic area enables shifts in strategy across a variety of stimulus dimensions; specifically, the prelimbic area may support the initial inhibition of a previously learned strategy and/or the ability to generate a new strategy (Ragozzino, 2007).

However, rats with infralimbic lesions have been shown to have difficulty forming new relevant choice patterns (Chudasama and Robbins, 2003). Supporting these findings, Rich and Shapiro (2009) revealed that the infralimbic cortex establishes new stable codes only after performance nears proficiency, which demonstrates the critical role of the infralimbic region in habit formation (Ragozzino, 2007).

The mammillary bodies form the principal functional route through which spatially relevant information passes from the hippocampus to the anterior thalamic nuclei (Neave et al., 1997). However, the role of the mammillary bodies of rats is not limited to allocentric spatial processing. Several studies have shown that the mammillary bodies are required for the rapid encoding of new spatial information (Vann and Aggleton, 2004). Indeed, damage to the mammillary bodies causes encoding deficits during the learning of new spatial tasks that result in suboptimal performance (Neave et al., 1997). The appearance of the supramammillary nucleus could be due to

386 the projections from the mammillary bodies. This connection suggests the combined
387 involvement of both the supramammillary and the mammillary bodies in spatial
388 memory (Santín et al., 2003).

389

390 The absence of the amygdala and hippocampus in the first principal component
391 can be understood to result from the cortically enhanced inhibition of the infralimbic
392 cortex that is produced in amygdalar circuits (Quirk et al., 2003) and from the
393 modulatory role that the prelimbic area has on the hippocampus (Rich and Shapiro,
394 2007).

395

396 The opposite effects were observed in the C-A groups; both the hippocampus
397 and amygdala appeared in the first component. The remarkable plasticity of the
398 hippocampal network has been suggested to underlie several neural processes, including
399 new acquisition of spatial memory (Goodrich-Hunsaker et al., 2008), matching to
400 position tasks (Méndez-López et al., 2010), and novelty exploration (Lever et al., 2006)
401 (via comparison of previously encountered information with novel information (Lisman
402 and Otmakhova, 2011)). The dentate gyrus is the ascending neuronal pathway to the
403 hippocampus. Saab et al. (2009) showed that selective manipulation of dentate gyrus
404 neurons in a mouse line promotes exploratory behaviour and enhances hippocampal
405 synaptic plasticity and the rapid acquisition of spatial memory. Recent reports suggest
406 that the dentate gyrus is strongly activated during the initial stages of spatial learning
407 (Poirier et al., 2008) in response to novel spatial conditions (Jenkins et al., 2004).
408 However, limitations in the application of PCA should be taken into account especially
409 those related to sample sizes and the subjects-to-item ratios (Osborne and Costello,
410 2004); this limitation highlights the exploratory nature of our findings.

411

412 To conclude, the present study showed facilitation in the acquisition of the
413 allocentric task when the cue-guided task had previously been applied and progressive
414 improvement in task performance when the switch between tasks occurred in the
415 opposite order. These data, along with the findings that the experimental groups shared
416 a common set of brain structures and that other structures were specifically involved in
417 only one strategy, will be helpful in promoting the understanding of the specific
418 subregional contributions that depend on task demands and other factors, such as the
419 amount of training and type of strategy (Rubio et al., 2012).

420 **Acknowledgments**

421 We thank O. Ruiz for his significant contributions to the improvement of this
422 manuscript. This work was supported by grants from the Spanish Ministry of Science
423 and Innovation (PSI2010-19348), FMMA (AP/6977-2009), MEC AP2009-1714 to NA
424 and BES-2008-002499 to CF.
425

References

Aller, M.A., Vara, E., Garcia, C., Palma, M.D., Arias, J.L., Nava, M.P., Arias, J. (2005). Proinflammatory liver and antiinflammatory intestinal mediators involved in portal hypertensive rats. *Mediators Inflamm*. 9:101-111. doi: 10.1155/MI.2005.101.

Amodio, P., Schiff, S., Del Piccolo, F., Mapelli, D., Gatta, A., Umiltà, C. (2005). Attention dysfunction in cirrhotic patients: An inquiry on the role of executive control, attention orienting and focusing. *Metab Brain Dis*. 20:115-127. doi: 10.1007/s11011-005-4149-3.

Arias, N., Álvarez, C., Conejo, N., González-Pardo, H., Arias, J.L. (2010). Estrous cycle and sex as regulating factors of baseline brain oxidative metabolism and behavior. *Revista Iberoamericana de Psicología y Salud.* 1:3-16.

Arias, N., Méndez, M., Arias, J., Arias, J.L. (2012). Brain metabolism and spatial memory are affected by portal hypertension. *Metab Brain Dis*. 27:183-191. doi: 10.1007/s11011-012-9276-z.

Bartsch, T., Schönfeld, R., Müller, F.J., Alfke, K., Leplow, B., Aldenhoff, J., Deuschl, G., Koch, J.M. (2010). Focal lesions of human hippocampal CA1 neurons in transient global amnesia impair spatial memory. *Science*. 328:1412-1415. doi: 10.1126/science.1188160.

Byrne, P., Becker, S., Burgess, N. (2007). Remembering the past and imagining the future: A neural model of spatial memory and imagery. *Psychol Rev*. 114:340-375. doi: 10.1037/0033-295X.114.2.340.

Camp, B.W., Gerson, J.E., Tsang, C.W., Villa, S.R., Acosta, J.I., Blair Braden, B., Hoffman, A.N., Conrad, C.D., Bimonte-Nelson, H.A. (2012). High serum androstenedione levels correlate with impaired memory in the surgically menopausal rat: A replication and new findings. *Eur J Neurosci*. 36:3086-3095. doi: 10.1111/j.1460-9568.2012.08194.x.

Chudasama, Y., Robbins, T.W. (2003). Dissociable contributions of the orbitofrontal and infralimbic cortex to Pavlovian autoshaping and discrimination reversal learning: Further evidence for the functional heterogeneity of the rodent frontal cortex. *J Neurosci*. 23:8771-8780.

Conejo, N.M., González-Pardo, H., Vallejo, G., Arias, J.L. (2007). Changes in brain oxidative metabolism induced by water maze training. *Neuroscience*. 145:403-412. doi: 10.1016/j.neuroscience.2006.11.057.

Corbit, L.H., Balleine, B.W. (2003). The role of prelimbic cortex in instrumental conditioning. *Behav Brain Res*. 146:145-157. doi: 10.1016/j.bbr.2003.09.023.

Córdoba, J. (2011). New assessment of hepatic encephalopathy. *J Hepatol*. 54:1030-1040. doi: 10.1016/j.jhep.2010.11.015.

Costello, A.B., Osborne, J.W. (2005). Best practices in exploratory factor analysis: four recommendations for getting the most from your analysis. *Practical Assessment, Research & Evaluation*. 10:1-9.

de Bruin, J.P., Sànchez-Santed, F., Heinsbroek, R.P., Donker, A., Postmes, P. (1994). A behavioural analysis of rats with damage to the medial prefrontal cortex using the Morris water maze: Evidence for behavioural flexibility, but not for impaired spatial navigation. *Brain Res*. 652:323-333. doi: 10.1016/0006-8993(94)90243-7.

de Bruin, J.P., Moita, M.P., de Brabander, H.M., Joosten, R.N. (2001). Place and response learning of rats in a Morris water maze: Differential effects of fimbria fornix and medial prefrontal cortex lesions. *Neurobiol Learn Mem*. 75:164-178. doi: 10.1006/nlme.2000.3962.

Dias, R., Robbins, T.W., Roberts, A.C. (1997). Dissociable forms of inhibitory control within prefrontal cortex with an analog of the Wisconsin Card Sort Test: Restriction to novel situations and independence from "on-line" processing. *J Neurosci*. 17:9285-9297.

Ferrando, P.J., Anguiano-Carrasco, C. (2010). El análisis factorial como técnica de investigación en psicología. *Papeles del Psicólogo*. 31:18-33. doi: 10.5231/psy.writ.2012.0609.

Fidalgo, C., Conejo, N.M., González-Pardo, H., Arias, J.L. (2011). Cortico-limbic-striatal contribution after response and reversal learning: A metabolic mapping study. *Brain Res*. 1368:143-150. doi: 10.1016/j.brainres.2010.10.066.

Fidalgo, C., Conejo, N.M., González-Pardo, H., Arias, J.L. (2012). Functional interaction between the dorsal hippocampus and the striatum in visual discrimination learning. *J Neurosci Res*. 90:715-720. doi: 10.1002/jnr.22774.

Floresco, S.B., Magyar, O., Ghods-Sharifi, S., Vexelman, C., Tse, M.T. (2006). Multiple dopamine receptor subtypes in the medial prefrontal cortex of the rat regulate set-shifting. *Neuropsychopharmacology*. 31:297-309. doi: 10.1038/sj.npp.1300825.

García-Martínez, R., Córdoba, J. (2011). Acute-on-chronic liver failure: The brain. *Curr Opin Crit Care*. 17:177-183. doi: 10.1097/MCC.0b013e328344b37e.

González-Lima, F., Cada, A. (1994). Cytochrome oxidase activity in the auditory system of the mouse: A qualitative and quantitative histochemical study. *Neuroscience*. 63:559-578. doi: 10.1016/0306-4522(94)90550-9.

Goodrich-Hunsaker, N.J., Hunsaker, M.R., Kesner, R.P. (2008). The interactions and dissociations of the dorsal hippocampus subregions: How the dentate gyrus, CA3, and CA1 process spatial information. *Behav Neurosci*. 122:16-26. doi: 10.1037/0735-7044.122.1.16.

Hochberg, Y. (1988). A sharper Bonferroni procedure for multiple tests of significance. *Biometrika*. 75:800–802. doi: 10.1093/biomet/75.4.800.

Jenkins, T.A., Amin, E., Pearce, J.M., Brown, M.W., Aggleton, J.P. (2004). Novel spatial arrangements of familiar visual stimuli promote activity in the rat hippocampal formation but not the parahippocampal cortices: A c-fos expression study. *Neuroscience*. 124:43-52. doi: 10.1016/j.neuroscience.2003.11.024.

505 Lever, C., Burton, S., O'Keefe, J. (2006). Rearing on hind legs, environmental novelty,
506 and the hippocampal formation. *Rev Neurosci*. 17:111-133.

507 Lisman, J.E., Otmakhova, N.A. (2011). Storage, recall, and novelty detection of
508 sequences by the hippocampus: Elaborating on the SOCRATIC model to account for
509 normal and aberrant effects of dopamine. *Hippocampus*. 11:551-568. doi:
510 10.1002/hipo.1071.

511 Méndez, M., Méndez-López, M., López, L., Aller, M.A., Arias, J., Cimadevilla, J.M.,
512 Arias, J.L. (2008). Spatial memory alterations in three models of hepatic
513 encephalopathy. *Behav Brain Res*. 188:32-40. doi: 10.1016/j.bbr.2007.10.019.

514 Méndez-López, M., Méndez, M., Begega, A., Arias, J.L. (2010). Spatial short-term
515 memory in rats: Effects of learning trials on metabolic activity of limbic structures.
516 *Neurosci Lett*. 483:32-35. doi: 10.1016/j.neulet.2010.07.054.

517 Menzie, J., Pan, C., Prentice, H., Wu, J.Y. (2012). Taurine and central nervous system
518 disorders. *Amino Acids*. 46:31-46. doi: 10.1007/s00726-012-1382-z.

519 Miyoshi, E., Wietzikoski, E.C., Bortolanza, M., Boschen, S.L., Canteras, N.S.,
520 Izquierdo, I., Da Cunha, C. (2012). Both the dorsal hippocampus and the dorsolateral
521 striatum are needed for rat navigation in the Morris water maze. *Behav Brain Res*.
522 226:171-178. doi: 10.1016/j.bbr.2011.09.011.

523 Mizumori, S.J., Ragozzino, K.E., Cooper, B.G. (2000). Location and head direction
524 representation in the dorsal striatum of rats. *Psychobiology*. 28:441-462.

525 Mizumori, S.J., Puryear, C.B., Martig, A.K. (2009). Basal ganglia contributions to
526 adaptive navigation. *Behav Brain Res*. 199:32-42. doi: 10.1016/j.bbr.2008.11.014.

527 Neave, N., Nagle, S., Aggleton, J.P. (1997). Evidence for the involvement of the
528 mammillary bodies and cingulum bundle in allocentric spatial processing by rats. *Eur J*
529 *Neurosci*. 9:941-955.

530 Owen, A.M., Downes, J.J., Sahakian, B.J., Polkey, C.E., Robbins, T.W. (1990).
531 Planning and spatial working memory following frontal lobe lesions in man.
532 *Neuropsychologia*. 28:1021-1034. doi: 10.1016/0028-3932(90)90137-D.

533 Paxinos, G., Watson, C.H. (2005). *The rat brain in stereotaxic coordinates-the new*
534 *coronal set*. 5th ed. San Diego: Elsevier Academic Press.

535 Poirier, G.L., Amin, E., Aggleton, J.P. (2008). Qualitatively different hippocampal
536 subfield engagement emerges with mastery of a spatial memory task by rats. *J Neurosci*.
537 28:1034-1045. doi: 10.1523/JNEUROSCI.4607-07.2008.

538 Poremba, A., Jones, D., González-Lima, F. (1998). Classical conditioning modifies
539 cytochrome oxidase activity in the auditory system. *Eur J Neurosci*. 10:3035-3043. doi:
540 10.1046/j.1460-9568.1998.00304.x.

Quirk, G.J., Likhtik, E., Pelletier, J.G., Paré, D. (2003). Stimulation of medial prefrontal cortex decreases the responsiveness of central amygdala output neurons. *J Neurosci*. 23:8800-8807.

Ragozzino, M.E., Detrick, S., Kesner, R.P. (1999). Involvement of the prelimbic-infralimbic areas of the rodent prefrontal cortex in behavioral flexibility for place and response learning. *J Neurosci*. 19:4585-4594.

Ragozzino, M.E. (2002). The effects of dopamine D(1) receptor blockade in the prelimbic-infralimbic areas on behavioral flexibility. *Learn Mem*. 9:18-28.

Ragozzino, M.E., Ragozzino, K.E., Mizumori, S.J., Kesner, R.P. (2002). Role of the dorsomedial striatum in behavioral flexibility for response and visual cue discrimination learning. *Behav Neurosci*. 116:105-115.

Ragozzino, M.E. (2007). The contribution of the medial prefrontal cortex, orbitofrontal cortex, and dorsomedial striatum to behavioral flexibility. *Ann N Y Acad Sci*. 1121:355-375. doi: 10.1196/annals.1401.013.

Rich, E.L., Shapiro, M.L. (2007). Prelimbic/infralimbic inactivation impairs memory for multiple task switches, but not flexible selection of familiar tasks. *J Neurosci*. 27:4747-4755.

Rich, E.L., Shapiro, M.L. (2009). Rat prefrontal cortical neurons selectively code strategy switches. *J Neurosci*. 29:7208-7219. doi: 10.1523/JNEUROSCI.6068-08.2009.

Rogers, J.L., Kesner, R.P. (2006). Lesions of the dorsal hippocampus or parietal cortex differentially affect spatial information processing. *Behav Neurosci*. 120:852-860.

Rubio, S., Begega, A., Méndez, M., Méndez-López, M., Arias, J.L. (2012). Similarities and differences between the brain networks underlying allocentric and egocentric spatial learning in rat revealed by cytochrome oxidase histochemistry. *Neuroscience*. 223:174-182. doi: 10.1016/j.neuroscience.2012.07.066.

Saab, B.J., Georgiou, J., Nath, A., Lee, F.J., Wang, M., Michalon, A., Liu, F., Mansuy, I.M., Roder, J.C. (2009). NCS-1 in the dentate gyrus promotes exploration, synaptic plasticity, and rapid acquisition of spatial memory. *Neuron*. 63:643-656. doi: 10.1016/j.neuron.2009.08.014.

Santín, L.J., Aguirre, J.A., Rubio, S., Begega, A., Miranda, R., Arias, J.L. (2003). c-Fos expression in supramammillary and medial mammillary nuclei following spatial reference and working memory tasks. *Physiol Behav*. 78:733-739. doi: 10.1016/S0031-9384(03)00060-X.

Stefani, M.R., Groth, K., Moghaddam, B. (2003). Glutamate receptors in the rat medial prefrontal cortex regulate set-shifting ability. *Behav Neurosci*. 117:728-737.

Vallejo, G., Fernández, M.P., Livacic-Rojas, P.E., Tuero-Herrero, E. (2011). Comparison of modern methods for analyzing unbalanced repeated measures data with missing values. *Multivariate Behav Res*. 46:900-937.

Vann, S.D., Aggleton, J.P. (2004). The mammillary bodies: two memory systems in one?. *Nat Rev Neurosci*. 5:35-44. doi: 10.1038/nrn1299.

White, N.M., McDonald, R.J. (2002). Multiple parallel memory systems in the brain of the rat. *Neurobiol Learn Mem*. 77:125-184. doi: 10.1006/nlme.2001.4008.

Wise, S.P., Jones, E.G. (1977). Cells of origin and terminal distribution of descending projections of the rat somatic sensory cortex. *J Comp Neurol*. 175:129-157.

Zahm, D.S. (2000). An integrative neuroanatomical perspective on some subcortical substrates of adaptive responding with emphasis on the nucleus accumbens. *Neurosci Biobehav Rev*. 24:85-105. doi: 10.1016/S0149-7634(99)00065-2.

Figure Captions

Figure 1: Cytochrome oxidase (COx) histochemistry in the sampled regions in which the squares used to take the measures were presented: cingulate (CG), prelimbic (PL) and infralimbic (IL) cortex, parietal cortex (Par), dorsal striatum (STR), accumbens core (Acc) and shell (Acs), dorsal hippocampus (CA1, CA3 and DG), basolateral (Bas) and central (Cen) amygdala, supramammillar (Supra) and medial mammillary nucleus (MM). Scale bar: 400µm.

Figure 2: Numbers of correct choices across training days for the A-C groups (A) and the C-A groups (B). Solid and dotted lines represent sham and hypertensive groups, respectively. * $p<0.05$ the numbers of correct choices were compared across training days.

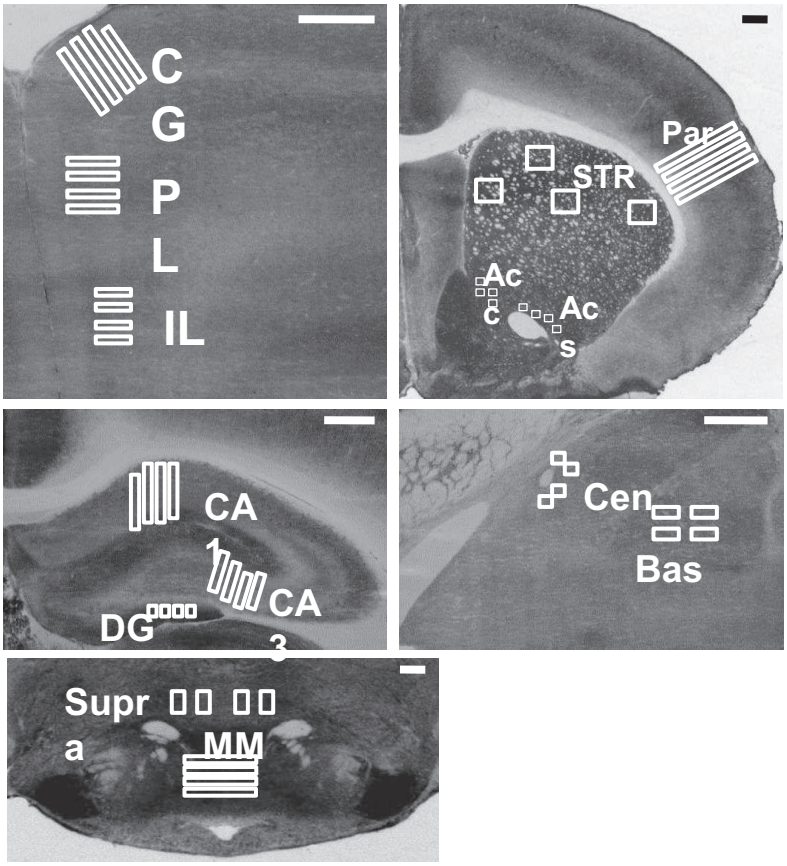
C
G
P
L
IL
Par
STR
Ac
c
Ac
s
CA
1
CA
3
DG
Cen
Bas
Supr
a
MM

Figure 2

A

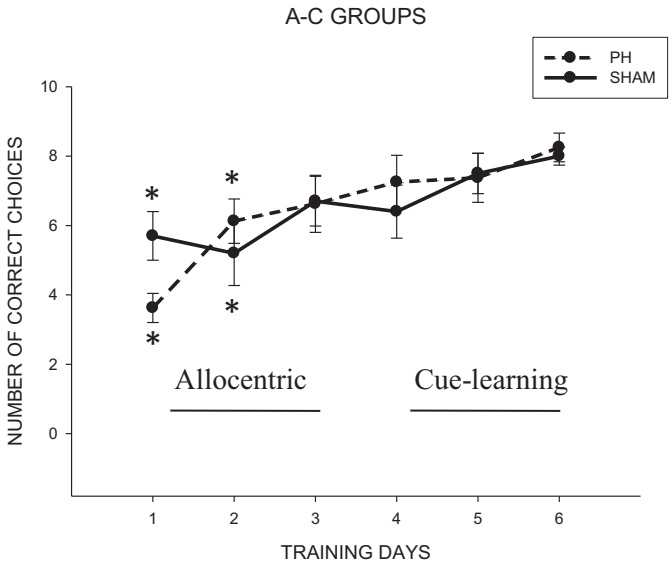
A-C GROUPS
PH
SHAM
NUMBER OF CORRECT CHOICES
10
8
6
4
2
0
Allocentric
Cue-learning
1
2
3
4
5
6
TRAINING DAYS

B

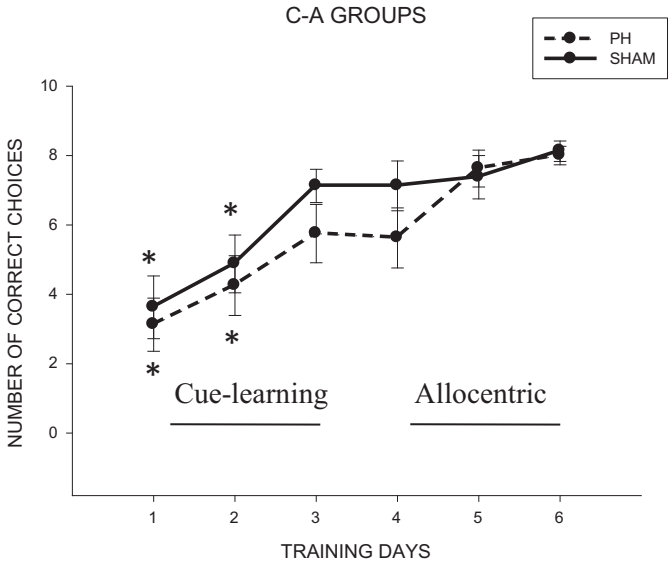
C-A GROUPS
PH
SHAM
NUMBER OF CORRECT CHOICES
10
8
6
4
2
0
Cue-learning
Allocentric
1
2
3
4
5
6
TRAINING DAYS

Table 1: Circuits of COx values activated in response to the experimental conditions as revealed by PCA. A: representative COx values for the A-C groups. B: representative COx values for the C-A groups.

A

	COMPONENT			
A-C GROUPS	1	2	3	4
Prelimbic cortex	**0.94**	0.19	0.41	0.50
Infralimbic cortex	**0.93**	0.30	0.41	0.59
Cingulate cortex	**0.94**	0.22	0.41	0.56
Parietal cortex	**0.74**	0.62	0.14	0.31
Dorsal striatum	**0.93**	0.33	0.19	0.70
Accumbens core	**0.91**	0.40	0.22	0.66
Accumbens shell	**0.93**	-0.02	0.25	0.62
CA1	0.60	0.20	0.27	**0.97**
CA3	0.54	0.17	0.30	**0.98**
Dentate gyrus	0.63	0.13	0.33	**0.91**
Basolateral amygdala	0.49	**0.90**	**0.93**	0.33
Central amygdala	0.23	-0.30	**0.96**	0.30
Supramammillar	0.53	**0.79**	0.04	0.56
Medial mammillary nucleus	0.10	**0.93**	0.02	0.07

B

	COMPONENT		
C-A GROUPS	1	2	3
Prelimbic cortex	0.47	-0.13	**0.96**
Infralimbic cortex	0.54	-0.14	**0.94**
Cingulate cortex	0.55	-0.12	**0.96**
Parietal cortex	**0.91**	0.03	0.61
Dorsal striatum	**0.91**	0.09	**0.75**
Accumbens core	**0.89**	-0.02	**0.75**
Accumbens shell	**0.84**	-0.10	**0.81**
CA1	0.68	0.59	0.72
CA3	0.60	0.63	0.67
Dentate gyrus	**0.77**	0.38	**0.81**
Basolateral amygdala	**0.79**	0.28	0.37
Central amygdala	**0.74**	0.54	0.22
Supramammillar	0.57	0.15	0.28
Medial mammillary nucleus	0.07	**0.81**	-0.21

V

DIFFERENTIAL CONTRIBUTION OF THE HIPPOCAMPUS IN TWO DIFFERENT DEMANDING TASKS AT EARLY STAGES OF HEPATIC ENCEPHALOPATHY

Arias N.[1,2], Méndez M.[1,2], Arias JL.[1,2]

[1] Laboratorio de Neurociencias, Departamento de Psicología, Universidad de Oviedo, Plaza Feijoo s/n, 33003 Oviedo, Spain

[2] INEUROPA, Instituto de Neurociencias del Principado de Asturias

HIPPOCAMPAL CONTRIBUTION IN EARLY HEPATIC ENCEPHALOPATHY

Text pages: 27

Number of Figures: 4

Corresponding author:

Natalia Arias

Plaza Feijoo s/n, CP: 33003, Oviedo, Asturias, Spain

Tel: +34 985103212

e-mail:ariasnatalia@uniovi.es

Grant Sponsor: Spanish Ministry of Science and Innovation; Grant number: PSI2010-19348; Grant Sponsor: FMMA; Grant number: AP/6977-2009; Grant Sponsor: MEC; Grant number: AP2009-1714.

Keywords: one-trial object-place recognition task, reversal learning, c-Fos immunoreactivity, hepatic encephalopathy, rat.

ABSTRACT

The hippocampus has been established as a site of plasticity during the acquisition of spatial memory. The memory for spatial locations is impaired in patients who develop hepatic encephalopathy (HE). We wondered how the hippocampus can deal with different levels of difficulty in hippocampal dependent tasks in a type B model of early evolutive phases of HE induced by triple portal vein ligation. We used a one-trial object-place recognition task which implies making judgments about whether a stimulus was encountered before in that location and a reversal learning, which involves reward-guided behavior and decision making, was also performed testing spatial learning in the Morris water maze. Our behavioral results showed impairment in the acquisition of both tasks by the portal hypertension group compared to sham-operated group. To label brain areas related to these tasks, we marked the expression of c-Fos protein, showing high c-Fos immunoreactivity in CA1, CA3 and Ent of the PH group compared to the SHAM group in the object-place recognition task, and a decrease in c-Fos positive cells in the reversal task, in the CA1, CA3, DG, CG, PL and IL in the PH group compared to the SHAM group. Concluding, the study corroborated the pivotal role of the hippocampus in spatial memory and pointed out its differential contribution in each of the tasks, not only in terms of recruitment different brain regions but also in terms of impairment of its function at early stages of type B HE when the requirements of the tasks are higher.

INTRODUCTION

The hippocampus has been established as a site of plasticity during the acquisition of spatial memory and its modification upon retrieval (Li *et al.*, 2013). The existence of individual place cells which are active not only to a first approximation to the environment, but even to ongoing dimensions of the rat's purposive behavior (Ainge *et al.*, 2007) indicate that the hippocampus may mediate spatial and episodic dimensions of the animal's experience (Ainge *et al.*, 2007). The implication of the hippocampus in the spatial memory has been revealed through numerous studies in working and reference memory tasks in a radial-arm maze (Olton & Papas, 1979; Poirier *et al.*, 2008), in Morris water maze (Morris *et al.*, 1982; Méndez-López *et al.*, 2010; Arias *et al.*, 2012), and even it supports spontaneous associative object-location and object-context information (Save *et al.*, 1992; Dix & Aggleton, 1999), indicating its involvement in the integration of multimodal information (Rajji *et al.*, 2006; Langston & Wood, 2010).

However, there is a different involvement of the hippocampal subfields during these spatial memory tasks. The dentate gyrus (DG) plays important role in spatial navigation (Derrick, 2007; Kesner, 2007), pattern separation (Leutgeb *et al.*, 2007; Clelland *et al.*, 2009), context-related functions (Lee & Kesner, 2004; Hernandez-Rabaza *et al.*, 2008) and encoding of spatial information (Lee & Kesner, 2004). Projections between DG, CA3 and hippocampal field CA1 have been broadly demonstrated. CA1 is critical for consolidation and retrieval of spatial information (Rolls & Kesner, 2006; Vago *et al.*, 2007), whereas CA3 has been more related to the process of encoding (Hunsaker *et al.*, 2008). This region also enables rapid associations between spatial locations or places and objects (Rolls, 2013).

The memory for spatial locations can be operationalized by stimuli (e.g., objects, platforms) encountered by animals and the occasion (contextual or temporal) in which the event took place (Eacott & Norman, 2004; Babb & Crystal, 2006). Impairments to this memory have been shown in numerous neurodegenerative diseases such as Korsakoff's syndrome (Kessels & Kopelman, 2012), Alzheimer's disease and patients who develop hepatic encephalopathy (HE) (Felipo *et al.*, 2012). HE can arise across

a spectrum of clinical severity, encompassing subtle loss of cognitive function, lethargy, depressed consciousness and coma (Tranah *et al.*, 2013). As the disease progresses, intellectual abilities deteriorate and patients show neuropsychological disturbances that affect orientation (Weissenborn *et al.*, 2003). In liver cirrhosis, between 60% and 80% of patients are estimated to suffer with minimal hepatic encephalopathy (Ortiz *et al.*, 2005). The functional neuroimaging of the brain in these patients shows alterations in the hippocampus and related regions that seems to be responsible for the clinical characteristics such as deficits in attention and spatial orientation (Weissenborn *et al.*, 2004).

In the current study, we wondered how the hippocampus can deal with different levels of difficulty in hippocampal dependent tasks in a model of early evolutive phases of HE. To address this issue, we used a simple spatial task where the animals have to recognize that an object they had experienced before had changed location (one-trial object-place recognition task), which implies making judgments about whether a stimulus was encountered before in that location. A more complex task assessing the ability to associate a reinforcement with previously neutral stimuli in the environment and to subsequently change this association (reversal learning), which, in turn, involves reward-guided behaviour and decision making, has also been used (Rudebeck & Murray, 2008).

To label the hippocampal regions and other brain areas, we marked the expression of c-Fos protein. The study of c-Fos can provide information about neuronal plasticity required for memory processes (Kaczmarek, 1993). The expression of c-Fos protein is induced after learning and is indicative of a change in neuronal activity (Kaczmarek, 1993; Radulovic *et al.*, 1998; Santín *et al.*, 2003). This technique allows the simultaneous examination of the activity of populations of neurons in multiple brain regions (Wan *et al.*, 1999). Because the hippocampus does not act as an isolated structure in these spatial learning tasks, other cerebral regions involved in them were studied. These were the prefrontal cortex and adjacent cortical areas within the temporal lobe, such as the entorhinal cortex and perirhinal cortex, based on the evidence that either ablation, electrophysiological lesions or dysfunctions suggest

that these structures might be involved in these spatial tasks (Zhu *et al.*, 1995; Schoenbaum *et al.*, 2003; Stalnaker *et al.*, 2007; Méndez *et al.*, 2010).

MATERIAL AND METHODS

1. Animals

We used 30 male Wistar rats from the vivarium of University of Oviedo, weighing 250-270 gm at the beginning of the study. Rats were housed in groups of three to five, three weeks prior to the beginning of the experiments and maintained under standard laboratory conditions (20-22 ºC, 65-70% relative humidity and a 12h light/dark cycle). Food and water were available ad libitum throughout the course of all experiments and sessions were performed during the light phase, between 9:00 a.m. and 13:00 p.m. All procedures were carried out according to the European Parliament and the Council of the European Union 2010/63/UE and were approved by the Oviedo University committee for animal studies. The animals were randomly distributed into two groups: portal hypertension (PH group, n = 14) and sham-operated (SHAM group, n = 16). Then, animals were distributed into a reversal task (SHAM group, n=10 and PH group, n=9) and a one-trial object-place recognition task (SHAM group, n=6 and PH group, n=5).

2. Procurement of experimental models

The experimental models that required surgery were anesthetized by i.m. injection of ketamine (100mg/kg) and xylazine (12 mg/kg). With regard to postsurgical care, rats were kept near a heat source (10-15 minutes) until they regained consciousness to prevent postoperative hypothermia. They were then introduced into individual polycarbonate cages for 15 days.

2.1. Portal hypertension

Portal hypertension was produced by triple stenosing ligation (Diéguez *et al.*, 2002). A midline abdominal incision was performed and a section of the intestinal loops was gently shifted to the left and covered with saline-moistened gauze. The portal vein was isolated and three ligatures, fixed on a sylactic

guide, were performed in its superior, middle and inferior portions. The stenoses were calibrated by simultaneous ligation (4-0 silk) around the portal vein and a 20-gauge blunt-tipped needle. The abdominal incision was closed in two layers with catgut and 2-0 silk. The postoperative period started immediately after the intervention and lasted until the behavioural evaluation 45 days later.

2.2. Sham-operated

A bilateral subcostal laparotomy with prolongation to the xyphoid apophysis, followed by isolation of the portal vein, was performed. The operative field was irrigated with saline solution during the intervention, like the portal hypertension ones. Finally, the laparotomics were closed by continuous suture on the two layers with catgut and 2-0 silk. The postoperative period started immediately after the intervention and lasted until the behavioural evaluation 45 days later.

2.3. Portal vein pressure measurement

In order to confirm the portal hypertension, splenic pulp pressure, an indirect measurement of portal pressure (PP), was measured by the method described by Aller *et al*. (2006) in 13 subjects randomly selected from the two groups (PH group, n = 7 and SHAM group, n = 6).

3. Apparatus

Object exploration was assessed in an square open field (100 x 100 x 40 (height) cm) with an open roof, placed in a rectangular room with several distal cues and a proximal cue, a small circular white sticker located on the east wall of the open field. The open field was made of grey fibreglass and two diffuse white lights, placed at sides of the room, provided an illumination density of approximately 50 lux at the centre of the open field. Two ventilation fans produced background noise at the east and west sides of the room. A video camera, connected to a video recorder, was mounted above the field to store sample and test trials on video files for off-line analysis. After each trial, the apparatus was thoroughly cleaned with a 75% ethanol solution. Four different objects were constructed from combinations of plastic pieces, varying in colour and size from 13 x 13 x 16 cm to 16 x 16 x 19 cm. All

objects had sufficient weight to ensure that the rats could not displace them and were counterbalanced within each group to avoid possible effects of preference. After each trial, objects were thoroughly cleaned with a 75% ethanol solution in order to remove odour cues.

3.1. Experiment 1: Object-Place recognition task

3.1.1. Habituation

Prior to testing, all the animals were handled for four consecutive days during 10 min/day and habituated to the empty arena for three consecutive days. On the first day of habituation, groups of between three and five rats were placed together in the open field and allowed to explore it for 6 min without objects. On the following day, rats were given another 6-min session of exploration but this time, only one rat at a time was placed in the open field. On the third and last habituation day, rats received three daily sessions of 6 min duration with 20 min of inter-trial interval with the presence of the two habituation objects placed opposite to each other, 10 cm, on two of the walls of the open field. This time, rats were also individually brought to the testing room and placed in the open field facing the centre of the wall where no objects were located. Habituation objects were not used in the assessment of memory for object place recognition.

3.1.2. Test phase

In the assessment for one-trial object-place recognition, these groups also received a sample and a test trial, both of 4 min duration, with an inter-trial interval of 50 min. In the sample trial condition, two copies of the same object were present. Nonetheless, in the test trial, one of the two copies was placed in a different corner of the open field. This task is used to determine whether rats can detect a mismatch between the past and present location of a familiar object.

3.2. Experiment 2: Reversal learning

Reversal learning was evaluated in the MWM (Morris, 1984). The MWM was made of fibreglass and measured 150 cm in diameter with a wall 40 cm high. The water level was 30 cm and its

temperature was 22±2°C. The platform used corresponded to a cylinder 10 cm in diameter and 28 cm high, of which 2 cm were below the surface of the water. The MWM was in the centre of a 16-m2 lit room (two halogen lamps of 4000 lx) and was surrounded by panels on which the spatial clues were placed. The pool was divided into four imaginary quadrants (quadrant A, B, C and D, or right, left, across and correct, respectively). The behaviour of the animal in the MWM was recorded by a video camera (Sony V88E) connected to a computer equipped with an EthoVision Pro programme.

The learning protocol consisted in the first day being destined for habituation of animals to the task, in which the animals carried out four trials with a visible platform, which juts out 4 cm from the water and is located in the centre of the pool. During the following 6 days, the animals were subjected to four acquisition trials in which the platform was hidden in the centre of quadrant D. After this training, the platform was moved to the opposite quadrant, C.

In each trial, the rats were allowed to swim to locate the platform, or were placed on it after 60 s, where they remained for 15 s before they were placed in the cage for 30 s. Latency to find the platform, defined as escape latency, were recorded during habituation and learning sessions. Daily, at the end of each learning session, rats were given a 25-second probe test, and selective quadrant search was evaluated by measuring the percentage of time spent in each quadrant of the pool. After this training, the rats were tested for reversal learning, for one day, using the same procedure. The animals were given four acquisition trials, where the hidden platform was located in the quadrant opposite from its previous location, quadrant C. As before, rats were given a probe test that was conducted at the end of the session.

4. c-Fos immunocytochemistry

To determine c-Fos activity, subjects that performed the reversal learning task (SHAM group n=6, PH group n=6) and object-place recognition task (SHAM group n=6, PH group n=5) were processed ninety minutes after the end of both tasks. The animals were decapitated, brains were removed intact,

frozen rapidly in isopentane (Sigma-Aldrich, Germany), and stored at −40 °C. Coronal sections (30 µm) of the brain were cut at −20 °C in a cryostat (Leica CM1900, Germany). The sections were mounted on gelatinized slides, which were post-fixed in buffered 4% paraformaldehyde (0.1M, pH 7.4) for 30 min and rinsed in phosphate-buffered saline (PBS) (0.01 M, pH 7.4). They were subsequently incubated for 15 min with 3% hydrogen peroxidase in PBS to remove endogenous peroxidase activity and were washed twice in PBS. After blocking with PBS solution containing 10% Triton X-100 (PBS-T) (Sigma, USA) and 3% bovine serum albumin for 30 min, sections were incubated with a rabbit polyclonal anti-c-Fos solution (1:10,000) (Santa Cruz Biotech, sc-52, USA) diluted in PBS-T for 24 h at 4° C in a humid chamber. Slides were then washed three times with PBS, and incubated in a goat anti-rabbit biotinylated IgG secondary antibody (Pierce, USA; diluted 1:200 in incubating solution) for 2 h at room temperature. They were washed three times in PBS and were reacted with avidin–biotin peroxidase complex (Vectastain ABC Ultrasensitive Elite Kit, Pierce) for 1 h. After two washes in PBS, the reaction was visualized treating the sections for about 3 min in a commercial nickel-cobalt intensified diaminobenzidine kit (Pierce). The reaction was finalized by washing the sections twice in PBS. Slides were then dehydrated through a series of graded alcohols, cleared with xylene and coverslipped with Entellan (Merck, USA) for microscopic observation. All immunocytochemistry procedures included sections that served as controls where the primary antibody was not added. Slides containing sections of a specific brain region were stained at the same time. Slides were coded so the investigator who performed the entire analysis would have no knowledge of the treatment of the individual subjects.

The number of c-Fos positive nuclei was quantified in two alternate sections 30 µm apart containing prelimbic (PL), infralimbic (IL) and cingulate (CG) cortex, septal hippocampus: cornu ammonis 1 (CA1), cornu ammonis 3 (CA3) and dentate gyrus (DG), the perirhinal cortex (Prh) and the entorhinal cortex (Ent). Coronal sections of these brain regions were located using the stereotaxic atlas of Paxinos and Watson (2005). Distance in mm of brain regions counted from bregma was: +3.0 mm for PL, IL and

CG cortex, -3.24 mm for septal hippocampus, -3.96 mm Prh and Ent. Quantification was done by systematically sampling each of the regions selected using counting frames superimposed over the region. Sizes of the counting frames range varied from 18000 µm2 (DG) to 121500 µm2 (CA1). The total area sampled by these frames per region in each section was: 214200 µm2 in PL, IL and CG cortex, 121500 µm2 in septal CA1, 58500 µm2 in septal CA3 and 18000 µm2 in septal DG, 40500 µm2 in Prh, Ent. Cell counts were conducted using a microscope (Olympus BH-2, Japan) coupled to an analogue camera (Sony XC-77, Japan) and a TV monitor (300x total magnification). c-Fos positive nuclei were defined based on homogenous gray-black stained elements with a well-defined border. Finally, the mean count of three sections was calculated for each subject and region.

STATISTICAL ANALYSIS

1. Object-Place recognition data

Exploration of an object was defined as directing the nose towards the object at a distance of less than 2 cm and actively exploring the object. Sitting and turning around on the object were not considered exploratory behaviour. For each rat, the time spent exploring the objects in both sample sessions and the test session were scored off-line from video files using stopwatches. Two researchers blind to the groups coded each video. A number of measurements were taken in order to examine exploration and discrimination. The proportion of exploration in the sample and test phases was considered as e1 and e2 respectively, and it was calculated by dividing the exploration of all objects in the phase divided by the total time available for exploration. Two measures of discrimination were taken: discrimination index (d1) and discrimination ratio (d2) (Ennaceur & Delacour, 1988). The discrimination index, d1, consisted of the difference in time spent exploring the two objects in the test phase, the object that changed position minus the object that remained in the same position. The discrimination ratio, d2, was also calculated in the test phase. This is the difference in the exploration time of the two objects divided by the total time spent exploring the objects, that is, d1/ time spent

exploring both objects. Exploration in the sample and the test phase (e1 and e2) was compared with a paired t-test. In addition, t-tests were performed on d1 and d2 to determine whether the mean scores differed from zero (chance performance indicating equal exploration of the two objects). This would indicate that the rats could successfully discriminate between the objects.

2. Reversal learning data

For the initial hidden platform test, the latencies to reach the hidden platform for each day (average of four trials) were analyzed using two-way repeated measures ANOVA (session x group). When a significant session effect was found, a further repeated measures ANOVA was conducted for each group. The time spent in each of the four quadrants during the probe test was analyzed separately for each group and day using a one-way ANOVA design, and Tukey's test was applied as a post hoc test. All data were analyzed in the Sigma-Stat 3.2 program (Systat, Richmond, USA) and were expressed as means±SEM. The results were considered as statistically significant if $P < 0.05$.

3. c-Fos data

For statistical analysis, cell counts from the three selected sections for a given brain region in each animal were averaged, and the mean was used for statistical analysis. Student *t*-test for independent samples was used to assess whether the number of c-Fos positive nuclei was different between experimental groups in each condition (reversal learning and object-place recognition) in each brain region. Moreover, a non-parametric Mann-Whitney *U* test (*H*) for independent samples was carried out when normality or equal group variances failed.

RESULTS

1. Portal vein pressure measurement

Portal pressure increases in rats with PH, showing mean values of 13.784 ± 1.45 compared to the SHAM group, where portal pressure values were 6.921 ± 0.52 ($t_{11} = -4.156$, $P = 0.002$).

2. Behavioural results

2.1. Experiment 1: Object-Place Recognition

The results showed that whereas SHAM rats were able to discriminate between an object that had remained in a constant position and one that had changed position, the PH group was not. Significant group differences were found in d1 and d2 (d1: $H = 15.000$, $n_1 = 5$, $n_2 = 6$, $P = 0.004$; d2: $t_9 = -3.681$, $P = 0.005$; Fig.1A). There was no significant group difference in the exploration index (e1: $t_9 = 0.591$, $P = 0.569$; e2: $t_9 = 1.104$, $P = 0.298$; Fig.1B).

2.2. Experiment 2: Reversal learning

There were no differences between groups in the habituation session. They show similar latencies to reach the visible platform (PH: 39.5 ± 3.807 and SHAM: 38.475 ± 3.184) $t_{17} = -0.208$, $P = 0.838$). Regarding the spatial learning task, the two-way repeated measures ANOVA showed no differences in escape latencies between the PH and SHAM groups ($F_{(1,17)} = 1.074$, $P = 0.315$). Test day or session had a significant effect ($F_{(5,85)} = 14.398$, $P < 0.001$). No interaction between factors (session and Group) was found ($F_{(5,85)} = 1.035$, $P = 0.403$). The repeated measures ANOVA that was conducted for each group revealed that both SHAM and PH groups improve over sessions (SHAM: $F_{(5,45)} = 13.292$, $P < 0.001$ and PH: $F_{(5,40)} = 4.297$, $P = 0.003$). The SHAM group presented shorter latencies to platform since the second session (2, 3, 4, 5 and 6) compared to the first ($P < 0.001$). However, the PH group improves in the last two sessions (5 and 6), where we can see a reduction in the escape latencies compared to the first one ($P \leq 0.041$) (Fig. 2). In the reversal session, both groups presented a similar performance ($t_{17} = 1.536$, $P = 0.143$) (Fig. 2).

In the probe test, the PH group learned the location of the platform on day 4. On this day, the PH group spent more time in the quadrant where the platform was located, quadrant D, than in the other quadrants ($F_{(3,32)} = 13.535$, $P < 0.001$). In days 5 and 6, this preference was also maintained ($F_{(3,32)} = 27.411$, $P < 0.001$ and $F_{(3,32)} = 45.331$, $P < 0.001$, respectively). In the SHAM group, spatial learning was demonstrated from day 2 ($F_{(3,36)} = 8.473$, $P < 0.001$). Tukey's test showed that quadrant D was preferred

by the SHAM rats over quadrants A, B and C ($P < 0.05$). The preference persisted during day 3 ($F_{(3,36)} = 20.180$, $P < 0.001$), day 4 ($F_{(3,36)} = 35.420$, $P < 0.001$), day 5 ($F_{(3,36)} = 12.775$, $P < 0.001$) and day 6 ($F_{(3,36)} = 58.593$, $P < 0.001$) (Fig.3).

As it was explained above, there were no differences between the PH and SHAM groups in the latencies to reach the hidden platform during the acquisition trials of the reversal test (Fig. 2). However, the groups differed in the probe test (Fig. 3). Regarding the SHAM group, the time of permanence in the four quadrants of the pool differed ($F_{(3,36)} = 58.593$, $P < 0.001$). The SHAM group preferred the new location of the platform position (quadrant C) versus the other quadrants, A, B and D ($P \leq 0.017$). However, the PH group did not learn the new location of the platform. In this group, the time of permanence in the quadrants of the pool also differed ($F_{(3,32)} = 5.973$, $P = 0.002$), but PH group preferred quadrant C over B ($P = 0.003$) and A ($P = 0.008$), but not D ($P = 0.151$) (Fig. 3).

3. c-Fos results

3.1. Experiment 1: Object-Place Recognition

There were group differences in the CA1 ($t_9 = 2.323$, $P = 0.045$), CA3 ($t_9 = 2.473$, $P = 0.035$) and Ent ($t_9 = 3.148$, $P = 0.012$). In these regions, the number of c-Fos positive nuclei was higher in the PH group than in the SHAM group. No group differences were found in PL ($t_9 = 1.046$, $P = 0.323$), IL ($t_9 = 0.947$, $P = 0.368$), CG ($t_9 = 0.481$, $P = 0.642$), DG ($t_9 = 0.991$, $P = 0.348$) or Prh ($t_9 = 1.453$, $P = 0.180$; Fig.4A).

3.2. Experiment 2: Reversal learning

The number of c-Fos positive nuclei was different in the two behavioural groups: lower in the PH group in the PL ($t_{10} = -2.918$, $P= 0.015$), IL ($t_{10}= -3.280$, $P = 0.008$) and CG ($H = 25.500$, $n_1 = 6$, $n_2 = 6$, $P = 0.026$); CA1 subfield of the septal hippocampus ($H = 45.000$, $n_1=5$, $n_2=6$, $P = 0.004$), septal CA3 ($t_{10} = -6.124$, $P < 0.001$) and septal DG ($t_{10} = -5.426$, $P < 0.001$; Fig.4B).

DISCUSSION

Our work revealed the presence of cognitive alterations in the processes of object-place recognition and reversal learning, and for the first time, these data demonstrated the differential contribution of hippocampal subfields and extrahippocampal structures associated with these spatial memories in a rat model of type B hepatic encephalopathy induced by triple portal vein ligation. We used different requirements of two spatial tasks, an object-place recognition task in which only involves the judgment of where an object was previously encountered, and a more complex task such as reversal learning, which implies contextual information, temporally extended behaviour, in which prospective and retrospective behaviour are implicit, and the integration of the journeys with reward expectancy to produce path selection (Young & Shapiro, 2011).

Experiment 1 showed that, unlike the SHAM group animals, the animals in the PH group were unable to remember the change of position of the displaced object. To solve the object-place recognition task, the animals must combine visual and spatial information and recognize the topographical location of the objects (Goodrich-Hunsaker *et al.*, 2005). The behavioural results indicated that this spatial memory was impaired in the PH animals, as they did not discriminate the new location of the object. It is important to note that the decreased discrimination ratio observed for the PH rats was not a consequence of decreased exploration, because the PH group exhibited no differences in total times of exploration when compared to the SHAM group.

Such judgment is supported by several regions. Traditionally, ablation or electrophysiological evidence have suggested that hippocampal formation, entorhinal cortex and adjacent cortical areas within the temporal lobe such as the perirhinal cortex might be involved in recognition memory (Zhu *et al.*, 1995). Detailed studies with bilateral hippocampal lesions revealed significantly impaired memory for object-place recognition, whereas lesions in the perirhinal cortex had no effect on it (Barker *et al.*, 2007; Barker & Warburton, 2011). These data highlighted the role of both structures in terms of the

type of information required for recognition memory judgment, with the hippocampus being more involved in recognition memory for places (Barker & Warburton, 2011). Furthermore, these lesion results were supported by other studies related to the recognition of familiar spatial arrangements in which significant increases in Fos levels in CA1 and significant decreases in the dentate gyrus were found (Aggleton *et al.*, 2012).

Regarding the entorhinal cortex, which is the major cortical input to the hippocampus (Warburton and Brown, 2010), its involvement in item and contextual novelty detection through object recognition paradigms has been broadly corroborated (Hunsaker *et al.*, 2013). Therefore, the involvement of the hippocampus and entorhinal cortex in one-trial object-place recognition are expected, as this is in agreement with previous studies reflecting the activation of these structures in the performance of object-place recognition tasks.

Experiment 2 revealed the inability of the PH group to remember the new location of the platform during the probe test of the reversal task, compared to SHAM group. Although portal hypertension animals take one day longer to reach the behavioral criterion during the performance of the spatial memory task, this delay is minimal and both groups acquire the spatial reference memory task. In fact, the portal hypertension animals show an excellent performance of the probe test that is maintained during the last three training days. This revealed a good consolidation and maintenance of the spatial information by this experimental group. However, when performing the reversal task, the PH group showed preference for the previous platform position, in contrast to SHAM group, which rapidly learned the new location. In this experiment, the demands to solve the task are higher than in Experiment 1, as the task involves complex processes such as the formation of associative paths, the maintenance in memory of sequences of goal-directed actions, withholding previously rewarded responses and producing previously unrewarded ones. Consequently, as the complexity of the task increases, the number of brain regions involved is higher.

The pivotal role of the hippocampus in reversal performance has been demonstrated when partial lesions of the hippocampus impair the task, revealing it as a component of a memory system necessary for the flexible use of relations between stimuli to guide behaviour (Eichenbaum & Cohen, 2001) and its implication in the ability to inhibit responses that the animal is predisposed to make (Kimble, 1968). Moreover, different subfields of the hippocampus have distinct functions in this learning. Whereas the dentate gyrus is more important for encoding spatial information, CA3 and especially CA1 are more critical for consolidation or retrieval processes (Rolls & Kesner, 2006; Vago *et al.*, 2007).

This strategy switching is impaired in rats with lesions to prelimbic-infralimbic cortex (Young & Shapiro, 2009). The relationship between both structures has also been reported by local field potential studies, suggesting the potential for mutual information exchange (Buzsáki & Draguhn, 2004), and revealing coherence between the hippocampus and rat PL-IL activity. This relationship has also been observed to correlate with spatial behaviour (Hyman *et al.*, 2005).

Taking together, the results of both experiments highlighted impairment in the performance of both hippocampal-dependent tasks of animals at early stages of HE. But more interesting data were revealed when we examined c-Fos results, which showed high c-Fos immunoreactivity in CA1, CA3 and entorhinal cortex of the PH group compared to the SHAM group in the object-place recognition task. However, the opposite pattern was found in the reversal learning task, where a decrease in c-Fos positive cells appeared in the CA1, CA3, DG, CG, PL and IL in the PH group compared to the SHAM group. Patients with minimal HE due to liver cirrhosis show neuropsychological disturbances that affect to spatial orientation (Weissenborn *et al.*, 2003). The functional neuroimaging of the brain in these patients shows alterations in the hippocampus and related regions that seems to be responsible for these deficits (Weissenborn *et al.*, 2004). Animal models of HE show slightly alterations of spatial memory at early stages of the disease and a clear impairment when macronodular cirrhosis progress

(Méndez *et al.*, 2008a; Arias *et al.*, 2012). It has been also demonstrated that spatial working memory is also affected in a model of liver cirrhosis and this deficit was related with less c-Fos protein expression in the hippocampus (Méndez *et al.*, 2008b).

In light of the results of the present study of the animal model of minimal HE, a differential contribution of the hippocampus has been revealed, depending on the requirement of the task. When the requirement is low, such as in the object-place recognition task, in which the structures recruited to perform the task form a "short neural circuit", increases in c-Fos positive nuclei have been normally found in the animals that perform the task correctly (SHAM group). However, when the SHAM group is compared to a group that has not reach the behavioural criterion (PH group), but is still trying to perform the task successfully, the number of c-Fos positive nuclei of the latter group is increased compared to the SHAM group. This reflects the need to recruit hippocampal subfields, such as CA1 and CA3, and entorhinal cortex in the acquisition of object-place recognition task (Aggleton *et al.*, 2012).

Conversely, an increase in the difficulty of a spatial task, reflected in reversal learning, is revealed by a recruitment of additional structures, forming a "long neural circuit". The entire subfields of the hippocampus and prefrontal cortex are needed to perform the task, which is shown in the SHAM group. But a deficit both in the acquisition of the task and the level of gene expression was found in the PH group compared to the SHAM group, as previously shown by Méndez *et al.* (2010) in cirrhotic rats.

At the same time, it is well-known that the hippocampus and prelimbic cortex are connected, and CA1 is the major efferent of prelimbic cortex projections (Jay *et al.*, 1989; 1991). Normal neurotransmission at hippocampal to prefrontal cortex synapses is AMPA glutamate receptor-dependent (Jay *et al.*, 1992; Gigg *et al.*, 1994). Different subfields of the hippocampus have distinct memory functions supported by the trysinaptic pathway, which is glutamate-dependent and distinguished by its one-way information flow, from entorhinal cortex to DG, to CA3, to CA1, and onto

the subiculum (Amaral & Witter, 1989; O'Reilly & McClelland, 1994; McClelland *et al.*, 1995; Eichenbaum, 2000; Witter *et al.*, 2000).

Seamans *et al.* (1998) suggest that dopamine can modulate the information flow between hippocampus and the prefrontal cortex. Both neurotransmission pathways are affected under HE. AMPA receptor densities were significantly increased in the cortex and decreased in the hippocampus (Oja *et al.*, 1996), together with the fact that a decrease in dopaminergic tone in HE has been reported (Albrecht & Jones, 1999). So, this dysfunction in the hippocampal-prefrontal pathway in the PH group is probably reflected not only in the inability to reach the behavioural criterion, but even in a lower c-Fos expression than in the SHAM group.

Concluding, the study corroborated the pivotal role of the hippocampus in spatial memory, highlighting three main findings: (i) Considerable variation in the expression of c-Fos in hippocampal subfields to reach and maintain distinctive levels of difficulty in spatial memory. (ii) Different recruitment of structures related to hippocampus based on the different requirements of the tasks, revealing short and long neural circuits (iii) The existence of brain damage at early stages of a model of type B hepatic encephalopathy, leading to behaviour and memory impairment through a hippocampal affectation.

ACKNOWLEDGEMENTS

This work was supported by grants from the Spanish Ministry of Science and Innovation (PSI2010-19348), FMMA (AP/6977-2009) and MEC AP2009-1714 to NA.

References

Aggleton, J.P., Brown M.W. & Albasser, M.M. (2012) Contrasting brain activity patterns for item recognition memory and associative recognition memory: insights from immediate-early gene functional imaging. *Neuropsychologia*, **50**, 3141-3155.

Ainge, J.A., Tamosiunaite, M., Woergoetter, F. & Dudchenko, P.A. (2007) Hippocampal CA1 place cells encode intended destination on a maze with multiple choice points. *J. Neurosci.*, **27**, 9769-9779.

Albrecht, J. & Jones, E.A. (1999) Hepatic encephalopathy: molecular mechanisms underlying the clinical syndrome. *J. Neurol. Sci.*, **170**, 138-146.

Aller, M.A., Vara, E., García, C., Nava, M.P., Angulo, A., Sánchez-Patán, F., Calderón, A., Vergara, P. & Arias, J. (2006) Hepatic lipid metabolism changes in short- and long-term prehepatic portal hypertensive rats. *World J. Gastroenterol.*, **12**, 6828-6834.

Amaral, D.G. & Witter, M.P. (1989) The three-dimensional organization of the hippocampal formation: a review of anatomical data. *Neuroscience*, **31,** 571–591.

Arias, N., Méndez, M., Arias, J. & Arias, J.L. (2012) Brain metabolism and spatial memory are affected by portal hypertension. *Metab. Brain Dis.*, **27**, 183-191.

Babb, S.J. & Crystal, J.D. (2006) Episodic-like memory in the rat. *Curr. Biol.*, **16**, 1317-1321.

Barker, G.R., Bird, F., Alexander, V. & Warburton, E.C. (2007) Recognition memory for objects, place, and temporal order: a disconnection analysis of the role of the medial prefrontal cortex and perirhinal cortex. *J. Neurosci*., **27**, 2948-2957.

Barker, G.R. & Warburton, E.C. (2011) When is the hippocampus involved in recognition memory?. *J. Neurosci*., **31**, 10721-10731.

Buzsáki, G. & Draguhn, A. (2004) Neuronal oscillations in cortical networks. *Science*, **304**, 1926-1929.

Clelland, C.D., Choi, M., Romberg, C., Clemenson, G.D., Fragniere, A., Tyers, P., Jessberger, S., Saksida, L.M., Barker, R.A., Gage, F.H. & Bussey, T.J. (2009) A functional role for adult hippocampal neurogenesis in spatial pattern separation. *Science*, **325,** 210–213.

Derrick, B.E. (2007) Plastic processes in the dentate gyrus: a computational perspective. *Prog. Brain Res.*, **163,** 417–451.

Diéguez, B., Aller, M.A., Nava, M.P., Palma, M.D., Arias, J.L., López, L. & Arias, J. (2002) Chronic portal hypertension in the rat by triple-portal stenosing ligation. *J. Invest. Surg.*, **15**, 329–336.

Dix, S.L. & Aggleton, J.P. (1999) Extending the spontaneous preference test of recognition: evidence of object-location and object-context recognition. *Behav. Brain Res.*, **99**, 191-200.

Eacott, M.J. & Norman, G. (2004) Integrated memory for object, place, and context in rats: a possible model of episodic-like memory?. *J. Neurosci.*, **24**, 1948-1953.

Eichenbaum, H. (2000) A cortical-hippocampal system for declarative memory. *Neuroscience.*, **1,** 41–50.

Eichenmaum, H. & Cohen, N.J. (2001) *From conditioning to conscious recollection*. New York, Oxford UP.

Ennaceur, A. & Delacour, J. (1988) A new one-trial test for neurobiological studies of memory in rats. 1: Behavioral data. *Behav. Brain Res.*, **31**, 47-59.

Felipo, V., Urios, A., Montesinos, E., Molina, I., Garcia-Torres, M.L., Civera, M., Olmo, J.A., Ortega, J., Martinez-Valls, J., Serra, M.A., Cassinello, N., Wassel, A., Jordá, E. & Montoliu, C. (2012) Contribution of hyperammonemia and inflammatory factors to cognitive impairment in minimal hepatic encephalopathy. *Metab. Brain Dis.*, **27**, 51-58.

Gigg, J., Tan, A.M. & Finch, D.M. (1994) Glutamatergic hippocampal formation projections to prefrontal cortex in the rat are regulated by GABAergic inhibition and show convergence with glutamatergic projections from the limbic thalamus. *Hippocampus*, **4**, 189-198.

Goodrich-Hunsaker, N.J., Hunsaker, M.R. & Kesner, R.P. (2005) Dissociating the role of the parietal cortex and dorsal hippocampus for spatial information processing. *Behav. Neurosci.*, **119**, 1307-1315.

Hernandez-Rabaza, V., Hontecillas-Prieto, L., Velazquez-Sanchez, C., Ferragud, A., Perez-Villaba, A., Arcusa, A., Barcia, J.A., Trejo, J.L. & Canales, J.J. (2008) The hippocampal dentate gyrus is essential for generating contextual memories of fear and drug-induced reward. *Neurobiol. Learn. Mem.*, **90**, 553–559.

Hunsaker, M.R., Tran, G.T. & Kesner, R.P. (2008) A double dissociation of subcortical hippocampal efferents for encoding and consolidation/retrieval of spatial information. *Hippocampus*, **18**, 699-709.

Hunsaker, M.R., Chen, V., Tran, G.T. & Kesner, R.P. (2013) The medial and lateral entorhinal cortex both contribute to contextual and item recognition memory: a test of the binding of items and context model. *Hippocampus*, **23**, 380-391.

Hyman, J.M., Zilli, E.A., Paley, A.M. & Hasselmo, M.E. (2005) Medial prefrontal cortex cells show dynamic modulation with the hippocampal theta rhythm dependent on behavior. *Hippocampus*, **15**, 739-749.

Jay, T.M., Glowinski, J. & Thierry, A.M. (1989) Selectivity of the hippocampal projection to the prelimbic area of the prefrontal cortex in the rat. *Brain Res.*, **505**, 337-340.

Jay, T.M. & Witter, M.P. (1991) Distribution of hippocampal CA1 and subicular efferents in the prefrontal cortex of the rat studied by means of anterograde transport of Phaseolus vulgaris-leucoagglutinin. *J. Comp. Neurol.*, **313**, 574-586.

Jay, T.M., Thierry, A.M., Wiklund, L. & Glowinski, J. (1992) Excitatory Amino Acid Pathway from the Hippocampus to the Prefrontal Cortex. Contribution of AMPA Receptors in Hippocampo-prefrontal Cortex Transmission. *Eur. J. Neurosci.*, **4**, 1285-1295.

Kaczmarek, L. (1993) Molecular biology of vertebrate learning: is c-fos a new beginning?. *J. Neurosci. Res.*, **34**, 377-381.

Kesner, R.P. (2007) A behavioral analysis of dentate gyrus function. *Prog. Brain Res.*, **163**, 567–576.

Kessels, R.P. & Kopelman, M.D. (2012) Context memory in Korsakoff's syndrome. *Neuropsychol. Rev.*, **22**, 117-131.

Kimble, D.P. (1968) Hippocampus and internal inhibition. *Psychol. Bull.*, **70**, 285-295.

Langston, R.F. & Wood, E.R. (2010) Associative recognition and the hippocampus: differential effects of hippocampal lesions on object-place, object-context and object-place-context memory. *Hippocampus*, **20**, 1139-1153.

Lee, I. & Kesner, R.P. (2004) Encoding versus retrieval of spatial memory: double dissociation between the dentate gyrus and the perforant path inputs into CA3 in the dorsal hippocampus. *Hippocampus*, **14**, 66–76.

Leutgeb, J.K., Leutgeb, S., Moser, M.B. & Moser, E.I. (2007) Pattern separation in the dentate gyrus and CA3 of the hippocampus. *Science*, **315**, 961–966.

Li, L., Sase, A., Patil, S., Sunyer, B., Höger, H., Smalla, K.H., Stork, O. & Lubec, G. (2013) Distinct set of kinases induced after retrieval of spatial memory discriminate memory modulation processes in the mouse hippocampus. *Hippocampus*, **23**, 672-683.

McClelland, J.L., McNaughton, B.L. & O'Reilly, R.C. (1995) Why there are complementary learning systems in the hippocampus and neocortex: insights from the successes and failures of connectionist models of learning and memory. *Psychol. Rev.*, **102**, 419–457.

Méndez, M., Méndez-López, M., López, L., Aller, M.A., Arias, J., Cimadevilla, J.M. & Arias, J.L. (2008a) Spatial memory alterations in three models of hepatic encephalopathy. *Behav. Brain Res.*, **188**, 32-40.

Méndez, M., Méndez-López, M., López, L., Aller, M.A., Arias, J. & Arias, J.L. (2008b) Working memory impairment and reduced hippocampal and prefrontal cortex c-Fos expression in a rat model of cirrhosis. *Physiol. Behav.*, **95**, 302-307.

Méndez, M., Méndez-López, M., López, L., Begega, A., Aller, M.A., Arias, J. & Arias, J.L. (2010) Reversal learning impairment and alterations in the prefrontal cortex and the hippocampus in a model of portosystemic hepatic encephalopathy. *Acta Neurol. Belg.*, **110**, 246-254.

Morris, R.G., Garrud, P., Rawlins, J.N. & O'Keefe, J. (1982) Place navigation impaired in rats with hippocampal lesions. *Nature*, **297**, 681-683.

Morris, R. (1984) Developments of a water-maze procedure for studying spatial learning in the rat. *J. Neurosci. Methods*, **11**, 47-60.

Oja, S.S., Borkowska, H.D., Albrecht, J. & Saransaari, P. (1996) Kainate and AMPA receptors in the rat brain in thioacetamide-induced hepatic encephalopathy. *Proc. West. Pharmacol. Soc.*, **39**, 15-17.

Olton, D.S. & Papas, B.C. (1979) Spatial memory and hippocampal function. *Neuropsychologia*, **17**, 669-682.

O'Reilly, R.C. & McClelland, J.L. (1994) Hippocampal conjunctive encoding, storage, and recall: avoiding a trade-off. *Hippocampus*, **4**, 661-682.

Ortiz, M., Jacas, C. & Cordoba, J. (2005) Minimal hepatic encephalopathy: diagnosis, clinical significance and recommendations. *J. Hepatol.*, **42**, S45–S53.

Paxinos, G. & Watson, C.H. (2005) *The rat brain in stereotaxic coordinates-the new coronal set*. Elsevier Academic Press, London.

Poirier, G.L., Amin, E. & Aggleton, J.P. (2008) Qualitatively different hippocampal subfield engagement emerges with mastery of a spatial memory task by rats. *J. Neurosci.*, **28**, 1034-1045.

Radulovic, J., Kammermeier, J. & Spiess, J. (1998) Relationship between fos production and classical fear conditioning: effects of novelty, latent inhibition, and unconditioned stimulus preexposure. *J. Neurosci.*, **18**, 7452-7461.

Rajji, T., Chapman, D., Eichenbaum, H. & Greene, R. (2006) The role of CA3 hippocampal NMDA receptors in paired associate learning. *J. Neurosci.*, **26**, 908-915.

Rolls, E.T. & Kesner, R.P. (2006) A computational theory of hippocampal function, and empirical tests of the theory. *Prog. Neurobiol.*, **79**, 1-48.

Rolls, E.T. (2013) The mechanisms for pattern completion and pattern separation in the hippocampus. *Front. Syst. Neurosci.*, **7**,74.

Rudebeck, P.H. & Murray, E.A. (2008) Amygdala and orbitofrontal cortex lesions differentially influence choices during object reversal learning. *J. Neurosci.*, **28**, 8338-8343.

Santín, L.J., Aguirre, J.A., Rubio, S., Begega, A., Miranda, R. & Arias, J.L. (2003) c-Fos expression in supramammillary and medial mammillary nuclei following spatial reference and working memory tasks. *Physiol. Behav.*, **78**, 733-739.

Save, E., Poucet, B., Foreman, N. & Buhot, M.C. (1992) Object exploration and reactions to spatial and nonspatial changes in hooded rats following damage to parietal cortex or hippocampal formation. *Behav. Neurosci.*, **106**, 447-456.

Schoenbaum, G., Setlow, B., Nugent, S.L., Saddoris, M.P. & Gallagher, M. (2003) Lesions of orbitofrontal cortex and basolateral amygdala complex disrupt acquisition of odor-guided discriminations and reversals. *Learn. Mem.*, **10**, 129-140.

Seamans, J.K., Floresco, S.B. & Phillips, A.G. (1998) D1 receptor modulation of hippocampal-prefrontal cortical circuits integrating spatial memory with executive functions in the rat. *J. Neurosci.*, **18**, 1613-1621.

Stalnaker, T.A., Franz, T.M., Singh, T. & Schoenbaum, G. (2007) Basolateral amygdala lesions abolish orbitofrontal-dependent reversal impairments. *Neuron*, **54**, 51-58.

Tranah, T.H., Vijay, G.K., Ryan, J.M. & Shawcross, D.L. (2013) Systemic inflammation and ammonia in hepatic encephalopathy. *Metab. Brain Dis.*, **28**, 1-5.

Vago, D.R., Bevan, A. & Kesner, R.P. (2007) The role of the direct perforant path input to the CA1 subregion of the dorsal hippocampus in memory retention and retrieval. *Hippocampus*, **17**, 977-987.

Wan, H., Aggleton, J.P. & Brown, M.W. (1999) Different contributions of the hippocampus and perirhinal cortex to recognition memory. *J. Neurosci.*, **19**, 1142-1148.

Warburton, E.C. & Brown, M.W. (2010) Findings from animals concerning when interactions between perirhinal cortex, hippocampus and medial prefrontal cortex are necessary for recognition memory. *Neuropsychologia*, **48**, 2262-2272.

Weissenborn, K., Heidenreich, S., Giewekemeyer, K., Rückert, N. & Hecker, H. (2003) Memory function in early hepatic encephalopathy. *J. Hepatol.*, **39**, 320-325.

Weissenborn, K., Bokemeyer, M., Ahl ,B., Fischer-Wasels, D., Giewekemeyer, K., van den Hoff, J., Köstler, H. & Berding, G. (2004) Functional imaging of the brain in patients with liver cirrhosis. *Metab. Brain Dis.*, **19**, 269-280.

Witter, M.P., Wouterlood, F.G., Naber, P.A. & Van Haeften, T. (2000) Anatomical organization of the parahippocampal-hippocampal network. *Ann. N. Y. Acad. Sci.*, **9**, 1–24.

Young, J.J. & Shapiro, M.L. (2009) Double dissociation and hierarchical organization of strategy switches and reversals in the rat PFC. *Behav. Neurosci.*, **123**, 1028-1035.

Young, J.J. & Shapiro, M.L. (2011) Dynamic coding of goal-directed paths by orbital prefrontal cortex. *J. Neurosci.*, **31**, 5989-6000.

Zhu, X.O., Brown, M.W., McCabe, B.J. & Aggleton, J.P. (1995) Effects of the novelty or familiarity of visual stimuli on the expression of the immediate early gene c-fos in rat brain. *Neuroscience*, **69**, 821-829.

FIGURE LEGENDS

Figure 1. Performance of the experimental groups in the object-place recognition task. **A**, Discrimination ratios (d1 and d2) for SHAM and PH groups. **B**, Exploration index (e1 and e2) for SHAM and PH groups, the asterisks indicate group differences (*$P < 0.05$).

Figure 2. Escape latencies (mean ± SEM) of the sham-operated group (SHAM) and the portal hypertension group (PH) during the training sessions of the spatial learning (day 1- day 6) and reversal learning (day 7). There is a reduction of escape latencies with respect to day 1 ($P < 0.05$, $ SHAM group and * PH group).

Figure 3. Probe test results from the spatial reversal task (mean ± SEM), showing the percentage time spent in each quadrant of the Morris water maze by both experimental groups (SHAM and PH groups) during the spatial learning (day 1- day 6) and reversal learning (day 7). * Significant difference in the time spent between quadrants ($P < 0.05$). The target or reinforced quadrant during the spatial learning was D (day 1- day 6). However, during reversal learning, C was reinforced (day 7).

Figure 4. Number of c-Fos immunoreactive cells for the two different groups (SHAM and PH) in the different brain regions: CG, PL, IL, CA1, CA3, GD and Ent. **A**, Fos counts in the animals who performed the object-place recognition task. **B**, represents the number of c-Fos positive nuclei in the animals under reversal task condition. Data are shown as mean ± SEM and significant differences between trained groups are represented as *($P < 0.05$).

Figure 1

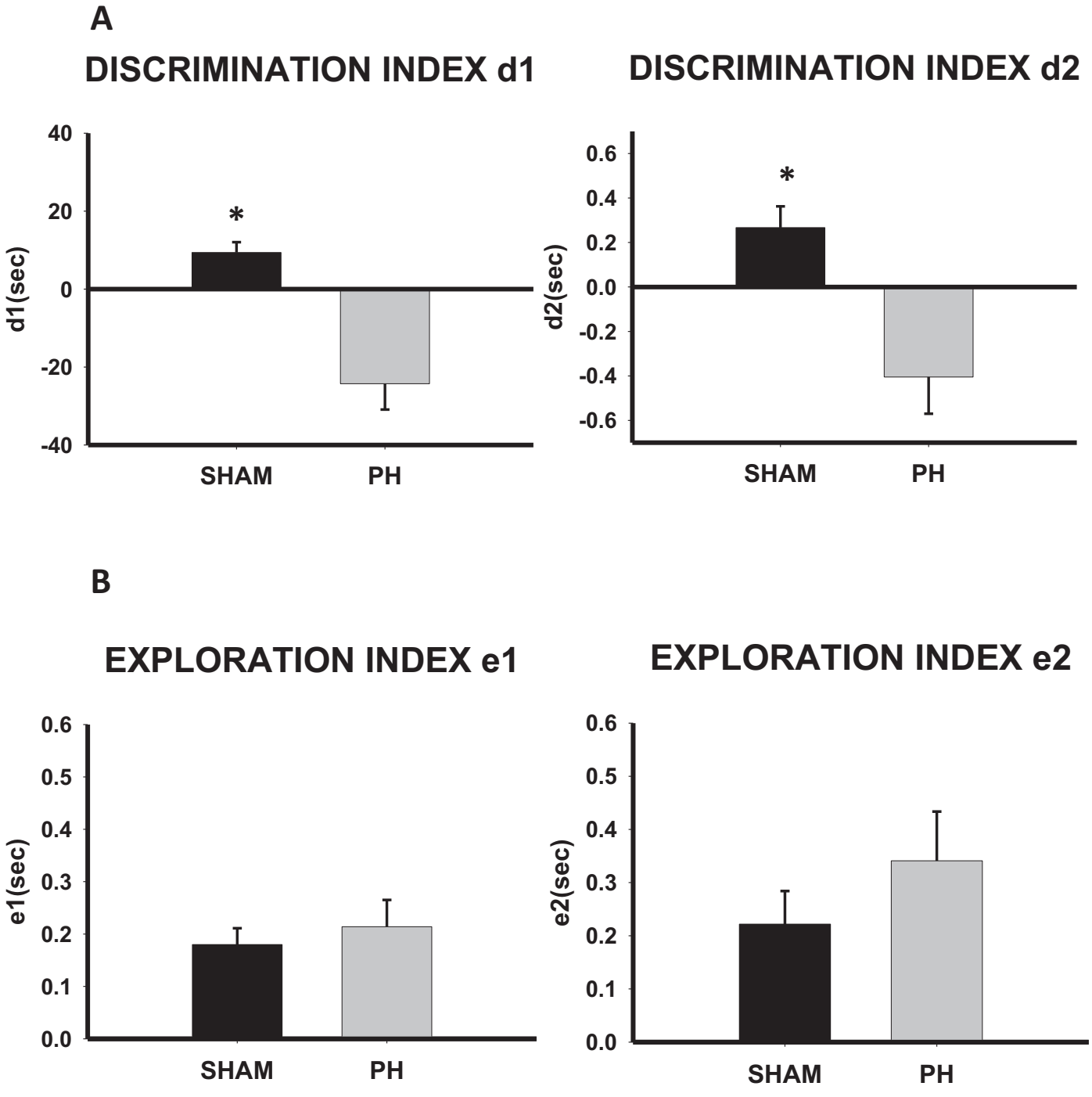
A
DISCRIMINATION INDEX d1
DISCRIMINATION INDEX d2
d1(sec)
d2(sec)
40
20
0
-20
-40
0.6
0.4
0.2
0.0
-0.2
-0.4
-0.6
*
*
SHAM
PH
SHAM
PH
B
EXPLORATION INDEX e1
EXPLORATION INDEX e2
e1(sec)
e2(sec)
0.6
0.5
0.4
0.3
0.2
0.1
0.0
SHAM
PH
SHAM
PH

Figure 2

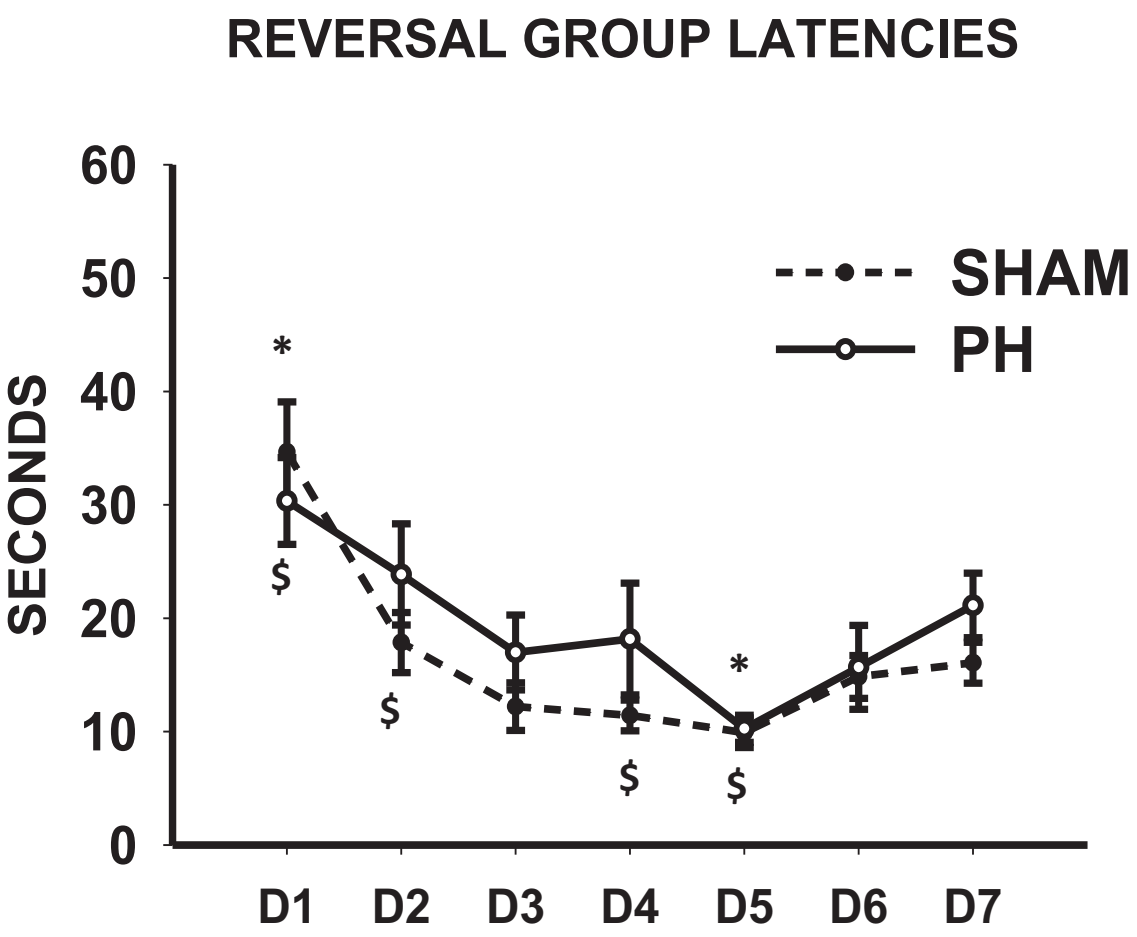
REVERSAL GROUP LATENCIES
SECONDS
60
50
40
30
20
10
0
SHAM
PH
*
$
$
$
$
*
D1
D2
D3
D4
D5
D6
D7

Figure 3

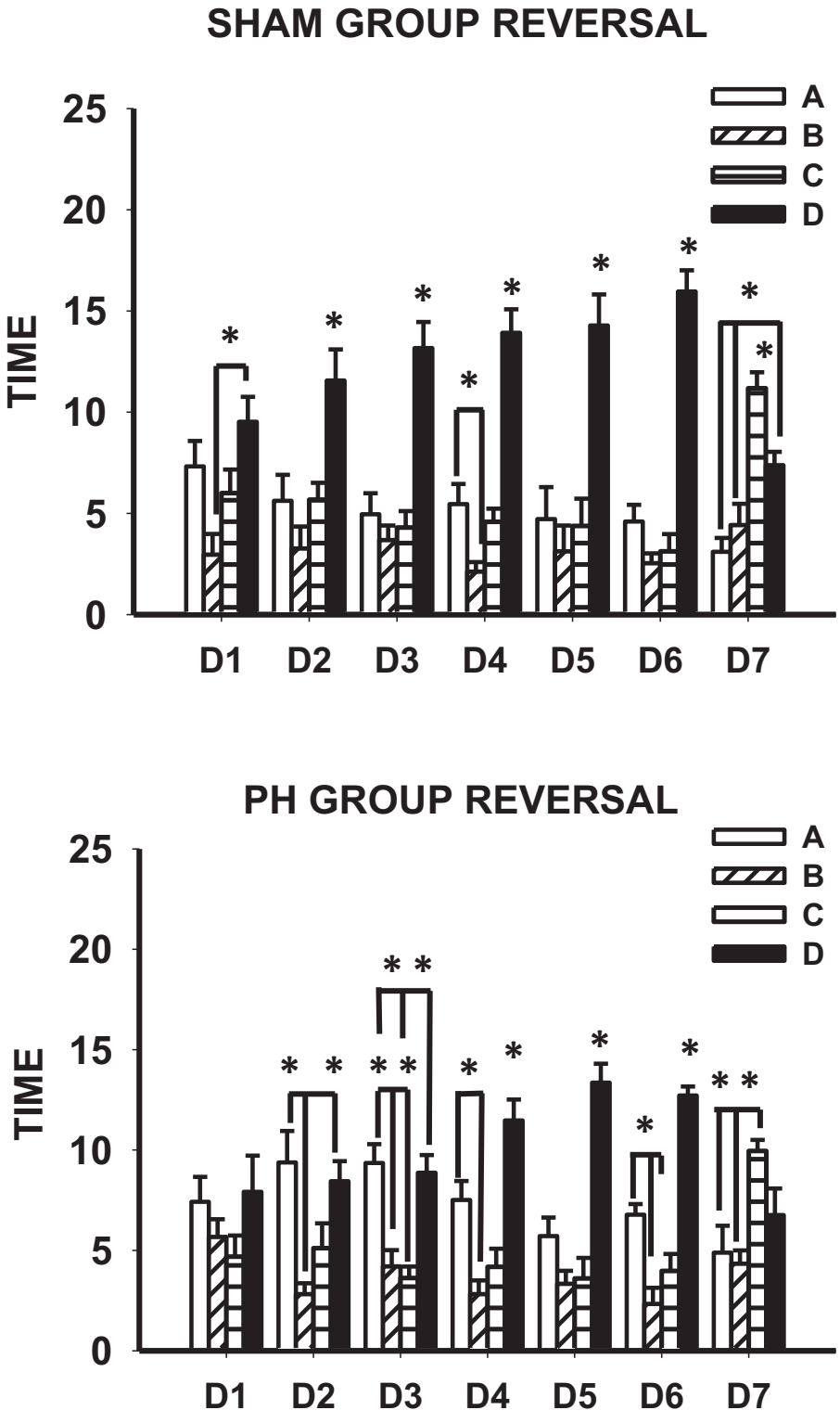
SHAM GROUP REVERSAL
A
B
C
D
TIME
25
20
15
10
5
0
D1
D2
D3
D4
D5
D6
D7
PH GROUP REVERSAL
A
B
C
D
TIME
25
20
15
10
5
0
D1
D2
D3
D4
D5
D6
D7

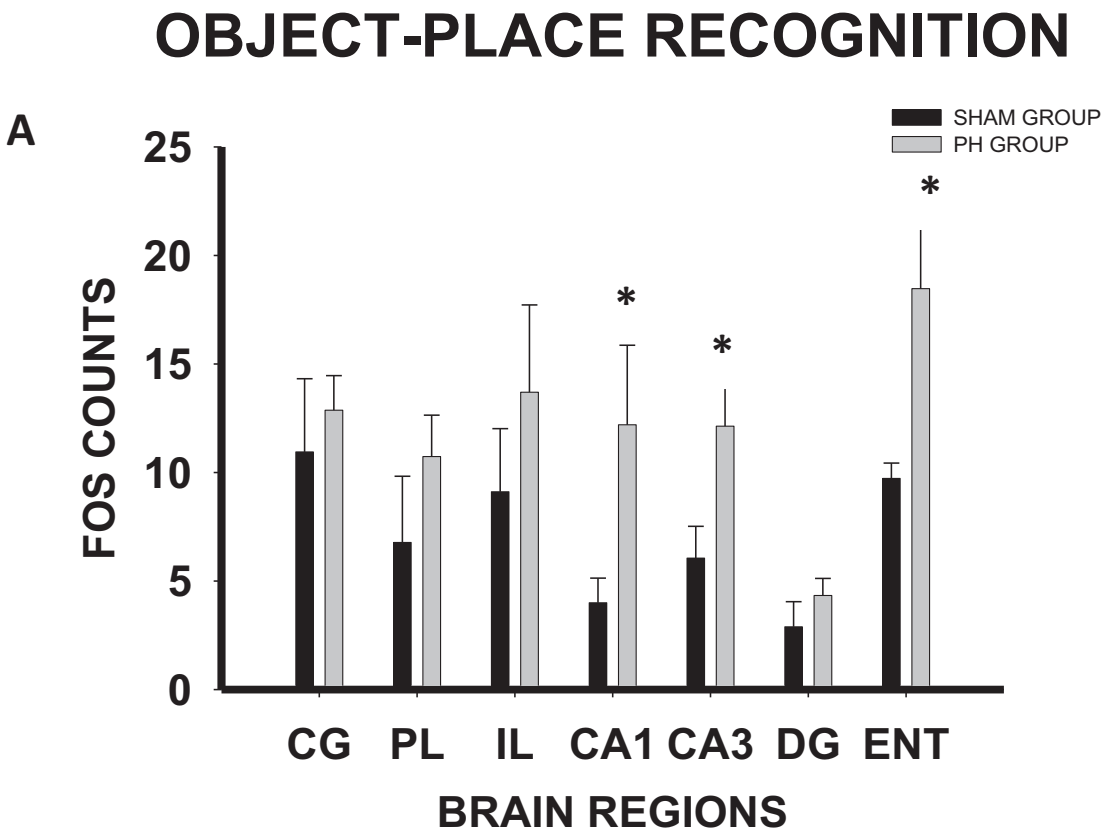
OBJECT-PLACE RECOGNITION
A
SHAM GROUP
PH GROUP
FOS COUNTS
25
20
15
10
5
0
*
*
*
CG
PL
IL
CA1
CA3
DG
ENT
BRAIN REGIONS

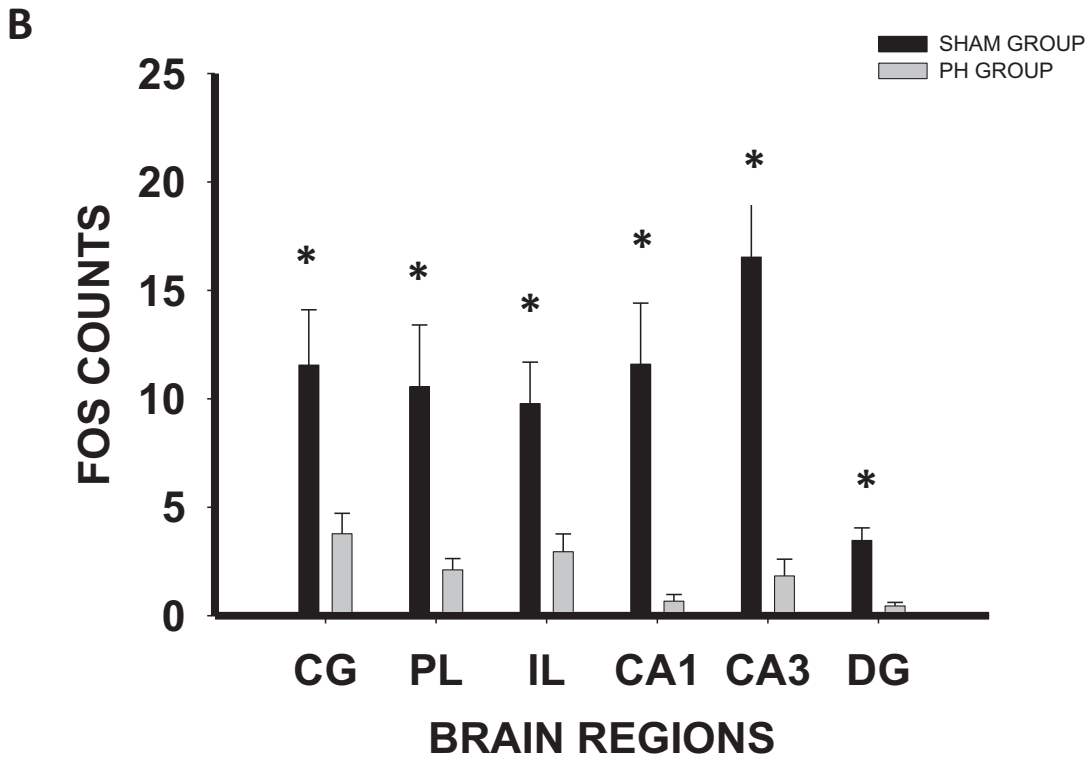
REVERSAL LEARNING
B
SHAM GROUP
PH GROUP
FOS COUNTS
25
20
15
10
5
0
*
*
*
*
*
*
CG
PL
IL
CA1
CA3
DG
BRAIN REGIONS

VI

Main target of minimal encephalopathy: morphophysiological, inflammatory and metabolic view

Natalia Arias[1,2*], Marta Méndez[1,2], Enertiz Gómez-Lázaro[3], Arantxa Azpiroz[3], Jorge L. Arias[1,2].

[1] Laboratorio de Neurociencias. Departamento de Psicología. Universidad de Oviedo. Plaza Feijoo s/n. 33003 Oviedo, Spain

[2] INEUROPA, Instituto de Neurociencias del Principado de Asturias

[3] Department of Basic Psychological Processes and their Development. Basque Country University. Avda. Tolosa 70, 20018 San Sebastian, Spain.

* Correspondence

Natalia Arias

Laboratorio de Neurociencias. Departamento de Psicología

Plaza Feijoo s/n 33003 Oviedo, Spain

Telephone: (+34) 985103273; Fax (+34) 985104144

Email: ariasnatalia@uniovi.es

ABSTRACT

Although often not considered clinically relevant and, therefore, not diagnosed or treated, minimal hepatic encephalopathy (MHE) has been shown to affect daily functioning, quality of life, driving and overall mortality. To discover early impairments involved in MHE, we studied one of its precipitating factors, portal hypertension. Rats were trained on a stimulus-response task using the Morris water maze. Two groups of animals were used: a SHAM (sham-operated) group (n=13) and a portal hypertension (PH) group (n=13). The triple portal vein ligation method was used to create an animal model of the early developmental phase of HE. The metabolic activity of the brains was studied with cytochrome c-oxidase histochemistry (C.O.). Neuronal nuclear volume was assessed by nucleator probe; the number of glial fibrillary acidic protein-immunoreactive astrocytes (GFAP-IR) and proinflammatory mediators were measured. The behavioural results revealed that the PH group was not able to reach the behavioural criterion, in contrast to the SHAM group. The metabolic brain consumption revealed decreased C.O. activity in the ventral striatum. The PH group showed decreased GFAP-IR and an increase in the tumour necrotic factor-α (TNF-α). The PH group showed decreased in neuronal nuclear volume in dorsal striatum and increased in ventral striatum. For the first time, a relationship has been established between inflammation, astrocytic and neural damage, and brain metabolism impairment in a model of MHE. Disruption of the striatum and related structures was highlighted as the main target in early stages of HE. Finally, a simple task is presented to evaluate the subtle impairments found in the clinic, which could provide fresh insights into the development of new tools for the assessment of MHE.

Keywords: minimal hepatic encephalopathy, stimulus-response task, cytochrome c-oxidase, inflammation, GFAP-IR, nucleator, striatum.

Introduction

Hepatic encephalopathy (HE) is a neuropsychiatric disorder that involves alterations in cerebral function resulting from liver failure, but HE is not an isolated syndrome. Liver disease (acute or chronic liver failure, as in cirrhosis), portal hypertension, and hyperammonemia appear to be the main contributing factors that lead to different cerebral and neurological alterations and to the occurrence of HE (Arias et al. 2013).

Patients with clinical HE show various neuropsychiatric symptoms, including impairments in the sleep-wake cycle, cognitive and intellectual function, and motor activity and coordination, as well as alterations in personality and consciousness that can get progressively worse. Before showing these symptoms, patients develop minimal HE (MHE), which can advance to clinical HE with the progressive deterioration of neurological function (Felipo 2013). By definition, it has no obvious clinical manifestation and is characterized by neurocognitive impairments in attention, vigilance and integrative function. Although often not considered clinically relevant and, therefore, not diagnosed or treated, MHE has been shown to affect daily functioning, quality of life, driving and overall mortality. The diagnosis of MHE has traditionally been achieved through neuropsychological examination, psychometric tests, or the newer critical flicker frequency test (Stinton and Jayakumar 2013).

Several animal models have been developed to study the pathogenic mechanism that may be responsible for HE symptoms (Butterworth et al. 2009; Arias et al. 2012). Difficulties in learning diverse types of tasks have been shown in these experimental models, such as classical conditioning (Aguilar et al. 2000), conditional discrimination (Erceg et al. 2005; Monfort et al. 2007), reference (Arias et al. 2012) and working memory (Méndez et al. 2009).

One way to assess the understanding of this pathology is to try to isolate each of the components. In fact, the presence of portal hypertension and ascites is frequently encountered in HE patients, followed by surgical portal decompression as a treatment (Butterworth 1994). Thus, a model of triple portal vein ligation, which reproduces portal hypertension in the early stages of development, can be studied to detect the early impairments present in MHE.

Another inconvenience when trying to study impairments in early stages of HE (MHE) is the existence of compensation mechanisms. For example, in the portal hypertension model, as in clinical MHE, portosystemic collaterals develop as a consequence of high pressure in the portal vein and ameliorate the increased resistance (Miñano and García-Tsao 2010; Méndez-López et al. 2007). Generally, portal hypertension can be accompanied by esophageal varices. Most studies have shown that platelet count and spleen diameters are directly or indirectly linked to the presence of esophageal varices (Baig et al. 2008). On the other hand, metabolic brain activity changes measured by cytochrome c-oxidase have been related to slight differences in the acquisition of reference memory by portal hypertension animals (Arias et al. 2012). Moreover, the presence of inflammatory factors such as chemokines could suggest that inflammation plays an important role in the pathogenesis of portal hypertensive encephalopathy in rats (Merino et al. 2011), which is in line with correlations found between

serum levels of pro-inflammatory interleukins and physically-related general health and mental abilities in the pathogenesis of patients with MHE (Wunsch et al. 2013).

However, less is known about the integrative role of all these factors in MHE. The aims of the present study are to: (i) Determine whether the acquisition of the stimulus-response (S-R) habit task could be an assessment tool for learning impairments in the MHE model; (ii) Measure portal hypertension and organ weight as an index related to MHE; (iii) Verify a hypothetic inflammatory etiopathogeny of MHE through the study of some mediators involved in an inflammatory response in the main brain areas related to the S-R task; and (iv) Try to link these learning impairments and brain inflammatory processes with morphologic changes in glial and neuronal cells and brain metabolic activity throughout the limbic system.

Material and methods

Subjects

We used 26 male *Wistar* rats from the vivarium of the University of Oviedo that weighed 290-330 gm at the beginning of the study. Rats were housed in groups of three to five, three weeks prior to the beginning of the experiments and maintained under standard laboratory conditions (20-22 ºC, 65-70% relative humidity and a 12h light/dark cycle). Food and water were available ad libitum throughout all of the experiments, and sessions were performed during the light phase, between 9:00 a.m. and 13:00 p.m. All procedures were carried out according to the European Parliament and the Council of the European Union 2010/63/UE, and approved by the Oviedo University committee for animal studies. The animals were randomly distributed into two groups: portal hypertension group (n=13) and sham-operated group (n=13). Their body weight, liver weight, adrenal weight, kidney weight, spleen weight and testis weight were determined.

Procurement of experimental models

The experimental models that required surgery were anesthetized by i.m. injection of ketamine (100mg/kg) and xylacine (12 mg/kg). With regard to postsurgical care, the rats were maintained close to a source of heat until they recovered consciousness (10-15 min) to avoid postoperative hypothermia. They were then introduced into individual polycarbonate cages for 15 days and subsequently grouped in cages of four animals each until their behavioural evaluation.

Portal hypertension

A midline abdominal incision was performed, and a section of the intestinal loop was gently shifted to the left and covered with saline-moistened gauze. The portal vein was isolated, and three ligatures, fixed on a sylactic guide, were performed in its superior, middle and inferior portions. The stenoses were calibrated by simultaneous ligation (4-0 silk) around the portal vein and a 20-gauge blunt-tipped needle. The abdominal incision was closed in two layers with vicryl and 2-0 silk. The

postoperative period started immediately after the intervention and lasted until the behavioural evaluation 45 days later.

Sham-operated

A bilateral subcostal laparotomy with prolongation to the xyphoid apophysis, followed by isolation of the portal vein, was performed. The operative field was irrigated with saline solution during the intervention, as in the portal hypertension interventions. Finally, the laparotomics were closed by continuous suture on the two layers with vicryl and 2-0 silk. The postoperative period started immediately after the intervention and lasted until the behavioural evaluation 45 days later.

Portal vein pressure measurement

Splenic pulp pressure, an indirect measurement of portal pressure (PP), was measured using the method described by Aller et al. (2006).

Determination of inflammatory response mediators

Processing the spleen to obtain mononuclear cells

After decapitation, the spleen was removed under sterile conditions and immediately processed to determine the in vitro T and B cell proliferative response to mitogenic stimulation. The spleen was immediately placed in sterile RPMI-1640 (Sigma-Aldrich, Madrid, Spain) and then passed through a sterile wire mesh to make single cell suspensions. The resulting cells were washed three times in a sterile medium, and viable cells were counted using the Trypan blue dye (0.5 % v/v) exclusion technique. Viability was always greater than 80%. Mononuclear cells were isolated from the splenic cell suspension using Ficoll-Paque ^{TM} PLUS (GE Healthcare Bio Sciences, Uppsala, Sweden) centrifugation (400g for 30 min) at room temperature. The density gradient established using Ficoll-Paque enabled the sedimentation of erythrocytes, granulocytes and dead cells underneath, with mononuclear cells (lymphocytes and monocytes) being distinguished as an interface between Ficoll-Paque and the RPMI-1640 medium. Cells collected in the interfaces were washed three times, their viability was re-determined, and their concentrations were adjusted to 2.5 x 10^6 cell/ml with RPMI-1640 supplemented with 10% fetal calf serum (Gibco, Life Technologies, MD, USA) 25mM HEPES, 2mM L-glutamine, 5 x 10^{-5}M 2-mercaptoethanol (Sigma-Aldrich, Madrid, Spain), and 2 g/l sodium bicarbonate (Sigma, Madrid, Spain). Once the spleen mononuclear cells had been obtained, cell cultures were prepared to determine *in vitro* the proliferative capacity of both the B and T lymphocytes.

Determination of the proliferative capacity of B and T lymphocytes in spleen

On a flat 96-well Falcon plate (Becton-Dickinson, Meylan, France), 15 wells per subject were injected with 100 µl of the medium in which the cells obtained in the extraction process were suspended. Next, in 5 of these wells, 100 µl of the RPMI-1640 medium supplemented with 20% fetal calf serum and without mitogenic stimulation were added; another five wells received 100 µl of the RPMI-1640 medium

supplemented with 20% fetal calf serum and 5 µg/ml of Concanavalin-A (Con-A, Sigma-Aldrich, Madrid, Spain), in order to stimulate the proliferation of T lymphocytes; and finally, the five remaining wells were injected with 100 µl of the RPMI-1640 medium supplemented with 20% fetal calf serum and 1 mg/ml of Lipopolysaccharides from Salmonela (LPS, Sigma-Aldrich, Madrid, Spain), in order to stimulate the proliferation of B lymphocytes. Once collected, all these samples were cultured for 72 h in a 95% air / 5% CO_2, humidified atmosphere in an incubator (Jouan, Saint Herblain, Cedex, France) at 37 ºC. Cell proliferation was determined using a II (XTT) colorimetric cell proliferation assay kit, according to the manufacturer's instructions (Roche, Mannheim, Germany), and measured with an Synergy HT colorimetric plate reader (BioTek Instruments, Inc., Winooski, VE., USA) using a 450 nm absorption filter. Data were expressed as a proliferative index (PI) score. PI of T lymphocytes = optic density (OD) of media of wells stimulated with ConA/OD of media of wells without mitogenic stimulation; PI of B lymphocytes = optic density (OD) of media of wells stimulated with LPS/OD of media of wells without mitogenic stimulation.

Real time RT-PCR measurement of mRNA expression of IL-1β, IL-6 and TNFα

Immediately after the spleen extraction, the brain was quickly removed, and the whole striatum, hippocampus, amygdala and prefrontal cortex were dissected. All dissections were performed under sterile conditions and under stereomicroscopic observation with reference to the rat brain atlas (Paxinos and Watson 2005). The samples were stored at -80 ºC to measure mRNA expression of IL-1ß, IL-6 and TNF-α in the prefrontal cortex, amygdala, hippocampus and striatum. Brain tissue was homogenized using the Trizol reagent (Invitrogen, Madrid, Spain), and total RNA was isolated utilizing a standard method of phenol: chloroform extraction (Chomczynski and Sacchi 1987). A UV spectrophotometric analysis of nucleic acid was performed at 260 nm to determine RNA concentrations, and the 260:280 absorption ratio was utilized to assess nucleic acid purity. Samples were DNase-treated (DNase I, Invitrogen, Madrid, Spain) to remove contaminating DNA prior to cDNA synthesis. The total RNA was then reverse-transcribed using the PrimeScript ^{TM} RT reagent kit (Takara Bio Inc., Madrid, Spain), and resulting cDNA levels were quantified by SybrGreen-based (SYBR® Premix Ex Taq^{TM}Takara Bio Inc., Madrid, Spain) real time PCR. Formation of PCR products was monitored in real time using the Applied Biosystems 7500 Real Time PCR System. The sequences of cDNA were obtained from Genbank at the National Center for Biotechnology Information (NCBI; www.ncbi.nlm.nih.gov). Glyceraldehyde-6-phosphate dehydrogenase (GAPDH) served as a housekeeping gene. Primer sequences were designed using the Primer Express Software v3.0 (Applied BioSystems). Primers were obtained from Applied Biosystems (Madrid, Spain). Prime specificity was verified by melt curve analysis. Relative gene expression was determined using the $2^{-\Delta\Delta t}$ method (Livak and Schmittgen 2001).

Primer sequences used for PCR were as follows (primer sequence direction is 5'….3'): IL-1β, forward: GCAACTGTCCCTGAACTAACTG, reverse: CTCATCTGGACAGCCAAGTC; IL-6, forward: CCACCAGGAACGAAAGTCAAC, reverse: CTTGCGGAGAGAAACTTCATAGC; TNF-α, forward: GCCACCGGCAAGGATTC, reverse: TCGACATTCCGGGATCCA; GAPDH, forward: GCTCTCTGCTCCTCCCTGTTC, reverse: GAGGCTGGCACTGCACAA.

Stimulus-response “habit” task

The water maze was made of fibreglass and measured 150 cm in diameter, with a 40-cm high wall. The water level was 30 cm, and its temperature was 22±2°C. The platform used corresponded to a cylinder that was 10 cm in diameter and 28 cm high, of which 2 cm was below the surface of the water. The water maze was in the centre of a 16 m^2 lit room (two halogen lamps of 4000 lx), surrounded by panels on which several extra-maze cues were placed. The pool was divided into four starting positions (north, south, east and west). For the visible water maze task, a white plastic glass was attached to the top of the submerged platform and protruded above the water surface. The platform could be used as a step to mount the glass to escape the water. The behaviour of the animal in the MWM was recorded by a video camera (Sony V88E) connected to a computer equipped with an EthoVision Pro programme.

Rats were trained in one session (which took on average of 10 min) to a pre-set criterion where sham-operated rats had to achieve two consecutive trials with retention latencies under 8 s, and it could take them no more than 10 trials to reach this criterion, as in previous studies (Teather et al. 2005). For each cued training trial, the animal was placed into the tank facing the wall at one of four designated start points (N, S, E and W) and allowed to escape onto the visibly cued platform. The visible escape platform was located in a different quadrant on each trial. A different starting point was used on each trial. Each trial ended once the animal had found the platform, or when 60 s had elapsed. If the animal had not reached the hidden platform after this time, it was placed on the platform for 15 s. During the inter-trial interval, the animals were placed in a black bucket for 30 s. The latency in reaching the escape platform was recorded and used as a measure of task acquisition.

Cytochrome oxidase histochemistry

The protocol used was the same one described by Arias et al (2010). 90 min after the last training day, the animals were decapitated. Brains were removed, frozen rapidly in N-methylbutane (Sigma-Aldrich, Madrid, Spain), and stored at -40ºC until processing with quantitative C.O. histochemistry. To quantify enzymatic activity and control staining variability across different baths, sets of tissue homogenate standards from the Wistar rat brain were cut into different thicknesses (10, 30, 40 and 60 µm) and included with each bath of slides. Quantification of C.O. histochemical staining intensity was done by densitometric analysis, using a computer-assisted image analysis workstation (MCID, Interfocus Imaging Ltd., Linton, England) made up of a high precision illuminator, a digital camera, and a computer with specific image analysis software. A total of twelve measurements were taken per brain region. These measures were averaged to obtain one mean per region for each animal, and they were expressed as arbitrary units of optical density (OD).

In all the animals, we measured the neuronal metabolic activity in the prefrontal cortex: infralimbic (IL), prelimbic (PL) and cingulate cortex (CG); the thalamus: anterodorsal (ADT), anteroventral (AVT) and mediodorsal (MDT); the striatum: anterodorsal (EAD), anterolateral (EAL) and anteromedial (EAM); the accumbens core (ACC) and shell (ACS); the septal hippocampus: dentate gyrus (DG), CA1 and CA3 areas; the central (Cen), medial (MeA) and basolateral (Bas) amygdala; the

mammillary bodies: supramammillary (SUPRA), medial (MM) and lateral (ML); the temporal hippocampus: dentate gyrus (tDG), tCA1 and tCA3 areas; and the temporal cortex: parietal (PAR), enthorinal (Ent) and perhirinal (Prh). The selected brains regions were anatomically defined according to the atlas by Paxinos and Watson (2005).

Brain histological methods

Six animals from the SHAM group and six from the PH group were used to quantify the density of GFAP-IR and neuronal nuclei volume in the septal hippocampus and dorsal striatum. They were anesthetized with sodium pentobarbital (100 mg/Kg) (Sigma-Aldrich) and intracardially perfused with phosphate buffer saline at 0.9% (PBS) (0.1 M; pH 7.4), followed by paraformaldehyde at 4% in PBS (0.1 M; pH 7.4). The brains were extracted and introduced in paraffin. Systematic cuts were performed on both regions with a microtome (Leica, Germany) in 30-μm thick serial sections at a known interval from the beginning to the end.

Staining procedures

GFAP Immunohistochemistry

We performed GFAP-IR immunocytochemistry on the sections of 12 animals (six SHAM and six PH), according to the method described by Blanco et al. (2006), which briefly consists of washing the previously deparaffinized sections in Tris Buffer saline (TBS) with Triton X-100 at 0.1% and blocking them with human serum. Afterwards, these were incubated for one day with rabbit polyclonal primary antibody anti GFAP (1:800 in bovine albumin, BSA). The next day, after rinsing in TBS with Triton X-100, we incubated with a biotinylated secondary antibody (goat anti-rabbit IgG, 1:30 in BSA) and applied the avidin-biotin horseradish peroxidase complex (Vectastain Ultra-Sensitive ABC Staining Kit), developed with diaminobenzidine tetrahydrochloride, and cover-slipped the sections.

Cresyl violet

Cresyl violet staining was performed on 12 animals (six SHAM and six PH), incubating the previously deparaffinised and hydrated sections in cresyl violet (Sigma-Aldrich) (0.5% in H_2O) for 3 min. Afterwards, the sections were washed with H_2O, dehydrated, and cover-slipped under Entellan.

Quantification

GFAP-IR

The entire quantification process was carried out using a Leica LAS Live Image Builder (Leica, Microsystems). To estimate the density of GFAP-IR, we used at least three equidistant sections in the selected structures from each animal. Quantification was done by placing four equidistant counting frames (frame size 0.150 mm × 0.150 mm) on the screen. Only the cell bodies within each quadrant or dissector focused on in the section were quantified. The total thickness measured on each slide was 30 μm, leaving out 5 μm of thickness above and below the *Z*-axis to avoid possible overestimations.

Neuronal Nuclei Volume

The volume of neuronal nuclei in EAD, EAM, EAL, CA1, CA3 and DG (subfields of the septal hippocampus) were quantified with the CAST2 System (Olympus, Denmark) in an Olympus-BX61 microscope. We only quantified the right side of every structure. Images of the cells were acquired with a ×100 oil objective. We used morphological criteria to identify neurons and glial cells. Neurons show clearly defined nucleolus, euchromatin in the nucleus, and visible surrounding cytoplasm, whereas glial cells show heterochromatin in the nucleus, no nucleolus, and no cytoplasm.

Our aim is to assess the neuronal nuclear volume in these structures in two rat groups: PH and SHAM. The nucleator method (Méndez et al. 2008) was applied to compare them. The nucleator probe was done by marking a unique point inside the neuron nucleus, the nucleolus. The system then created 6 test lines intersecting the point. We marked the intersections of the test lines with the membrane. Only defined cellular nuclei within the 1141 μm^2 dissector area that came into focus as the optical plane moved through the height of the dissector were sampled. Four sections of each animal and nucleus were sampled with a constant and known distance between them (30 µm). Twenty five cell measurements were performed on each section, obtaining a total of 100 sampled neurons.

Statistical analysis

All data were analyzed in the Sigma-Stat 3.2 program (Systat, Richmond, USA) and expressed as the mean ± SEM. The results are considered statistically significant if $p<0.05$.

A *t*-test for independent samples was used for the statistical comparison of portal pressures, physiological determinations, C.O. activity values, density of GFAP-IR, and neuronal nuclei volume results. The mean path length, the swimming speed, and the latencies to reach the visibly cued platform during the training phase of the stimulus-response "habit" task were analysed with a one-way ANOVA. Post hoc multiple comparison analyses were carried out when allowed, using pair-wise Tukey tests. Moreover, a non-parametric Mann–Whitney U test (H) for independent samples was carried out when normality or equal group variances failed.

Results

Portal pressure

Portal pressure in all the animals with portal hypertension increased ($t_{14} = -7.152$; $p < 0.001$) in comparison with that of the control animals (Table 1).

Organ Weight

Adrenal weight was lower ($t_{12} = 3.358$; $p = 0.006$) in PH rats compared to control rats (Table 1). Moreover, portal hypertension caused splenomegaly ($U_7 = 36.00$, $p = 0.038$). Although body weight in the PH group was slightly lower, no significant differences were found when compared to the SHAM group.

Physiological determinations

The expression of TNF-α increased ($p = 0.024$) in the striatum of the portal hypertensive rats compared to the levels in the SHAM rats (Table 2). No differences were found between groups in the prefrontal cortex, hippocampus and amygdala in the expression of IL-1β, IL-6, TNF-α and cell proliferation of T and B cells in the spleen.

Stimulus-response "habit" task

The one-way ANOVA did not reveal differences in velocity ($F_{(1,12)} = 0.821$, $p = 0.383$), but significant differences were found in distance covered ($F_{(1,12)} = 9.806$, $p = 0.009$) between PH and SHAM. At the same time, the one-way ANOVA showed differences in escape latencies between the PH and SHAM groups ($F_{(1,12)} = 7.809$, $p = 0.016$). When a one-way repeated measures ANOVA was carried out in both groups, the PH group did not show differences in the escape latencies during trials ($F_{(6,54)} = 1.201$, $p = 0.313$). However, there were significant effects of the variable trial ($F_{(6,54)} = 4.563$, $p < 0.001$) in the SHAM group. This interaction revealed a progressive latency reduction on the training days in both groups, with the SHAM group showing significant differences until trial two ($p = 0.034$) (Fig.1).

C.O. activity

The group comparison of C.O. activity revealed lower C.O. activity in the PH group than in the SHAM group in the ACC ($t_{11} = 2.613$; $p = 0.024$), DG ($t_{12} = 2.222$; $p = 0.046$), Bas ($t_{12} = 2.759$; $p = 0.017$), Lat ($t_{12} = 2.870$; $p = 0.014$) and Cen ($t_{12} = 3.266$; $p = 0.007$). The groups did not differ in their C.O. activity in the PL ($t_{12} = 0.661$; $p = 0.521$), IL ($t_{12} = 1.408$; $p = 0{,}185$), CG ($t_{12} = 0.298$; $p = 0.771$), ADT ($t_{10} = -1.065$; $p = 0.312$), AVT ($t_{10} = 0.527$; $p = 0.610$), MD ($t_{10} = 0.114$; $p = 0.911$), ACS ($t_{11} = 1.410$; $p = 0.186$), EAD ($t_{11} = 1.388$; $p = 0.193$), EAL ($t_{11} = 0.850$; $p = 0.414$), EAM ($t_{11} = 0.572$; $p = 0.579$), CA1 ($t_{12} = 1.036$; $p = 0.321$), CA3 ($t_{12} = 0.684$; $p = 0.507$), MeA ($t_{12} = 1.764$; $p = 0.103$), tCA1 ($t_{12} = 1.241$; $p = 0.238$), tCA3 ($t_{12} = 1.975$; $p = 0.072$), tDG ($t_{12} = 1.779$; $p = 0.101$), SUPRA ($t_{12} = 0.724$; $p = 0.483$), MML ($t_{12} = 2.104$; $p = 0.057$), ML ($t_{12} = 1.563$; $p = 0.144$), PAR ($t_{11} = 0.357$; $p = 0.728$), Prh ($t_{12} = 2.037$; $p = 0.064$) or Ent ($t_{12} = 1.208$; $p = 0.250$). See Fig.2.

GFAP counting

Differences in the GFAP-IR astrocyte number were found between groups in EAD ($t_8 = 4.393$, $p = 0.002$) and EAM ($t_8 = 4.365$, $p = 0.002$), where the number was significantly greater in the SHAM group than in the PH group. However, no differences were found in EAL ($t_8 = 2.010$, $p = 0.079$), ACC ($U_5 = 4.000$, $p = 0.095$) or ACS ($t_8 = 0.160$, $p = 0.877$). See Fig.3.

Neuronal nuclear volume

There were differences between the SHAM and PH groups in terms of volume of the neuronal nuclei (Fig.4). Larger nuclei were found in the SHAM group in the EAD ($t_9 = 2.645$, $p = 0.027$), EAL (t_9

= 2.845, p = 0.019), EAM (t_9 = 3.113, p = 0.012), ACC (U_6 = 3.000, p = 0.015) and ACS (U_6 = 1.000, p = 0.004).

Discussion

Hepatic encephalopathy (HE) is characterized by cognitive impairment and usually seen in patients with advanced liver disease or porto-systemic shunts. The HE spectrum varies from minor cognitive dysfunction to lethargy, depressed consciousness and coma (Dhiman 2013). Minor cognitive dysfunction in patients with cirrhosis is termed minimal hepatic encephalopathy (MHE), which is estimated to affect up to 60% to 80% of patients with cirrhosis and may seriously impair a patient's daily functioning and health-related quality of life (Dhiman et al. 2010). Despite its importance, none of the neuro or psychophysiological methods used competitively has proven to be of greater use in diagnosing MHE (Weissenborn 2008).

Therefore, in our work we studied one of the main contributing factors to HE, portal hypertension, reproduced by a model of triple portal vein ligation (Arias et al. 2013). Differences in portal pressure between the PH and SHAM groups were found. Moreover, portal hypertension was confirmed by the presence of splenomegalia (Aller et al. 2005) and adrenal insufficiency, which is common in critically ill patients with cirrhosis and severe sepsis. However, we found its presence in early stages of HE, which could help to formulate a physiopathological definition of MHE. Adrenal insufficiency is related to functional liver reserve and disease severity and associated with hemodynamic instability, renal dysfunction and increased mortality (Tsai et al. 2006). In this study, we tried to develop a simple task that animals with PH (developing MHE) would be unable to perform successfully. For this purpose, we evaluated the performance of MHE animals on a stimulus-response task in which the visible platform was pseudo-randomly repositioned across trials to render its relation with distal cues trivial (Morris 1981).

In rats, behaviour may be guided by a double dissociation between the mnemonic functions of the hippocampal system and the dorsal striatum (caudate-putamen), with the acquisition of this visible platform task being more striatum-dependent (Packard and McGaugh 1992; McDonald and White 1994). Behavioural results showed the inability of PH animals to reach the behavioural criterion compared to the SHAM group. Several studies have reported that lesions in the caudate-putamen can impair acquisition of the hidden platform version of the task (Block et al. 1993; Dunbar et al. 1993), and these impairments are not due to gross deficits in motor performance (Furtado and Mazurek 1996; Arias et al. 2012). These results could suggest impairment in the striatum as one of the first targets in early stages of MHE.

Rapidly growing evidence has supported the role of inflammation in exacerbating the neurological manifestations in HE. Inflammation in the context of HE can arise directly within the brain itself, resulting in astrocytic, microglial and neuronal dysfunction and taking part in the development of brain failure (Tranah et al. 2013). Inflammation may also develop systemically and indirectly influence brain function, as Aller et al. (2005) showed. In this model there is an increase in pro-inflammatory factors in the liver, such as tumour necrosis factor-α (TNF-α) and interleukin-1β (IL-1β), among others, pointing out their systemic presence in early phases of HE. Regarding the role of inflammation in

developing MHE, we considered it interesting to determine the mRNA expression level in some mediators involved in inflammatory response, including TNF-α, IL-1β and IL-6, in order to verify a hypothetic inflammatory brain etiopathogeny of MHE. Our results showed no differences in IL-1β and IL-6 expression between the PH and SHAM groups in the main brain structures of the limbic system related to this learning task. No differences in the proliferation of T and B cells in the spleen were found. However, an increase in TNF-α mRNA was found in the PH group. TNF-α production often has synergistic activities on inflammatory pathways and processes, and it amplifies these responses by inducing secondary mediators (Moore et al. 2001).

With regard to these findings, we wanted to map the metabolic activity in the brain limbic structures involved in learning processes. To accomplish this goal, histochemical labelling of cytochrome c-oxidase (C.O.) was performed. C.O. is a mitochondrial enzyme that reflects changes in tissue metabolic capacity that are induced by the sustained energy requirements of the nervous system associated with learning (Poremba et al., 1998) and spatial memory in the Morris water maze (MWM) (Conejo et al. 2007). Decreases in C.O. in the PH group were found in the ventral striatum, hippocampus, and amygdala nuclei.

The low metabolic activity found in the ventral striatum correlates with the poor performance of the PH group during the stimulus-response task and the increase in TNF-α mRNA in these animals. In fact, TNF-α could decrease C.O. activity in two ways: directly, by inhibiting the mitochondrial oxidative phosphorylation, which involves C.O. as a mitochondrial enzyme involved in the phosphorylation process that generates ATP; and indirectly, because TNF-α could increase the synthesis of NO by iNOS up-regulation (Aller et al. 2005). Brain oxidative and nitrosative stress could cause neural mitochondrial damage and defective oxidative phosphorylation, which are reflected in impaired C.O. activity (Arias et al. 2013).

Through the years, evidence has suggested that different neural systems contribute to each form of learning (O´Keefe and Nadel 1978). In fact, lesions in the dorsal striatum and hippocampus have been found to have opposite effects on behaviour in cued and spatial versions of the radial maze task (White and McDonald 1993). These findings are consistent with the hypothesis that a corticostriatal system mediates stimulus-response habit formation, whereas a hippocampus-based system contributes to cognitive-spatial impairment (Petri and Mishkin 1994). However, Rubio et al. (2012) support a possible functional interaction between the two memory systems, as their structural convergence may facilitate functional cooperation in behaviours guided by more than one strategy (Rubio et al. 2012). Moreover, there is a well-known projection that the ventral striatum receives from the hippocampus, which is capable of modulating its firing (Pennartz et al. 2011). In fact, a model of the hippocampal-ventral striatum circuit has been proposed in which the hippocampus is primarily involved in the mental simulation of possible navigation paths, and the ventral striatum is involved in the evaluation of the value of locations (Chersi and Pezzulo 2012). Our C.O. results highlight this relationship between the dentate gyrus and ventral striatum, and they point out that it is unlikely that a single neural structure is solely responsible for processing information on a specific task; while one structure may be primarily involved,

other structures may make some contributions. The lack of differences between groups in the dorsal striatum was expected, based on recent studies showing that the dorsal striatum may not be required when rats have to adopt a particular strategy (Botreau and Gisquet-Verrier 2010).

Furthermore, anatomical studies have shown that the dorsal striatum is a heterogeneous structure, both in terms of its intrinsic compartmentalization of neurochemical constituents (Groves et al. 1995) and its regionally diverse connectivity with other cortical/subcortical structures (Groenewegen et al. 1990). One example of this is the amygdala-striatal projection, which in the rat originates primarily in the basolateral nucleus of the amygdala and innervates ventral regions of the striatum such as the nucleus accumbens, as well as the dorsomedial, caudal, rostroventral, central and dorsolateral portions of the striatum (McDonald 1991; Fass et al. 1984).

Regarding the amygdala, studies have shown that the amygdala incidentally acquires information during the acquisition of a task (McDonald et al. 2004), suggesting that the basolateral and lateral nuclei of the amygdala are essential for the acquisition and storage of stimulus-reward associations (McDonald and White 1993). At the same time, recent results have pointed out that the central nucleus of the amygdala is involved in the acquisition of habits (Lingawi and Balleine 2012). Another important feature of the basolateral complex and the central nucleus of the amygdala is the presence of glutamate receptors (NMDA), which are presented along the projection from the basolateral amygdala to the nucleus accumbens (Lee et al. 2013). Animal models of HE reveal increased glutamate levels (Palomero-Gallagher and Zilles 2013), which are linked to a down-regulation of these receptors in the striatum (Oja et al. 1996).

Taking into account that we found impairment in the acquisition of a stimulus-response task, an increase in pro-inflammatory factors in the striatum, and a decrease in C.O. activity in the striatum and brain structures with connections to it, neural and glial impairments were studied in order to explore to what extent MHE cellular damage underlies learning impairments. We attempted to assess neural and glial damage through the study of brain neuronal nuclear volume changes and the cytoskeletal protein glial acidic fibrillary protein (GFAP). We found decreased GFAP-IR in the dorsal striatum in the PH group compared to the SHAM group. Among other functions, GFAP modulates astrocyte motility and shape by providing structural stability to astrocytic processes. GFAP represents the most specific astrocytic marker under normal and pathological conditions (Bélanger et al. 2002), and GFAP-immunoreactive astrocytes were found to be decreased in number in the cerebral cortex of rats with chronic liver failure resulting from portocaval anastomosis (Norenberg 1977). Similarly, decreased GFAP-IR was reported in human chronic liver failure in the basal ganglia, cerebral cortex and thalamic structures (Sobel et al. 1981). In fact, pro-inflammatory mediators (TNF-α) even led to decreased GFAP expression (Chastre et al. 2010). This is the first study to reveal GFAP changes in the striatum and their relationship with learning impairment in MHE.

At the same time, there is evidence suggesting that, in acute liver failure, pro-inflammatory cytokines may act synergistically with brain ammonia to cause brain edema and its complications

(Chastre et al. 2010). An increased neuronal nuclear volume in the ventral striatum, the structure on which correct performance of the task rests, has been found.

Neuronal damage and death are documented in end-stage chronic liver failure, usually accompanied by astrocytic swelling. Increased neuronal nuclear volume in mammillary nuclei and hippocampus were identified in a thioacetamide-induced cirrhosis model (Méndez et al. 2008). However, this functional impairment of neurons is suggested to be secondary to damage in the astrocytes. This increased nuclear neuronal volume could be due to increased oxidative stress (Méndez et al. 2008), which can occur through the mediation of pro-inflammatory factors such as TNF-α, which produce NO in this region. Nuclear hypertrophy of neurons due to oxidative stress could cause mitochondrial damage and defective oxidative phosphorylation, and this has been reflected in the decreased C.O. activity found in the PH group.

To conclude, our work provides a novel insight into correlating impairment in performance on a stimulus-response task with energetic and morphologic disturbances in the brain limbic system involved in learning processes in early stages of HE. Our results suggest that neuronal and astroglial alterations highlight the double action of astroglial dysfunction and neuronal disturbances, and that the consequent disruption in neuron-glia interactions might lead to the dysfunction of the striatum and related structures involved in learning. For the first time, we have established the relationship between inflammation, astrocytic and neural damage, and brain metabolism impairment in a model of MHE. We have highlighted the disruption of the striatum and related structures as the main target in early stages of HE. Finally, we presented a simple task to evaluate subtle impairments found in the clinic, which could provide fresh insights into the development of new tools for the assessment of MHE. Our research opens a new door to future treatments for the early targets of dysfunction in patients with minimal hepatic encephalopathy.

Acknowledgments

This research was supported by Grants MICINN PSI2010-19348, MEC AP2009-1714 to NA and Project Grants of Spanish Ministry of Economy and Competitiveness: PSI 2012-35352.

Figure Captions

Fig.1 Latencies to reach the platform were calculated. * represent differences in escape latencies between the PH and SHAM groups. # represent shorter latencies during trials 5, 8, 9 and 10 compared to trial 1, and during trial 2 compared to trial 10 for the SHAM group ($p<0.05$). Data represent mean±SEM.

Fig.2 Cytochrome oxidase (C.O.) histochemistry in the sampled regions where significant differences were found: ventral striatum (ACC), hippocampus (DG) and amygdala nuclei (Cen, Bas, Lat).

Fig.3 Number of GFAP-IR cells (mean±SEM) related to the studied structures. *$p<0.05$ was significantly higher in the SHAM group compared to the PH group.

Fig.4 Nuclear volume of neurons in dorsal and ventral striatum. Volume was measured by the nucleator probe. SHAM group showed an enlarged volume in dorsal striatum, and PH group showed an enlarged volume in ventral striatum. Asterisks indicate statistically significant differences between groups. Data represent mean values±SEM.

REFERENCES

Aguilar MA, Miñarro J, Felipo V (2000) Chronic moderate hyperammonemia impairs active and passive avoidance behavior and conditional discrimination learning in rats. Exp Neurol 161: 704–713.

Aller MA, Vara E, García C, Nava MP, Angulo A, Sánchez-Patán F, Calderón A, Vergara P, Arias J (2006) Hepatic lipid metabolism changes in short- and long-term prehepatic portal hypertensive rats. World J Gastroenterol 12: 6828-6834.

Aller MA, Vara E, Garcia C, Palma MD, Arias JL, Nava MP, Arias J (2005) Proinflammatory liver and antiinflammatory intestinal mediators involved in portal hypertensive rats. Mediators Inflamm 2: 101-111.

Arias N, Álvarez C, Conejo N, González-Pardo H, Arias JL (2010) Estrous cycle and sex as regulating factors of baseline brain oxidative metabolism and behavior. Revista Iberoamericana de Psicología y Salud 1: 3-16.

Arias N, Méndez M, Arias J, Arias JL (2012) Brain metabolism and spatial memory are affected by portal hypertension. Metab Brain Dis 27: 183–191.

Arias N, Méndez M, Fidalgo C, Aller MA, Arias J, Arias JL (2013) Mapping metabolic brain activity in three models of hepatic encephalopathy. Int J Hypertens 390872.

Baig WW, Nagaraja MV, Varma M, Prabhu R (2008) Platelet count to spleen diameter ratio for the diagnosis of esophageal varices: Is it feasible? Can J Gastroenterol 22: 825-828.

Bélanger M, Desjardins P, Chatauret N, Butterworth RF (2002) Loss of expression of glial fibrillary acidic protein in acute hyperammonemia. Neurochem Int 41: 155-160.

Blanco E, Picón IM, Miranda R, Begega A, Conejo NM, Arias JL (2006) Astroglial distribution and sexual differences in neural metabolism in mammillary bodies. Neurosci Lett 395: 82-86.

Block F, Kunkel M, Schwarz M (1993) Quinolinic acid lesion of the striatum induces impairment in spatial learning and motor performance in rats. Neurosci Lett 149: 126-128.

Botreau F, Gisquet-Verrier P (2010) Re-thinking the role of the dorsal striatum in egocentric/response strategy. Front Behav Neurosci 4:7.

Butterworth RF (1994) Hepatic encephalopathy. In: Arias IM, Boyer JL, Fausto N, Jakoby WB, Schachter DA, Shafritz DA (ed) The liver: Biology and Pathology, 3rd ed, New York: Raven Press, pp 1193-1208.

Butterworth RF, Norenberg MD, Felipo V, Ferenci P, Albrecht J, Blei AT (2009) Members of the ISHEN Commission on Experimental Models of HE. Experimental models of hepatic encephalopathy: ISHEN guidelines. Liver Int 29: 783-788.

Chastre A, Jiang W, Desjardins P, Butterworth RF (2010) Ammonia and proinflammatory cytokines modify expression of genes coding for astrocytic proteins implicated in brain edema in acute liver failure. Metab Brain Dis 25: 17-21.

Chersi F, Pezzulo G (2012) Using hippocampal-striatal loops for spatial navigation and goal-directed decision-making. Cogn Process 13: S125-129.

Chomczynski P, Sacchi N (1987) Single-step method of RNA isolation by acid guanidinium thiocyanate-phenol-chloroform extraction. Anal Biochem 162: 156-159.

Conejo NM, González-Pardo H, Vallejo G, Arias JL (2007) Changes in brain oxidative metabolism induced by water maze training. Neuroscience 145:403-412.

Dhiman RK (2013) Gut microbiota and hepatic encephalopathy. Metab Brain Dis 28: 321-326.

Dhiman RK, Saraswat VA, Sharma BK, Sarin SK, Chawla YK, Butterworth R, Duseja A, Aggarwal R, Amarapurkar D, Sharma P, Madan K, Shah S, Seth AK, Gupta RK, Koshy A, Rai RR, Dilawari JB, Mishra SP, Acharya SK (2010) Indian National Association for Study of the Liver. Minimal hepatic encephalopathy: consensus statement of a working party of the Indian National Association for Study of the Liver. J Gastroenterol Hepatol 25: 1029-1041.

Dunbar GL, Lescaudron LL, Stein DG (1993) Comparison of GM1 ganglioside, AGF2, and D-amphetamine as treatments for spatial reversal and place learning deficits following lesions of the neostriatum. Behav Brain Res 54: 67-79.

Erceg S, Monfort P, Hernández-Viadel M, Rodrigo R, Montoliu C, Felipo V (2005) Oral administration of sildenafil restores learning ability in rats with hyperammonemia and with portacaval shunts. Hepatology 41: 299–306.

Fass B, Talbot K, Butcher LL (1984) Evidence that efferents from the basolateral amygdala innervate the dorsolateral neostriatum in rats. Neurosci Lett 44: 71-75.

Felipo V (2013) Hepatic encephalopathy: effects of liver failure on brain function. Nat Rev Neurosci 14: 851-858.

Furtado JC, Mazurek MF (1996) Behavioral characterization of quinolinate-induced lesions of the medial striatum: relevance for Huntington's disease. Exp Neurol 138: 158-168.

Groenewegen HJ, Berendse HW, Wolters JG, Lohman AH (1990) The anatomical relationship of the prefrontal cortex with the striatopallidal system, the thalamus and the amygdala: evidence for a parallel organization. Prog Brain Res 85: 95-118.

Groves PM, García-Munoz M, Linder JC, Manley MS, Martone ME, Young SJ (1995) Elements of the intrinsic organization and information processing in the neostriatum. In: Houk JC, Davis JL, Beiser DG (ed) Models of information processing in the basal ganglia. Cambridge: MIT, pp 51-96.

Lee BR, Ma YY, Huang YH, Wang X, Otaka M, Ishikawa M, Neumann PA, Graziane NM, Brown TE, Suska A, Guo C, Lobo MK, Sesack SR, Wolf ME, Nestler EJ, Shaham Y, Schlüter OM, Dong Y (2013) Maturation of silent synapses in amygdala-accumbens projection contributes to incubation of cocaine craving. Nat Neurosci 16: 1644-1651.

Lingawi NW, Balleine BW (2012) Amygdala central nucleus interacts with dorsolateral striatum to regulate the acquisition of habits. J Neurosci 32: 1073-1081.

Livak KJ, Schmittgen TD (2001) Analysis of relative gene expression data using real-time quantitative PCR and the 2(-Delta Delta C(T)) Method. Methods 25: 402-408.

McDonald AJ (1991) Topographical organization of amygdaloid projections to the caudatoputamen, nucleus accumbens, and related striatal-like areas of the rat brain. Neuroscience 44: 15-33.

McDonald RJ, Hong NS (2004) A dissociation of dorso-lateral striatum and amygdala function on the same stimulus-response habit task. Neuroscience 124: 507-513.

McDonald RJ, White NM (1993) A triple dissociation of memory systems: hippocampus, amygdala, and dorsal striatum. Behav Neurosci 107: 3-22.

McDonald RJ, White NM (1994) Parallel information processing in the water maze: evidence for independent memory systems involving dorsal striatum and hippocampus. Behav Neural Biol 61: 260-270.

Méndez M, Méndez-López M, López L, Aller MA, Arias J, Arias JL (2008) Mammillary body alterations and spatial memory impairment in Wistar rats with thioacetamide-induced cirrhosis. Brain Res 1233: 185-195.

Méndez M, Méndez-López M, López L, Aller MA, Arias J, Arias JL (2009) Associative learning deficit in two experimental models of hepatic encephalopathy. Behavioural Brain Research 198: 346–351.

Méndez-López M, Méndez M, Sánchez-Patán F, Casado I, Aller MA, López L, Corcuera MT, Alonso MJ, Nava MP, Arias J, Arias JL (2007) Partial portal vein ligation plus thioacetamide: a method to obtain a new model of cirrhosis and chronic portal hypertension in the rat. J Gastrointest Surg 11: 187–194.

Merino J, Aller MA, Rubio S, Arias N, Nava MP, Loscertales M, Arias J, Arias JL (2011) Gut-brain chemokine changes in portal hypertensive rats. Dig Dis Sci 56: 2309-17.

Miñano C, Garcia-Tsao G (2010) Clinical pharmacology of portal hypertension. Gastroenterol Clin North Am 39: 681–695.

Monfort P, Erceg S, Piedrafita B, Llansola M, Felipo V (2007) Chronic liver failure in rats impairs glutamatergic synaptic transmission and long-term potentiation in hippocampus and learning ability. Eur J Neurosci 25: 2103–2111.

Moore KW, de Waal Malefyt R, Coffman RL, O'Garra A (2001) Interleukin-10 and the interleukin-10 receptor. Annu Rev Immunol 19: 683–765.

Morris RGM (1981) Spatial localization does not require the presence of local cues. Learn Motiv 12: 239-260.

Norenberg MD (1977) A light and electron microscopic study of experimental portal-systemic (ammonia) encephalopathy. Lab Investigat 36: 618–627.

O´Keefe J, Nadel L (1978) The hippocampus as a cognitive map. Oxford: Clarendo.

Oja SS, Borkowska HD, Albrecht J, Saransaari P (1996) Kainate and AMPA receptors in the rat brain in thioacetamide-induced hepatic encephalopathy. Proc West Pharmacol Soc 39: 15-17.

Packard MG, McGaugh JL (1992) Double dissociation of fornix and caudate nucleus lesions on acquisition of two water maze tasks: further evidence for multiple memory systems. Behav Neurosci 106: 439-446.

Palomero-Gallagher N, Zilles K (2013) Neurotransmitter receptor alterations in hepatic encephalopathy: a review. Arch Biochem Biophys 536: 109-121.

Paxinos G, Watson CH (2005) The rat brain in Stereotaxic Coordinates — the new coronal set 5th ed. Elsevier Academic Press.

Pennartz CM, Ito R, Verschure PF, Battaglia FP, Robbins TW (2011) The hippocampal-striatal axis in learning, prediction and goal-directed behavior. Trends Neurosci 34: 548-559.

Petri HL, Mishkin M (1994) Behaviorism, cognitivism and the neuropsychology of memory. Am Scientist 82: 30-37.

Poremba A, Jones D, González-Lima F (1998) Classical conditioning modifies cytochrome oxidase activity in the auditory system. Eur J Neurosci 10: 3035-3043.

Rubio S, Begega A, Méndez M, Méndez-López M, Arias JL (2012) Similarities and differences between the brain networks underlying allocentric and egocentric spatial learning in rat revealed by cytochrome oxidase histochemistry. Neuroscience 223: 174-82.

Sobel RA, DeArmond SJ, Forno LS, Eng LF (1981) Glial fibrillary acid protein in hepatic encephalopathy. An immunohistochemical study. J Neuropathol Exp Neurol 40: 625–632.

Stinton LM, Jayakumar S (2013) Minimal hepatic encephalopathy. Can J Gastroenterol 27: 572-574.

Teather LA, Packard MG, Smith DE, Ellis-Behnke RG, Bazan NG (2005) Differential induction of c-Jun and Fos-like proteins in rat hippocampus and dorsal striatum after training in two water maze tasks. Neurobiol Learn Mem 84: 75-84.

Tranah TH, Vijay GK, Ryan JM, Shawcross DL (2013) Systemic inflammation and ammonia in hepatic encephalopathy. Metab Brain Dis 28: 1-5.

Tsai MH, Peng YS, Chen YC, Liu NJ, Ho YP, Fang JT, Lien JM, Yang C, Chen PC, Wu CS (2006) Adrenal insufficiency in patients with cirrhosis, severe sepsis and septic shock. Hepatology 43: 673-681.

Weissenborn K (2008) PHES: one label, different goods?! J Hepatol 49: 308-312.

White NM, McDonald RJ (1993) Acquisition of a spatial conditioned place preference is impaired by amygdala lesions and improved by fornix lesions. Behav Brain Res 55: 269-281.

Wunsch E, Koziarska D, Milkiewicz M, Naprawa G, Nowacki P, Hartleb M, Milkiewicz P (2013) In patients with liver cirrhosis, proinflammatory interleukins correlate with health-related quality of life irrespective of minimal hepatic encephalopathy. Eur J Gastroenterol Hepatol 25: 1402-1407.

Group	PP (mmHg)	FBW (g)	LW (g)	AW (g)	KW (g)	SW (g)	TW (g)
SHAM (n=7)	6,80±0,47 *	415,71±13,34	2,90±0,08	0,017±0,0024 *	0,28±0,0041	0,21±0,013 *	16,20±0,73
PH (n=7)	12,74±0,69	368,90±18,34	2,72±0,16	0,0087±0,0006	0,28±0,017	0,33±0,06	13,11±1,71

Table 1. Measurements in sham-operated and portal hypertension rats at 45 days of evolution.

PP: Portal Pressure, FBW: final body weight, LW: liver weight, AW: adrenal weight, KW: kidney weight, SW: spleen weight, TW: testis weight. Results are the mean ± SEM *$p<0.05$, statistically significant difference when compared to group portal hypertension.

Group	CPF IL1β	CPF IL6	CPF TNF	HC IL1β	HC IL6	HC TNF
SHAM (n=6)	2,718±0,596	4,015±1,712	2,293±0,670	3,442±1,139	2,217±0,719	1,587±0,169
PH (n=6)	2,388±0,144	6,685±2,671	2,780±0,422	1,737±0,163	1,993±0,541	1,613±0,183

Group	AMIG IL1β	AMIG IL6	AMIG TNF	STRI IL1β	STRI IL6	STRI TNF
SHAM (n=6)	3,318±0,792	2,517±0,652	7,097±2,213	2,050±0,586	2,344±0,480	2,354±0,147 *
PH (n=6)	2,160±0,398	2,207±0,681	3,980±0,976	2,403±0,364	2,973±0,374	4,805±0,810

Group	T 450	B 450
SHAM (n=6)	3,317±0,518	1,389±0,172
PH (n=6)	4,344±0,479	1,515±0,0973

Table 2. Prefrontal cortex, hippocampus, amygdala and striatum content of IL1β, IL6 and TNF in sham-operated and portal hypertension rats. Cell proliferation of T and B cells measured at 450 nm. Results are the mean±SEM. TNF: tumor necrosis factor; IL1β: interleukin 1β; IL6: interleukin 6. * p=0.024.

Figure 1

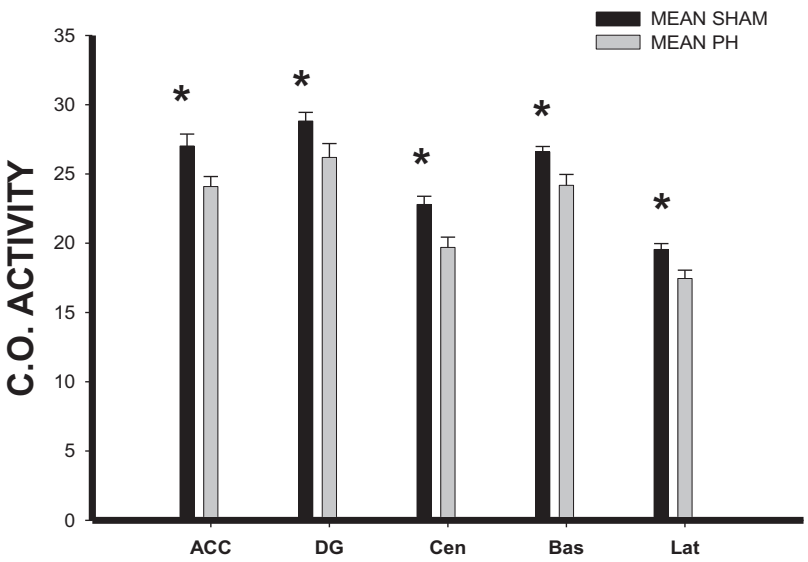

Figure 2

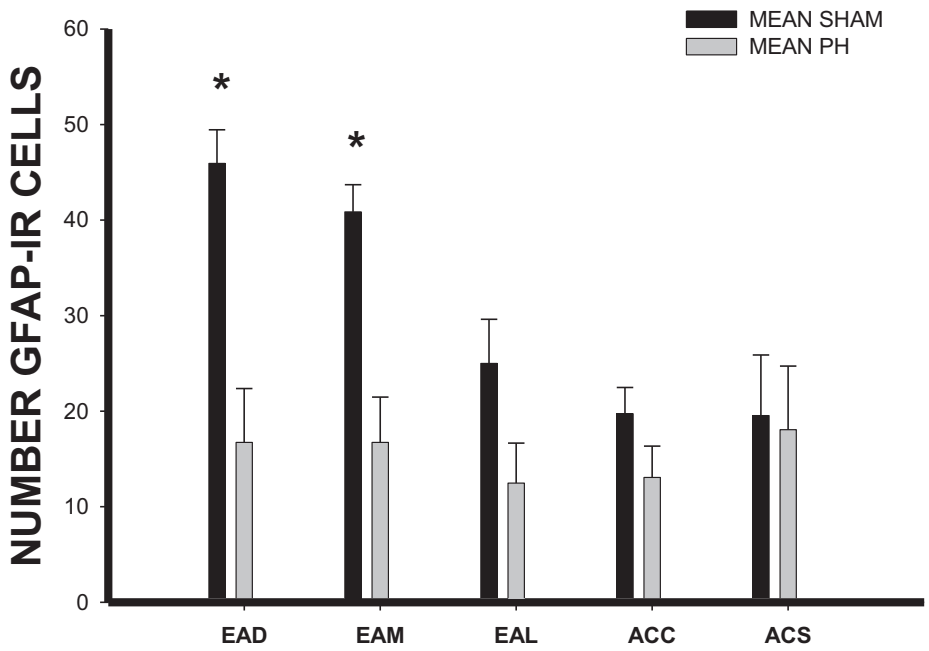

Figure 3

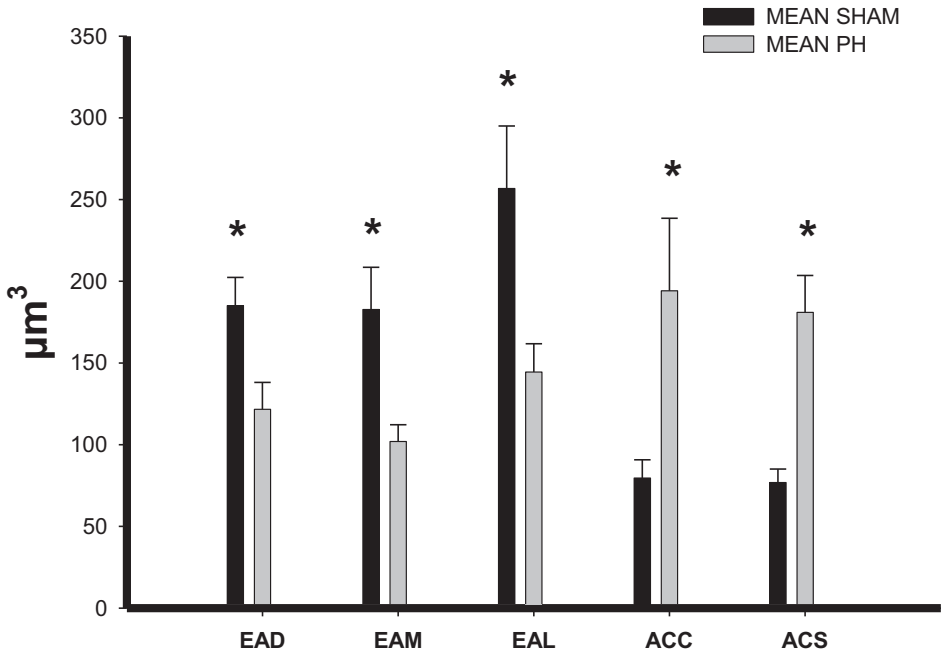

Figure 4

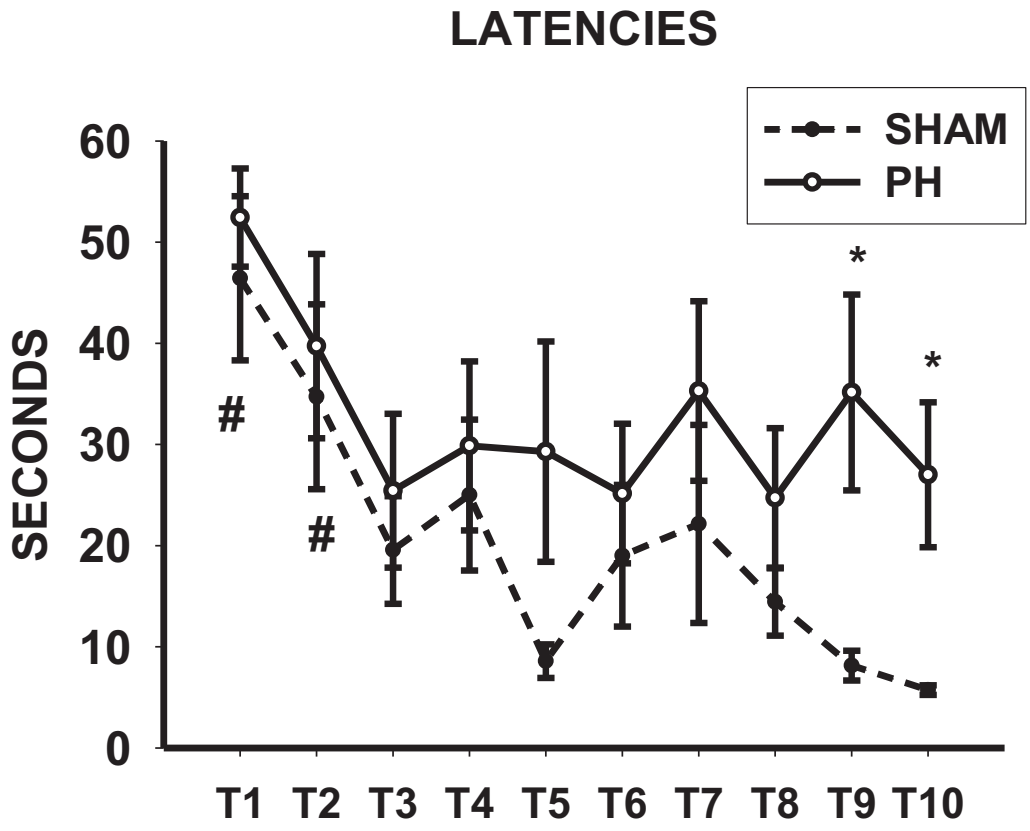

VII

Medical Hypotheses 78 (2012) 721–731

Contents lists available at SciVerse ScienceDirect

Medical Hypotheses

journal homepage: www.elsevier.com/locate/mehy

Coupling inflammation with evo-devo

María-Angeles Aller [a], Natalia Arias [b], Sherezade Fuentes-Julian [c], Alejandro Blazquez-Martinez [c], Salvador Argudo [d], Maria-Paz de Miguel [c], Jorge-Luis Arias [b], Jaime Arias [a,*]

[a] Surgery I Department, School of Medicine, Complutense University of Madrid, Spain
[b] Neurosciences Laboratory, Psychobiology Department, School of Psychology, University of Oviedo, Asturias, Spain
[c] Cell Engineering Laboratory, La Paz Hospital, Autonomous University of Madrid, Madrid, Spain
[d] General Surgery Unit, Sudeste Hospital, Arganda del Rey, Madrid, Spain

ARTICLE INFO

Article history:
Received 13 April 2011
Accepted 15 February 2012

ABSTRACT

Inflammation integrates diverse mechanisms that are associated not only with pathological conditions, such as cardiovascular diseases, type 2 diabetes, obesity, neurodegenerative diseases and cancer, but also with physiological processes like reproduction i.e. oogenesis and embryogenesis as well as aging. In the current review we firstly propose that the inflammatory response could recapitulate the phylogenia. In this way, highly conserved inflammatory mechanisms that play a main role in the evolutive development of different animal species, both invertebrates as well as vertebrates, are identified. Therefore, we also hypothesize that inflammation could represent a key tool used by nature to modulate organisms according to the environmental conditions in which these develop. Thus, inflammation could be the pathway by which the environmental factors could be related to the evolutionary development. If so, the diverse human chronic inflammatory diseases that nowadays the Western society suffer would represent the way for adapting to the abrupt changes in their lifestyle. Nonetheless, the distribution of the different pathological conditions varies in terms of intensity and magnitude among Western country populations depending on their genetic polymorphism. In this case, it should be considered that this set of diseases, distributed between all the individuals that constitute the Westernized society, would represent a true Social Inflammatory Syndrome whose final result is its remodeling. In this context, the use of inflammation by the Western society could represent the camouflaged expression of efficient mechanisms of evolution and development. In addition, if the different types of the inflammatory response involved in these diverse chronic pathological conditions could trace the biochemical origins of life, perhaps inflammation could represent an archaeological tool of unsuspected usefulness for understanding our own origin.

Introducing the inflammation

Nowadays, inflammation is considered a highly beneficial and adaptive response triggered by noxious stimuli and conditions, such as infection and tissue injury [1,2]. However, this standard view of inflammation as a reaction to injury or infection might need to be expanded to account of the inflammatory processes induced by other types of adverse conditions [1]. The human diseases that are associated with these conditions, including atherosclerosis, asthma, type 2 diabetes and neurodegenerative diseases, are all characterized by chronic low-grade inflammation. Since these chronic pathological processes are intermediate between basal and inflammatory states, they have been termed para-inflammation [1].

Furthermore, human aging can be explained by the emerging concept of para-inflammation-driven inflammageing, i.e. a combination of inflammation and aging [3–5]. Inflammageing seems to favor the onset of typical age-related diseases like atherosclerosis, dementia, osteoporosis and cancer [6,7] (Fig. 1).

However, a key adaptive characteristic of inflammation, whether acute, chronic or acute-on-chronic, is that it produces tissue, organ or even organism remodeling [8,9]. In this way, it has been proposed that the inflammatory response has features in common with tissue development, which requires involution of pre-existing tissue elements [8–10]. The ability of the tissues to involute or dedifferentiate could represent a return to early stages of development [11]. Particularly, involution or dedifferentiation could form an effective defense mechanism to escape death after injury. In this way, this mechanism could make retracing an ancient, efficient and well-known route possible for repairing the injured tissue, just like the initial phases of embryonic development [8,10,11]. The correlation that can be established between the embryonic and the inflammatory events suggests that the

* Corresponding author. Address: Cátedra de Cirugía, Facultad de Medicina, Universidad Complutense de Madrid, Pza. de Ramón y Cajal s.n., 28040 Madrid, Spain. Tel.: +34 91 394 1388; fax: +34 91 3947115.
E-mail address: jariasp@med.ucm.es (J. Arias).

0306-9877/$ - see front matter © 2012 Elsevier Ltd. All rights reserved.
doi:10.1016/j.mehy.2012.02.018

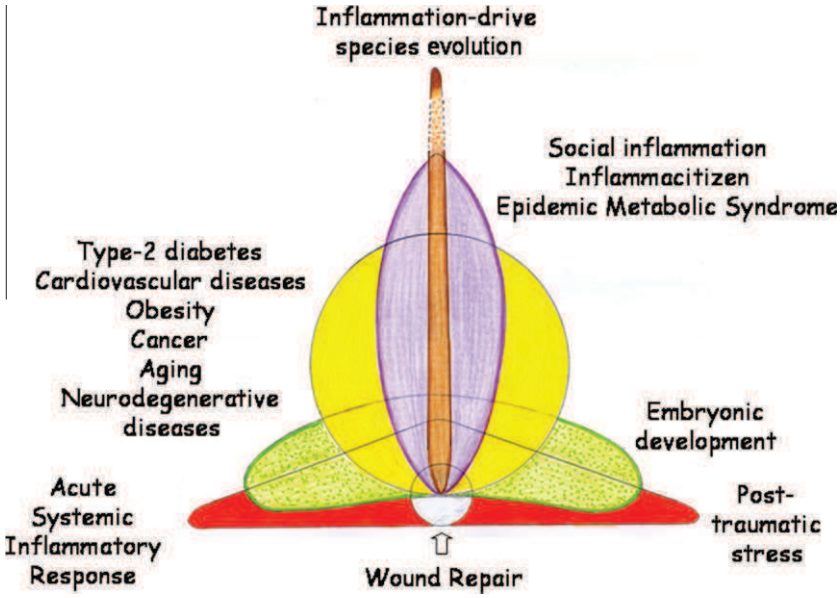

Fig. 1. The different physiological and pathological processes in which inflammation is involved are represented in superimposed areas with different forms. The central common area would integrate the basic mechanisms that are shared by all these processes. At the same time, the different forms try to represent the different expression types that the inflammatory response can adopt as time and space change when they take place.

results obtained from research into both great fields of knowledge would favor each other and promote their development [11].

In the adult body, many pathways that play an essential role during embryological development are inactivated later in life, although some of them may be transiently expressed during adult repair processes [11,12]. This ability of the tissues to involute or dedifferentiate could constitute an effective solution against whatever type of injury. Through differentiation, tissues can have the chance to reform and remodel themselves according to the new environmental situations imposed on them.

Nonetheless, it can be hypothesized that the inflammatory response also seems to compile mechanisms that have a great value from a phylogenetic point of view. It would be explained how similar mechanisms are shared in essence by the diverse types of the inflammatory response, from acute high-grade to chronic low-grade inflammation.

The hypothesis: inflammation as a very useful tool for evo-devo

There are highly conserved inflammatory mechanisms that play a main role in embryonic development as well as in the evolution of different animal species, both invertebrates as well as vertebrates. Consequently, we propose that inflammation could represent a key tool used by nature to modulate organisms according to the environmental, both intra- and extrauterine, conditions in which these develop and therefore could be the pathway by which the environmental factors could drive evolutionary development.

In this context, multiple chronic inflammatory conditions that are suffered by Western society today could represent mechanisms that are used by the organism to successfully adapt to the environmental changes imposed by the lifestyle in developed countries. With this idea in mind, we hypothesize that inflammation, in addition to being a recapitulating tool of ontogeny and phylogeny, would be useful to living beings to adapt to the new environmental changes created by nature. Therefore, and even though these inflammatory mechanisms are considered pathological, they could in fact represent adaptive pathways for remodeling the organism according to the environmental changes where the organism lives, so it can survive the continuous changes imposed upon it. In summary, we propose that inflammation, a recapitulating tool of ontogeny and phylogeny, could also involve the mechanisms by which diverse chronic pathological conditions adapt the organism to survive in view of the abrupt environmental changes caused by Western lifestyle. In addition, if the different types of inflammatory responses involved in diverse chronic pathological conditions could trace the biochemical origins of life, perhaps inflammation could represent an archaeological tool of unsuspected usefulness for understanding our own origin.

Evaluation of the hypothesis

Inflammation, an essential process in the production of diseases in living beings, could be defined as a succession of phases during which increasingly complex mechanisms are expressed. The final aim of these mechanisms could be trophism of the injured body and, finally its remodeling [13]. In the evaluation of our proposed hypothesis, one also will have to consider that these inflammatory mechanisms are also essential pathways for the embryonic development and the phylogenetic evolution of the living beings. Actually, the inflammatory mechanisms would orchestrate the pathogenesis as well as the ontogeny and phylogeny of the living beings while their common objective in all these processes would be to remodelate the organism according to the different environmental factors leading to them. This is the reason why we carried out a comparative description of these mechanisms in order to evaluate if they would be valid to participate in the inflammatory response as well in evolution and development.

Essential mechanisms of the inflammatory response and their involvement in ontogeny and phylogeny

The inflammatory pathology shares fundamental mechanisms with evo-devo, which in turn could entail that these mechanisms would be the real mediators of the remodeling of living beings during all these processes, whether physiological, like embryogenesis and phylogenesis, or pathological, like the inflammatory diseases. This is the reason why we have proposed the hypothesis that the inflammatory response could recapitulate phylogeny and

ontogeny. The systemic inflammatory response that is induced in the injured organism could be described as a succession of three overlapped phases, during which the phenotypes of metabolic progressive complexity related to the use of oxygen are expressed [14].

In the first phase of the inflammatory response, hydroelectrolytic alterations stand out, with edema secondary to the ischemia–reperfusion phenomenon and nutrition by diffusion, which predominates [13,14]. In the following phase, the metabolic response is characterized by hypermetabolism and enzymatic stress associated with immunological and endocrinological responses [14]. In this phase, oxygen is not correctly used since the inability to obtain energy through the electron transport chain persists and the systemic alterations produced are referred collectively as the acute response (APR) [15]. Enzymatic stress favors extracellular (fermentation) and intracellular (phagocytosis) digestion [8]. The last phase of the inflammatory response is characterized by the capacity to use the oxygen in oxidative metabolism, i.e. oxidative phosphorylation. In this phase, patients recover their capillary function, and therefore, nutrition is mediated by them. This type of metabolism is characterized by a large production of ATP, which is fundamentally used by epithelial cells and fibroblasts to drive specialized multiple cellular processes. In the case of epithelial cells, or parenchymatous cells, the substrates interchange with the environment and, in the case of fibroblasts, or stromal-resident cells, extracellular matrix production. These specialized functions would finally determine the onset of the healing [8,14].

Since these trophic mechanisms are of increasing complexity, progressing from anoxia to total specialization in the use of oxygen to obtain usable energy, it could be speculated that they represent the successive reappearance of the stages that took place during the evolution of life without oxygen on earth from ancient times. In this sense, the inflammatory response not only could recapitulate ontogeny [11], but also phylogeny, through the successive expression of phenotypes that have a trophic meaning. However, this "constructive" concept of the inflammatory response does not rule out its noxious or "destructive" effect. In particular, during the evolution of the inflammatory response some of the abovementioned mechanisms can induce cellular death. Thus, oxidative and nitrosative stress, acidosis, edema, enzymatic stress or a dysfunctional or excessive acute phase response can induce the destruction of the injured tissue.

The great ubiquity in the body of the basic mechanisms that manage the inflammatory response suggests that they are inseparably linked to cell survival and development and possibly to cell evolution as well. In this way, these said mechanisms could bury their roots in the origin of eukaryotic life.

Some of the fundamental mechanisms of inflammation, both acute and chronic, can be recognized in the origin and evolutive development of different animal species and, for this reason, in the current paper we are aiming at establishing a corresponding relation between both of them. Thus, the functions that characterize each phase of the inflammatory response of the body to the injury or to stress could represent regression to remote stages of the species evolution.

Ischemia and hydration: the common beginning

The inflammatory response irrespective of the specific cause, i.e. allergic, infections, ischemia, toxins or stress, could have basic mechanisms shared by all of these types of diseases. We have previously proposed that whatever the cause of the inflammatory response its principal objective could be to provide nutrition to the injured tissues [8,16]. Particularly, the inflammatory response related to surgery and trauma, also named surgical inflammation, seems to recapitulate diverse trophic mechanisms, like interstitial diffusion, enzymatic (intra and extracellular) digestion, leukocyte-mediated nutrition or blood capillaries-vehiculed substrates, all of which are related to developmental processes [11].

The interstitial space always seems to be the battlefield for inflammation, whether it is due to trauma [8,10], infection [17] or tumors [18,19]. The successive pathophysiological mechanisms that develop in the interstitial space of tissues when they undergo surgical inflammation are considered increasingly complex trophic functional systems for using oxygen because they go from ischemia to the development of an oxidative mechanism [16]. Therefore, a correlation between the increased organism complexity and the development of the use of the atmospheric oxygen could be established [20,21]. This correlation seems to exist in the evolutive phases of the surgical inflammatory response since progressive cellular and tissue complexity occur parallel to a gradual oxygenation process from ischemia after severe traumatic injury, to progressive reoxygenation until the correct revascularization by capillarogenesis occurs in the injured organism [14].

A successive molecular and cellular infiltration of the interstitial space is produced during the evolution of the surgical inflammatory response [10,14]. This space is occupied by the extracellular matrix that is not an inert substance [22]; rather it plays a significant role in different physiological processes and disease conditions [22–24]. Phylogenetic data generated from recently completed genome sequencing projects have shown that the molecules of the extracellular matrix, i.e. collagen, laminins, integrins, nidogens, perlecan, especially those related to cell-matrix adhesion, are ancient and exquisitely conserved in multicellular animals [23,25]. Perhaps this is the reason why the extracellular matrix performs a key role in both the evolution of surgical inflammation and the early stages of animal development.

The inflammatory mechanisms that drive the successive molecular and cellular infiltration of the interstitial space recall some of the fundamental mechanisms of the distinct steps of the early stages of invertebrate and vertebrate development. Perhaps, first we should highlight hydration because it is a prime and initial step of inflammation [14], and development as well [26–29].

Interstitial and cellular edema

Hydration is a fundamental step of inflammation and development, probably because it favors nutrition by diffusion in both cases. In injured tissue hydration, i.e. cellular and interstitial edema, is secondary to ischemia-revascularization phenomenon with oxidative and nitrosative stress [14]. Increased degradation of the extracellular matrix with accumulation of fragments of glycosaminoglycans has been proposed as an important mechanism for edema formation because of the hydrophilic properties of glycosaminoglycans and particularly of hyaluronan [30]. Glycosaminoglycans attract and entrap water and ions, thereby forming hydrated gels, while permitting the flow of cellular nutrients and favoring edematous infiltration of the tissue as well as the interstitial fluid flow and the tissue lymph pressure gradient [31].

In several animal species hydration is one of the initial events in development. Thus, in lepidoptera dormant follicles, which include a single oocyte and 7 nurse cells encased in an epithelium of follicle cells, they become active when they suffer an increase in turgor pressure and are visibly swollen [26]. The follicle cells, as an epithelium, have a system of intercellular channels containing a matrix of sulfated glycosaminoglycans that enable hemolymph to reach the oocyte [26]. In fish, fertilized eggs are activated by exposure to fresh water. After activation, the zona radiata or acellular eggshell, takes up water, gains resistance to breakage and can support up to 100 times more weight than oviductal eggs [32]. In marine fish, the final volume of the egg is acquired during oocyte maturation due to water uptake. During oocyte hydration and

maturation, amino acids derived of yolk protein hydrolysis are osmotic effectors but hydration of oocyte also depends on the accumulation of ions like K^+, Mg^{2+}, Ca^{2+}, Cl^- and ammonium (NH_4^+) [28]. Early preimplantation mouse embryos also require intracellular accumulation of glycine to provide osmotic support and thus control cell volume [27].

The liquid that is accumulated in the interstitial space of the inflamed tissues or organs, and which infiltrates the extracellular matrix, progressively adopts some of the properties that have been described in the hemolymph [33,34]. The circulatory system depending on whether blood and interstitial fluid mix, can be divided into two major groups: the open circulatory system and the closed circulatory system. In this last system, the blood circulates only within the internal lumen of the blood vessels and does not mix with interstitial fluid. On the contrary, in the phyla with the open circulatory system such as *Arthropoda*, the blood can freely blend into the interstitial fluid to generate hemolymph [35]. The internal organs in these animals are submerged within an internal cavity called the hemocoel and directly receive oxygen and nutrients, and deposit metabolic wastes [35,36]. Therefore, it could be considered that in the inflamed tissue the closed circulatory system suffers a switch to acquire some of the characteristics of the open circulatory system and perhaps of the hemolymph. In this way, the inflammatory exudates bathes the cells of the injured tissues and organs, thanks to the quick infiltration of the extracellular matrix [14].

The open circulatory system in the inflamed tissue, like in insects, permits coagulation to be more exuberant to quickly seal wounds, limit fluid loss, entrap microbes at wound sites and restore the tissue [34]. The great increase of the endothelial permeability in the inflamed organs also allows selective diffusion through the interstitial space of circulating substances in the blood that have been released as a neuroendocrine system response to stress i.e. the hypothalamic–pituitary-adrenal and sympathetic-adrenal medullary or sympathetic nervous system [14]. This selectivity in the localization of the inflammatory response that induces interstitial edema could also favor the interstitial accumulation of substances derived from the acute phase response (APR) [37].

However in this initial phase of the systemic inflammatory response in mammals, it could be considered that hypometabolism, anaerobic glycolisis, low temperature and a decrease in energy expenditure [14] reduces the expression of specialized functions with a high energetic expense for the traumatized organism, drives the catabolism and therefore, favors its deconstruction.

Vitellogenesis and acute-phase response: the lipoprotein-related metabolism

In oviparous animals, accumulation of yolk materials into oocytes during oogenesis and their mobilization during embryogenesis are key processes for successful reproduction [26,28,32]. All oviparous species, including insects, provide their eggs with vitellin as a major yolk storage glycolipoprotein [38]. The precursor vitellogenin is synthesized by the fat body, the main organ of the intermediate metabolism of insects [38]. Moreover, the majority of proteins of the hemolymph are synthesized in the fat body. In this organ vitellogenin is modified to facilitate the transport of carbohydrates, lipids and other nutrients into oocyte during vitellogenesis. In fact it has been suggested that the lipid would be used as an energy source for oogenesis, in addition to being incorporated with the oocytes in the vitellogenesis process [38] (Table 1).

Vitellogenins are stored in oocytes as vitellin, a reserve foodsource for the future embryo [38]. In the insects, vitellogenins are involved in the regulation of hormonal dynamics, antioxidant activity, immune defense, longevity and social behavior [38,39].

Table 1
Related factors involved in the inflammatory response and in development.

Inflammatory response	Development
Innate immune response	**Oviparous animals:*
Acute phase response	Vertebrate and invertebrate-vitellogenin genes
Pentraxins	Pentraxins
C-reactive protein-bound to LDL	
Fibrinogen	Vitellogenesis
Serum amiloid A increases the ability of HDL to accept cholesterol	Fat body
Hydrolisis of adipose tissue	
Increased lymph production	Hemolymph lipids from the fat body
Coagulation	Melanin
Factor XIIIa	Transglutaminase
IL-6-induced changes in the lipoprotein profile	Vitellin (glycolipoproteins)
Mast cell activation	Granulocyte/hemocyte activation
Apolipoprotein-B-containing particles	Apolipoprotein B
LDL	
VLDL	
Corticoids-aldosterone: oxidative stress fibrogenesis	Steroid producing follicle cells
	Oenocyte accumulation of lipid droplets
	**Mammalian embryos:*
Atherogenic dyslipidemia	Accumulation of cholesterol
Hepatic steatosis	Accumulation of lipids into the yolk sac
Insulin resistance	Embryo environment rich in glutamine and glucose:
	Lipid synthesis
	Cell growth and division
Obesity	
Metabolic syndrome	

IL: interleukin; LDL: low density lipoprotein; HDL: high density lipoprotein; VLDL: very low density lipoprotein.

Furthermore, it has been postulated, based on phylogenetic studies, that the entire vitellogenin sequence should be used when searching for phylogenetic inferences [38]. Vitellogenins are part of a multi-gene family that includes insect apolipophorins and human apolipoprotein B [38].

Vitellogenesis in fishes also describes the incorporation of vitellogenin protein carbohydrates and lipids by the oocyte. The lipids accumulating within the oocyte originate from plasma – very low density lipoproteins (VLDL) and from vitellogenins [28]. Lipids could be sequestered from the plasma VLDL by the binding to apolipoprotein B [28,32]. The ability to transport fat, in the form of lipoprotein, through the circulatory system by eukaryotes is one of their most significant functions right from the beginning of existence [32].

The reason and functional basis for why the vitellogenin transport system initially evolved provides information about how energy in the form of fat can be distributed. Thus, the evolutionary advancement of storing energy in the form of fat has provided organisms with an enormous advantage in adapting to environmental and developmental changes [32]. Comparative studies based on amino acid sequences and gene organization support the hypothesis of a common evolutionary origin of the vertebrate and invertebrate vitellogenin genes [32,40]. The immune phenotype associated with the evolution of the inflammatory response is coupled with the development of dyslipidemia [11]. Hence, we suggest that the inflammatory response seems to be associated with an alteration of the lipid metabolism. In turn, the pathophysiological basis of this lipid metabolic impairment could be compared to the accumulation of lipids in the yolk sac during the early phases of embryo development.

An isoform of apolipoprotein B and apoB48 particles are chylomicrons, which transport dietary cholesterol and triglycerides from the intestine to the site of storage for use within the body, such as the adipose tissue, skeletal and cardiac muscle and the liver [41]. This is one of the reasons why considering digestion as a physiologic inflammatory state is allowed. However, during cardiovascular inflammation, cholesterol esters may be transferred from high density lipoprotein (HDL) to apolipoprotein B-containing particles, such as low-density lipoprotein (LDL cholesterol) or VLDL [42]. Trapping of apolipoprotein B containing particles within the arterial wall is unquestionably the essential initiating event for the development of complex atherosclerotic lesions [41]. Hepatic steatosis also results from increased hepatic uptake of free fatty acids derived mainly from the hydrolysis of adipose-tissue triglycerides, increased because of insulin resistance, but also from dietary chylomicrons and hepatic biogenesis [43]. Hepatic steatosis in turn might play a key role in the pathogenesis of cardiovascular disease through the systemic release of several inflammatory mediators and/or through the production of insulin resistance and atherogenic dyslipidemia [43,44] (Table 1).

The acute phase response and the inflammatory lipoprotein metabolism

The acute phase response is a core part of the innate immune response and produces changes in more than 200 proteins grouped as either positive or negative acute phase proteins [37,45]. Positive acute phase proteins include C-reactive protein, fibrinogen, haptoglobin, α_2-macroglobulin, α_1-acid glycoprotein, transferrin, ceruloplasmin and serum amyloid A [45]. IL-6, produced in response to tissue damage and infection, is a central mediator of the immune system inducing the liver acute-phase response [46].

Inflammation and the concomitant acute phase response induce marked changes in the lipoprotein profile [47]. Likewise, IL-6 and acute phase proteins, particularly C-reactive protein, have been correlated to disease severity and outcome in most of the chronic low-grade inflammatory conditions like cardiovascular diseases, obesity, metabolic syndrome, type-2 diabetes, non-alcoholic fatty liver disease (NAFLD), which includes a large spectrum that ranges from fatty liver, non-alcoholic steatohepatitis and cryptogenetic cirrhosis and depression [43,44,48–51].

There are conflictive results as to whether IL-6 is a beneficial or harmful cytokine [52]. There is, however, increasing evidence to show that IL-6 has a protective role during neural and liver injury [46]. In this context, it has been suggested that IL-6 favors hepatic secretion of VLDL triglyceride by increasing the availability of apoB and thereby, reducing hepatic lipid content by increased triglyceride export [52]. In addition, acute phase proteins, particularly the lipoprotein serum amyloid A, increase the ability of acute phase HDL to serve as an acceptor for cellular cholesterol efflux promoting the removal of excess cholesterol from macrophages as well as increasing the availability of cellular free cholesterol [47,53].

The predominance of the lipid metabolism with accumulation of cholesterol within embryos [26,32] as well as in the chronic inflamed tissue [43,44], could also be attributed to it being a precursor molecule of many hormones, like aldosterone, corticoids, progesterone, androgens and estrogen [28]. Particularly, endogenous sex steroids have been implicated in the pathology of, and protection against, a limited number of inflammatory disorders. Indeed estrogens limit while androgens could increase wound inflammation [54]. Also mineralocorticoids, i.e. aldosterone and glucocorticoids, are involved in the pathophysiology of inflammation because they produce oxidative stress, insulin resistance and fibrogenesis, as well as the promotion of adipogenesis [55]. Maybe due to the imperious need of this hormone potential, the developing oocyte is located in the center of the follicle and is surrounded by steroid producing follicle cells [32]. It has also been considered that endogenous lipid stores in fish oocytes and early embryos could be used as an energy substrate [56].

Mammalian embryos, however, have a changing pattern of energy metabolism, i.e. ATP generation, during early development. The most abundant energetic substrates in the embryo environment are glucose, pyruvate, lactate and glutamine [57]. For most mammalian proliferative cells the fundamental molecules catabolized are glucose and glutamine. This means that glucose and glutamine supply most of the carbon, nitrogen and free energy and reducing equivalents necessary to support cell growth and division [58]. Particularly interesting is the fact that some glucose is diverted to macromolecular precursor such as acetyl-CoA for fatty acids. Glutamine uptake also appears to be critical for lipid synthesis in that it supplies carbon in the form of mitochondrial oxalacetate to maintain citrate production in the first step of tricarboxylic acid [58].

The close relationship between lipid metabolism and inflammation has been emphasized in obesity. Thus, it has been suggested that current life style trends in modern society, characterized by excess of nutrients, reduced physical activity and increased lifespan could alter immune signaling and produce a chronic low-grade inflammatory state [59]. Because obesity-associated inflammation is considered a novel form of inflammation triggered by metabolic cues, the term of *"metaflammation"* has been proposed for its name [59,60].

The acute phase response is a pervasive physiological response of the body to injury [61]. Acute-phase changes may be divided into changes in the concentrations of many plasma proteins, known as the acute phase proteins and a large number of behavioral, physiologic, biochemical, and nutritional changes [37]. In nearly all animal species, albumin represents the major negative acute-phase protein which, during the acute phase response, decreases in blood concentration and increases in the inflammatory interstitial space [45]. Proteolysis during the acute phase response favors a protein-switch, because the resulting increase of amino acids is used for the synthesis of positive acute phase proteins, between which pentraxins i.e. serum amyloid P and C-reactive protein, stand out [61,62].

Pentraxins are a super-family of multifunctional conserved proteins, some of which are components of the humoral arm of innate immunity and behave as functional ancestors of antibodies [62,63]. Pentraxins are ancient proteins with high phylogenetic conservation. They are considered highly conserved acute phase innate immune proteins [61–64]. The classic short pentraxins, C-reactive protein and serum amyloid P component, are produced in the liver in response to inflammatory signals, most prominently IL-6 [62].

C-reactive protein circulates as a disc shaped pentamer and is dissociated by exposure of bioactive lipids on activated cell membrane and exhibit anti-inflammatory properties [63]. After dissociation, monomeric C-reactive protein could deposit in the inflamed tissue and represent an *"activation signal"* for inflammatory cells [63], but may also be able to minimize inflammation while enhancing apoptotic cell clearance [64]. Serum amyloid-P is closely related to C-reactive protein [64] and could promote anti-inflammatory responses [65].

C-reactive protein and serum amyloide-P are considered the main acute-phase reactants in humans, but also in arthropods different forms of C-reactive protein and serum amyloid-P are abundant constituents of the hemolymph [62]. In addition, it's noteworthy that C-reactive protein can bind to LDL and co-localize with LDL in human atherosclerotic lesions [62].

The long pentraxin PTX3 may play a regulatory role in inflammation but also is required for cumulus matrix organization [66]. Cumulus cells are closely connected to the oocyte during follicular development and ovulation, forming a reciprocal functional

interconnection [67,68]. Therefore, PTX3 that allows the formation of a highly organized hyaluronan-rich cumulus matrix favors ovulation and subsequent fertilization [62,66,68,69]. It has been proposed that PTX3 could have a similar function in hyaluronic acid-enriched inflammatory tissues [62,69].

PTX3 also plays an important role in humoral innate immunity and inflammation [70]. Levels of circulating PTX3 increase in humans during systemic inflammatory response syndrome, myocardial infarction or septic shock [71]. In this inflammatory context the high levels of PTX3 found associated with macrophages and endothelial cells in atherosclerotic plaques acting as a natural angiogenic inhibitor stand out [71,72].

Because both invertebrates and vertebrates detect and respond to microbial antigens, it is likely that a system recognizing these epitopes emerged at a very early stage in the evolution of animal species. In invertebrates, hemolymph coagulation and melanin formation are prominent as such responses [33]. Transglutaminase appears to be a common coagulation factor because it is involved in coagulation in arthropods and also acts as vertebrate clotting factor XIIIa [34]. The clots of large insects first form as a soft, initial, *"primary"* clot that is subsequently melanized [34]. Coagulation in insects contributes to wound healing and both processes depend on hemocytes, also called granulocytes [33,34]. In humans, activation of factor XIII is involved in atherogenesis and polymorphisms are related to the risk of coronary artery disease, atherothrombotic ischemic stroke and peripheral artery disease [73]. Procoagulant factors, i.e. plasminogen activator inhibitor I (PAI-1), fibrinogen and factor VII are also highest in patients with NAFLD, which explains the risk of the incidence of cardiovascular events among these patients [43].

Mast cells and the adipose-liver axis

Granulocytes may be close to the most ancient precursor of mast cells in invertebrates. In ascidians, the basophil/mast cell like granular hemocyte have been considered a potential mast cell progenitor and some granular hemocytes in *arthropoda* also closely approximate the ultrastructure of modern mast cells [74]. During evolution mast cells might have lost their potential to circulate in the blood once differentiated into sessile, tissue-homing cells [74].

Mast cells, strategically located in the interstitial space, could be among the first responders to orchestrate mechanical and biochemical stimuli that initiate inflammation [75]. Mast cells have the ability to produce vasoactive amines, enzymes i.e. proteases, cytokines, chemokines and growth factors through degranulation. This plasticity of the mast cells, which is the base for the called *"mast cell heterogeneity"* [75] suggest that mast cells can also show diverse responsiveness during the successive phases of the inflammatory response [11]. Mast cells stimulated through Toll-like receptors (TLRs) express "surgical" cytokine responses consisting mainly of IL-4, IL-8, tumor necrosis factor (TNF)-α and IL-6 [74,76]. In turn, IL-6, not only is the major mediator for the hepatocyte secretion of most of the acute phase proteins, but actually is also considered the major cytokine produced by activated mast cells, as well as a key factor that can trigger mast cell differentiation [77]. The acute phase response in the intestine resembles that seen in the liver. Indeed IL-6 mRNA is increased in the intestine during inflammation [78–80]. Among the cytokines produced during inflammation in the gut-liver axis, IL-6 is particular important because of its multiple biological effects both in the liver, intestine and other organs and tissues, including thermogenesis, stimulation of the hypothalamic–pituitary-adrenal axis and stimulation of growth hormone secretion [80]. Moreover, the pro-inflammatory cytokine IL-6 is critically involved in the pathophysiology of various aspects of NAFLD. Particularly, serum levels of this cytokine correlate remarkably well with the presence of insulin resistance and IL-6 has been shown to regulate hepatic insulin resistance [81].

Mast cells have well established roles as mediators of allergic, fibrotic and angiogenic diseases [14] and increasing evidence has implicated these cells in atherosclerotic plaque development [82,83]. Mast cells also produce serine proteases that could activate metalloproteinases leading to extracellular matrix remodeling [74,82]. The tissue distribution of mast cells containing serine proteases varies across animal species and the large number of functions described to these enzymes clearly indicates their importance in mast cell biology [74]. In this way, serine proteases appear to be a major link between innate immunity and tissue remodeling [74]. This is one of the reasons why it has been proposed that the mast cell phylogenetic progenitor evolved from a primitive local innate immunity cell into a tissue regulatory and remodeling cell [74].

White adipose tissue may represent an important source of mast cells in physiological and pathological situations [84]. Moreover, homeostasis of lipid metabolism is essential for mast cell survival and dysregulation of lipid metabolism, with oxysterols accumulation, the derivates of cholesterol, which may induce mast cell apoptosis [85].

Oenocytes, specialized hepatocyte-like cells [86], are found in a wide range of insects [87]. The presence of densely packed smooth and rough endoplasmic reticulum, together with other morphological features characteristic of mammalian steroidogenic cells and hepatocytes, indicates that oenocytes are cells with specialized secretory functions [87]. Oenocytes accumulate large numbers of lipid droplets specifically during fasting. As this is a hallmarks of hepatocytes, the possibility is raised that insect oenocytes might process lipids in a similar way to the mammalian liver [86]. Analogous to the mammalian adipose-liver axis, lipid mobilization from the fat body, the main organ of the intermediate metabolism of insects [39] during starvation produces lipid droplet accumulation in *Drosophila* oenocytes, a metabolic change resembling hepatic steatosis [86,88] (Table 1).

Increasingly sophisticated approaches are required to understand the critical roles of energy homeostasis. Several disorders have comparable syndromes in lower metazoans, like worms, flies and zebrafish [88]. Unbiased methods have been used to identify more genes where mutation in lower metazoans leads to phenotypes that are comparable to human syndromes of altered energy homeostasis like NAFLD, diabetes mellitus and obesity [88]. In this context, it has been speculated that *Drosophila* may prove useful, not only for modeling hepatic steatosis, but also the regulation of body fat content [89]. Indeed multiple genes have been identified that either positively or negatively regulate whole fly triglyceride levels when targeted specifically in neurons, the fly liver i.e. oenocytes, the fat body or muscle cells. Since more than 60% of the candidate genes with strong lipid storage regulatory potential linked with regulation of adiposity is conserved across animal phyla to humans, screening genes is considered a unique starting point to the elucidation of novel regulatory modalities in mammals [89].

Metamorphosis and remodeling: gastrulation dictates their rules

When talking about metamorphosis the caterpillar-to-butterfly and tadpole-to-frog transition immediately come to mind. However, most metazoan phyla metamorphose: for example, in cnidarians, flat worms or mollusks [90]. It has been also considered that all chordates have a homologous metamorphosis stage during their post-embryonic development. If vertebrate metamorphosis has been molecularly well characterized only in anurans, which could be probably for historical, anthropocentric, epistemological as well as technical reasons [90].

We have hypothesized that the phylogenetic evolution of our body is written in the successive phases which make up the acute inflammatory response. Therefore, it could be considered that when evolution of a serious traumatized patient is favorable, he could first undergo a dedifferentiation followed by a process of differentiation or specialization which would represent a complete metamorphosis program, as which occurs with lepidoptera [91]. This specialization would require the return of the prominence of oxidative metabolism and angiogenesis in the affected tissues and epithelial organs to create the capillary bed that would make the repair possible [8].

Nutrition mediated by blood capillaries is established because of angiogenesis. The new functional properties of microcirculation include the exchange of oxygen, nutrients and waste products. This oxygen support induces oxidative metabolism, an efficient method for extracting energy from blood molecules, which begins with the Krebs cycle and ends with oxidative phosphorylation [8]. Oxygen and oxidative metabolism are an excellent combination through which cells can obtain an abundant energy supply for tissue repair by specialized cells, but this combination has the inconvenience that it produces energetic stress [14].

Nonetheless, little is known about the capacity of eukaryotic cells to monitor the redox state for supporting specialized functions [92]. Although NF-kB acts mainly as an initiator of inflammation, recent studies suggest that it also functions in the equally complex process of resolution of inflammation [93]. Obviously, the mechanisms that promote tissue structure and restoring of functions also include the mechanisms involved in the resolution of inflammation [94]. In particular, endogenous pro-resolving lipid mediators, i.e. lipoxins, resolvins and protectins, have been the most studied. In essence, pro-resolution factors revert back the pro-inflammatory phenotype to its prior physiological state and therefore the microcirculatory functions of tissues and organs return to homeostasis [95].

A common complication of the post-natal inflammatory response in mammals is fibrosis. Scar formation and fibrosis are processes incompatible with tissue regeneration [96]. It has been suggested that molecular and cellular mechanisms involved in gastrulation during embryo development return when the activation of a fibrotic process occurs, whether by local remodeling i.e. wound repair, or systemic remodeling i.e. aging [11].

Gastrulation is a developmental phase that delineates the three embryogenic germ layers: ectoderm, endoderm and mesoderm [97]. Although the details of gastrulation differ among different species, the cellular mechanisms involved in gastrulation are common to all animals ([97]. The molecular and cellular contribution to gastrulation may be made by the two halves of the egg and early embryo structures: The amnion or *"animal"* side, thus named because it suggests movement and activity, which has the egg nucleus and the central nervous system form from *"animal"* cells; and the yolk sac or *"vegetal"*, because it suggests sluggishness, which is filled with yolk material (*vitellum*) for nutrition [98]. Moreover, the amnion could be considered as an embryonic functional axis with the ability to manage the embryo interstitial fluid, as well as with a strong neurogenic phenotype [99,100]. In regards to the yolk sac, it could be considered, not only a yolk deposit for nutrition but also a hematopoietic-angiogenic axis with a strong immune-endocrine potential phenotype [11,101].

In essence, during gastrulation it could be considered that the extraembryonic mesoderm with its amniotic and yolk-sac-derived functions internalizes to form the primary mesenchyma [11]. Afterward this is followed by mesenchymal-epithelial transition to create secondary epithelium [102]. The vast arrangement of the mesenchyma around and between the developing amniotic and yolk sac cavities suggests an important role of the mesenchyma in orchestrating embryo development. Mesenchymal stem cells are a versatile group of cells derived from mesodermal progenitors and can be found in several fetal and adult tissues [103]. The concept that fibroblasts are simple residual embryonic mesenchymal cells explains the incorrect and often interchangeable substitution of the term *"fibroblast"* for *"mesenchymal"* [104]. However, this hypothetical internalization process of the plurifunctional extraembryonic mesoderm to form the mesenchyma could explain the amazing quick capacity of the fibroblast not only to transform in epithelial cells but also to create a heterogeneous population capable to express neuro (contractile cells i.e. smooth muscle cells and pericytes), immune (myofibroblasts), endocrine (adipocytes) as well as remodeling (profibrogenic cells) phenotypes [11].

This amazing property of the mesenchymal or stromal cells to conserve a memory of its early embryonic origin undergoing reprogramming events could allow them post-injury to re-enter the embryonic programs of tissue formation and obtain regeneration [105]. Generally, while the monopotent and tissue-committed stem cells were described in the adult tissue, stem cells with a pluripotent/multipotent capacity were thought to be restricted to the early embryonic stages. However, recent evidence challenged this idea by confirming the presence of pluripotent/multipotent stem cells in adult tissues and organs [106]. Particularly, adult human mesenchymal cell populations contain distinctly multipotent stem cells. These stem cells have the ability to generate the multiple cell types of the three germ layers, like ectodermal, endodermal and mesodermal lineage cells [107]. Therefore, it is accepted that after the tissue is damaged, the inflammatory response induces the activation and mobilization of stem cells capable of regenerating the tissue, or by default, of repairing it by fibrosis, a process whose essential mechanisms have been compared to those that are responsible for gastrulation during embryonic development [11].

During vertebrate gastrulation, the cell behavior is strictly coordinated in time and space by various signaling pathways. In vertebrates, the non-canonical Wnt/planar cell polarity (Wnt/PCP) pathway is a key regulator of convergence and extension movements also involved in the internalization of mesodermal cells and their migration [108]. The Wnt/ßcatenin pathway is a developmental pathway that is highly conserved throughout evolution. Wnt signaling is initiated by the binding of secreted Wnt ligands to frizzled receptors, leading to the activation of canonical and non-canonical signaling. Canonical signaling activates ß-catenin mediated gene transcription [109]. Wnt signaling regulates many aspects of vertebrate development and adult stem cells. During development, non-canonical Wnt signaling is required for tissue formation and also is required for maintenance of adult stem cells [110].

Wnt represents a large morphogenic family of secreted lipid-modified glycoproteins that during embryogenesis controls multiple developmental processes [108,111] and during adult life regulates tissue maintenance and remodeling [110,112]. These physiological, developmental and oncogenic effects are mediated by the regulation of different specific programs, the nature of which depends on temporal and spatial factors and the tissues in question [109]. Binding of Wnts to their receptors activates the disheveled scaffolding protein, which in turn inhibits a "destruction complex" including Axin, Adenomatous Polyposis coli, and the serine/threonine kinase GSK-3beta. The destruction complex promotes the phosphorylation of beta-catenin/Armadillo, which is then targeted for proteasome-dependent degradation. Inhibition of this complex by Wnt signaling leads to a rise in cytoplasmic beta-catenin levels, and in its translocation into the nucleus, where it associates with the transcription factor TCF/LEF/Pangolin to regulate Wnt target genes [113].

At the cellular level, Wnt signals coordinate changes in cellular metabolism favoring either a "quiescent metabolism" or a "proliferating metabolism" [111,112]. This is why it is tempting to

speculate that common alterations in metabolic programming may accompany embryonic and/or stem cell differentiation and these may also be involved in adult tissue development and/or remodeling [111].

Moreover, synthesis and deposition of extracellular matrix are key features of fibroblasts [114]. Components of the extracellular matrix, including fibronectin, laminin and collagen are essential regulators of cell migration, adhesion and polarity during both normal vertebrate development [115] and the progression of diseases, such as age-related diseases [116]. It has been suggested that the extracellular matrix network should be present during zebrafish gastrulation and that this network should be positioned to affect, at a minimum, the polarized behavior of mesodermal cells [115]. Furthermore, age-related changes in cell behavior and morphology of fibroblasts appear to be linked to alterations [116]. In chronically inflamed tissues there is increasing evidence to suggest that aberrant expression of extracellular matrix molecules and fragments of the extracellular matrix that are derived from tissue-remodeling processes can influence immune cell activation, differentiation and survival [22].

Taken all together the exposed mechanisms mentioned above, it would be concluded that the inflammatory pathology is supported by evo-devo sharing mechanisms. Moreover, these mechanisms represent a very useful and universal tool for remodeling organisms in harmony with continuous environmental changes. If so, the inflammatory mechanisms would be effective mediating pathways between the environment and the genetic potential of living beings, which in turn give them an epigenetic character.

Consequences of the hypothesis and discussion

Today, evo-devo research is characterized by a dialectical approach that, on the one hand, looks at how developmental systems have evolved and, on the other hand, probes the consequences of these historically established systems for organism evolution [117]. A further question is how evolutionary developmental interactions relate to environmental conditions [117]. In this context, it could be hypothesized that, since inflammation could be a hypothetical recapitulator response of the fundamental mechanisms that govern the phylogeny and the ontogeny, it would constitute a useful tool of nature to integrate both processes.

The inflammatory response, thanks to its supposed ability to recreate primitive or ancestral evolutive states of animal life, could also exploit the possibility to induce genetic and epigenetic regulations to create a new developmental context in accordance with today's environmental factors. In this way, under the inflammatory influence, chromatin can undergo changes in its conformation in response to various cellular metabolic demands [118], but can also undergo epigenetic regulation, in which case, the same genotype can produce different phenotypes in response to the actually external conditions [117,118]. Therefore, maybe the plasticity that animal organisms have for achieving a successful adaption to the environmental changes could be related to inflammation.

Chronic low-grade metabolic inflammation-related Evo-Devo

Through the recovery of ancient evolutive phenotypes during the inflammatory response, the body could have the chance of choosing the most appropriate phenotype to survive according to the harmful circumstances that fall upon it. The equivalent pathological response of a population could be explained by this mechanism when similar harmful factors fall upon it, such as chronic psychosocial stress, sedentary lifestyle, a Western diet, alcohol intake or smoking [119]. The metabolic syndrome refers to the clustering of cardiovascular risk factors that include dyslipidemia, obesity, diabetes and hypertension [119,120]. However, youths that are overweight and obesity in youth is also a worldwide public health problem. Overweight and obesity in childhood and adolescents affects many systems, resulting in clinical conditions such as metabolic syndrome, early atherosclerosis, dyslipidemia, type 2 diabetes and hypertension [121,122] (Fig. 2). Due to the high incidence of this complex syndrome, both among children and adolescents as well as in aging people, it has been proposed that this disease spreads like an epidemic and, therefore it indeed must be scrutinized for an infectious cause [123].

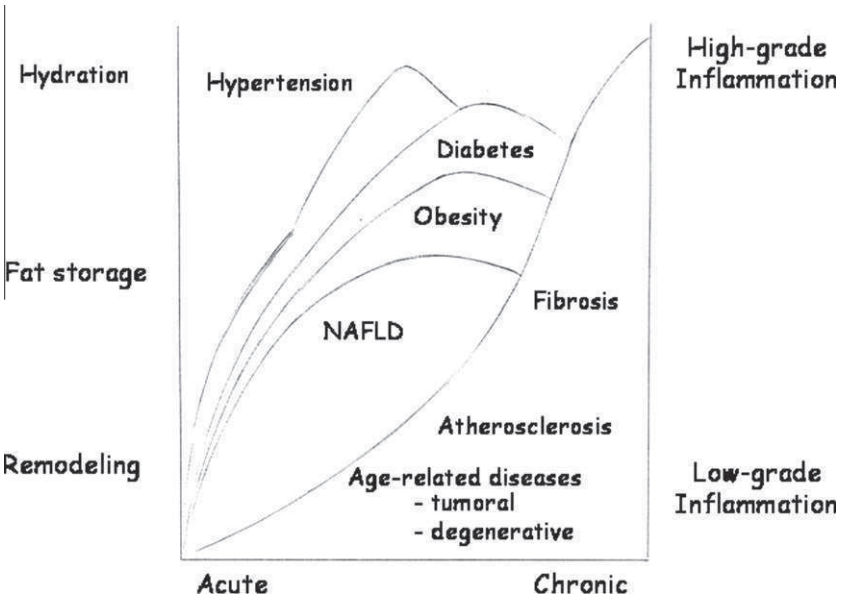

Fig. 2. The distribution of the different pathological conditions, i.e. hypertension, diabetes, non-alcoholic fatty liver disease (NAFLD) that integrate the metabolic syndrome varies in terms of intensity and magnitude among Western country populations. Such a varying manifestation depends on the different expressions of the basic inflammatory mechanisms that govern each one of the pathologies making up the metabolic syndrome due to human genetic diversity. Therefore, there is ischemia-revascularization in the case of arterial hypertension, the vitellogenic phenotype in cases where obesity with NAFLD predominate, and the remodeling phenotype when atherosclerosis or premature aging stand out.

Furthermore obesity may exaggerate the inflammatory response to stressors [124] and there is also a robust association between metabolic syndrome, obesity, NAFLD and encephalopathy-associated depression [13,124]. The inflammatory mediators have the capacity to induce depression, sleep and appetite disturbances and fatigue, which characterize depression, and they are part of a cytokine-triggered syndrome termed "sickness behavior", that also occurs when an organism has a wound or an infection [51,124].

In turn, this vicious cycle, that seems to be generated around inflammation, seems to close when it is assumed that the psychophysiological stress- originating from the masterfully created human mind with biological, social, behavioral, psychological, transcendental and religious components – is a risk factor for cardiovascular and metabolic diseases [125]. In this way, it has been suggested that inflammation could be a psychophysiological biomarker in chronic psychosocial stress, generated by example by low socioeconomic status, job stress/burnout, childhood adversity and life event stress, caregiver stress and loneliness [126]. In this way, the individual with an inflammatory pathology secondary to the conditions of life imposed upon him by the Western society could be considered an "*inflammacitizen*". If so, it's possible that the society, composed of these people sensitized by inflammation, cannot avoid their modulator influence. Particularly, obesity is considered from a global population perspective as an epidemic condition [127].

The hypothetical distribution of the pathophysiological mechanisms related to low-grade inflammatory response in the Western society

Chronic low-grade inflammation, also named metabolic inflammation or "metaflammation" [60] is believed to be a key pathogenic mechanism of several metabolic disorders including metabolic syndrome and their related diseases mentioned above [50,59]. The metabolic inflammation hypothesis has gained popularity with the demonstration of the central involvement of the stress-activated protein kinases c-Jun N terminal Kinase 1 (JNK1) and I Kappa Kinase beta (IKKβ) in their pathogenesis [48,50]. These enzymatic complexes in turn are situated at the focal points of different signaling pathways involved in innate immunity, inflammation and stress [50].

Nonetheless, the association of diseases shared by the same key pathogenic mechanism, i.e. inflammation, in the metabolic syndrome, could be also the result of the tissue, organic and systemic recapitulation of ancestral phylogenic ontogenic mechanisms. Through the expression of old mechanisms regulating: (1) the interstitial hydroelectrolytic distribution with cell hydration; (2) vitellogenesis related to the acute-phase-response and (3) gastrulation with mesenchymal remodeling, the basic physiopathological mechanisms leading to the development of an array of pathological conditions would be established in the animal body. In addition, the expression of these three pathological phenotypes could be distributed between all the individuals that constitute the Westernized society depending on their genetic polymorphism. If so, these three basic mechanisms could be related with the development of the pathological conditions associated with the metabolic syndrome, such as hypertension, type 2 diabetes, dyslipidemia, NAFLD, sickness behavior, depression, atherosclerosis, and aging-related diseases, i.e. profibrotic degenerative and tumoral diseases (Fig. 2).

In this context, the use of inflammation by the body could represent the camouflaged expression of efficient mechanisms of evolution and development that would allow survival although the drastic environmental conditions are imposed upon it. Maybe this is the reason that the body attempts to inhibit certain types of the inflammatory response, particularly when chronic, are very difficult or unsuccessful, since their mechanisms would take root in their own mechanisms of adaptive survival.

If the different types of inflammatory response, both acute and chronic, marking the life of human beings, integrate evolutive ancestral mechanisms, it could also be considered that through research we could "trace" the biochemical origins of our life, as if we were carrying out an archaeological dig. On the contrary, we could ask ourselves with respect to the role that inflammation could play in our future evolution. Since the final objective of this amazing response always seems to be a remodeling of the organism in harmony with the correlative environmental conditions, which are partially modulated by the human being, we are indeed sculpting the future of our species.

It is most likely that this set of diseases suffered by our Western society represents the distribution of the abovementioned phenotypes among those individuals who form part of this society. In this case, it should be considered that this set of diseases would represent a true "Social Inflammatory Syndrome". This hypothetical social approach of the inflammatory response would imply the existence of individual groups who suffer a similar pathology, and at the same time, this common pathological characteristic would define them as true pathological bodies of the society they belong to. Therefore, the set of pathologies considered, if grouped based on the different and hypothetical phylogenic or ontogenic phenotype expressed (i.e. hypertensive, arterial, pulmonary or portal pathology with sodium and water retention, oxidative stress, increased hydrostatic pressure and hemodynamic alterations; lipoprotein related pathology with hyperinsulinemia, due to resistance to insulin, dyslipidemia, enzymatic stress, obesity, NAFLD and early atherosclerosis; and age-related pathology with profibrotic alterations, degenerative stress and tumoral pathology) would represent three social pathological phenotypes.

Conclusion

In summary, if the different types of the inflammatory response, both acute and chronic, that mark the life of the human being integrate ancestral evolutive mechanisms, it is possible that through careful and intentional research, we could trace the biochemical origins of life. The biochemical impairments that play the leading role in the early phases of the inflammatory response could be a reflection of those primitive mechanisms that began life on our planet. In this way, maybe inflammation represents an archaeological tool of unsuspected usefulness. On the contrary, we could also ask ourselves in terms of the role that inflammation could be playing regarding our future evolution as an animal species. Since the final objective of this amazing response seems to be to make the organism survive, whether individual or socially, in harmony with the correlative environmental conditions, perhaps we could try to foresee our immediate future if we were able to discover the laws that govern the predominating expression of the different phenotypes composing the inflammatory response.

Conflict of interest statement

The authors declare that they have not conflict of interest.

Acknowledgements

We would like to thank Maria-Elena Vicente for preparing the manuscript, Elizabeth Mascola for translating it into English and the Complutense University Medical School Director and Chief Section librarians, Javier de Jorge García-Reyes and María-José Valdemoro, respectively.

This study was supported in part, with a Grant from the Mutua Madrileña Automovilista, Ref. No. AP6977/2009.

References

[1] Medzhitov R. Origin and physiological roles of inflammation. Nature 2008;454:428–35.
[2] Smale ST. Selective transcription in response to an inflammatory stimulus. Cell 2010;140:833–44.
[3] Franceschi C, Bonafe M, Valensin S, et al. Inflamm-aging. An evolutionary perspective on immunosenescence. Ann N Y Acad Sci 2000;908:244–54.
[4] Franceschi C, Capri M, Monti D, et al. Inflammaging and anti-inflamming: a systemic perspective on aging and longevity emerged from studies in humans. Mech Ageing Dev 2007;128:92–105.
[5] Goto M. Inflammaging (inflammation + aging): a driving force for human aging based on an evolutionarily antagonistic pleiotropy theory? Biosci Trends 2008;2:218–30.
[6] Caruso C, Lio D, Cavallone L, Franceschi C. Aging, longevity, inflammation and cancer. Ann N Y Acad Sci 2004;1028:1–13.
[7] Bürkle A, Caselli G, Franceschi C, et al. Pathophysiology of ageing, longevity and age related diseases. Immunol Aging 2007;4:4.
[8] Aller MA, Arias JL, Nava MP, Arias J. Post-traumatic inflammation is a complex response based on the pathological expression of the nervous, immune, and endocrine functional systems. Exp Biol Med (Maywood) 2004;229:170–81.
[9] Nathan C, Ding A. Non resolving inflammation. Cell 2010;140:871–82.
[10] Aller MA, Arias JL, Sanchez-Patan F, Arias J. The inflammatory response: an efficient way of life. Med Sci Monit 2006;12:RA225–34.
[11] Aller MA, Arias JI, Arias J. Pathological axes of wound repair: gastrulation revisited. Theor Biol Med Model 2010;7:37.
[12] Selman M, Pardo A, Kaminski N. Idiopathic pulmonary fibrosis: aberrant recapitulation of developmental programs? Plos Med 2008;5:e62.
[13] Aller MA, Arias JL, Arias JI, Sanchez-Patan F, Arias J. The inflammatory response recapitulates phylogeny through trophic mechanisms to the injured tissue. Med Hypotheses 2007;68:202–9.
[14] Aller MA, Arias JI, Alonso-Poza A, Arias J. A review of metabolic staging in severely injured patients. Scand J Trauma Resusc Emerg Med 2010;17:18–27.
[15] Cone JB. Inflammation. Am J Surg 2001;182:558–62.
[16] Aller MA, Arias JL, Arias J. Post-traumatic inflammatory response: perhaps a sucesión of phases with a nutricional purpose. Med Hypotheses 2004;63:42–6.
[17] Arias JI, Aller MA, Arias J. Surgical inflammation: a pathophysiological rainbow. J Transl Med 2009;7:19.
[18] Arias JI, Aller MA, Arias J. The use of inflammation by tumor cells. Cancer 2005;104:223–8.
[19] Arias JI, Aller MA, Arias J. Cancer cell: using inflammation to invade the host. Mol Cancer 2007;6:29.
[20] Raymond J, Segre D. The effect of oxygen on biochemical networks and the evolution of complex life. Science 2006;311:1764–7.
[21] Acquisti C, Klefe J, Collins S. Oxygen content of transmembrane proteins over macroevolutionary time scales. Nature 2007;445:47–52.
[22] Sorokin L. The impact of the extracellular matrix on inflammation. Nat Rev Immunol 2010;10:712–23.
[23] Rhodes JM, Simons M. The extracellular matrix and blood vessels formation: not just a scaffold. J Cell Mol Med 2007;11:176–205.
[24] Dhar A, Ray A. The CCN family proteins in carcinogenesis. Exp Oncol 2010;32:2–9.
[25] Hynes RO, Zhao Q. The evolution of cell adhesion. J Cell Biol 2000;150:F89–96.
[26] Telfer WH. Egg formation in lepidoptera. J Insect Sci 2009;9:1–21.
[27] Baltz JM, Tartia AP. Cell volume regulation in oocytes and early embryos: connecting physiology to successful culture media. Hum Reprod Update 2010;16:166–76.
[28] Lubzens E, Young G, Bobe J, Cerda J. Oogenesis in teleosts: how fish eggs are formed. Gen Comp Endrocrinol 2010;165:367–89.
[29] Skoblina MN. Hydration of oocytes in bony-fishes. Ontogenez 2010;41:5–18.
[30] Jiang D, Liang J, Noble PW. Hyaluronan in tissue injury and repair. Ann Rev Cell Dev Biol 2007;23:435–61.
[31] Chen B, Fu B. A model for charged molecule transport in the interstitial space Conf Proc IEEE Eng. Med Biol Sci 2005;1:55–8.
[32] Arukwe A, Goksyr A. Eggshell and egg yolk proteins in fish: hepatic proteins for the next generation: oogenetic, population, and evolutionary implications of endocrine disruption. Comp Hepatol 2003;2:4.
[33] Muta T, Iwanaga S. The role of hemolymph coagulation in innate immunity. Curr Opin Immunol 1996;8:41–7.
[34] Dushay MS. Insect hemolymph clotting. Cell Mol Life Sci 2009;66:2643–50.
[35] Jin S-W, Patterson C. The opening act. Vasculogenesis and the origins of circulation. Arterioscler Thromb Vasc Biol 2009;29:623–9.
[36] Wasserthal LT. *Drosophila* flies combine periodic heartbeat reversal with circulation in the anterior body mediated by a newly discovered anterior pair of ostial valves and "venous" channels. J Exp Biol 2007;210:3707–19.
[37] Gabay C, Kushner I. Acute-phase proteins and other systemic responses to inflammation. N Engl J Med 1999;340:448–54.
[38] Tufail M, Takeda M. Molecular characteristics of insect vitellogenins. J Insect Physiol 2008;54:1447–58.
[39] Münch D, Amdam GV. The curious case of aging plasticity in honey bees. FEBS Lett 2010;584:2496–503.
[40] Davis RA. Evolution of processes and regulators of lipoprotein synthesis: from birds to mammals. J Nutr 1997;127:7955–8005.
[41] Sniderman A, Couture P, De Graaf J. Diagnosis and treatment of apolipoprotein B dyslipoproteinemias. Nat Rev Endocrinol 2010;6: 335–46.
[42] Natarajan P, Ray KK, Cannon CP. High-density lipoprotein and coronary heart disease. J Am Coll Cardiol 2010;55:1283–9.
[43] Targher G, Day CP, Bonora E. Risk of cardiovascular disease in patients with nonalcoholic fatty liver disease. N Engl J Med 2010;363:1341–50.
[44] Tarantino G, Savastano S, Colao A. Hepatic steatosis, low-grade chronic inflammation and hormone/growth factor/adipokine imbalance. World J Gastroenterol 2010;16:4773–83.
[45] Cray C, Zaias J, Altman NH. Acute phase response in animals: a review. Comp Med 2009;59:517–26.
[46] Kopf M, Bachmann MF, Marsland BJ. Averting inflammation by targeting the cytokine environment. Nat Rev Drug Discov 2010;9:703–18.
[47] Jahangiri A. High-density lipoprotein and the acute phase response. Curr Opin Endrocrinol Diabetes Obes 2010;17:156–60.
[48] Czaja MJ. JNK regulation of hepatic manifestation of the metabolic syndrome. Trends Endocrinol Metab 2010;21:707–13.
[49] Marsland AL, McCaffery JM, Muldoon MF, Manuck SB. Systemic inflammation and the metabolic syndrome among middle-aged community volunteers. Metabolism 2010;59:1801–8.
[50] Solinas G, Karin M. JNK1 and IKKβ: molecular links between obesity and metabolic dysfunction. FASEB J 2010;24:2596–609.
[51] Wager-Smith K, Markou A. Depression: a repair response to stress-induced neuronal microdamage that can grade into a chronic neuroinflammatory condition? Neurosci Biobehav Rev 2011;35:742–64.
[52] Sparks JD, Cianci J, Jokinen J, Chen LS, Sparks CE. Interleukin-6 mediates hepatic hypersecretion of apolipodrotein B. Am J Physiol Gastrointest Liver Physiol 2010;299:G980–9.
[53] Van der Westhuyzen DR, De Beer FC, Webb NR. HDL cholesterol transport during inflammation. Curr Opin Lipidol 2007;18:147–51.
[54] Gilliver SC. Sex steroids as inflammatory regulators. J Steroid Biochem Mol Biol 2010;120:105–15.
[55] Whaley-Connell A, Johnson MS, Sowers JR. Aldosterone: role in the cardiometabolic syndrome and resistant hypertension. Prog Cardiovasc Dis 2010;52:401–9.
[56] Sturmey RG, Reis A, Leese HJ, McEvory TG. Role of fatty acids in energy provision during oocyte maturation and early embryo development. Reprod Domest Anim 2009;44:50–8.
[57] Dumollard R, Carroll J, Duchen MR, Campbell K, Swann K. Mitochondrial function and redox state in mammalian embryos. Semin Cell Dev Biol 2009;20:346–53.
[58] Vander Heiden MG, Cantley LC, Thompsson CB. Understanding the Warburg effect: the metabolic requirements of cell proliferation. Science 2009;324:1029–33.
[59] Hummasti S, Hotamislïgil GS. Endoplasmic reticulum stress and inflammation in obesity and diabetes. Circ Res 2010;107:579–91.
[60] Hotamisligil GS. Inflammation and metabolic disorders. Nature 2006;444:860–7.
[61] Bayne CJ, Gerwick L. The acute phase response and innate immunity of fish. Dev Comp Immunol 2001;25:725–43.
[62] Bottazzi B, Garlanda C, Salvatori G, Jeannin P, Manfredi A, Mantovani A. Pentraxins as a key component of innate immunity. Curr Opin Immunol 2010;18:10–5.
[63] Martinez de la Torre Y, Fabbri M, Jaillon S, et al. Evolution of the pentraxin family: the new entry PTX4. J Immunol 2010;184:5055–64.
[64] Litvack ML, Palaniyar N. Soluble innate immune pattern-recognition proteins for clearing dying cells and cellular components: implications on exacerbating or resolving inflammation. Innate Immun 2010;16:191–200.
[65] Castaño AP, Lin S-L, Surowy T, et al. Serum amyloid P inhibits fibrosis through FcRγ-dependent monocyte-macrophage regulation in vivo. Sci Transl Med 2009;1:1–11.
[66] Inforzato A, Rivieccio V, Morreale AP, et al. Structural characterization of PTX3 disulfide bond network and its multimeric status in cumulus matrix organization. J Biol Chem 2008;283:10147–61.
[67] Cillo F, Brevini TAL, Antonini S, Paffoni A, Ragni G, Gandolfi F. Association between human oocyte developmental competent and expression levels of some cumulus genes. Reproduction 2007;134:645–50.
[68] Pisani LF, Antonini S, Pocar P, et al. Effects of pre-mating nutrition on mRNA levels of developmentally relevant genes in sheep/oocytes and granulosa cells. Reproduction 2008;136:303–12.
[69] Scarchilli L, Camaioni A, Bottazzi B, et al. PTX3 interacts with Inter-α-trypsin inhibitor. Implications for hyaluronan organization and cumulus oophorous expansion. J Biol Chem 2007;282:30161–70.
[70] Deban L, Jaillon S, Garlanda C, Bottazzi B, Mantovani A. Pentraxis in innate immunity: lessons from PTX3. Cell Tissue Res 2011;343:237–49.
[71] Rusnati M, Camozzi M, Moroni E, et al. Selective recognition of fibroblast growth factor-2 by the long pentraxin PTX3 inhibits angiogenesis. Blood 2004;104:92–9.
[72] Leali D, Alessi P, Coltrini D, Rusnati M, Zetta L, Presta M. Fibroblast growth factor-2 antagonist and antiangiogenic activity of long-pentraxin 3-derived synthetic peptides. Curr Pharm Des 2009;15:3577–89.

[73] Muszbek L, Bereczky Z, Bagoly Z, Shemirani AH, Katona E. Factor XIII and atherothrombotic diseases. Semin Thromb Hemost 2010;36:18–33.
[74] Crivellato E, Ribatti D. The mast cell: an evolutionary perspective. Biol Rev 2010;85:347–60.
[75] Galli SJ, Kalesnikoff J, Grimbaldeston MA, Piliponsky AM, Williams CMM, Tsai M. Mast cells as "tunable" effector and immunoregulatory cells: recent advances. Ann Rev Immunol 2005;23:749–86.
[76] Bachelet I, Levi-Schaffer F. Mast cells as effector cells, a costimulating question. Trends Immunol 2007;28:360–5.
[77] Hu Z-Q, Zhao W-H, Shimamura T. Regulation of mast cell development by inflammatory factors. Curr Top Med Chem 2007;14:3044–50.
[78] Molmenti EP, Ziambaras T, Perlmutter DH. Evidence for an acute phase response in human intestinal epithelial cells. J Biol Chem 1993;288: 14116–24.
[79] Wang Q, Wang JJ, Boyce S, Fischer J, Hasseigren PO. Edotoxemia and IL-1β stimulate mucosal IL-6 production in different parts of the gastrointestinal tract. J Surg Res 1998;76:27–31.
[80] Pritts T, Hungness E, Wang Q, Robb B, Hershko D, Hasselgren P-O. Mucosal and enterocyte IL-6 production during sepsis and endotoxemia-role of transcription factors and regulation by the stress response. Am J Surg 2002;183:372–83.
[81] Tilg H. The role of cytokines in non-alcoholic fatty liver disease. Dig Dis 2010;28:179–85.
[82] Bui QT, Prempeh M, Wilensk RL. Atherosclerotic plaque development. Int J Biochem Cel Biol 2009;41:2109–13.
[83] Yeong P, Ning Y, Xu Y, Li X, Yin L. Tryptase promotes human monocyte-derived macrophage from cell formation by suppressing LXRα activation. Biochem Biophys Acta 2010;1801:567–76.
[84] Poglio S, De Toni-Costes F, Arnaud E, et al. Adipose tissue as a dedicated reservoir of functional mast cell progenitors. Stem Cell 2010;28: 2065–72.
[85] Fukunaga M, Nunomura S, Nishida S, et al. Mast cell death induced by 24(S), 25-epoxycholesterol. Exp Cell Res 2010;316:3272–81.
[86] Gutierrez E, Wiggins D, Fielding B, Gould AP. Specialized hepatocyte-like cells regulate *Drosophila* lipid metabolism. Nature 2007;445:275–80.
[87] Gould AP, Elstob PR, Brodu V. Insect oenocytes: a model system for studying cell-fate specification by Hox genes. J Anat 2001;199:25–33.
[88] Schlegel A, Stainier DYR. Lessons from "lower" organisms: what worms, flies and zebra fish can teach us about human energy metabolism. Plos Genet 2007;3:e199.
[89] Pospisilik JA, Schramek D, Schnidar H, et al. *Drosophila* genome-wide obesity screen reveals hedgehog as a determinant of brown versus white adipose cell fate. Cell 2010;140:148–60.
[90] Paris M, Laudet V. The history of a developmental stage: metamorphosis in chordates. Genesis 2008;46:657–72.
[91] Aller MA, Arias JL, Nava MP, Arias J. Evolutive trophic phases of the systemic acute inflammatory response, oxygen use mechanisms and metamorphosis. Psicothema 2004;16:369–72.
[92] Agarwal AK, Auchus RJ. Minireview: cellular redox state regulates hydroxysteroid dehydrogenase activity and intracellular hormone potency. Endocrinology 2005;146:2531–8.
[93] Ghosh S, Hayden MS. New regulators of NF-κB in inflammation. Nat Rev 2008;8:837–49.
[94] Serhan CN, Brain SD, Buckley CD, et al. Resolution of inflammation: state of the art, definitions and terms. FASEB J 2007;21:325–32.
[95] Lawrence T, Gilroy DW. Chronic inflammation: a failure of resolution? Int J Exp Path 2007;88:85–94.
[96] Buchanan EP, Longaker MT, Lorenz HP. Fetal skin wound healing. Adv Clin Chem 2009;48:137–61.
[97] Mikawa T, Poh AM, Kelly KA, Ishii Y, Reese DE. Induction and patterning of the primitive streak, and organizing center of gastrulation in the amniote. Dev Dyn 2004;229:422–32.
[98] Elinson RP, Beckham Y. Development in frogs with large eggs and the origin of amniotes. Zoology 2002;105:105–17.
[99] Bellini C, Boccardo F, Bonioli E, Campisi C. Lymphodynamics in the fetos and newborn. Lymphology 2006;39:110–7.
[100] Chang YJ, Hwang SM, Tseng CP, et al. Isolation of mesenchymal stem cells with neurogenic potentials from the mesoderm of the amniotic membrane. Cells Tissues Organs 2010;192:93–105.
[101] De Miguel MP, Arnalich-Montiel F, Lopez-Iglesias P, Blázquez-Martinez A, Nistal M. Epiblast-derived stem cells in embryonic and adult tissue. Int J Dev Biol 2009;53:1529–40.
[102] Acloque H, Adams MS, Fishwick K, Bronner-Fraser M, Nieto MA. Epithelial-mesenchymal transitions: the importance of changing cell state in development and disease. J Clin Invest 2009;119:1438–49.
[103] Feng B, Chen L. Review of mesenchymal stem cells and tumors: executioner or conspirator? Cancer Biother Radiopharm 2009;24:717–21.
[104] Kalluri R, Neilson EG. Epithelial-mesenchymal transition and its implications for fibrosis. J Clin Invest 2003;112:1776–82.
[105] Kragl M, Knapp D, Nacu E, et al. Cells keep a memory of their tissue origin during axo to limb regeneration. Nature 2009;460:60–5.
[106] Zuba-Surma EK, Kucia M, Ratajczak J, Ratajczak MZ. "Small stem cells" in adult tissues: very small embryonic-like stem cells (VSELs) stand up. Cytometry 2010;75:4–13.
[107] Kuroda Y, Kitada M, Wakao S, et al. Unique multipotent cells in adult human mesenchymal cell populations. PNAS 2010;107:8639–43.
[108] Roszko I, Sawada A, Solnica-Krezel L. Regulation of convergent and extension movements during vertebrate gastrulation by the Wnt/PCP pathway. Semin Cell Develop 2009;20:986–97.
[109] Torre C, Perret C, Colnot S. Transcription dynamics in a physiological process: β-catenin signaling directs liver metabolic zonation. Int J Biochem Cell Biol 2011;43:271–8.
[110] Sugimura R, Li L. Non canonical Wnt signaling in vertebrate development, stem cells and diseases. Birth Defects Res C Embryo Today 2010;90:243–56.
[111] Sethi JK, Vidal-Puig A. Wnt signalling and the control of cellular metabolism. Biochem J 2010;427:1–17.
[112] Li L, Clevers H. Coexistance of quiescent and active adult stem cells in mammals. Science 2010;327:542–5.
[113] Budnik V, Salinas PC. Wnt signaling during synaptic development and plasticity. Curr Opin Neurobiol 2011;21:151–9.
[114] Krenning G, Zeisberg EM, Kalluri R. The origin of fibroblasts and mechanism of cardiac fibrosis. J Cell Physiol 2010;225:631–7.
[115] Latimer A, Jessen JR. Extracellular matrix assembly and organization during zebrafish gastrulation. Matrix Biol 2010;29:89–96.
[116] Wolfson M, Budovsky A, Tacutu R, Fraifeld V. The signaling hubs at the cross road of longevity and age-related disease networks. Int J Biochem Cell Biol 2009;41:516–20.
[117] Muller GB. Evo-devo: extending the evolutionary synthesis. Nat Rev Genet 2007;8:943–9.
[118] Choudhuri S, Cui Y, Klaassen CD. Molecular targets of epigenetic regulation and effectors of environmental influences. Toxicol Appl Pharmacol 2010;245:378–93.
[119] Duvnjak L, Duvnjak M. The metabolic syndrome – an ongoing story. J Physiol Pharmacol 2009;60:19–24.
[120] Grundy SM, Adams-Huet B, Vega GL. Variable contributions of fat content and distribution to metabolic syndrome risk factors. Metab Syndr Relat Disord 2008;6:281–8.
[121] Halpern A, Mancini MC, Magalhães ME, et al. Metabolic syndrome, dyslipidemia, hypertension and type 2 diabetes in youth: from diagnosis to treatment. Diabetol Metab Syndr 2010;2:55.
[122] Blüher M. Fat tissue and long life. Obesity Facts 2008;1:176–82.
[123] Nathan C. Epidemic inflammation: pondering obesity. Mol Med 2008;14:485–92.
[124] Kiecolt-Glaser JK, Gouin JP, Hantsoo L. Close relationships, inflammation and death. Neurosci Biobehav Rev 2010;35:33–8.
[125] Hamer M, Malan L. Psychophysiological risk markers of cardiovascular disease. Neurosci Biobehav Rev 2010;35:76–83.
[126] Hänsel A, Hong S, Camara RJA, Von Kämel R. Inflammation as a psychophysiological biomarker in chronic psychosocial stress. Neurosci Biobehav Rev 2010;35:115–21.
[127] Hansen CH, Gilman AP, Odland JO. Is thermogenesis a significant causal factor in preventing the "globesity" epidemic? Med Hypotheses 2010;75:250–6.